AFRRI REPORTS

January
February
March
1986

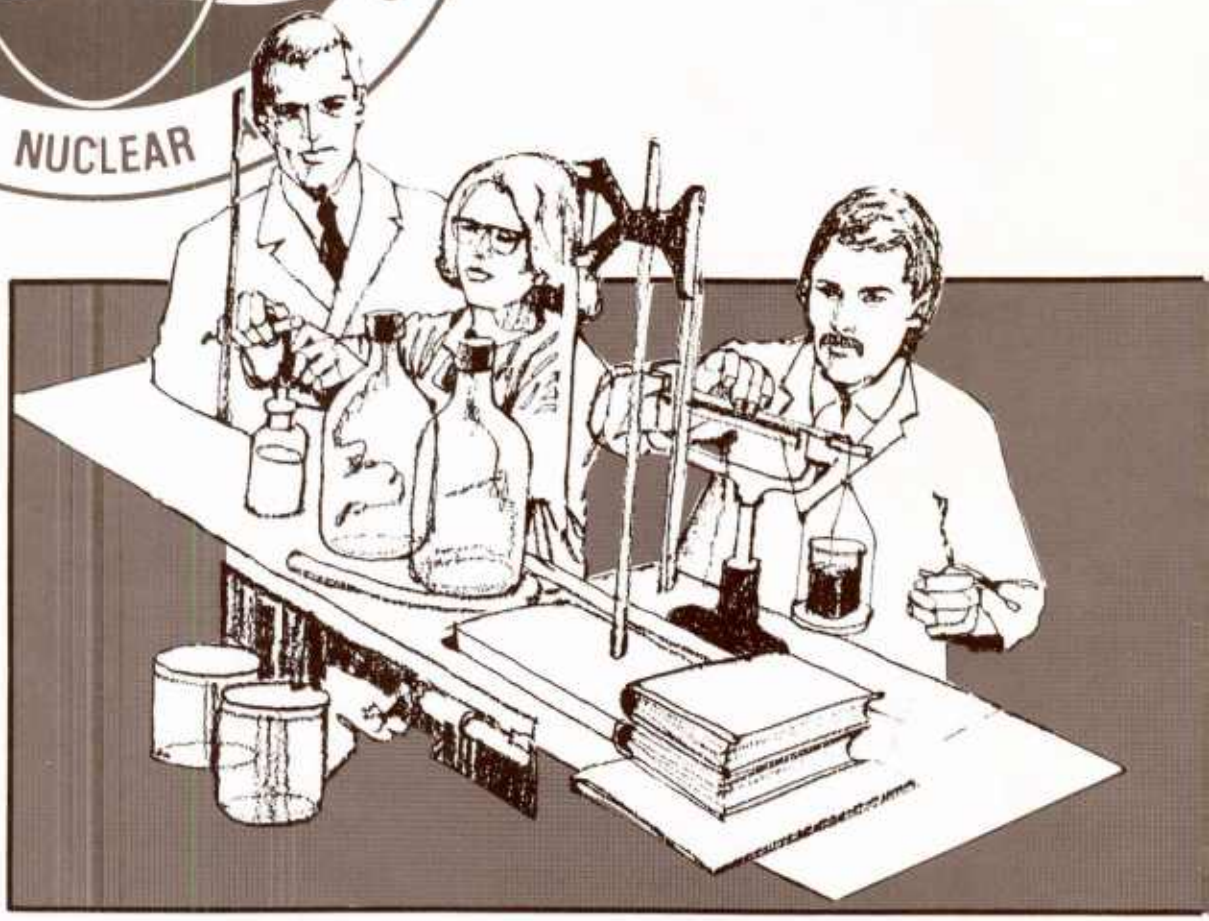

Defense Nuclear Agency

Armed Forces Radiobiology Research Institute

Bethesda, Md 20814-5145

REPORT DOCUMENTATION PAGE

1a. REPORT SECURITY CLASSIFICATION UNCLASSIFIED	1b. RESTRICTIVE MARKINGS
2a. SECURITY CLASSIFICATION AUTHORITY	3. DISTRIBUTION/AVAILABILITY OF REPORT Approved for public release; distribution unlimited.
2b. DECLASSIFICATION/DOWNGRADING SCHEDULE	
4. PERFORMING ORGANIZATION REPORT NUMBER(S) AFRRI SR86-1 through 86-13	5. MONITORING ORGANIZATION REPORT NUMBER(S)
6a. NAME OF PERFORMING ORGANIZATION Armed Forces Radiobiology Research Institute 6b. OFFICE SYMBOL (If applicable) AFRRI	7a. NAME OF MONITORING ORGANIZATION
6c. ADDRESS (City, State and ZIP Code) Defense Nuclear Agency Bethesda, Maryland 20814-5145	7b. ADDRESS (City, State and ZIP Code)
8a. NAME OF FUNDING/SPONSORING ORGANIZATION Defense Nuclear Agency 8b. OFFICE SYMBOL (If applicable) DNA	9. PROCUREMENT INSTRUMENT IDENTIFICATION NUMBER
8c. ADDRESS (City, State and ZIP Code) Washington, DC 20305	10. SOURCE OF FUNDING NOS. PROGRAM ELEMENT NO.: NWED QAXM PROJECT NO.: TASK NO.: WORK UNIT NO.:
11. TITLE (Include Security Classification) AFRRI Reports, Jan-Mar 1986	
12. PERSONAL AUTHOR(S)	
13a. TYPE OF REPORT Reprints/Technical 13b. TIME COVERED FROM _____ TO _____	14. DATE OF REPORT (Yr., Mo., Day) 15. PAGE COUNT 127
16. SUPPLEMENTARY NOTATION	

17. COSATI CODES			18. SUBJECT TERMS (Continue on reverse if necessary and identify by block number)
FIELD	GROUP	SUB. GR.	
			N/A

19. ABSTRACT (Continue on reverse if necessary and identify by block number)

This volume contains AFRRI Scientific Reports SR86-1 through 86-13 for Jan-Mar 1986.

20. DISTRIBUTION/AVAILABILITY OF ABSTRACT UNCLASSIFIED/UNLIMITED ☒ SAME AS RPT. ☐ OTIC USERS ☐	21. ABSTRACT SECURITY CLASSIFICATION UNCLASSIFIED
22a. NAME OF RESPONSIBLE INDIVIDUAL Junith A. Van Deusen	22b. TELEPHONE NUMBER (Include Area Code) (301) 295-3536 22c. OFFICE SYMBOL ISDP

DD FORM 1473, 83 APR EDITION OF 1 JAN 73 IS OBSOLETE.

CONTENTS

ARMED FORCES RADIOBIOLOGY
RESEARCH INSTITUTE
SCIENTIFIC REPORT
SR86-1

Brain Research, 364 (1986) 199–203
Elsevier

BRE 21329

Desensitization to glutamate and aspartate in rat olfactory (prepyriform) cortex slice*

DAVID J. BRAITMAN

Physiology Department, Armed Forces Radiobiology Research Institute, Bethesda, MD 20814-5145 (U.S.A.)

(Accepted September 24th, 1985)

Key words: glutamate — aspartate — olfactory cortex — prepyriform cortex — amino acid receptor — desensitization — brain slice

Olfactory cortex brain slices were subject to multiple bath applications of either glutamate or aspartate. The effectiveness of these amino acids (measured by quantitating the amplitude of lateral olfactory tract-stimulated field potentials) was progressively reduced with each successive perfusion of the agonist. However, the effectiveness of the endogenous neurotransmitter recovered to control in each intervening wash period. Thus, repeated applications of glutamate or aspartate desensitized olfactory cortex receptors to these amino acids but did not desensitize the receptors to the endogenous transmitter. These data support the hypothesis that neither glutamate nor aspartate is the neurotransmitter released from the lateral olfactory tract onto pyramidal cells of the olfactory cortex.

A critical criterion for establishing a substance as a neurotransmitter is identity of action, i.e., it must be demonstrated that the postsynaptic actions of the candidate substance are identical to those of the endogenously released transmitter[14]. A major problem with meeting this criterion for glutamate and aspartate is that their excitatory actions are ubiquitous in the central nervous system (CNS). To circumvent this problem, another characteristic of transmitter action, desensitization, has been used to suggest identity of action. Desensitization is expressed as a reduction in the biological response to an agonist after prolonged or repeated exposure to that agonist. This reduction in response has been shown to be receptor-mediated[10].

At the invertebrate neuromuscular junction, prolonged exposure to exogenously applied glutamate results in (1) desensitization of glutamate receptors and (2) a significant reduction in the magnitude of synaptic responses[11]. This observation is consistent with the transmitter role suggested for glutamate in this system. However, in rat hippocampal slice, desensitization to glutamate occurs without any change in synaptic transmission[4,5], an observation inconsistent with the putative transmitter role for glutamate in this area of the CNS.

The present study was designed to elucidate the role of glutamate and aspartate in synaptic transmission from the lateral olfactory tract (LOT) to the olfactory cortex. Repeated exposure of olfactory cortex brain slices to exogenously applied glutamate or aspartate during LOT stimulation resulted in a powerful and reversible desensitization to these amino acids. However, the synaptic responses to the endogenous transmitter released by LOT stimulation did not densensitize. These results support previous pharmacological observations from this laboratory[8,9] that indicate that neither glutamate nor aspartate is the transmitter released at the terminal synapses of LOT onto pyramidal cells of the olfactory cortex[2].

Tissue preparation, stimulation and recording were as previously described[9]. Tangential slices (300–400 μm) of rat olfactory cortex were placed in a total submersion chamber at 32 °C and constantly perfused with normal Ringer's solution (5 ml/min). L- or D-glutamate or L-aspartate was added to the Ringer's and bath applied to the slice for 3–5 min. This was followed by a wash in normal Ringer's for

* The views presented in this paper are those of the author: no endorsement by the Defense Nuclear Agency has been given or should be inferred.

Correspondence: D.J. Braitman, Physiology Department, Armed Forces Radiobiology Research Institute, Bethesda, MD 20814-5145, U.S.A.

10–15 min. This procedure was repeated with the same drug concentration as many as 6 ×. Field potentials, evoked by 0.25-Hz orthodromic stimulation to the LOT, were recorded from the pial surface of the prepyriform cortex throughout the experiment. Five consecutive evoked potentials were computer-averaged at intervals of 1–5 min. To quantify the actions of amino acids, the peak amplitude of the monosynaptic slow-wave component of the averaged field potential, i.e., the population excitatory postsynaptic potential, was measured before, during, and after drug application. Drug effects were studied on 16 slices. Each slice was used for only one experiment.

Initial application of 2–5 × 10^{-3} M L-glutamate significantly decreased the amplitude of the field potential evoked by lateral olfactory tract stimulation (Table I). This effect was dose- and time-dependent and stabilized within 5 min. The decrease in amplitude of the field potential during glutamate perfusion presumably was due to the depolarizing action of glutamate on this tissue[3]. Successive perfusions of the same concentration of glutamate were less effective in attenuating the amplitude of the field potential (Fig. 1A). Synaptic potentials in the wash period returned to within 5.9 ± 2.1% of the control field potential amplitude (i.e., predrug values) 10–15 min after termination of the final drug application (mean ± S.E.M. of 7 experiments). The reduced efficacy observed during successive glutamate applications suggests that the reduction in depolarization was due to desensitization of glutamate receptors.

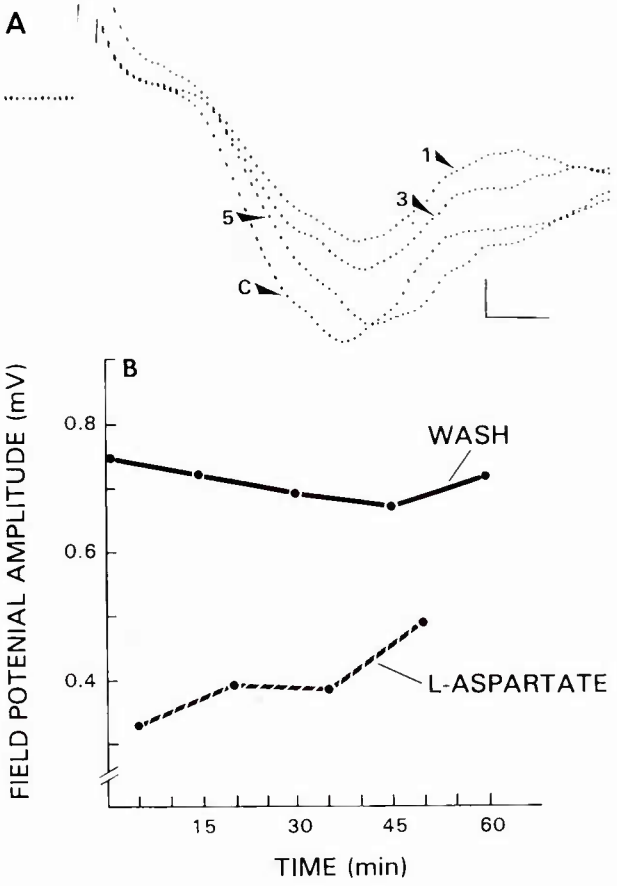

Fig. 1. Desensitization to repeated applications of L-glutamate or L-aspartate. A: examples of field potentials evoked by stimulation of LOT (average of 5 successive potentials) in a representative experiment. The trace labeled C is potential prior to application of any drugs. Other traces represent field potentials after first, third and fifth successive application of 2 × 10^{-3} M glutamate. Each subsequent 5-min perfusion of glutamate resulted in reduced efficacy to decrease the amplitude of field potential. By the fifth application almost no response to glutamate perfusion is seen. Calibration bar is 0.4 mV and 2 ms. B: in another experiment, peak field potential amplitude was plotted at the end of each 5-min perfusion with 10^{-2} M L-aspartate (dashed line) and after each 10-min perfusion with drug-free medium (solid line). First point in wash data is control amplitude. This tissue did not respond to 5 × 10^{-3} M aspartate. Note that there was a dissociation between (1) time course and magnitude of aspartate desensitization and (2) fluctuations in synaptic response in the wash. The dissociation between desensitization and synaptic responses to the endogenous transmitter was observed in 4 of the 5 aspartate experiments.

TABLE I

Effects of multiple applications of excitatory amino acids on field potentials evoked by LOT-stimulation

Each excitatory amino acid was bath applied for 3–5 min followed by a 10–15-min wash in normal Ringer's. The percent depolarization at the end of the first (Initial) and third or fourth (Final) amino acid perfusion was calculated (wash–drug/wash × 100). The percent desensitization was determined for each experiment by calculating the difference between the first and last depolarization divided by the first and multiplying by 100. Each value represents the mean ± S.E.M. of the indicated number of experiments (n). Desensitization to L-glutamate ranged from 36 to 94% and to L-aspartate from 38 to 71%.

Amino acids	*n*	*Decrease of field potential amplitude (%)*		*Desensitization (%)*
		Initial	*Final*	
L-Glutamate	7	39.6 ± 4.8	16.9 ± 3.6	63.4 ± 6.7
D-Glutamate	2	49.2 ± 14.8	26.4 ± 1.0	33.4 ± 19.4
L-Aspartate	5	52.5 ± 7.1	24.7 ± 4.7	55.0 ± 7.0

Desensitization to repeated applications of L-aspartate was similar to that demonstrated for glutamate (Table I). In the experiment illustrated in Fig. 1B, the first application of aspartate produced a 55% decrease in the peak amplitude of the field potential,

while a fourth perfusion of aspartate resulted in only a 27% decrease in amplitude. This indicates that aspartate receptors became progressively more desensitized with each successive drug perfusion. In contrast, synaptic potentials recovered to within 10% of control amplitude by the end of each intervening 10-min wash (see legend and Fig. 1B). In the final wash synaptic potentials recovered to within 19.5 ± 3.4% of control and 6.0 ± 1.9% relative to the wash after the first amino acid perfusion (mean ± S.E.M. for 5 experiments). Thus, the receptors responding to the endogenous transmitter released by LOT stimulation were not desensitized as were the aspartate receptors. These results suggest that the olfactory pyramidal cell receptors that receive input from the LOT are not aspartate or glutamate receptors.

In order to test whether desensitization to glutamate and aspartate was reversible or due to a permanent alteration in receptor function, 4 slices were given an extended wash in drug-free Ringer's solution following desensitization. Fig. 2 illustrates data from an experiment in which an olfactory cortex slice

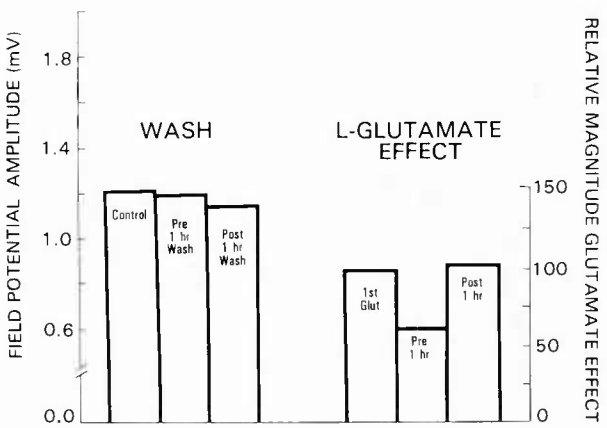

Fig. 2. Reversible desensitization to glutamate. L-glutamate effect (right side) expressed as percent efficacy in decreasing field potential amplitude relative to first glutamate application (1st Glut, 100% effect). After 4 successive applications of 2×10^{-3} M glutamate (pre 1 h), a large reduction in response to glutamate, i.e. desensitization, was seen. After a 1-h wash in normal Ringer's, response to a fifth application of glutamate (post 1 h) was as great as to first glutamate application. Synaptic responses in absence of glutamate (left side, wash), expressed in mV field potential amplitude, exhibited little net change over the 2.5-h course of this experiment. Wash control is field potential amplitude before any drug application. Pre 1-h wash shows field potential amplitude at the end of a 10-min wash period following fourth glutamate application (prior to a 1-h wash in normal Ringer's). Post 1-h wash was the field potential amplitude at the end of a 1-h wash (preceding fifth glutamate application).

was desensitized by 4 successive perfusions of L-glutamate. As can be seen in the right side of Fig. 2 (L-glutamate effect) the fourth application of glutamate (pre 1 h) was only 54% as effective as the first glutamate application (1st Glut). Following the fourth perfusion of glutamate, the slice was washed in drug-free Ringer's for 1 h then exposed to a fifth glutamate application (post 1 h). After this long wash desensitization was abolished and the response to the fifth application of glutamate (L-glutamate effect, post 1 h) was as great as to the first glutamate application (1st Glut). Throughout the experiment synaptic responses in the absence of drugs (wash) exhibited recovery to control amplitude at the end of each intervening wash period (Fig. 2, left side). Thus, glutamate and aspartate receptors exhibited progressive desensitization when exposed to multiple applications of these amino acids. Desensitization persisted during the short intervening washes but receptors returned to a nondesensitized state after a 1-h wash (e.g., Fig. 2, L-glutamate effect). On the other hand, receptors to the endogenous transmitter were not desensitized and maintained responsiveness at control levels throughout the experiment (e.g., Fig. 2, wash).

To ensure that desensitization was not due to a modification of glutamate uptake, experiments were conducted with the D-isomer of glutamate which is taken up only weakly by high-affinity transport[1]. Desensitization and reversal of desensitization similar to that observed with L-glutamate was seen with D-glutamate (Table I). These results indicate that desensitization was not due to the facilitation of a high-affinity uptake inactivation mechanism.

The desensitization to glutamate and aspartate seen in this study was qualitatively similar to the desensitization to glutamate at the invertebrate neuromuscular junction[11], where glutamate is a strong candidate for the excitatory transmitter. However, in contrast to the neuromuscular junction experiments, synaptic responses to the endogenous transmitter released by LOT stimulation in the present experiments were not markedly reduced during glutamate desensitization. The most parsimonious explanation for the failure of synaptic receptors to desensitize during repeated exposure to millimolar concentrations of glutamate and aspartate is that neither amino acid is the excitatory transmitter from LOT to olfactory cortical cells. Although it may be argued that ex-

trasynaptic receptors are responsible for the results seen here, this is unlikely because (1) synaptic responses desensitize along with glutamate receptors at the invertebrate neuromuscular junction where extrasynaptic receptors have been shown to exist[12], and (2) glutamate and aspartate receptors in the rat have been reported to be enriched at synaptic junctions[7]. Furthermore, the design of the experiments reported here allowed all receptors to be exposed to glutamate or aspartate since high agonist concentrations were bath perfused onto totally submerged slices.

The observation of a small but consistent decrease in the amplitude of the synaptic potentials during the wash period may be due to an excitotoxic action of glutamate and aspartate and/or down regulation of a subpopulation of receptors by the initial application of these amino acids. In accord with this suggestion is the observation that the decrease in amplitude between the control field potential and the synaptic potential during the first wash following the initial drug application was 7.4 ± 1.5% for L-glutamate and 16.3 ± 3.5% for L-aspartate (mean and S.E.M. for 7 and 5 experiments, respectively). The decrease in field potential amplitude in the wash following the first amino acid perfusion was equivalent to the mean decrease in synaptic potentials over the course of the entire experiment.

Alternatively, the decrease in the amplitude of the synaptic potentials during the wash period may be due to a weak cross-sensitivity of the endogenous LOT receptor with these amino acids. If the endogenous transmitter is an amino acid analog or a small glutamyl and/or aspartyl peptide, one might expect to see some effect of glutamate and aspartate at this receptor, given the cross-sensitivity of excitatory amino acid receptors[13]. Recently, it has been shown that the endogenous dipeptide N-acetylaspartylglutamate (NAAG) has the same pharmacological profile as the LOT neurotransmitter[6]. Further experiments, including the bath application of NAAG, are required to distinguish between these alternatives.

The excitatory action of glutamate and aspartate[3,8,9] as well as their presence and release in olfactory cortex[2] supports the possibility of a transmitter role for these amino acids. However, their specific role is in doubt. It has been reported[6,8,9] that 2-amino-4-phosphonobutyrate, an excitatory amino acid antagonist, blocks neuronal responses evoked by the endogenous lateral olfactory tract transmitter and NAAG but not responses elicited by glutamate or aspartate themselves. The present results, as well as those previous observations[6,8,9], indicate that neither glutamate nor aspartate is the primary neurotransmitter released from lateral olfactory tract onto pyramidal cells of the olfactory (prepyriform) cortex.

The author thanks Drs. J.R. ffrench-Mullen, T. Pellmar and B. Waldbillig for valuable comments on the manuscript. Expert typing was provided by Ms. Marianne Owens. Editorial and graphics support was provided by the AFRRI Administration Department. Supported by the Armed Forces Radiobiology Research Institute, Defence Nuclear Agency, under Research Work Unit MJ00005.

1 Balcar, V.J. and Johnston, G.A.R., The structured specificity of high affinity uptake of L-glutamate and L-aspartate by rat brain slices, *J. Neurochem.*, 19 (1972) 2657–2666.

2 Collins, G.G.S., Anson, J. and Probett, G.A., Patterns of endogenous amino acid release from slices of rat and guinea-pig olfactory cortex, *Brain Research*, 204 (1981) 103–120.

3 Constanti, A., Connor, J.D., Galvan, M. and Nistri, A., Intracellularly recorded effects of glutamate and aspartate on neurones in the guinea-pig olfactory cortex slice, *Brain Research*, 195 (1980) 403–420.

4 Fagni, L., Baudry, M. and Lynch, G., Desensitization to glutamate does not affect transmission in rat hippocampal slices, *Brain Research*, 261 (1983) 167–171.

5 Fagni, L., Baudry, M. and Lynch, G., Classification and properties of acidic amino acid receptors in hippocampus. I. Electrophysiological studies of an apparent desensitization and interactions with drugs which block transmission, *J. Neurosci.*, 3 (1983) 1538–1546.

6 Ffrench-Mullen, J.M.H., Zaczek, R., Koller, K.J., Coyle, J.T., Hori, N. and Carpenter, D.O., N-acetylaspartylglutamate: possible role as the neurotransmitter of the lateral olfactory tract, *Proc. Natl. Acad. Sci. U.S.A.*, 82 (1985) 3897–3900.

7 Foster, A.C., Mena, E.E. and Cotman, C.W., Glutamate and aspartate binding sites are enriched in synaptic junctions isolated from rat brain, *J. Neurosci.*, 1 (1981) 620–625.

8 Hori, N., Auker, C.R., Braitman, D.J. and Carpenter, D.O., Lateral olfactory tract transmitter: glutamate, aspartate or neither?, *Cell Mol. Neurobiol.*, 1 (1981) 115–120.

9 Hori, N., Auker, C.R., Braitman, D.J. and Carpenter, D.O., Pharmacological sensitivity of amino acid responses and synaptic activation of in vitro prepyriform neurons,

J. Neurophysiol., 48 (1982) 1289–1301.

10 Katz, B. and Theleff, S., A study of the desensitization produced by acetylcholine at the motor end-plate, *J. Physiol. (London)*, 138 (1957) 63–80.

11 Takeuchi, A. and Takeuchi, N., The effect on crayfish muscle of iontophorectically applied glutamate, *J. Physiol. (London)*, 170 (1964) 296–317.

12 Usherwood, P.N.R., Glutamate synapses and receptors on insect muscle. In G. DiChiara and G.L. Gessa (Eds.), *Glutamate as a Neurotransmitter. Advances in Biochemical Psychopharmacology, Vol. 27*, Raven, New York, 1981, pp. 183–193.

13 Watkins, J.C. and Evans, R.H., Excitatory amino acid receptors, *Annu. Rev. Pharmacol. Toxicol.*, 21 (1981) 165–204.

14 Werman, R., Criteria for identification of a central nervous system transmitter, *Comp. Biochem. Physiol.*, 18 (1966) 745–766.

ARMED FORCES RADIOBIOLOGY
RESEARCH INSTITUTE
SCIENTIFIC REPORT
SR86-2

Journal of Leukocyte Biology 39:241–254 (1986)

Ionic Channels in Leukocytes

Elaine K. Gallin

Physiology Department, Armed Forces Radiobiology Research Institute, Bethesda, Maryland

In the past several years, with the advent of the patch clamp technique, the field of leukocyte electrophysiology has grown considerably. With the exceptions of the neutrophil and the eosinophil, electrophysiological and biochemical techniques have been used to characterize a number of types of voltage- or ligand-gated ionic channels in the different classes of leukocytes. This article reviews each of the ionic channels described in leukocytes and their functional relevance. It should be emphasized that this is by no means a final listing of the ionic channels in leukocytes, but merely a summary of the studies to date. It is highly likely that there are many other ionic channels in leukocytes with important functional implications that have not yet been discovered.

Key words: leukocytes, ionic channels, lymphocytes, basophils, macrophages

INTRODUCTION

Ionic channels are integral membrane proteins through which ions passively flow down their electrochemical gradient at rates exceeding 10^6 ions/sec. They can be characterized by their gating properties (the factors that control their opening and closing) as well as their conductance (a measure of the ease with which ions flow), kinetics (rates at which the channels open and close), ionic selectivity (differential permeability), and pharmacology (the action of specific agents in blocking or changing the flow of ions). Many different ionic channels have been described, opening and closing in response to specific chemical ligands (ligand-gated), voltage (voltage-gated), and other factors [28].

Ionic channels have been studied most extensively in the nervous system, where they function in information processing and signaling. While ionic channels in general and voltage-gated channels in particular were originally thought to be unique to cells of neuronal origin, it is now evident that similar channels are present in most types of

The views presented in this paper are those of the author; no endorsement by the Defense Nuclear Agency has been given or should be inferred.

Received September 6, 1985; accepted September 20, 1985.

Reprint requests: Elaine K. Gallin, Physiology Department, Armed Forces Radiobiology Research Institute, Bethesda, MD 20814-5145.

© 1986 Alan R. Liss, Inc.

TABLE 1. Ionic Channels in Leukocytes

Channel	Cell type	Reference	Gating[a]	Blockers	Possible physiological role
K^+ Channels					
Outward rectifying K^+	T cells Macrophages B-cells	[2,35] [59,22] [14]	V	D-600, verapamil TEA, 4-AP, Ni, Co, quinidine	In T cells: cytotoxicity mitogenesis volume regulation
Inward rectifying K^+	Macrophages Basophils	[21,22] [29]	V	Ba, Cs, Rb	Setting membrane potential to E_k
Ca-activated K^+	Macrophages	[19,43]	V, Ca	Ba[b]	—
Na^+ channel	T-cells	[2]	V	TTX	—
Ca^{++} channel	B-cells	[12]	V	Mn	Secretion
Cl^- channels	Macrophages	[45]	V	—	—
Fc-receptor cation channel	Macrophages	[58]	L (IgG)	—	Phagocytosis secretion
Cromolyn binding receptor calcium channel	Basophils	[57]	L (IgE)	—	Secretion

[a]Gating refers to whether channel is opened and closed in response to voltage (V), an ion (such as calcium), or a ligand (L).
[b]Unpublished observations (Gallin, E.K.)

cells and that they provide a crucial link between events occurring at the cell surface and a variety of cell functions. For example, voltage-gated ionic channels control the motile response of paramecium [39], whereas in egg cells, ionic channels mediate the block of polyspermy and may also play a role in egg cell activation [27]. Secretion in cells of neuronal origin, as well as in many nonneuronal cell types, is modulated or controlled by ionic channels [44].

It follows from studies on other cell types that ionic channels probably also play an important role in the cell physiology of leukocytes. In the last several years, with the advent of the patch clamp technique developed by Sigworth and Neher [51], it has become feasible to study small cells, such as leukocytes, that had been difficult to study with intracellular microelectrode techniques. For this reason, the area of leukocyte electrophysiology has progressed considerably in recent years, and a number of voltage-gated and ligand-gated ionic channels have been described in these cells. In addition, it has become evident that leukocytes have extremely high input resistances (on the order of 10^9 ohms); that is, their plasma membrane has a low permeability to ions [2,22]. Therefore, the opening of several channels, or even a single channel, on the surface of the leukocyte can produce a significant change in the membrane potential and the conductance of the leukocyte. The purpose of this article is to review the recent advances made in characterizing the ionic channels present in leukocytes and their functional relevance. Table 1 summarizes the ionic channels described in leukocytes. It should be emphasized that because this is a relatively new area of investigation, there are undoubtedly other ionic channels in these cells that have not yet been detected, and many questions pertaining to their role in cell function that remain unanswered.

METHODS

The studies reviewed in this paper have used three types of electrophysiological techniques to monitor either current flow or voltage changes induced by current flow. The earliest studies used high resistance ($>30 \times 10^6$ ohms) intracellular microelectrodes to puncture the cell membrane and to monitor either voltage or current [23]. This technique is difficult to use in small cells, such as leukocytes, where microelectrode penetration can produce a significant leak current, thereby damaging the cells [30]. Nonetheless, these earlier studies demonstrated that leukocytes could exhibit voltage-gated ionic channels similar to those found in neuronal cells [17]. More recent studies have used patch clamp recording techniques in which a low resistance (5×10^6 ohms) electrode is placed against the surface of a cell, and suction is applied to the electrode, resulting in the formation of a very high resistance ($>10^9$ ohms) seal between the plasma membrane and the patch electrode. The high-resistance seal minimizes leak current and reduces the noise level so that small current fluctuations (on the order 10^{-12} A), which represent the opening and closing of single ion channels, can be recorded. In addition, currents across the whole cell membrane can be measured with a patch electrode by simply destroying the membrane beneath the electrode with additional suction, so that the inside of the cell becomes contiguous with the inside of the electrode [44]. This technique has the additional advantage (or disadvantage, depending on the purpose of the study) of perfusing the inside of the cell with the solution inside the patch electrode so that the effects of ions, regulatory proteins, pH, or other factors on ionic channels can be studied. The third technique, used in studies characterizing ionic channels in leukocytes, measures current fluctuations across lipid bilayers containing either membrane fractions or purified membrane proteins from leukocytes [58]. This technique has been particularly useful in studying ligand-gated ion channels. In addition to these techniques, numerous studies have used indirect probes of the membrane potential to monitor membrane potential changes occurring during stimulation in leukocytes [47]. This paper does not attempt to review those studies except in cases where they pertain to the discussion of specific ionic channels.

Terminology

Voltage-gated ionic channels are usually referred to in terms of the ion(s) to which they are permeable. For example, a channel that is much more permeable to potassium (K^+) than other cations is designated a K^+ channel, even though it may have a finite permeability to other cations. Since there may be more than one type of channel in a cell that is permeable to a particular ion, it is often necessary to specify additional properties of the channel in order to uniquely identify it. For example, if a K^+ channel is activated (opened) only when the membrane potential of the cell is -40 mV or less negative (more depolarized) and the equilibrium potential for potassium (E_k) is normally -80, then K^+ will only flow out of the cell through this channel. That is, for K^+ to flow into the cell the membrane potential across the cell would have to be more negative than -80 mV, and the channels would be closed at those potentials. The K^+ current that flows through this channel is referred to as an outward rectifying current, since the current will flow out of the cell more easily than into the cell.

Ligand-gated ionic channels are usually referred to by the specific ligand that opens the channel rather than by the ions that permeate the channel. For example,

even though the acetylcholine channel is permeable to Na^+ and K^+, it is referred to by its ligand.

The conductance of an ionic channel is a measure of the ease with which current flows through the channel. From Ohms' law, it is equal to the current divided by the potential across the channel. It is expressed in siemens, and its value is the inverse of the resistance.

IONIC CHANNELS IN T-LYMPHOCYTES

At present, three different voltage-gated channels have been described in T-lymphocytes: two K^+ channels with different characteristics and a Na^+ channel [2,7,35]. Each of these currents is described below. A slow outward current present at very positive potentials also has been noted in human T-cells, which indicates the presence of at least one other voltage-dependent channel [2]. This outward current has not been studied in detail, but it had little ion selectivity and was not sensitive to K^+ channel blockers. It had been postulated that T-cells have voltage-gated calcium channels, since extracellular calcium is required for T-cell activation, and activation is associated with a rise in intracellular calcium [51]. However, calcium channels have not been detected in T-cells [2].

Potassium Channels

Voltage-gated K^+ currents were first described in human T-lymphocytes by Matteson and Deutsch [35] and DeCoursey et al [5]. These currents activated when the cells were depolarized beyond -50 mV. Increasing the external K^+ changed the currents in a manner indicating that the current was carried by K^+. Therefore, the channels underlying the current are referred to as outward rectifying K^+ channels. This channel is 100 times more permeable to K^+ than Na^+ and has a steep voltage dependency, activating at potentials positive to -50 mV and saturating at -20 mV [2]. In addition, the currents flowing through this channel decrease with time when the cell is stepped to potentials positive to -80. Since the resting membrane potential (estimated by using voltage sensitive dyes) is -50 to -70 mV [9,52], these channels are probably partially inactivated at rest. The channel is blocked by classical K^+ channel blockers such as tetraethylammonium and 4-aminopyridine as well as quinine [5] and the calcium channel antagonists diltiazem and verapamil [4]. The cations nickle, cobalt, zinc, and lanthanum are also effective blockers of the channel [6,35]. Single channel currents with conductances of 9 and 16×10^{-12} siemens exhibiting a similar voltage dependence to the whole cell currents have been described in human T-cells [2].

Similar currents have since been described in mouse-derived T-cells as well as a variety of T-cell lines, although the relative number of the K^+ channels expressed on the surface of the different types of T-cells varies [6,13]. For instance, human T-lymphocytes express several hundred K^+ channels whereas normal mouse T-cells have on the order of 10 K^+ channels per cell [6]. T-cells isolated from MRL mice (a strain of mice that develops a disease similar to human systemic lupus erythematosus) also exhibit a second type of K^+ channel [7]. This channel activates at more positive potentials, inactivates more slowly, is more sensitive to block by TEA, and is less sensitive to block by cobalt than the K^+ channel most prevalent in other T-cells. These channels also have a higher unitary conductance (21×10^{12} siemens) than the first type of K^+ channel [7].

Physiological Significance

Several findings strongly implicate the voltage-gated K^+ ehannels in T-cell activation, although they provide little information about their mechanism of action. First, it has been known for some time that the mitogen phytohemagglutinin (PHA) increases the passive K^+ efflux from T-eells [46]. DeCoursey et al [5] reported that the addition of PHA to human T-lymphoeytes rapidly shifted the eonductance-voltage relationship for the K^+ channel to the left by approximately 10 mV; thus, more channels are open at the resting membrane potential, and K^+ efflux will increase. The measured K^+ efflux during PHA stimulation can be accounted for solely by estimates of the flux through the voltage-gated K^+ channels [2]. However, contradictory findings were reported by Deutseh et al [10]. They found no shift in the conductance-voltage relationship of the K^+ current in human T-lymphoeytes during the first several hours following exposure to either PHA or 12-O-tetradeeanoylphorbol-13 aeetate (TPA), although they described an increase ($\times 1.7$) in the amplitude of the K^+ current 24 hours after addition of the mitogen TPA. The reason for the discrepancy between the results of the two laboratories is unclear.

The second and more consistent (albeit indirect) piece of evidenee supporting the involvement of this K^+ channel in T-cell aetivation is that agents that block the K^+ channel are very effective in blocking PHA-stimulated DNA synthesis, protein synthesis, and interleukin 2 (IL 2) production, although they do not block the expression of IL 2 receptors on the T-eell surface [4]. More recently, these studies have been extended to demonstrate that K^+ channel blockers also inhibit T-eell activation induced by allogenic cells, conconavalin A (Con A), and antibody against the T3 reeeptor [6]. The data obtained with the K^+ channel blockers indicate that the blockers must be added to the T-cells within the first 24 hours of exposure to the mitogen in order to show maximal inhibition [4]. However, these studies provide no information about whether the blockers affect the initial events of activation or some later step during the first 24 hours of exposure to mitogens. Studies assessing the effects of K^+ channel blockers on early events in T-cell activation such as the rise in intracellular calcium (rather than thymidine incorporation or protein synthesis measured 2 days after mitogen addition) would address this point.

If K^+ channels are required for all types of T-cell activation, then T-cell lines that do not have K^+ channels should not be sensitive to mitogenic stimulation. Two T-cell lines, CTLL-2 (mouse) and P12 Ichikawa (human), lack K^+ channels [6]. However, CTLL-2 cells respond mitogenically to T-cell growth factor (IL 2) [24], indicating that K^+ channels are not required for mitogenic responsiveness to all stimuli.

The mechanism by which K^+ channels function in the mitogenic response is not known. Several possibilities have been discussed. Cahalan et al [2] proposed that the rise in intracellular calcium that occurs following mitogen stimulation is due to calcium entry through voltage-gated K^+ channels, whieh open during stimulation. Although the calcium permeability of these channels in the T-cell has not been measured, there is precedent for a significant calcium flux through K^+ channels from work done in the squid axon [31]. If calcium enters through K^+ channels, then K^+ channel blockers should block the rise in intracellular calcium concentration that occurs within minutes of adding Con A or PHA [52]. Unfortunately, these experiments have not been reported at this time. In addition, as mentioned above, resting mouse T-lymphocytes express many fewer K^+ channels than resting human lympho-

cytes (10 versus >200). Since both resting mouse T-cells and human T-cells are responsive to a variety of mitogens, there appears to be no correlation between the responsiveness to mitogens and the number of K^+ channels. Although Cahalan et al [2] calculated that sufficient calcium (to trigger mitogenesis) can flow through the K^+ channels in human lymphocytes (assuming a calcium permeability similar to that in the squid axon), it is not clear whether this is a viable possibility in mouse T-cells containing only 10 channels. By day 1 after exposure to a mitogen, the number of K^+ channels in mouse T-cells increases significantly [8], indicating that these channels may be involved in a later step in mitogenesis.

An alternative suggestion is that the K^+ channels are important in T-cell activation because of their role in volume regulation [10]. Lymphocytes exposed to hypotonic medium initially swell and then shrink, exhibiting a regulatory volume decrease (RVD) [25]. This response is blocked by quinine, 4-aminopyridine, and tetraethylammonium (TEA), which are blockers of the K^+ channel [10]. Interestingly, T-lymphocytes exhibit a more complete RVD response than B-lymphocytes, and K^+ channels are much more prevalent in T-lymphocytes than in B-lymphocytes.

In addition to the role of K^+ channels in T-cell activation, there is evidence that these channels may play a role in cytotoxicity. Cytotoxic T-cells exhibit K^+ channels and target cell lysis is blocked by K^+ channel blockers [3]. Fukushima and Hagiwara [13] reported that, in mouse cytotoxic T-lymphocyte clones, the K^+ current increased in magnitude under conditions (high calcium) in which killing occurred.

Sodium Channels

Small inward currents that have the kinetics and voltage dependence of Na^+ currents found in nerve and muscle cells have been described in 3% of human T-cells, 14% of activated mouse T-cells, and a few human T-cell lines [6]. Although tetrodotoxin (TTX), a very specific Na^+ channel blocker, is effective (in nanomolar concentrations) in blocking the Na current in T-cells, TTX (at similar concentrations) has no effect on mitogenesis, indicating that this conductance is not required for mitogenesis [2].

IONIC CHANNELS IN B-LYMPHOCYTES

B-lymphocytes, unlike T-cells, exhibit a prominent voltage-gated calcium channel, which has been well characterized and is described in detail below [12]. Sodium currents have not been reported in these cells, but an outward K^+ current, similar to the K^+ currents described in T-cells, was noted in 10% of the B-cell lines examined by Fukushima et al [14]. Since this outward current has not been characterized yet, it will not be discussed further here.

Calcium Channels

Fukushima and Hagiwara [12] have described inward currents in the mouse mycloma cell line S194/5.XXO that were dependent on the presence of extracellular calcium, unaffected by sodium removal, and blocked by manganese. Strontium and barium could substitute for calcium in carrying the current through these channels. These results indicated that S194 cells exhibit calcium currents similar to those found in excitable cells. Calcium currents also have been described in mouse hybridoma cell lines (derived from S194 cells and splenic B-cells) as well as splenic B-cells

[14,15]. In cardiac cells and other cell types, the calcium current has been separated into different currents (channels) by virtue of the kinetic and gating properties [26]. However, at this time no evidence exists for more than one type of calcium channel in B-cells. Recently Fukushima and Hagiwara [15] have taken advantage of the fact that B-cells appear to have only one type of calcium channel and that they usually exhibit no other voltage-gated conductances (which might interfere with analysis) to demonstrate that monovalent cations can permeate through calcium channels [15].

Physiological Significance

The opening of voltage-dependent calcium channels serves to increase the intracellular calcium concentration, thereby triggering secretion in nerve cells and other cell types [28]. Since B-cells function primarily as secretory cells, it is logical to hypothesize that the calcium channels present in these cells function in the secretory response. Fukushima and Hagiwara [14] have shown that the addition of new medium to mouse hybridoma cell lines increases their immunoglobulin production. Along with the increased secretion of immunoglobulin, there was a parallel increase in the magnitude of the inward calcium current, supporting the view that the calcium channel is associated with immunoglobulin secretion [14]. However, Fukushima and Hagiwara's studies with the calcium channel blocker D-600 indicated that the relationship between secretion and the calcium channels in these cells is unclear [14]. The calcium currents in these cells were surprisingly insensitive to D-600 (compared to other calcium channels), being only 37% blocked by 100 μM D-600. On the other hand, immunoglobulin secretion was completely blocked by 100 μM D-600. The observation that calcium channels in B-cells are relatively insensitive to calcium channel blockers, together with the results by Chandy et al [3] showing that K^+ channels in T-cells are quite sensitive to calcium channel blockers, indicates that the inhibition of a cell function by calcium channel blockers cannot be used as strong evidence that voltage-gated calcium channels are involved in a response, unless a direct block (in a similar concentration range) of those channels is demonstrated.

IONIC CHANNELS IN MACROPHAGES

Macrophages exhibit at least three different voltage-gated K^+ channels: 1) an inward rectifying K^+ channel that activates at potentials negative to -60 mV [16,21]; 2) an outward rectifying K^+ channel that activates at potentials positive to -40 mV [21,57]; and 3) a calcium- and voltage-activated K^+ channel [19]. A large conductance voltage-gated chloride channel has also been reported in macrophages [48], as well as slow spike-like potentials activating at potentials positive to zero [38]. The ionic basis of the spikes has not been determined, but their occurrence indicates the presence of another current that turns on at very depolarized potentials. In addition to exhibiting a number of voltage-gated channels, it has recently been demonstrated that the receptor for the γ2b/γ1 Fc portion of IgG is a ligand-dependent ion channel permeable to K^+ and Na^+ [58].

Potassium Channels

Inward rectifying K^+ channel. An inward rectifying K^+ current that activates at voltages negative to -60 mV was first described in mouse spleen and thioglycolate-induced macrophages that had been cultured for several weeks [16,21]. It has been

observed more recently in cultured human macrophages (Gallin,E.K., unpublished observations) and in the mouse-derived macrophage-like cell line J774 [22]. This conductance is very similar to the inward rectifying K^+ conductance that has been extensively characterized in both muscle and egg cells [27,28]. It has a steep voltage dependence, activating at potentials negative to −50 mV and plateauing at potentials negative to −100 mV [22]. Addition of the cations barium, cesium, and rubidium to the bathing medium blocks this channel [21,22]. In macrophages as in other cells, this channel is unique in that its gating depends not only on voltage but also on the extracellular K^+ concentration [22,28]. Thus when the external K^+ concentration is increased, these channels open at more depolarized potentials. The macrophage is often found at sites of dead and dying tissue where K^+ concentrations are higher than normal (Gallin,J.I., unpublished observations), and the gating of this K^+ channel will be influenced by these changes.

The expression of the inward rectifier in J774.1 cells is affected by culture conditions. That is, cells grown in suspension and then plated do not exhibit this conductance unless they have been adherent for several hours [22]. All long-term adherent (plated for >24 hours) J774 cells exhibit inward rectifying K^+ channels. Ypey and Clapham [59] reported that the inward rectifying K^+ conductance was absent in mouse peritoneal macrophages maintained in culture for 4 days, whereas 2–4-week-old cultured mouse peritoneal macrophages exhibit a prominent inward rectifying K^+ conductance [16]. These findings indicate that the inward rectifying K^+ channel is probably associated with older, more mature macrophages comparable to the tissue macrophage.

Physiological significance. In both J774 cells and mouse spleen and peritoneal macrophages, blockage of these K^+ channels by barium depolarizes the cells from −76 mV to approximately −50 mV. These observations indicate that these channels are responsible for setting the resting membrane potential of the macrophage near the equilibrium potential for K^+, normally about −80 mV. Interestingly, the resting membrane potential of suspended J774.1 cells was estimated employing the lipophilic cation tetraphosphonium to be −14 mV [56]. This data fits with the observation of Gallin and Sheehy [22] that the inward rectifying K^+ channel is expressed in J774 cells only after several hours of adherence. Cells exhibiting this conductance have a high K^+ permeability at rest, but because of the voltage dependence of the inward K^+ channel (it closes as the macrophage is depolarized and thereby increases the membrane resistance), small inward currents can produce large potential changes in these cells. Therefore, depolarizing stimuli will be amplified in cells with inward rectifying K^+ channels.

Outward rectifying K^+ channel. The outward rectifying K^+ current was first described in resident mouse peritoneal macrophages by Ypey and Clapham [59]. This current is very similar to that described in T-cells, activating at potentials positive to −50 mV, inactivating with time, and being blocked by 4-aminopyridine. Ypey and Clapham [59] reported that this channel was absent during the first day following isolation of the resident peritoneal macrophages, but was present in 96% of the cells cultured for 1 to 4 days. On the other hand, this channel was not seen in long-term (2–6 weeks) cultured mouse peritoneal and spleen macrophages [16,21]. The mouse-derived cell lines J774 [22] and P388D1 (Gallin, unpublished observations) also express a similar K^+ channel. In J744 cells, the channel is present only 1 to 8 hours after adherence, and is not present in long-term adherent cultures where the inward rectifying potassium channel is the predominant channel [22].

Physiological significance. The finding that in J774 cells this conductance is absent immediately after adherence but is expressed soon after (within 30 minutes) indicates that these channels may 1) normally be present on the surface of the cells, but that their expression is modulated by intracellular factors such as protein phosphorylation, or 2) that there is a preexisting pool of channels that can be inserted into the membrane. Future studies need to be done to determine the factors controlling channel expression and the physiological implication of its expression in terms of macrophage function.

Calcium- and Voltage-Activated K^+ Channel. A calcium-activated K^+ current has been attributed to macrophages as early as 1975, when spontaneous membrane hyperpolarizations involving increases in potassium permeability were described [23]. The hyperpolarizations could be triggered by the calcium ionophore A23187, and they were blocked by the addition of EGTA to the bath. More direct support for the existence of a calcium-activated K^+ channel in macrophages came when Persechini et al [43] demonstrated that injection of calcium into mouse macrophages triggered hyperpolarizations. With the aid of patch clamp recording techniques, large conductance (200 psiemens in symmetrical K^+) calcium-activated K^+ channels have been described in human macrophages [19]. The channels are activated both by voltage and intracellular calcium. As the membrane potential becomes more depolarized and/or the calcium concentration increases (in the concentration range of 10^{-7} to 10^{-4}), the probability of these channels opening increases. These channels are very similar to the large conductance calcium- and voltage-gated channels described in muscle and other cells [1].

Physiological significance. Single channel data indicate that the intracellular free calcium must go above 10^{-6} M for the channels to be activated at physiological potentials. There is evidence, employing the calcium indicator Quin 2, that intracellular calcium levels increase to micromolar levels during phagocytosis [54]. If the calcium-activated K^+ channels in situ have the same calcium sensitivity that they have in isolated membrane patches, then an increase in calcium to micromolar levels may be sufficient to open a few channels (although most would remain closed) if the cell is depolarized by 20 mV. However, the physiological relevance of activating the calcium-activated K^+ channel in the macrophage is unknown. This channel, by increasing the membrane permeability to potassium may serve in volume regulation or to modulate the intracellular K^+ concentration. There is evidence, in other cell types, that changes in intracellular K^+ can influence synthetic processes [34,49] as well as receptor-mediated endocytosis [33]. In addition, in macrophages the contractile machinery also may be influenced by changes in K^+, since these cells contain an actin modulating protein, acumentin, whose activity is modified by changes in potassium concentration in the physiological range (100–200 mM) [50].

Recent studies have demonstrated that freshly isolated human monocytes do not exhibit calcium-activated K^+ channels but that they are expressed by the cells after 2 to 4 days in culture [18]. After 7 days in culture, 90% of patches from the cells contained three or more channels. During this time, the monocytes are maturing into macrophages. This maturation process produces a variety of morphological and functional changes in these cells, including increases in protein content and decreases in H_2O_2 production [40]. Gallin and Gallin [20] demonstrated that chemotactic factors induced membrane hyperpolarizations in long-term cultured human macrophages. It is likely that these hyperpolarizations involved the activation of calcium-activated K^+

channels. However, the fact that freshly isolated human peripheral blood monocytes (which lack these calcium- and voltage-activated K^+ channels) are phagocytic and chemotactic implies that these channels are not essential for those events.

Chloride Channel

Schwarze and Kolb [48] have described a chloride channel in mouse peritoneal macrophages, that has a very large conductance (340 psiemens) which is five times more selective for chloride than Na^+. This channel is activated by both depolarizing and hyperpolarizing voltage jumps and exhibits voltage-dependent inactivation. Schwarze and Kolb [48] also reported that addition of the calcium ionophore A23187 to the bath during cell-attached patch recordings increased the probability of recording these channels, thus implicating calcium in these events. However, the channels exhibited no calcium sensitivity when recorded in excised patches of membrane. Schwarze and Kolb [48] fit the complex kinetics of this channel to a model, describing a single channel controlled by two independent voltage-sensitive gates. Similar models have been used to describe the behavior of voltage-dependent gap junctions, and it was suggested that the chloride channel plays a role in intercellular communication [48]. If these channels play a role in intercellular communication, they might be important in macrophage-macrophage or macrophage-lymphocyte interactions. There is a preliminary report (that uses intracellular microelectrodes) demonstrating that macrophages grown in tissue culture can be electrically coupled to each other [42].

Fc Receptor Channel

Ligand binding to the macrophage receptor for the Fc portion of immunoglobulin and its subsequent cross-linking mediates the ingestion of particles and the secretion of a number of mediators [53]. Experiments in the macrophage-like cell line J774, indirectly monitoring membrane potential with tetraphenylphosphonium ions, demonstrated that a transient membrane depolarization occurs following the addition of ligands that bind to the Fc receptor [56]. In subsequent studies, these investigators inserted isolated IgG γ2b/γ1 Fc receptors (FcR) into lipid vesicles. They demonstrated a membrane depolarization after exposure to IgG, which involved an increase in permeability to Na^+ and K^+ ions. These findings indicated that the ligand-FcR complex may form an ion channel that is permeable to cations [57]. Subsequently, this was demonstrated directly by incorporating FcR into lipid bilayers and recording the discrete current fluctuations produced across the bilayer after the addition of immunoglobulin to the cis side (the side that the FcR was added to) [58]. The ligand-FcR channel inactivated, remaining open transiently following the addition of ligand, and it was permeable to both K^+ and Na^+ but had a low calcium permeability. Young [54] has recently shown that the calcium concentration on the trans side of the membrane (the side opposite to the binding site for IgG) modulates channel activity. That is, the conductance across the bilayer decreased, and the channel gating properties changed when the calcium concentration on the trans side was increased from 0.1 μM to 1 μM. Previous studies that used Quin 2 studies had shown that the concentration of intracellular calcium in J774 cells increases to micromolar levels following ligand-FcR binding [55]. Therefore, changes in intracellular calcium that occur during phagocytosis can modulate channel activity.

The studies directly measuring conductance changes following ligand binding in artificial bilayers have recently been extended to intact cells by Nelson et al [41].

They demonstrated that large-conductance channels were formed in intact membranes from human alveolar macrophages after the addition of aggregated IgG to the bath. Whole cell recordings from macrophages exposed to aggregated IgG resulted in large inward currents. The role of the ion fluxes through the ligand-FcR channel in mediating phagocytosis and secretion is unknown. However, it is likely that these fluxes are important in triggering the physiological events that occur following ligand binding and cross-linking.

BASOPHILS

The rat basophilic leukemia cell line RBL 2H3, which has been extensively used as a model cell for studies of secretion, exhibits an inward rectifying K^+ conductance [30] as well as a ligand-dependent ionic channel involved in the secretory response [36]. The degranulation of RBL-2H3 cells is associated with an influx of calcium and a membrane depolarization [11,32]. These events might be due to the opening of a voltage-gated calcium channel. However, no inward currents were noted during depolarizing voltage steps in RBL-2H3 cells (Ikeda, personal communication).

Potassium Channel

The inward rectifying K^+ conductance in RBL 2H3 cells is similar to that described in macrophages [30]. It is increased by raising the external K^+, activated at potentials negative to -60 mV, and blocked by barium or cesium. As with the macrophage, this conductance will set membrane potential at E_k (usually about -80 mV), but because of the steep voltage dependence, the conductance will turn off when the cells are depolarized. In this way, the cells will have a high permeability to K^+ at rest and a low K^+ permeability (high resistance) during depolarization. However, as with the macrophage, the functional relevance of these channels, other than maintaining the resting potential near E_k while still keeping the cell sensitive to depolarizing stimuli, is not known.

Cromolyn-Binding Protein Receptor Channel

Recent studies by Mazurek et al [37] indicate that the calcium influx that occurs during degranulation results from the opening of a ligand-dependent channel formed by the aggregation of the cromolyn-binding protein (CBP) rather than a voltage-gated channel. The antihistamine cromolyn binds to a specific membrane protein, and blocks mediator-induced calcium influx and secretion in RBL-2H3 cells [37]. The membrane protein that cromolyn binds to has been isolated and purified [36]. This protein has been implicated in the secretory response, because cells lacking this protein do not degranulate in response to immunological stimuli. Furthermore, the insertion of CBP into these cells restores their secretory response [36]. In more recent studies, lipid bilayers were formed that contained either CPB or plasma membrane isolated from RBL-2H3 cells. The addition of monoclonal antibody against CBP to these bilayers results in the formation of ion channels that are permeable to calcium (and to K^+ and Na^+ when calcium is absent). Channel formation required aggregation of CBP. These data provide strong evidence that binding to and crosslinking of the CBP result in the formation of an ion channel responsible for the calcium influx and subsequent degranulation in RBL-2H3 cells.

In related studies on intact RBL 2H3 cells, Kanner and Metzger [32] demonstrated that the aggregation of the receptor for IgE in the presence of millimolar

external calcium resulted in a calcium influx, whereas in the absence of calcium, receptor aggregation increased sodium influx. In addition, they found that depolarization of the membrane by high potassium in the presence of calcium did not induce degranulation, and in the presence of IgE, high K^+ diminished degranulation [32]. These findings agree with those of Mazurek et al [37] and indicate that the secretory response in RBL cells is mediated by a voltage-independent ion channel permeable to calcium that forms following ligand receptor binding and aggregation.

ACKNOWLEDGMENTS

The author thanks Drs. John Gallin, Leslie McKinney, Paul Sheehy, and Arie Moran for their helpful comments on the manuscript. This work was supported by Armed Forces Radiobiology Research Institute, Defense Nuclear Agency, under Research Work Unit MJ00020.

REFERENCES

1. Barrett, J.N., Magleby, K.L., and Pallota, B.S. Properties of single calcium-activated potassium channels in cultured rat muscle. J. Physiol. (Lond.) 331,211,1982.
2. Cahalan, M.D., Chandry, K.G., DeCoursey, T.E., and Gupta, S. A voltage-gated potassium channel in human T lymphocytes. J. Physiol. (Lond.) 358,197,1985.
3. Chandy, K.G., DeCoursey, T.E., Sharma, B., Cahalan, M., and Gupta, S. "Voltage gated K^+ channels are required for target cell lysis by human alloreactive cytotoxic T-cells. J. Exp. Med. (in press).
4. Chandy, K.G., DeCoursey, T.E., Cahalan, M.D., McLaughlin, C., and Gupta, S. Voltage gated potassium channels are required for human T-lymphocyte activation. J. Exp. Med. 160,369,1984.
5. DeCoursey, T.E., Chandry, K.G., Gupta, S., and Cahalan, M.D. Voltage-gated K^+ channels in human T lymphocytes: A role in mitogenesis? Nature 307,465,1984.
6. DeCoursey, T.E., Chandry, K.G., Gupta, S., and Cahalan, M.D. Voltage dependent ion channels in T lymphocytes. J. Neuroimmunol. (in press).
7. DeCoursey, T.E., Chandy, S., Gupta, S., and Cahalan, M.D. Two types of K^+ channels in murine T lymphocytes. J. Gen. Physiol. (in press).
8. DeCoursey, T.E., Chandy, S., Gupta, S., Fischbach, M., Talal, N., and Cahalan, M.D. Ion channel expression in resting and proliferating murine T lymphocytes. J. Gen. Physiol. (in press).
9. Deutsch, C., Holian, A., Holian, S.K., Danielle, R.P., and Wilson, D.F. Transmembrane electrical and pH gradients across human erythrocytes and human peripheral lymphocytes. J. Cell. Physiol. 99,79,1979.
10. Deutsch, C., Krause, D., and Lee, S. Voltage-gated K^+ conductance in T-lymphocytes stimulated with phorbol esters or plant lectin. J. Physiol. (Lond.) (in press).
11. Eisenberg, R., and Pecht, I. Membrane potential changes during IgE mediated histamine release in rat basophilic leukemia cells. J. Membr. Biol. 75,97,1983.
12. Fukushima, Y., and Hagiwara, S. Voltage gated calcium channel in mouse myeloma cells. Proc. Natl. Acad. Sci. USA 80, 2240,1983.
13. Fukushima, Y., Hagiwara, S., and Henkart, M. Potassium current in clonal cytotoxic T lymphocytes from the mouse. J. Physiol. (Lond.) 351,645,1984.
14. Fukushima, Y., Hagiwara, S., and Saxton, R.E. Variation of calcium current during the cell growth cycle in mouse hybridoma lines secreting immunoglobulins. J. Physiol. (Lond.) 355,313,1984.
15. Fukushima, Y., and Hagiwara, S. Currents carried by monovalent cations through calcium channels in mouse neoplastic B lymphocytes. J. Physiol. (Lond.) 358,255,1985.
16. Gallin, E.K. Voltage clamp studies in cultured mouse spleen cells. Science 214,458,1981.
17. Gallin, E.K. Electrophysiological properties of macrophages. Fed. Proc. 43,2385,1984.
18. Gallin, E.K. Expression of calcium-activated potassium channels in human monocytes with time after culture. Biophys. J. 47,135a,1985.
19. Gallin, E.K. Calcium and voltage activated potassium channels in human macrophages. Biophys. J. 46,821,1984.
20. Gallin, E.K., and Gallin, J.I. Interaction of

chemotactic factors with human macrophages: Induction of transmembrane potential changes. J. Cell. Biol. 75:277,1977.

21. Gallin, E.K., and Livengood, D.R. Inward rectification in mouse macrophages: Evidence for a negative resistance region. Am. J. Physiol. 214,C9,1981.
22. Gallin, E.K., and Sheehy, P.A. Differential expression of inward and outward potassium currents in the macrophage-like cell line J774. J. Physiol. (Lond.) 369,475,1985.
23. Gallin, E.K., Wiederhold, M., Lipsky, P., and Rosenthal, A. Spontaneous and induced membrane hyperpolarizations in macrophages. J. Cell. Physiol. 86,653,1975.
24. Gillis, S., Ferm, M., Ou, W., and Smith, K.T. Cell growth factor: Parameters of production and a quantitative microassay for activity. J. Immunol. 120,2027,1978.
25. Grinstein, S., Rothstein, A., Sarkadi, B., and Gelfand, E.W. Responses of lymphocytes to anisotonic media: Volume regulating behavior. Am. J. Physiol. 246,C204,1984.
26. Hagiwara, S., and Byerly, L. The calcium channel. Trends Neurosci. 6,189,1983.
27. Hagiwara, S., and Jaffe, L. Electrical properties of egg cell membranes. Ann. Rev. Biophys. Bioeng. 8,385,1979.
28. Hille, B. Ionic Channels in Excitable Membranes. Sunderland, MA: Sinauer Assoc., 1984.
29. Ikeda, S., and Weight, F. Inward rectifying K^+ currents recorded from rat basophilic leukemia cells by whole cell patch clam. Neurosci. Abstr. 10,870,1984.
30. Ince, C., Ypey, D., Van Furth, R., and Verveen, A. Estimation of the membrane potential of cultured macrophages from the fast potential transient upon microelectrode entry. J. Cell. Biol. 96,796,1983.
31. Inoue, I. Activation and inactivation of potassium channels and development of the potassium channel spike in internally perfused squid giant axons. J. Gen. Physiol. 78,43,1981.
32. Kanner, B., and Metzger, H. Initial characterization of the calcium channel activated by the cross-linking of the receptors for immunoglobulin E. J. Biol. Chem. 259,10188,1984.
33. Larkin, J., Brown, M., Goldstein, J., and Anderson, R. Depletion of intracellular potassium arrests coated pit formation and receptor-mediated endocytosis in fibroblasts. Cell 33,273,1983.
34. Lopez-Rivas, A., Adelberg, E., and Rozengurt, E. Intracellular K^+ and the mitogenic response of 3T3 cells to peptide factors in serum-free medium. Proc. Natl. Acad. Sci. USA 79,6275,1982.
35. Matteson, D.R., and Deutsch, C. K channels in T lymphocytes: A patch clamp study using monoclonal antibody adhesion. Nature 307,468,1984.
36. Mazurek, N., Bashkin, P., Loyter, A., and Pecht, I. Restoration of calcium influx and degranulation capacity of variant RBL-2H3 cells upon implantation of isolated cromolyn binding protein. Proc. Natl. Acad. Sci. USA 80,6014,1983.
37. Mazurek, N., Schindler, H., Schurhols, T.H., and Pecht, I. The cromolyn binding protein constitutes the Ca channel of basophils opening upon immunological stimulus. Proc. Natl. Acad. Sci. USA 81,6841,1984.
38. McCann, F., Cole, J., Guyre, P., and Russell, J. Action potentials in human macrophages derived from human monocytes. Science 219,991,1983.
39. Naitoh, Y., and Eckert, R. The control of ciliary activity in Protozoa. In Cilia and Flagella. (Sleigh, ed.) London: Acacemic Press p.305, 1972.
40. Nakagawara, A., Nathan, C., and Cohn, Z. Hydrogen peroxide metabolism in human monocytes during differentiation in vitro. J. Clin. Invest. 68,1243,1981.
41. Nelson, D., Jacobs, E.R., Tang, J.M., Zeller, J.M., and Bone, R.C. Immunoglobulin G-induces single ionic channels in human alveolar macrophage membranes. J. Clin. Invest. 76,500,1985.
42. Ori, M., Shiba, Y., and Kanno, Y. Facillitation of cell coupling formation between mouse macrophages with an increase in the external calcium concentration. Cell Struct. Function 5,259,1980.
43. Persechini, P., Araujo, E., and Oliviero-Castro, G. Electrophysiology of phagocytic membranes: Induction of slow membrane hyper polarizations on macrophages and macrophage polykaryond by intracellular calcium injection. J. Membrane Biol. 61,81,1981.
44. Peterson, O.H. Electrophysiology of mammalian gland cells. Physiol. Rev. 56,535,1976.
45. Sakmann, B., and Neher, E. Single Channel Recording. New York: Plenum Press, 1983.
46. Segal, G.B., Simon, W., and Lichtman, M.A. Regulation of sodium and potassium transport in phytohemagglutinin-stimulated human blood lymphocytes. J. Clin. Invest. 64,834, 1979.
47. Seligmann, B.E., and Gallin, J.I. Comparison of indirect probes of membrane potential utilized in studies of human neutrophils. J. Cell. Physiol. 115,105,1983.
48. Schwarze, W., and Kolb, H.A. Voltage dependent kinetics of an ion channel of large

conductance in macrophages and myotube membranes. Pfluegers Arch. 402:281,1984.
49. Shinohara, T., and Piatigorsky, J. Regulation of protein synthesis, intracellular electrolytes and cataract formation in vitro. Nature 270,406,1977.
50. Southwick, F., Tatsumi, N., and Stosdsel, T. Acumentin, an actin-modulating protein of rabbit pulmonary macrophages. Biochemistry 21,6321,1982.
51. Sigworth, F.J., and Nehr, E. Single Na^+ channel currents observed in cultured rat muscle cells. Nature 287,447,1980.
52. Tsien, R.Y., Pozzan, T., and Rink, T.J. T-cell mitogens cause early changes in cytoplasmic free Ca^{++} and membrane potential in lymphocytes. Nature 285,68,1982.
53. Unkeless, J.C., Fleit, H., and Mellman, I.S. Structural aspects and heterogeneity of immunoglobulin Fc receptors. Adv. Immunol. 31,247,1981.
54. Young, J.D. Properties of the mouse Fc receptor reconstitutes into model lipid membranes: The effect of calcium on the ligand activated conductance. Biophys. J. (in press).
55. Young, J.D., Ko, S., and Cohn, Z. The increase in intracellular free calcium associated with IgG γ2b/γ1Fc receptor-ligand interactions: Role in phagocytosis. Proc. Natl. Acad. Sci. USA 81,5430,1984.
56. Young, J.D., Unkeless, J., Kaback, H., and Cohn, Z. Macrophage membrane potential changes associated with γ2b/γ1 Fc receptor-ligand binding. Proc. Natl. Acad. Sci. USA 1357,1982.
57. Young, G.D., Unkeless, J.C., Kaback, H.R., and Cohn, Z. Mouse macrophage Fc receptor for IgG γ2b/γ1 in artificial and plasma membrane vesicles functions as a ligand-dependent ionophore. Proc. Natl. Acad. Sci. USA 80,1636,1983.
58. Young, J.D., Unkeless, J.C., Young, T.M., Mauro, A., and Cohn, Z.A. Role for mouse macrophage IgG Fc receptor as ligand-dependent ion channel. Nature 306,186,1983.
59. Ypey, D.L., and Clapman, D.E. Development of a delayed outward-rectifying potassium conductance in cultured mouse peritoneal macrophages. Proc. Natl. Acad. Sci. USA 81,3083,1984.

ARMED FORCES RADIOBIOLOGY
RESEARCH INSTITUTE
SCIENTIFIC REPORT
SR86-3

J. Physiol. (1985), **369**, *pp.* 475–499
With 13 *text-figures*
Printed in Great Britain

DIFFERENTIAL EXPRESSION OF INWARD AND OUTWARD POTASSIUM CURRENTS IN THE MACROPHAGE-LIKE CELL LINE J774.1

BY ELAINE K. GALLIN* AND PAUL A. SHEEHY†

From the Armed Forces Radiobiology Research Institute, Bethesda, MD 20814-5145, U.S.A. and Departments of Physiology, Uniformed Services University of the Health Sciences

(*Received 27 February 1985*)

SUMMARY

1. J774.1 cells, a mouse-derived macrophage-like tumour cell line, were voltage clamped using whole-cell patch-clamp techniques. Cells were maintained in suspension cultures and plated at varying times before recording.

2. The average zero-current potential of long-term adherent (> 24 h) cells was −77·6 mV. A tenfold increase in $[K]_o$ produced a 49 mV shift in zero-current potential.

3. Freshly plated cells (< 24 h) expressed two voltage-dependent currents: an outward current expressed transiently from 1 to 12 h post-plating and an inward current expressed 2–4 h post-plating which persisted in 100 % of long-term adherent cells.

4. Inward current was dependent upon voltage, time and $[K]_o^{1/2}$, similar to the anomalous rectifier of other tissues. The conductance activated at potentials negative to −50 mV and plateaued at potentials negative to −110 mV. Inactivation was evident at potentials negative to −100 mV. Both the rate and extent of inactivation increased with hyperpolarization. Inward rectification was blocked by external $BaCl_2$ or CsCl.

5. The outward current was time- and voltage-dependent. The instantaneous I/V curves derived from tail experiments reversed at the potassium equilibrium potential (E_K). A tenfold change of $[K]_o$ shifted the reversal potential 52 mV, indicating that the current was carried by potassium. This conductance activated at potentials positive to −50 mV, plateaued at potentials positive to −10 mV and inactivated completely with an exponential time course at all potentials. At voltages positive to −25 mV the rate of inactivation was independent of voltage. The outward current was blocked by 4-aminopyridine or D600.

6. During the first 10 min after attaining a whole-cell recording, the conductance/voltage relation of the outward current shifted to more negative voltages and peak conductance showed a slight increase; recordings then stabilized. The voltage

* To whom correspondence should be addressed.
† Present address: Laboratory of Neurophysiology, NINCDS, Bethesda, MD 20205, U.S.A.

dependence of the inward current did not shift with time but wash-out of inward current was observed in some cells.

7. The J774.1 cell line can serve as a model for the study of the role of voltage-dependent ionic conductances in macrophages.

INTRODUCTION

Leukocytes exhibit a number of voltage-dependent ionic conductances which may be related to such cellular processes as secretion, chemotaxis, and mitogenesis (Gallin & Gallin, 1975; Fukushima, Hagiwara & Saxton, 1984; DeCoursey, Chandy, Gupta & Cahalan, 1984). Three different voltage-dependent potassium currents have been described in macrophages. Long-term cultured mouse macrophages exhibit an inward rectifying potassium current activating at potentials negative to −70 mV (Gallin, 1981). An outward potassium current activating at potentials positive to −40 mV has been described in shorter-term cultures (Ypey & Clapham, 1984). In addition, a calcium-activated potassium current has been described in cultured macrophages from a variety of sources (Gallin, Weiderhold, Lipsky & Rosenthal, 1975; Olivera-Castro & Dos Reis, 1981). Recent single-channel studies have demonstrated large conductance calcium- and voltage-activated potassium channels in cultured human macrophages (Gallin, 1984) and large conductance chloride-selective channels in mouse macrophages (Schwarze & Kolb, 1984).

In this study we used whole-cell patch-clamp techniques (Hamill, Marty, Neher, Sakmann & Sigworth, 1981) to characterize both inward and outward voltage-dependent potassium conductances in J774.1 cells. These cells, derived from a mouse reticulum sarcoma (Ralph & Nakoinz, 1975), have been extensively studied because they provide homogeneous populations that express many properties characteristic of macrophages, including receptor-mediated endocytosis, secretion of enzymes and immunomodulatory factors, and chemotaxis (Snyderman, Pike, Fischer & Koren, 1977). In addition, the existence of variant clones defective in specific functions may make them particularly useful in relating ionic conductances to macrophage function (Unkeless, Kaplan, Plutner & Cohn, 1979; Bloom, Diamond, Muschel, Rosen, Schneck, Damiani, Rosen & Scharff, 1978; Damiani, Kiyotaki, Soeller, Sasada, Peisach & Bloom, 1980).

Macrophages express a variety of activities depending on their activation state or, *in vitro*, upon culture conditions. For example, adherent culture conditions (in contrast to suspension culture) decrease the phorbol-ester-induced release of superoxide anion (Berton & Gordon, 1983) and alter the membrane transport of certain nutrients (Pofit & Strauss, 1977). Indirect estimates of membrane potential using tetraphenylphosphonium (TPP^+) indicated that J774.1 cells in suspension had a resting membrane potential of −14 mV (Young, Unkeless, Kaback & Cohn, 1983) whereas both intracellular and patch micro-electrode studies of adherent J774.1 cells have reported values considerably more negative (Sheehy & Gallin, 1984). These and other observations suggest that the biophysical properties of the macrophage plasma membrane may depend on whether the cell is in suspension or is adherent. In this work we demonstrate the differential expression of two voltage-dependent potassium currents in J774.1 cells upon transition from suspension to an adherent form. During

the first hours after plating, an outward potassium current is evident which closely resembles that described in other leukocytes (Cahalan, Chandy, DeCoursey & Gupta, 1985; Matteson & Deutsch, 1984; Ypey & Clapham, 1984). This current disappears and is followed by an inward potassium current which is similar to the inward rectifier described in long-term cultures of primary macrophages as well as in egg and muscle cells (Gallin, 1981; Hagiwara & Takahashi, 1974; Leech & Stanfield, 1981).

METHODS

Cell culture

J774.1 cells obtained from the American Type Culture Collection (Rockville, MD, U.S.A.) were maintained in tissue culture medium containing RPMI 1640 (Flow Labs, McLean, VA, U.S.A.) supplemented with penicillin 10 u./ml, streptomycin 10 μg/ml (Difco Labs, Detroit, MI, U.S.A.), 0·03 % glutamine (w/v) (Sigma, St. Louis, MO, U.S.A.), and 10 % fetal bovine serum (v/v) (Hyclone, Logan, UT, U.S.A.). Stock cultures were maintained as a non-adherent population in spinner flasks treated with Sigmacote (Sigma, St. Louis, MO, U.S.A.). For experiments, cells were withdrawn and plated in 35 mm tissue culture Petri dishes (Corning Glass Works, Corning, NY, U.S.A.). Cultures were kept at 37 °C in a 7 % CO_2 incubator and fed every 2–3 days. Cells were 12–14 μm in diameter.

Electrical recordings

Recordings were made using the whole-cell variation of the patch-electrode voltage-clamp technique (Hamill *et al.* 1981). Electrodes were filled with 150 mM-KCl, 10 mM-NaCl, 1·0 mM-$MgCl_2$, 1·1 mM-EGTA, 0·1 mM-$CaCl_2$ (pCa = 7·7) and 10 mM-HEPES, and brought to pH 7·3. The bath solution contained 155 mM-NaCl, 4·6 mM-KCl, 1·6 mM-$CaCl_2$, 0·6 mM-$MgCl_2$, and 10 mM-HEPES (pH = 7·30). The liquid junction potential between the electrode and bath solutions (typically 4·5–5·5 mV, electrode negative) was subtracted from the voltage record. Ionic concentrations were used to calculate reversal potentials because at these ionic strengths, internal and external activities of sodium and potassium were within 2 % of each other (Fujimoto & Kubota, 1976). Experiments were performed at room temperature (22–25 °C). In experiments where $[K]_o$ was raised, KCl was substituted for NaCl. Electrodes were fire polished and coated with beeswax to reduce electrode capacitance. Resistances ranged from 2 to 10 MΩ; seal resistances ranged from 5 to 20 GΩ. Confluent cultures were not studied to avoid the possibility of recording from electrically coupled cells.

The output of a Dagan 8900 patch-clamp amplifier with a 1 GΩ feed-back resistor (Dagan Corp, Minneapolis, MN, U.S.A.) was filtered through a low-pass filter at 1 kHz; the output was displayed on the oscilloscope and a strip-chart recorder. The output was also tape-recorded (Ampex PR2200, Ampex Corp, Redwood City, CA, U.S.A.). I/V relations generated using slow voltage ramps (dV/dt = 20 mV/s) were plotted directly onto an X–Y recorder (Hewlett Packard 7015B, Hewlett Packard, San Diego, CA, U.S.A.). No series resistance compensation was performed. Since the maximum amplitude of currents measured in this study was < 0·5 nA, the error due to series resistance was no more than 5 mV and usually much less. Unless otherwise noted, cells were maintained at the initial zero-current holding potential and voltage steps were separated by 10 s. This was subtracted from the voltage records.

Statistical analysis and curve fitting were performed on a VAX 750 computer (DEC, Boston, MA, U.S.A.) using the RS1 software package (BBN Inc., Cambridge, MA, U.S.A.).

RESULTS

Resting membrane potential

Initial studies were done on long-term adherent cultures (> 24 h) of J774.1 cells because they were judged more comparable to previous intracellular micro-electrode studies of macrophages (Gallin, 1981; Gallin & Livengood, 1981). The zero-current holding potential determined within seconds of attaining the whole-cell configuration

was used as an estimate of resting membrane potential. The zero-current potential of thirty-seven cells averaged $-77{\cdot}6$ mV $\pm 0{\cdot}78$ (S.E. of mean); values ranged from -66 to -85 mV. The observation that the zero-current potential was within 10% of the potassium equilibrium potential ($E_K = -87$ mV assuming 2·3 $RT/F = 57$ mV where R, T and F have their usual meaning, $[K]_o = 4{\cdot}6$ and $[K]_i = 150$ mM) indicates that shunt to ground across the pipette/cell seal or conductance to ions other than K^+ was no more than 10% of the whole-cell conductance. Zero-current potentials of long-term adherent J774.1 cells were routinely stable for greater than 30 min and as long as 90 min.

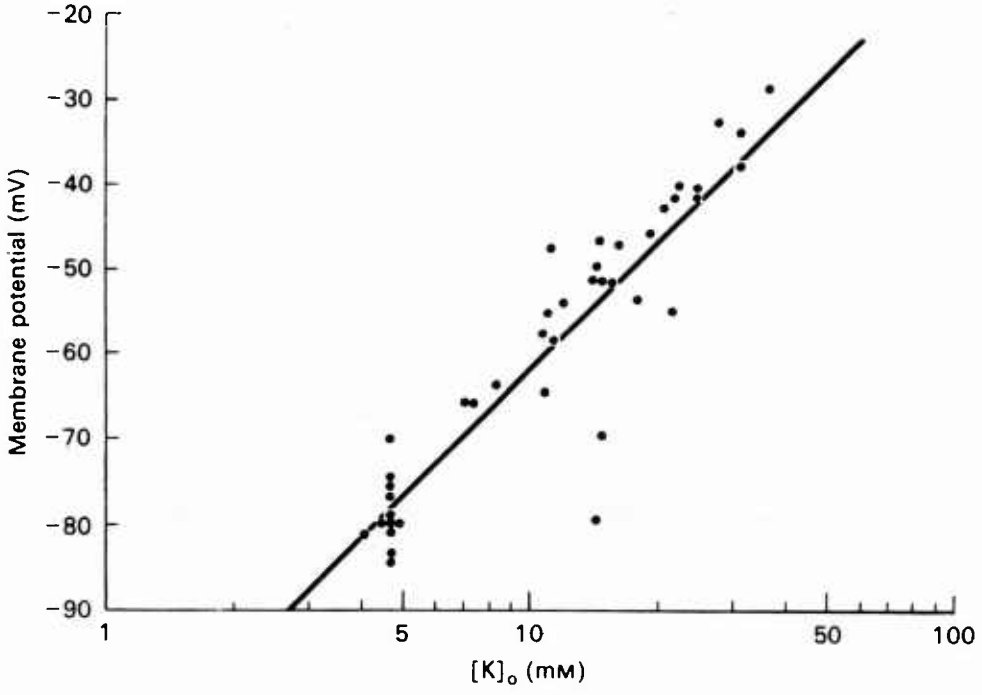

Fig. 1. Relation between membrane potential (estimated as zero-current holding potential) and $[K]_o$. Data are the summary of twelve different cells exposed to three or four increases in $[K]_o$.

To determine the relation between the resting membrane potential and the potassium equilibrium potential, studies were done in which the extracellular potassium was varied and the zero-current membrane potential was measured. The data obtained from twelve different cells each exposed to three or four different $[K]_o$ are shown in Fig. 1. The linear regression line drawn through these points has a slope of 49 mV/tenfold increase in $[K]_o$ (correlation coefficient $-0{\cdot}90$) compared to a predicted slope of 57 mV/decade change in $[K]_o$ for a potassium electrode.

I/V relations

All long-term adherent J774.1 cells showed marked inward rectification. Fig. 2*A* depicts the current responses of a cell to voltage steps taken from its zero-current potential of -80 mV. Hyperpolarizing voltage steps produced large inward currents which activated rapidly. For steps beyond -120 mV, the currents show a decrease with time. The current elicited by depolarizing steps was considerably smaller and

exhibited no time dependenee. The I/V relations of this cell obtained from both voltage steps (circles) and a voltage ramp (continuous line, $dV/dT = 20$ mV/s) is shown in Fig. 2*B*. The apparent peak current, measured 10 ms after the beginning of the step (a time when the ionie eurrent could be clearly distinguished from the capaeitive transient) and the steady-state current obtained with voltage steps are

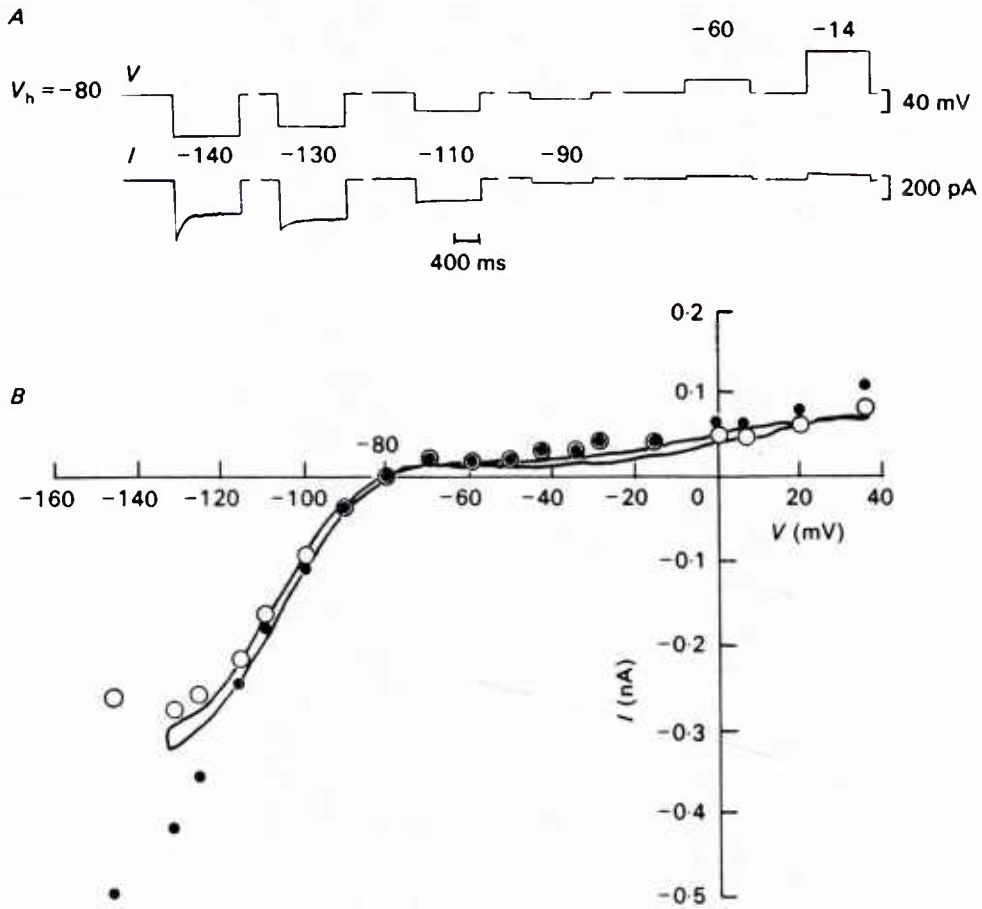

Fig. 2. *A*, current responses to a series of voltage steps from zero-current holding potential (−80 mV). Cell plated for > 24 h. *B*, I/V relation of cell shown in Fig. 2*A*. Filled circles represent current measured 10 ms after start of step. Open circles represent current measured at end of step (1 s). Voltage steps were applied every 10 s. Continuous line represents current generated by injection of a voltage ramp ($dV/dT = 20$ mV/s).

both plotted. Since there was no time dependence to current in the voltage range of +40 to −110 mV, the peak and steady-state curves as well as the ramp-derived curve are identical. However, at voltages negative to −110 mV they diverge. In other studies in which ramps to more negative potentials were done, a prominent hysteresis was evident (see Fig. 3*C* and *D*) due to time-dependent inactivation of the inward current. The cell in Fig. 2 had a maximum slope conductance of 9·6 nS for inward current calculated between −100 and −120 mV (for both the ramp- and step-derived curves) and a leak slope conductance, calculated from −50 to −40 mV, of 0·9 nS. The leak conductance of long-term adherent cells, calculated from −50 to −40 mV, was 1·01 nS ± 0·12 (mean ± S.E. of mean, $n = 22$).

Effect of adherence on zero-current potential and I/V relations

The resting membrane potential of non-adherent J774.1 cells as measured with TPP^+, an indirect probe of membrane potential, is significantly more positive than our values obtained on adherent J774.1 cells (Young *et al.* 1983). To investigate the cause of this difference, we measured the zero-current membrane potential of J774.1 cells previously grown in spinner culture and plated shortly before recordings were done. The zero-current holding potentials of cells studied at 30 min–24 h post-plating were similar to those of long-term adherent cultures (−66 mV or more negative), indicating that J774.1 cells probably hyperpolarize rapidly upon plating.

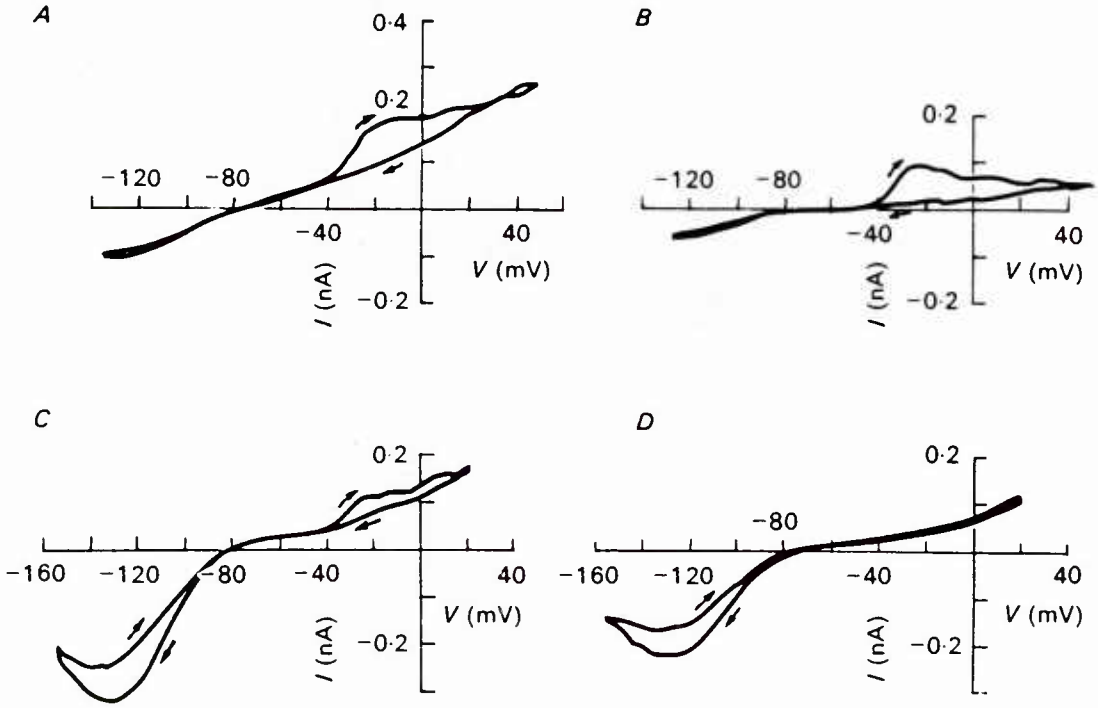

Fig. 3. *I/V* relations of four cells obtained by voltage ramp at various times after plating from suspension culture. Cells were held at zero-current potential. *A*, 1 h after plating. $V_h = -77$ mV. *B*, 3 h. $V_h = -78$ mV. *C*, 7 h. $V_h = -81$ mV. *D*, > 24 h. $V_h = -72$ mV.

The *I/V* characteristics of J774.1 cells varied considerably with time after plating. Four *I/V* curves representative of the pattern seen in the 195 cells analysed in this paper are shown in Fig. 3. Cells showed no evidence of inward rectification immediately after plating (< 1 h) although small inactivating, outward currents were sometimes noted. The increase in the slope of the *I/V* curve at voltages positive to −40 mV in the rising limb of the depolarizing ramp in Fig. 3*A* reflects activation of an outward current. The returning limb of the ramp was flat due to inactivation of this outward current. This inactivating outward current was observed up to 8 h after plating (Fig. 3*B* and *C*) but was absent in cultures more than 12 h old (Fig. 3*D*). The outward current is described in a later section of this paper. Inward rectification usually became evident about 2–4 h after plating (Fig. 3*C*) and was the characteristic feature of *I/V* curves obtained from cells plated 24 h or longer (Fig. 3*D*). Experiments with voltage steps confirmed the results obtained with ramps.

While the inward rectifier was always present in long-term cultures, expression of the outward current was variable. The fraction of cells expressing the outward current 2–4 h after plating could vary from 90 to 20%. The consistent observation was that the inward current was not expressed upon plating and took 2 h or more to manifest. The inactivating outward current was seen between 1 and 12 h after plating and, with only one exception, never thereafter.

Analyses of the voltage dependence of the inward and outward currents which are presented later in this paper were all performed on stabilized cells. Apart from an occasional transient increase in leak current during the first 10 min of a recording, holding currents were stable throughout an experiment.

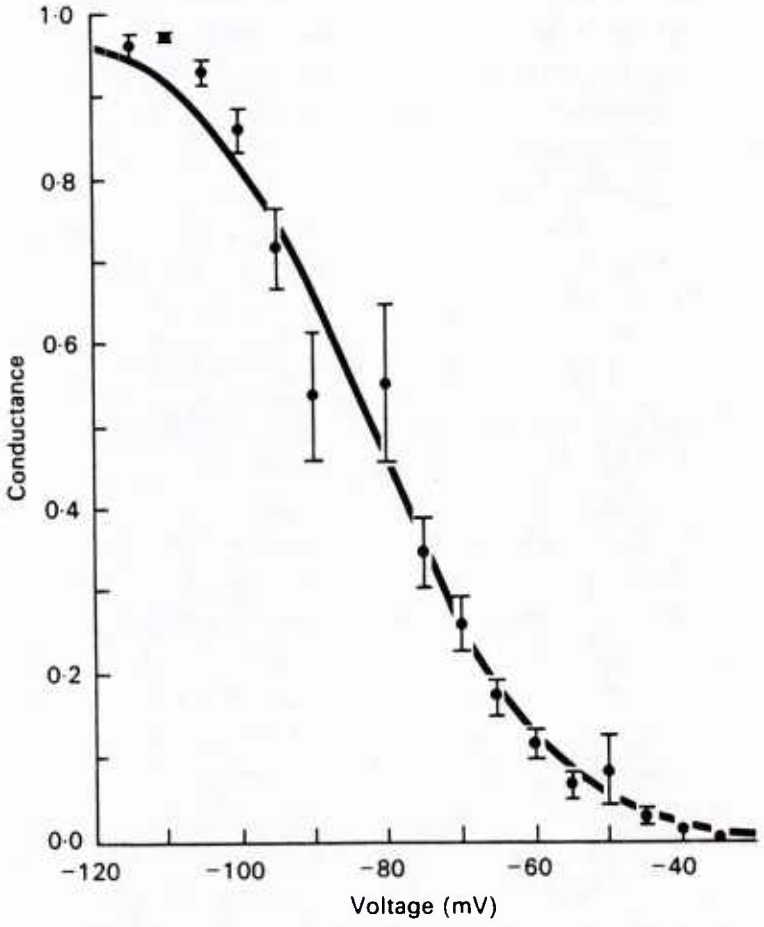

Fig. 4. Chord conductance *versus* voltage of twelve long-term adherent J774.1 cells. Leak conductance (calculated at −30 mV) was subtracted; each cell's curve was normalized by its peak conductance. Reversal potential was assumed to be −87 mV. Each point is the mean ± S.E. of mean. Continuous line conforms to eqn. (1).

Inward rectification

The conductance/voltage relation. Comparison of I/V curves obtained with voltage steps to those obtained with voltage ramps demonstrated that ramp-derived curves provided faithful representations of the peak instantaneous I/V relation up to −110 mV (Fig. 2*B*). Therefore the chord conductance of the inward current was calculated from I/V curves generated from ramps. Leak conductance, determined at −30 mV, was subtracted. The reversal potential (E_R) of the inward rectifying current

was assumed to be E_K (−87 mV). The conductance/voltage relations of twelve long-term adherent cells obtained in $[K]_o = 4{\cdot}6$ mM are presented in Fig. 4. The conductance values of each cell were normalized to 1·0 by its maximum (G_{max}) so that they could be pooled. The voltage at which the peak was observed varied from −110 to −120 mV; consequently, the pooled conductances at these potentials are slightly less than 1·0. The conductance is substantially activated at rest (about 39 % at −77 mV) and thus contributes to the resting membrane potential of the cell. At potentials beyond −110 mV the data indicate a drop in the inward rectifying conductance (this is more evident in Fig. 5*B*). This is an artifact resulting from time-dependent inactivation of the conductance during the ramp, since experiments with steps demonstrated that the inward conductance peaked by −110 mV and remained constant at more negative voltages. With the exception of the drop in conductance at potentials negative to −110 mV, the conductance/voltage parameters determined from peak currents in response to voltage steps agreed closely with those determined from current responses to voltage ramps. This indicates that inactivation positive to −110 mV during the course of the voltage ramp was insignificant.

The continuous line drawn through the points in Fig. 4 represents an empirical relation reported by Hagiwara for the anomalous rectifier in egg cells (Hagiwara & Takahashi, 1974). This relation is described by the equation:

$$G/G_{max} = 1/[1+\exp((V-V_h)/v)], \quad (1)$$

where v is a constant that characterizes the slope of the relation and V_h represents a constant that locates the curve along the voltage axis; at $V = V_h$ the conductance is half-maximal. $V = (V_m - E_K)$, the driving force of the current where V_m is the membrane potential. The data shown in Fig. 4 were fitted by non-linear least-squares regression. Values of $2{\cdot}85 \pm 0{\cdot}08$ and $11{\cdot}57 \pm 0{\cdot}25$ were obtained for V_h and v, respectively (coefficient of multiple determinations = 0·993). The relation is steep near rest; fractional activation drops from 66 % at −90 mV to 26 % at −70 mV. The average G_{max} of the cells in Fig. 4 was $6{\cdot}57$ nS $\pm 1{\cdot}06$ (mean ± S.E. of mean). Condutance/voltage characteristics of long-term adherent cells were routinely stable for greater than 30 min.

Effects of $[K]_o$. The inward rectifying potassium conductance in egg and muscle cells is a function of both the membrane potential and the $[K]_o$ (Hagiwara & Takahashi, 1974; Leech & Stanfield, 1981). To determine if this is also the case for macrophages, the effect of varying external potassium was investigated in J774.1 cells. Four I/V curves of a single cell taken after equilibration in sequentially increasing $[K]_o$ are shown in Fig. 5*A*. In addition to depolarizing the cell, raising $[K]_o$ increased the slope conductance for inward currents and shifted the voltage dependence of inward rectification to the right. In Fig. 5*B* the conductance/voltage relations of the cell are displayed for each of the four potassium concentrations shown in Fig. 5*A*. The continuous lines in Fig. 5*B* represent fits of each set of conductance data (not normalized by G_{max}) to eqn. (1); V_h and v determined at each $[K]_o$ were not substantially different from the values at $[K]_o = 4{\cdot}6$ mM when the appropriate values of E_K and G_{max} were substituted. A log–log plot of G_{max} *versus* $[K]_o$ is shown in Fig. 5*C*; linear least-squares regression gives a slope of 0·56 ($r = 0{\cdot}97$). Similar data from six different cells were normalized by dividing G_{max} determined at each $[K]_o$ by

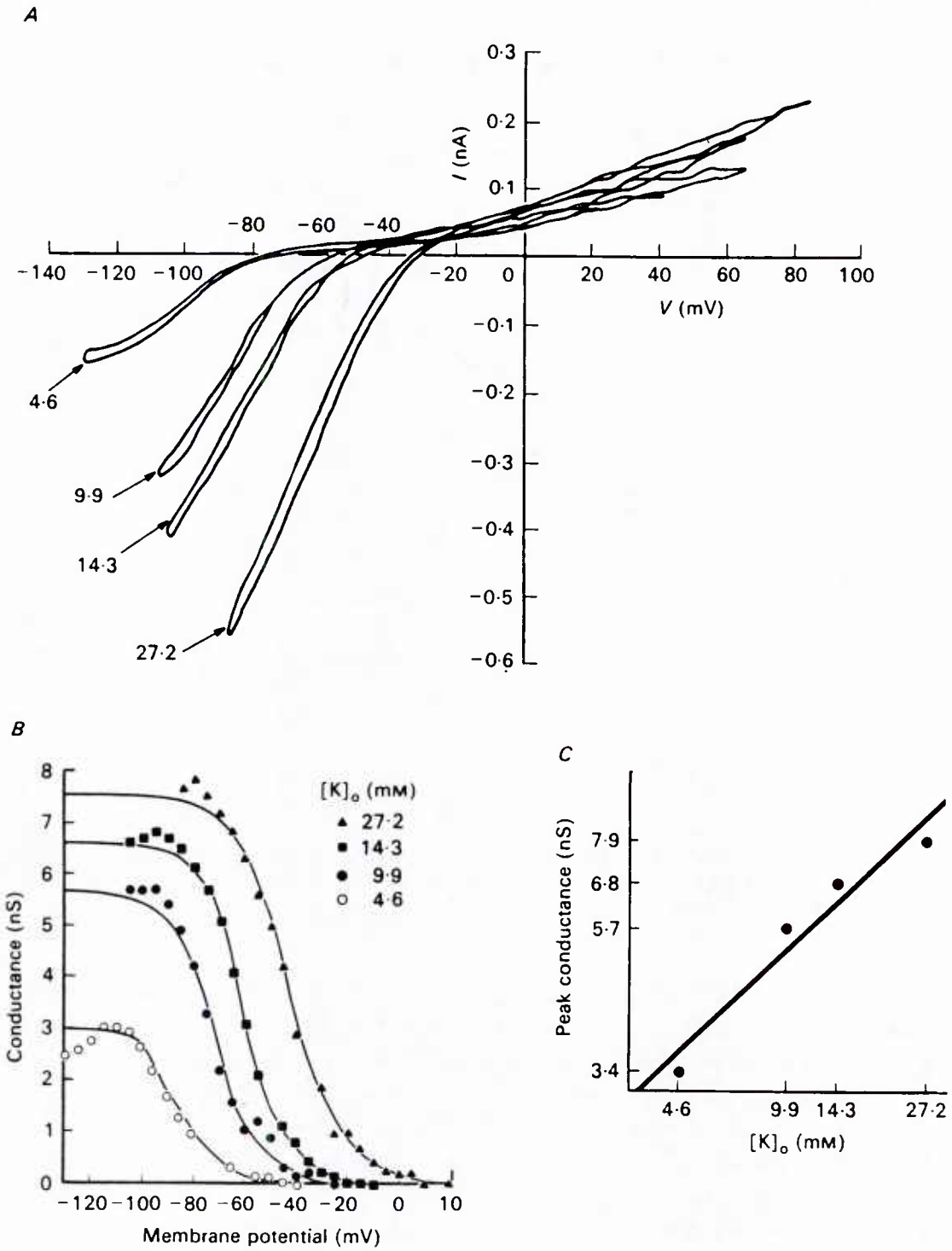

Fig. 5. *A*, *I/V* relations of the same cell taken sequentially in $[K]_o = 4{\cdot}6$, 9·9, 14·3 and 27·2 mM. Holding potentials were zero-current potentials: $V_h = -75$, -56, -50 and -33 mV, respectively. *B*, chord conductance *versus* voltage for each $[K]_o$ calculated as in Fig. 4; conductance 40 mV positive to rest was used as estimate of leak. *C*, log peak conductance *versus* log $[K]_o$. Data in panels *B* and *C* were fitted by least-squares regression ($r > 0{\cdot}97$).

G_{max} determined in $[K]_o$ 4·6 mM. The slope of a log–log plot of the normalized G_{max} *versus* $[K]_o$ for the six cells was 0·49. Thus, there is a square-root relation between the peak inward rectifying conductance and $[K]_o$, similar to that observed in egg and muscle cells (Hagiwara & Takahashi, 1974; Leech & Stanfield, 1981).

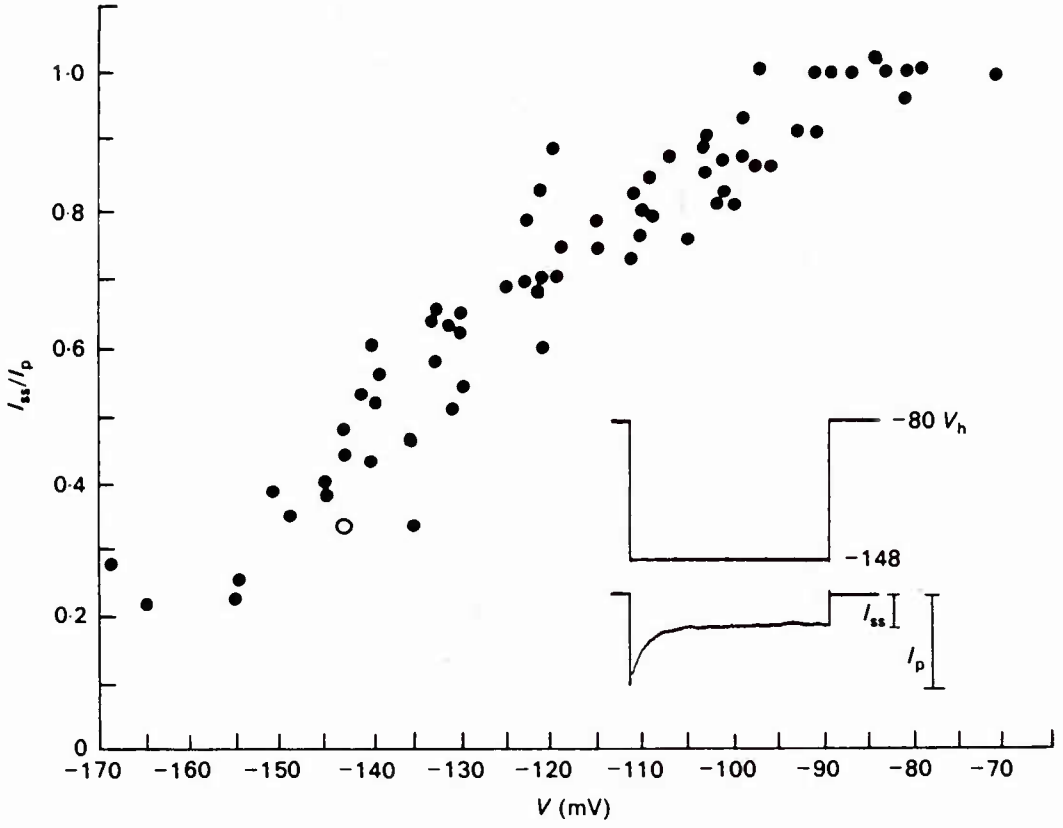

Fig. 6. Steady-state current/peak current (I_{ss}/I_p) *versus* voltage. Data from eight cells. I_p determined 10 ms after start of step, I_{ss} determined at end of 1 s step. Inset represented by open circle at −148 mV.

Inactivation. The *I/V* relations in Fig. 2*A* and *B* show that inward current was time independent for voltage steps up to −110 mV but decreased with time at more negative voltages and suggest that the inactivating component of total inward current increases with hyperpolarization. The ratio of the steady-state current (I_{ss}) to the apparent peak current (I_p) is plotted *versus* voltage for eight cells in Fig. 6. The peak was measured 10 ms after the initiation of the voltage step when the capacitive transient was clearly over. The data in Fig. 6 indicate that inactivation occurs at voltages negative to −100 mV and that the inactivating component of inward current increases with hyperpolarization. At the most negative voltages studied (−150 to −175 mV), the steady-state inward current was still greater than leak. It was not possible to determine whether the ratio of I_{ss}/I_p plateaued at very negative voltages since it was difficult to apply voltage steps to −150 mV or greater.

Fig. 7*A* shows the time-dependent current ($I_p - I_{ss}$) measured from current records as a function of time for four different voltage steps. The current relaxations were fit by single exponentials ($P < 0·01$). The time constants determined for voltage steps

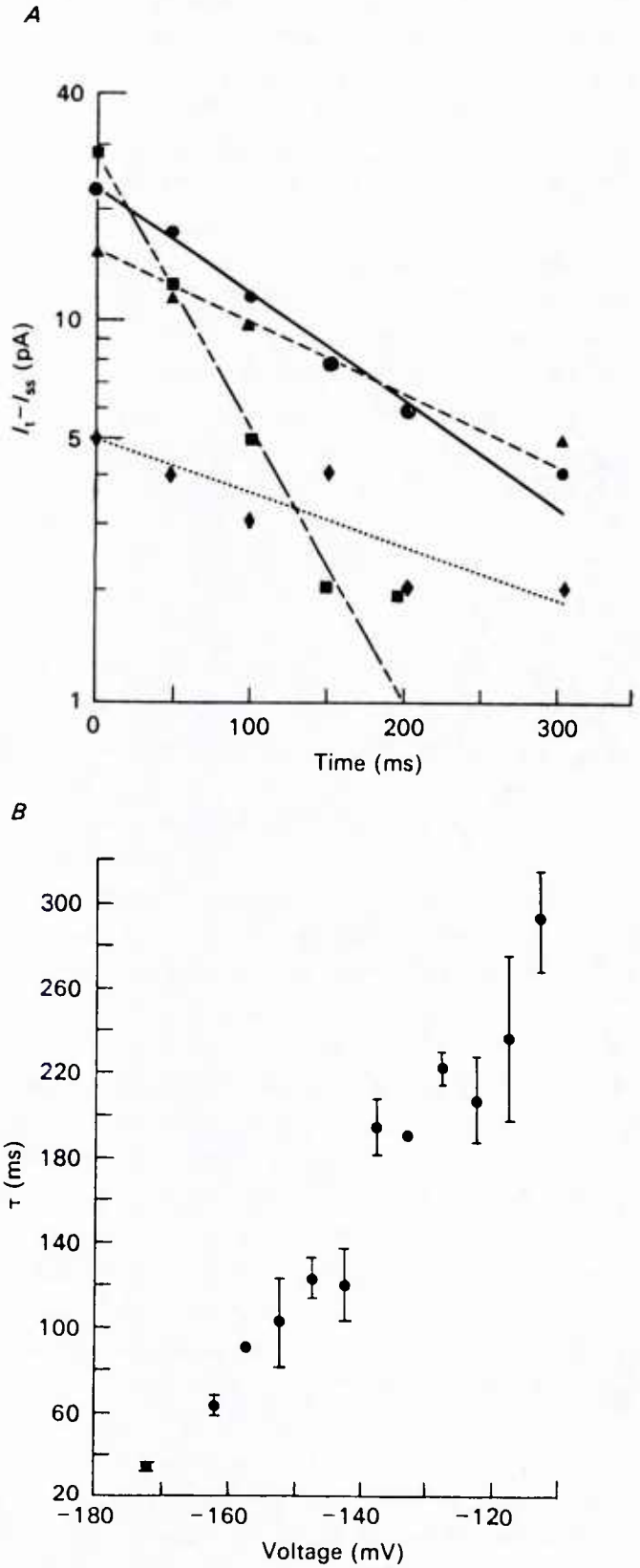

Fig. 7. *A*, semilog plot of inactivating inward current as function of time for voltage steps to −154 (square), −145 (filled circle), −136 (triangle) and −114 (diamond) mV. *B*, time constant of decay (τ) *versus* voltage for cells of Fig. 6. Individual points represent average time constant from a number of cells (one to five) ± S.E. of mean. The two points with no error bar represent single cells; eight different cells were analysed in all.

to −154, −145, −136, and −114 mV were 58, 148, 218, and 298 ms, respectively. Fig. 7*B* shows the time constants of decay as a function of voltage for the same eight cells analysed in Fig. 6. Time constants decreased with increasing hyperpolarization.

Blockers. Addition of barium (2–3 mM) to the bathing medium blocked inward rectification in J774.1 cells. The *I/V* curves from a cell before and after the application of barium are shown in Fig. 8*A*. The *I/V* curve of the cell following addition of barium became linear with a slope resistance of 3·7 GΩ, a value equal to its resistance in the voltage range −60 to −40 mV before the addition of barium. The zero-current holding potential of this cell shifted from −81 to −51 mV. Barium completely eliminated inward rectification in all cells tested. The average zero-current holding potential after barium was −49 mV ± 11·3 (n = 18). Block was not voltage dependent at the barium concentrations and voltages studied. Note that the control and barium-tested *I/V* curves intersect at −84 mV, indicating that barium-sensitive current was carried by K^+ (E_K = −87 mV).

Caesium (1–3 mM) reduced the inward rectifying conductance in J774.1 cells (n = 5). Block was voltage dependent, as shown in the *I/V* curves of Fig. 8*B*. Block was incomplete at rest and increased with hyperpolarization, producing a region of negative slope resistance.

Outward rectification

I/V relation. As noted earlier, outward currents were obtained in cells that had been plated for 1–8 h. Fig. 9*A* shows current responses of a cell, plated for 3 h, to voltage steps from a holding voltage of −80 mV. Cells in these studies were held at −80 mV regardless of their actual zero-current potential and a 40 s interpulse interval was used. A 10 min interval after attaining the whole-cell confirmation was instituted before initiating voltage steps to allow the conductance to stabilize (see section on *Stability of currents*, p. 493). Fig. 9*A* shows that voltage steps positive to −40 mV activated an outward current that declined with time. The outward current produced by the step to −32 mV peaked at 30 ms. With increasing depolarization, the time to peak was reduced (Fig. 9*B*). The time course of the rise of the outward current was not systematically investigated because the capacitative transients obscured very early events. Fig. 9*C* shows the *I/V* curve plotting the steady-state and peak currents from the cell in Fig. 9*A* and *B*. The peak outward currents were measured at least 10 ms after the voltage step (at a time when the capacitative transient was over). The measured values for the peak currents for large depolarizing steps (where the current activates rapidly) therefore underestimate the actual peak current. It is evident from the steady-state *I/V* curve that the current completely inactivates.

Ionic basis of outward rectification. The ionic basis of the outward current was investigated using a two-step pulse protocol. Fig. 10*A* presents oscilloscope records of tail currents obtained in $[K]_o$ = 4·6, 9·7, 14·8 and 20 mM. The first pulse was to −10 mV which fully activated the outward conductance. The instantaneous *I/V* curves (Fig. 10*B*) were generated by plotting the amplitude of the tail current (measured 10 ms after the second step minus steady-state current) *versus* the voltage of the second step. The tail currents measured in this way underestimate the actual tail currents, particularly for large currents and therefore were not used to calculate conductance. However, they can be used to determine the reversal potential of the

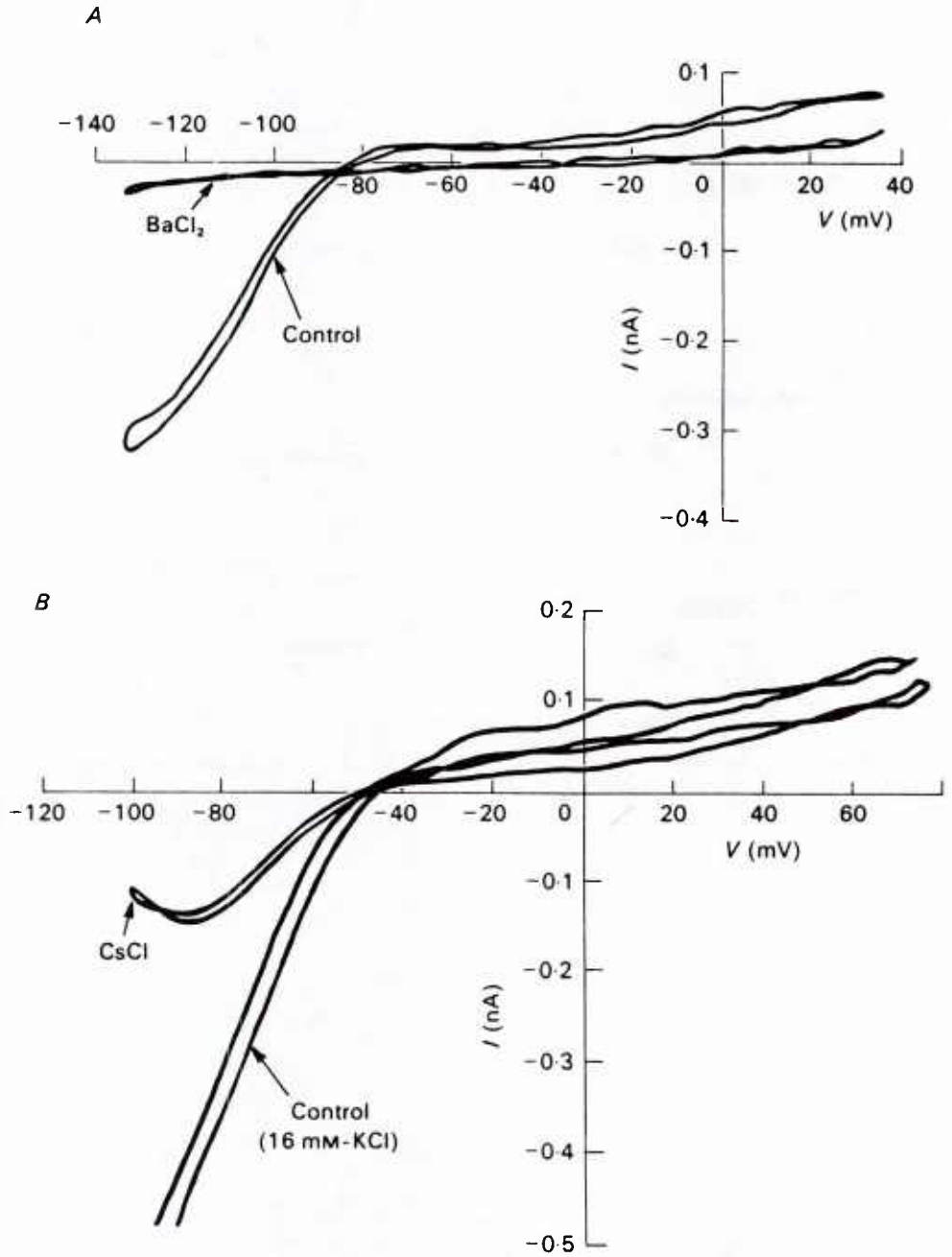

Fig. 8. *A*, *I/V* relations before and after addition of 2·5 mM-$BaCl_2$ to bath. $V_h = -80$ mV. *B*, *I/V* relations before and after addition of 1 mM-CsCl to bath. $[K]_o = 16$ mM. $V_h = -46$ mV.

current. It is evident from Fig. 10*B* that the reversal potential of the outward current shifted to the right as $[K]_o$ increased. A plot of the reversal potentials *versus* log $[K]_o$ for these data is shown in Fig. 10*C*. The points were fit by linear-regression analysis, and they have slope of -52 mV per tenfold increase in potassium ($r = 0{\cdot}96$) indicating that these outward currents are carried by potassium.

Conductance/voltage relations. The chord conductance of the outward rectifying current was calculated assuming potassium as the predominant charge carrier and E_K as -87 mV. Fig. 11 presents results from three cells. The rectifying current

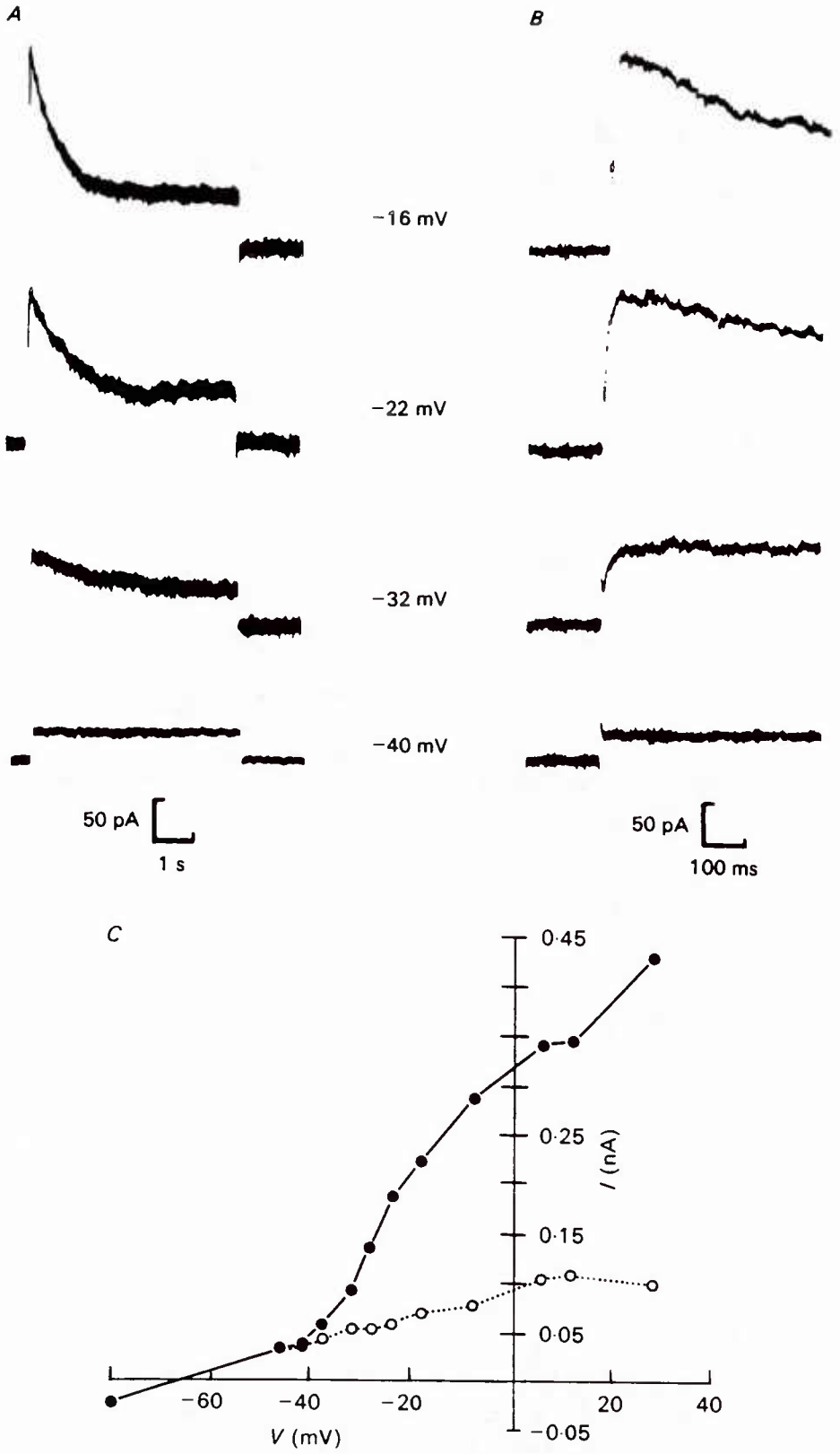

Fig. 9. *A*, current responses to series of voltage steps taken from −80 mV. Cell plated for 3 h. *B*, same currents as in Fig. 9*A* but at 10 times sweep speed. *C*, *I*/*V* relation of cell in Fig. 9*A*. Each point is mean of three steps. Filled circles represent current measured 10 ms after start of step, open circles represent the current at end of 5 s step. Voltage steps were applied every 40 s.

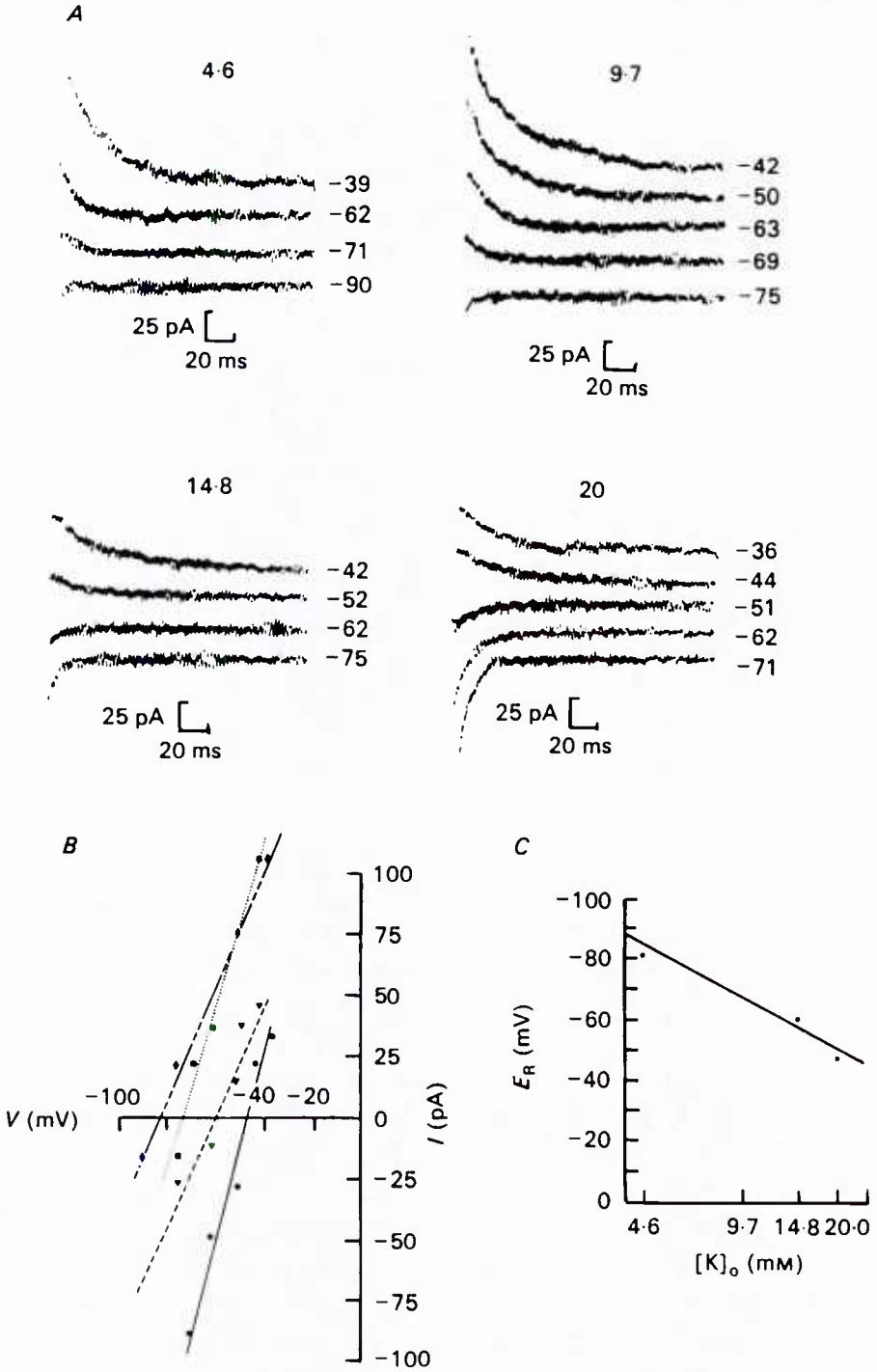

Fig. 10. Tail current analysis of ionic basis of outward rectification. Cell was held at −80 mV and outward conductance fully activated by a step to −10 mV. *A*, current responses of same cell obtained in $[K]_o$ = 4·6, 9·7, 14·8 and 20 mM. *B*, instantaneous *I*/*V* relations from data of Fig. 10*A*. *C*, reversal potential determined from Fig. 11*B* plotted *versus* log $[K]_o$. Lines in both Fig. 10*B* and *C* were fitted by least-squares linear regression ($r > 0{\cdot}98$).

activated positive to −50 mV and plateaued around −10 mV. The dashed line corresponds to a best fit of the data to the Hodgkin–Huxley equation for the delayed rectifier:

$$G/G_{max} = 1/(1+\exp[-(V_m-V_h)/v])^x, \quad (2)$$

where V_m and V_h have the same meanings as in eqn. (1) and x indicates an unknown degree of exponentiation. The values of V_h and v determined from these data using a first-power relationship are −31 and 5·7 mV, respectively (non-linear least-squares fit, coefficient of multiple determinations = 0·98). Statistically significant fit could be obtained for both first- or fourth-power relations.

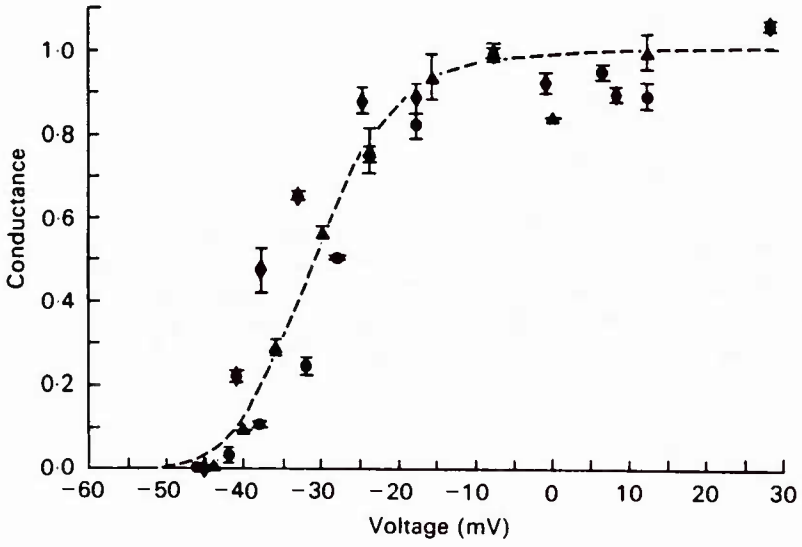

Fig. 11. Chord conductance *versus* voltage of three freshly plated J774.1 cells ($V_h = -80$ mV), each pulsed to same voltage three times (each point is mean ± S.E. of mean). Conductances were leak subtracted (calculated at −60 mV) and normalized by peak conductance for each cell. Reversal potential was estimated as −85 mV. Dashed line conforms to eqn. (2), $x = 1$.

Inactivation. As shown in Fig. 9, the outward currents completely inactivated with time during the voltage step. The time course of the inactivation process was described by a single exponential (Fig. 12*A*). Fig. 12*B* plots the time constant of inactivation as a function of voltage for three different cells. Positive to −25 mV the time constant was insensitive to voltage, averaging 538 ± 25 ms (mean ± S.D.); negative to this potential, inactivation was consistently slower and appeared to show some voltage dependence. However, since the amount of inactivating current negative to −25 mV was very small, reliable estimates of the time constants at these voltages could not be made.

The outward rectifying current recovered relatively slowly from inactivation. Recovery from inactivation was examined using paired 250 ms pulses to −10 mV separated by a variable interval. The summary of three experiments is shown in Fig. 13 in which the ratio of the peak current elicited by the second pulse to the first pulse is plotted *versus* the interpulse interval. The time course of recovery was described by a single exponential with a time constant of 13·7 s.

Blockers. The effects of 4-aminopyridine (4-AP) and D600 on the outward currents

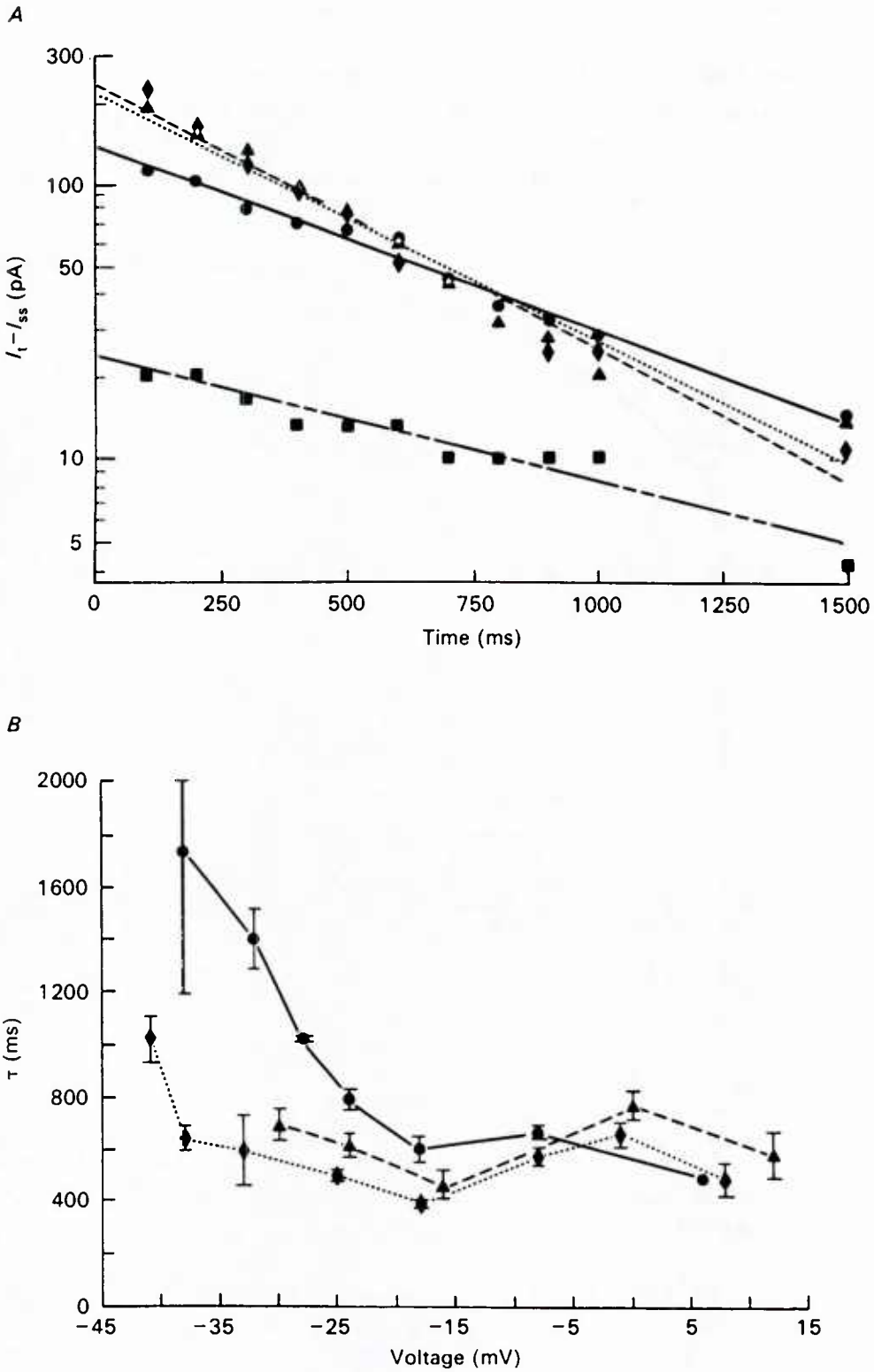

Fig. 12. Time course of inactivation of outward rectification. *A*, semilog plot of inactivating outward current as a function of time for steps to −32 mV (squares), −24 mV (circles), −8 mV (triangles) and +12 mV (diamonds). *B*, time constant of outward current decay *versus* voltage for three different cells.

were investigated because it has been shown that 4-AP (DeCoursey *et al.* 1984; Ypey & Clapham, 1984), and verapamil (Chandry, DeCoursey, Cahalan, McLaughlin & Gupta, 1984) block outward potassium currents in other leukocytes. Addition of 10 mM-4-AP (introduced at pH 7·4) or 1 mM-D600 (methoxyverapamil) to the bath during recordings from cells exhibiting inactivating outward currents produced a block of the current within 3–5 min. Lower concentrations of these agents (1 mM-4-AP or 500 μM-D600) had only partial blocking action.

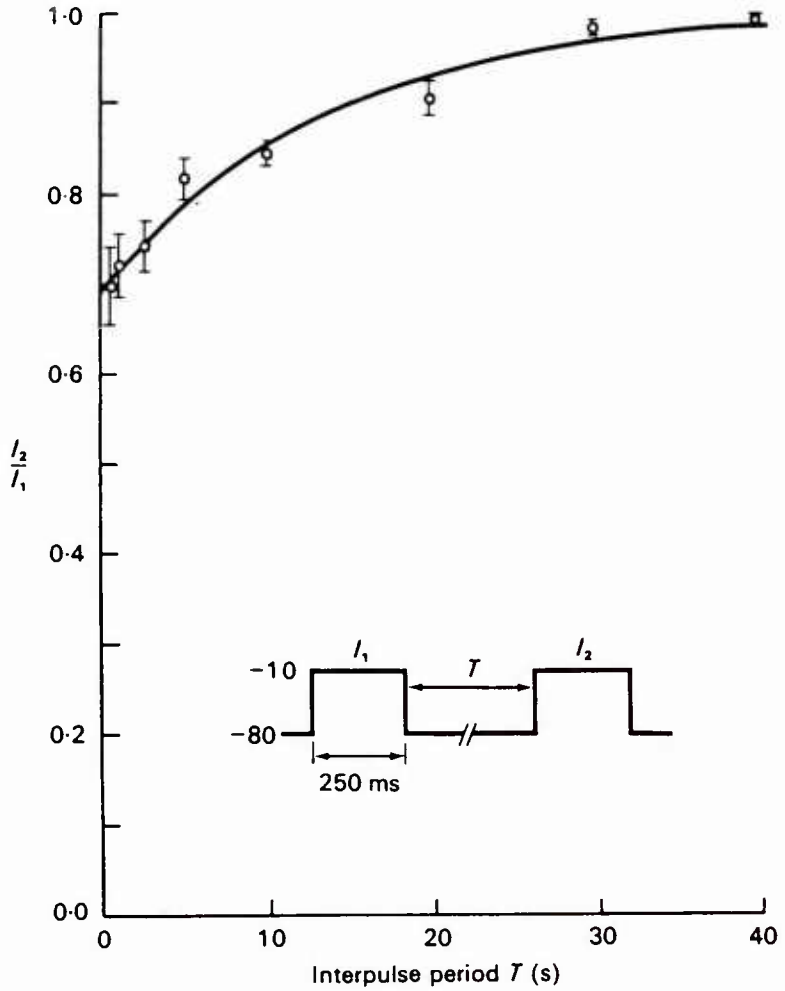

Fig. 13. Time course of recovery from inactivation of outward rectification. The ratio of the peak current during the second pulse (I_2) to that during the first pulse is plotted as a function of the interpulse interval. The continuous line conforms to $I_2/I_1 = 1-0{\cdot}30 \exp(t/-13{\cdot}7)$ where t is seconds ($P < 0{\cdot}01$).

The concentration of 4-AP needed to completely block the outward currents produced rapid and extensive vacuolization of the cells and whole-cell recordings were often lost following block of the outward current. To ensure that the outward current block was not related to a general run down of the cells, the following study was done. Recordings were obtained from different cells in the same culture dish before and after a 20 min incubation in 10 mM-4-AP and the resting membrane potential, leak conductance, and outward currents measured. Both populations before and after 4-AP addition had the same average resting membrane potential and leak conductance

(−78·7 *versus* −78·5 mV and 1·1 *versus* 1·2 nS, respectively). However, the expression of outward rectification decreased from six of seven cells observed before addition of 4-AP to none of eight after. No release of the intracellular enzyme lactate dehydrogenase was detected during a 1·5 h incubation in 10 mM-4-AP (S. W. Green & E. K. Gallin, unpublished observations).

Stability of currents

Several groups of investigators have reported that some parameters of voltage-dependent sodium, potassium and calcium conductances change with time during patch-clamp recordings (Fenwick, Marty & Neher, 1982; Cahalan *et al.* 1985; Fernandez, Fox & Krasne, 1984). In J774.1 cells, the outward current increased and its activation shifted over the course of the first 10 min of a whole-cell recording. After an initial stabilization period, outward current routinely remained stable for up to an hour. I/V curves generated with voltage steps immediately after attaining the whole-cell conformation and again after stabilization indicated that peak outward conductance increased and activation shifted. The conductance/voltage curves from four different cells fitted to eqn. (2) exhibited a 8 mV shift in V_h to the left; no change was found in v. The 8 mV shift may be an underestimate since it was apparent that a significant shift occurred even as the first I/V curve was obtained. The inward potassium current showed a different pattern of changes with time under whole-cell recording conditions. The conductance/voltage relation did not shift and, in most cells, maximum inward current was stable. In a few cells, voltage-dependent inward current disappeared within 10–20 min without a detectable shift in its conductance/voltage relation. Activation of the outward current shifted in such cells but no run-down was observed.

DISCUSSION

This report describes two time- and voltage-dependent potassium currents in J774.1 cells, a macrophage-like cell line derived from a mouse reticulum sarcoma (Ralph & Nakoinz, 1975). The two currents have different voltage sensitivities: one activating at voltages negative to −60 mV, and the other activating at voltages positive to −40 mV. The former is similar to the inward rectifying potassium conductance described in long-term cultures of mouse spleen and thioglycolate-elicited peritoneal macrophages (Gallin, 1981; Gallin & Livengood, 1981). The latter is similar to the outward rectifying potassium conductance described in mouse resident peritoneal macrophages (Ypey & Clapham, 1984). These conductances are sequentially expressed after J774.1 cells are switched from suspension to adherent culture.

Resting membrane potential

The relation of the zero-current potential to $[K]_o$ indicates that approximately 90 % of the resting membrane potential of J774.1 cells is determined by the potassium electrochemical gradient. The remaining component, i.e. permeability to other ions, may be induced by the recording system (i.e. it may reflect a shunt conductance across the electrode–cell seal), or may normally be present in unperturbed J774.1 cells. Our previous studies using intracellular micro-electrodes demonstrated a broad distri-

bution of resting membrane potentials in J774.1 cells, with resting membrane potentials ranging from −18 to −86 mV (Sheehy & Gallin, 1984). A bimodal distribution of resting membrane potentials, from −20 to −40 and −50 to −90 mV, was found in primary cultures of mouse spleen and peritoneal macrophages (Gallin & Livengood, 1981; Gallin, 1981). In those studies it was suggested that the depolarized cells might represent a damaged subpopulation. The patch-clamp data in this paper, demonstrating a unimodal distribution of hyperpolarized resting membrane potentials, indicate that this is the case.

The values of resting membrane potential for adherent J774.1 cells are very different from the value of −14 mV obtained by Young *et al.* (1983) using the lipophilic cation TPP^+ to indirectly monitor membrane potential. However, TPP^+ measurements on adherent cells yield resting membrane potential values of −70 mV, which are similar to those obtained in these studies (J. Young, personal communication). Therefore, it is likely that the process of adherence produces a rapid (within 30 min) increase in the resting membrane potential. The change in resting membrane potential must involve either an increase in potassium permeability or a decrease in other permeabilities. The depolarization induced by barium indicates that the inward rectifier contributes significantly to the resting membrane potential of long-term adherent cells. On the other hand, cells soon after plating have −77 mV potentials but do not exhibit inward rectification, indicating that the inward rectifier is not essential for the establishment of negative resting membrane potential.

Conductance changes following adherence

J774.1 cells express both voltage-dependent inward and outward potassium currents at different times after plating. The outward current appears first, about an hour after plating, and is lost within 12 h post-plating. In these studies the number of cells exhibiting outward current in any given dish was variable, but the time frame of its expression remained consistent. With only a single exception (in 195 cells), outward currents were not observed more than 12 h post-plating. All long-term cultured J774.1 cells express the inward rectifying potassium current; it was only occasionally seen in cells plated for less than 3 h. As already noted, similar inward and outward rectifications have been described in primary cultures of mouse peritoneal macrophages (Gallin & Livengood, 1981; Ypey & Clapham, 1984). Ypey & Clapham (1984) reported that the outward current was not present until cells had been cultured under adherent conditions for 12 h and was expressed for at least 4 days (the duration of the studies). They did not observe inward rectification during the 4 day culture period. Previous work in this laboratory has demonstrated that 2–4 week cultured mouse peritoneal macrophages exhibit prominent inward rectification (Gallin & Livengood, 1981). Although these two conductances are expressed at later times after plating in primary macrophages than in J774.1 cells, the expression of the inward rectifying current appears to follow the expression of the outward current in both cell types.

The differential appearance of these two conductances could result from any one or a combination of the following processes: (1) the synthesis and subsequent insertion of new channels in the membrane, (2) the insertion of pre-existing channels in the membrane, and (3) the modulation of membrane channels. Since the expression

of the outward rectifier in J774.1 cells occurs rapidly, as early as 25 min following plating, it is unlikely that *de novo* protein synthesis is required. Inward rectification develops slightly later, 2–4 h after plating; therefore, its full expression may involve synthetic processes. Studies examining this possibility are in progress.

In addition to influencing the expression of potassium conductances, adherence produces other physiological changes in macrophages. For example, Lazdins, Koech & Karnovsky (1980) have shown that within 3 h after plating, the glycogen levels in mouse peritoneal macrophages triple. Furthermore, Cohen, Ryan & Root (1981) have demonstrated that 90 min after adherence, the release of reactive oxygen metabolites increases in response to phagocytosis or phorbol myristate acetate. An increase in a voltage-dependent inward calcium current which parallels the development of immunoglobulin-secreting activity has been reported in lymphocyte–myeloma hybridomas, another cell type of leukocyte origin (Fukushima *et al.* 1984). It is possible that the expression of the two potassium conductances in J774.1 cells relates to a functional change(s) occurring following adherence.

The two conductances will have different effects on a cell. In response to depolarizing stimuli the inward rectifier shuts off whereas the outward rectifier activates; thus voltage responses to depolarizing stimuli will be amplified for a cell exhibiting inward rectification but blunted for a cell exhibiting outward rectification. Future studies using pharmacological agents to block the inward and outward potassium conductances in J774.1 cells may be useful in elucidating the relation between these conductances and cell function.

Inward rectification

The dependence of the inward current in J774.1 cells on both voltage and $[K]_o^{\frac{1}{2}}$ is similar to that described for the anomalous rectifying potassium conductance in muscle and egg cells (Leech & Stanfield, 1981; Hagiwara & Takahashi, 1974). Previous work in this laboratory using intracellular micro-electrodes has demonstrated a similar inward rectification blocked by barium and enhanced by increasing $[K]_o$ in mouse spleen and thioglycollate-induced peritoneal macrophages cultured for 2–4 weeks (Gallin & Livengood, 1981). Thus, J774·1 cells can serve as a model to study the role of the inward rectifying current in macrophages.

The unique relation of the anomalous rectifier to $[K]_o$ is particularly interesting in the context of the role of the macrophage as a scavenger. Macrophages are commonly found in sites of dead and dying tissue where $[K]_o$ may be locally elevated, and the increased inward rectifying conductance could be associated with enhanced expression of some effector function. Macrophages are not unique among leukocytes in expressing this conductance. A similar inward rectifying potassium current has recently been observed in a rat-derived basophil leukaemic cell line (Ikeda & Weight, 1984).

The conductance/voltage relation of the inward current (eqn. (1)) was similar to that of egg cells (Hagiwara & Takahashi, 1974). However, in J774.1 cells, activation was faster than in skeletal muscle or starfish eggs (Leech & Stanfield, 1981; Hagiwara, Miyazaki & Rosenthal, 1976), usually fully activated before the capacitative transient was over (< 10 ms). In contrast to activation, the voltage dependence of both the rate and extent of inactivation of the inward current in J774.1 cells generally

paralleled that of muscle and egg cells. Inactivation followed first-order kinetics with a rate that increased with membrane hyperpolarization, similar to the process described in skeletal muscle (Standen & Stanfield, 1979) and tunicate egg cells (Ohmori, 1978). However, the time constant of decay was generally longer in J774.1 cells than in muscle and egg cells. As in muscle and egg cells, the amount of inactivation in J774.1 cells increased with voltage, resulting in steady-state I/V relations with regions of negative-slope resistance for potentials negative to -150 mV.

In other cells, inactivation of the inward rectifying potassium conductance has been shown to result from one or a combination of three possible mechanisms: (1) a change in driving force due to a potassium redistribution (Almers, 1971*a*, *b*), (2) block of the open channel by weakly permeant ions such as Na^+ (Standen & Stanfield, 1979), and (3) actual channel closure (Sakmann & Trube, 1984). It is unlikely that there is a significant change in K^+ gradient in J774.1 cells since they are isolated in tissue culture, and there is no evidence that they contain an extensive system of membrane invaginations. The issue of open-channel block *versus* true channel closure would best be approached by single-channel techniques rather than the whole-cell method used in this study. However, the observation that significant current decay (up to 40%) was seen at potentials where Na^+ block is not thought to predominate in other cells (Standen & Stanfield, 1979) suggests that channel closure is the predominant mechanism in J774.1 cells in the voltage range studied in these experiments.

Outward rectification

The inactivating outward potassium current of J774.1 cells is very similar to that of peritoneal macrophages and T lymphocytes (Ypey & Clapham, 1984; Cahalan *et al.* 1985; Fukushima, Hagiwara & Henkart, 1984). The voltage dependence of activation of the outward conductance in J774.1 cells could be described by Hodgkin–Huxley-type kinetics. The values of V_h and v determined in this study (-31 and 5·7 mV, respectively) are quite close to those reported in T lymphocytes (-37 and 4·2 mV) by Cahalan *et al.* (1985).

The time course of inactivation of the outward current followed a single exponential at all voltages studied, and showed no systematic voltage dependence at voltages positive to -25 mV. In two cells studied at potentials negative to -25, the rate of decay clearly decreased, but the measurement error was too large to make accurate estimates for the whole population. These results are similar to the findings of Cahalan *et al.* (1985) in T lymphocytes.

The inactivating outward current in J774.1 cells was completely blocked by 10 mM-4-AP. This concentration, although high, is similar to the blocking concentration reported in mouse peritoneal macrophages (5 mM-4-AP; Yepey & Clapham, 1984) and human T lymphocytes (10 mM; DeCoursey *et al.* 1984). The sensitivity of the outward current to D600, an agent which blocks calcium channels suggests that the conductance might be activated by the influx of calcium. Studies of excised patches from human macrophages have demonstrated large conductance calcium- and voltage-dependent potassium channels (Gallin, 1984). If similar channels exist in J774.1 cells (and were to play a role in these outward currents), the internal calcium

would have to be in the order of 10^{-5} M to produce the voltage dependence reported here. This is unlikely since the electrode contains 1·1 mM-EGTA and inward (calcium) currents were not seen in these cells. Furthermore, the time course of the activation and inactivation are inconsistent with a calcium-activated potassium conductance. Thus, this conductance differs from the calcium-dependent potassium conductance previously described in human macrophages. In T lymphocytes, the outward potassium conductance also is blocked by high concentrations of calcium antagonists but shows no apparent calcium dependence (DeCoursey *et al.* 1984).

Stability of currents

The zero-current holding potential recorded immediately after obtaining a whole-cell patch recording usually remained stable for an hour or longer. However, I/V curves frequently changed during the first 10 min of recording. After stabilization, all cells showed a decrease in steady-state current at voltages positive to −40 mV. Activation of the inactivating outward current shifted to more negative voltages in cells exhibiting this current. Our estimate of a 8 mV shift in the conductance/voltage relation is most likely an underestimate because of the time (3–4 min) required to obtain the initial I/V relation. The time course and magnitude of the shift in these macrophage-like cells is similar to that seen in lymphocytes by Fukushima *et al.* (1984). Two general mechanisms have been proposed to account for the conductance changes with time seen using patch electrodes: (1) dilution/loss of intracellular modulatory substances, and (2) alterations of membrane surface charge (Fernandez *et al.* 1984). The observation that activation of the inward current did not shift under whole-cell recording conditions suggests that the shift of the activation of the outward current was not due to a generalized phenomenon such as a change in surface charge.

The authors would like to acknowledge Drs L. McKinney and J. Freschi for their critical reading of the manuscript. The work has been submitted in partial fulfilment of the requirements for the Ph.D. degree for P.A.S. who was supported by a Graduate Fellowship from USUHS. The work was supported by the Armed Forces Radiobiology Research Institute, Defense Nuclear Agency under Research Work Unit 00020. The views presented in this paper are those of the authors; no endorsement by the Defense Nuclear Agency has been given or should be inferred.

REFERENCES

ALMERS, W. (1972*a*). Potassium conductance changes in skeletal muscle and the potassium concentration in the transverse tubules. *Journal of Physiology* **225**, 33–56.

ALMERS, W. (1972*b*). The decline of potassium permeability during extreme hyperpolarization in frog skeletal muscle. *Journal of Physiology* **225**, 57–83.

BERTON, G. & GORDON, S. (1983). Superoxide release by peritoneal and bone marrow derived mouse macrophages. Modulation by adherence and cell activation. *Immunology* **49**, 693–704.

BLOOM, B. R., DIAMOND, B., MUSCHEL, R., ROSEN, N., SCHNECK, J., DAMIANI, G., ROSEN, O. & SCHARFF, M. (1978). Genetic approaches to the mechanism of macrophage functions. *Federation Proceedings* **37**, 2765–2771.

CAHALAN, M. D., CHANDY, K. G., DECOURSEY, T. E. & GUPTA, S. (1985). A voltage-gated potassium channel in human T lymphocytes. *Journal of Physiology* **358**, 197–237.

CHANDRY, K. G., DECOURSEY, T. E., CAHALAN, M. D., MCLAUGHLIN, C. & GUPTA, S. (1984). Voltage gated potassium channels are required for human T lymphocyte activation. *Journal of Experimental Medicine* **160**, 369–385.

COHEN, M. S., RYAN, J. L. & ROOT, R. K. (1981). The oxidative metabolism of thioglycollate-elicited mouse peritoneal macrophages: The relationship between oxygen, superoxide and hydrogen peroxide and the effect of monolayer formation. *Journal of Immunology* **127**, 1007–1011.

DAMAINI, G., KIYOTAKI, C., SOELLER, W., SASADA, M., PEISACH, J. & BLOOM, B. R. (1980). Macrophage variants in oxygen metabolism. *Journal of Experimental Medicine* **152**, 808–822.

DECOURSEY, T. E., CHANDY, K. G., GUPTA, S. & CAHALAN, M. D. (1984). Voltage-gated K^+channels in human T lymphocytes: A role in mitogenesis? *Nature* **307**, 465–468.

FENWICK, E. M., MARTY, A. & NEHER, E. (1982). Sodium and calcium channels in bovine chromaffin cells. *Journal of Physiology* **331**, 599–635.

FERNANDEZ, J. M., FOX, A. P. & KRASNE, S. (1984). Membrane patches and whole-cell membranes: a comparison of electrical properties in rat clonal pituitary (GH3) cells. *Journal of Physiology* **356**, 565–585.

FUJIMOTO, M. & KUBOTA, T. (1976). Physicochemical properties of a liquid ion exchanger microelectrode and its application to biological fluids. *Japanese Journal of Physiology* **26**, 631–650.

FUKUSHIMA, Y., HAGIWARA, S. & HENKART, M. (1984). Potassium current in clonal cytoxic lymphocytes from the mouse. *Journal of Physiology* **351**, 645–656.

FUKUSHIMA, Y., HAGIWARA, S. & SAXTON, R. E. (1984). Variation of calcium current during the cell growth cycle in mouse hybridoma lines secreting immunoglobulins. *Journal of Physiology* **355**, 313–321.

GALLIN, E. K. (1981). Voltage clamp studies on macrophages from mouse spleen cultures. *Science* **21**, 458–460.

GALLIN, E. K. (1984). Calcium- and voltage-activated potassium channels in human macrophages. *Biophysical Journal* **46**, 821–825.

GALLIN, E. K. & GALLIN, J. I. (1977). Interaction of chemotactic factors with human macrophages. *Journal of Cell Biology* **75**, 277–289.

GALLIN, E. K. & LIVENGOOD, D. R. (1981). Inward rectification in mouse macrophages: Evidence for a negative resistance region. *American Journal of Physiology* **241**, C9–17.

GALLIN, E. K., WEIDERHOLD, M. L., LIPSKY, P. E. & ROSENTHAL, A. S. (1975). Spontaneous and induced membrane hyperpolarizations in macrophages. *Journal of Cellular Physiology* **86**, 653–662.

HAGIWARA, S., MIYAZAKI, S. & ROSENTHAL, N. P. (1967). Potassium current and the effect of caesium on this current during the anomalous rectification of the egg cell membrane of a starfish. *Journal of Physiology* **67**, 621–638.

HAGIWARA, S. & TAKAHASHI, K. (1974). The anomalous rectification and cation selectivity of the membrane of a starfish egg cell. *Journal of Membrane Biology* **18**, 61–80.

HAMILL, O. P., MARTY, A., NEHER, E., SAKMANN, B. & SIGWORTH, F. (1981). Improved patch-clamp techniques for high-resolution current recording from cells and cell-free membrane patches. *Pflügers Archiv* **391**, 85–100.

IKEDA, S. R. & WEIGHT, F. F. (1984). Inward rectifying potassium currents recorded from rat basophilic leukemia cells by whole cell patch clamp. *Society for Neuroscience Abstracts* **10**, 870.

LAZDINS, J. K., KOECH, D. K. & KARNOVSKY, M. L. (1980). Oxidation of glucose by mouse peritoneal macrophages: A comparison of suspensions and monolayers. *Journal of Cellular Physiology* **195**, 191–196.

LEECH, C. A. & STANFIELD, P. R. (1981). Inward rectification in frog skeletal muscle and its dependence on membrane potential and external potassium. *Journal of Physiology* **319**, 295–309.

MATTESON, D. R. & DEUTSCH, C. (1984). K channels in T lymphocytes: A patch clamp study using monoclonal antibody adhesion. *Nature* **307**, 468–471.

OHMORI, H. (1978). Inactivation kinetics and steady-state current noise in the anomalous rectifier of tunicate egg cell membranes. *Journal of Physiology* **281**, 77–90.

OLIVERA-CASTRO, G. M. & DOS REIS, G. A. (1981). Electrophysiology of phagocytic membranes: III. Evidence for a calcium-dependent permeability change during slow hyperpolarizations of activated membranes. *Biochimica et biophysica acta* **640**, 500–511.

POFIT, J. F. & STRAUSS, P. R. (1977). Membrane transport by macrophages in suspension and adherent to glass. *Journal of Cell Physiology* **92**, 249–256.

RALPH, P. & NAKOINZ, I. (1975). Phagocytosis and cytolysis by a macrophage tumor and its cloned cell line. *Nature* **257**, 393–394.

SAKMANN, B. & TRUBE, G. (1984). Conductance properties of single inwardly rectifying potassium channels in ventricular cells from guinea-pig heart. *Journal of Physiology* **347**, 641–657.

SCHWARZE, W. & KOLB, H. A. (1984). Voltage-dependent kinetics of an ionic channel of large unit conductance in macrophages and myotube membranes. *Pflügers Archiv* **402**, 281–291.

SHEEHY, P. A. & GALLIN, E. K. (1984). Electrophysiological properties of the macrophage-like cell line J774.1. *Biophysical Journal* **45**, 58a.

SNYDERMAN, R., PIKE, M., FISCHER, D. & KOREN, H. (1977). Biologic and biochemical activities of macrophage cell lines P388D1 and J774.1. *Journal of Immunology* **119**, 2060–2066.

STANDEN, N. B. & STANFIELD, P. R. (1979). Potassium depletion and sodium block of potassium currents under hyperpolarization in frog skeletal muscle. *Journal of Physiology* **294**, 497–520.

UNKELESS, J. C., KAPLAN, G., PLUTNER, H. & COHN, Z. A. (1979). Fc-Receptor variants of a mouse macrophage cell line. *Proceedings of the National Academy of Sciences of the U.S.A.* **761**, 1400–1404.

YOUNG, J., UNKELESS, J. C., KABACK, H. R. & COHN, Z. A. (1983). Macrophage membrane potential changes associated with γ_2b/γ_1Fc receptor-ligand binding. *Proceedings of the National Academy of Sciences of the U.S.A.* **80**, 1357–1361.

YPEY, D. L. & CLAPHAM, D. E. (1984). Development of a delayed outward-rectifying K^+ conductance in cultured mouse peritoneal macrophages. *Proceedings of the National Academy of Sciences of the U.S.A.* **81**, 3083–3087.

ARMED FORCES RADIOBIOLOGY RESEARCH INSTITUTE
SCIENTIFIC REPORT
SR86-4

0022-3565/86/2361-0037$00.00/0
THE JOURNAL OF PHARMACOLOGY AND EXPERIMENTAL THERAPEUTICS
Vol. 236, No. 1
Copyright © 1986 by The American Society for Pharmacology and Experimental Therapeutics
Printed in U.S.A.

In Vivo Dephosphorylation of WR-2721 Monitored by ^{31}P NMR Spectroscopy[1]

S. A. KNIZNER, A. J. JACOBS, R. C. LYON[2] and C. E. SWENBERG

Departments of Radiation Sciences (S.A.K., R.C.L., C.E.S.) and Biochemistry (A.J.J.), Armed Forces Radiobiology Research Institute, Bethesda, Maryland

Accepted for publication September 30, 1985

ABSTRACT

The *in vivo* dephosphorylation of the radioprotective agent S-2-[3-(aminopropylamino)]ethylphosphorothioic acid (WR-2721) in male CD2F$_1$ mice was measured by ^{31}P NMR spectroscopy after i.p. injection. The disappearance of the WR-2721 phosphate NMR signal with time was concurrent with an increase and splitting of the inorganic phosphate NMR signal. The more acidic inorganic phosphate resonance is shown to be attributed to phosphate (inorganic phosphate) in the urine. Using regression first-order kinetic analysis of data, after i.p. injection of 600 mg/kg, the half-life of WR-2721 was determined to be 40.9 ± 5.9 (S.D.) min (n = 10).

^{31}P NMR spectroscopy has been used to observe small, highly mobile phosphate compounds, such as ATP, PCr, sugar phosphates and Pi, in tissues (Gadian *et al.*, 1979; Gadian and Radda, 1981). *In vivo* studies have been limited to the observation of endogenous phosphate metabolites. In this investigation, the metabolism of an exogenously administered phosphate containing radioprotectant has been monitored *in vivo* by ^{31}P NMR. The NMR technique has the dual advantage of being noninvasive and nondestructive, which makes it ideal for performing serial examinations of the same subject.

WR-2721, S-2-[3-(aminopropylamino)]ethylphosphorothioic acid, is a phosphorothioate that exerts a radioprotective effect in several animal species (Davidson, 1980). Because this drug protects normal tissues to a greater extent than most malignant tissues (Yuhas and Storer, 1969), its use in cancer radiotherapy is being investigated. Phase I and II clinical trials are currently under way (Kligerman *et al.*, 1980). Presumably this drug is dephosphorylated *in vivo* to yield the active thiol form of the drug (WR-1065) and Pi (Yuhas, 1970; Harris and Phillips, 1971) as illustrated by the reaction

$$H_2N(CH_2)_3HN(CH_2)_2SPO_3H_2 \rightarrow H_2N(CH_2)_3HN(CH_2)_2SH + H_3PO_4.$$

Most previous studies investigating the metabolism of this drug have used ^{35}S radiolabeled WR-2721 (Kollman *et al.*, 1971; Washburn *et al.*, 1974; Utley *et al.*, 1976; Yuhas, 1980). However, this technique does not monitor the conversion of WR-2721 to WR-1065. The appearance of WR-1065 can be monitored by a combination of radiolabel and high-performance liquid chromatography techniques (Utley *et al.*, 1984), although this requires time consuming tissue extractions and several mice to assemble a time study. Inasmuch as only phosphorylated compounds can be observed by ^{31}P NMR, the rate of decrease of the WR-2721 phosphate signal constitutes a direct measure of the dephosphorylation process. The ^{31}P signal from WR-2721 can be easily observed *in vivo* as its resonance is clearly resolved and is well separated from endogenous phosphate signals. Furthermore, this technique allows the increase in Pi to be monitored simultaneously. In this study we report the determination of the rate of *in vivo* dephosphorylation of WR-2721 in mice.

Methods

Phosphorus NMR spectra were acquired using a Nicolet NT-200 Wide Bore NMR, equipped with an Oxford magnet (4.7 Telsa) and a Nicolet 1280 Computer. A 25 mm ^{31}P probe was used in all experiments. Spectra were acquired without a field frequency lock, and without proton decoupling. Magnetic field homogeneity was adjusted by maximizing the proton free induction decay from water in the sample.

^{31}P NMR spectra were obtained at 80.98 mHz, with a sweep width

Received for publication May 20, 1985.
[1] This work was supported by Armed Forces Radiobiology Research Institute, Defense Nuclear Agency, under Research Work Unit MJ 00083. Views presented in this paper are those of the authors; no endorsement by the Defense Nuclear Agency has been given or should be inferred. Research was conducted according to the principles enunciated in the "Guide for the Care and Use of Laboratory Animals" prepared by the Institute of Laboratory Animal Resources, National Research Council.
[2] Present address: Clinical Pharmacology Branch, National Cancer Institute, National Institutes of Health, Bethesda, MD 20205.

ABBREVIATIONS: PCr, phosphocreatine; Pi, inorganic phosphate.

of ± 3000 Hz, using 8K data points. A one-pulse sequence, consisting of a 78° pulse (35 μsec), repeated every 1.56 seconds, was time averaged for 192 acquisitions (5 min). The broad spectral component, consisting of contributions from bone phosphates and phospholipids, was removed by the convolution difference technique (Campbell *et al.*, 1973). The signal was enhanced further by summing sequential pairs of spectra. Resulting spectra therefore represent average concentrations over a 10-min period. Relative concentrations of phosphorus-containing compounds in each spectrum were determined by computer integration of peak areas using standard Nicolet software. The pH was calculated using the formula $pH = 6.72 + \log_{10}(\delta - 3.27)/(5.69 - \delta)$, where δ is the difference in chemical shift between PCr and Pi (Dawson *et al.*, 1977; Bailey *et al.*, 1981).

Male $CD2F_1$ mice (Charles River Breeding Laboratories, Inc., Wilmington, MA), 8 to 10 weeks old and weighing 20 to 25 g, were used in this study. The maximum tolerated dose ($LD_{10/30}$) for WR-2721 in this strain of mice is approximately 800 mg/kg. WR-2721 was obtained from Division of Experimental Therapeutics, Walter Reed Army Institute of Research (Wash. DC). Solutions of WR-2721 were prepared in neutralized sterile water immediately before use, and mice were injected i.p. or s.c. behind the neck, with 600 mg/kg of drug. In one experiment, 0.5 ml of 0.5 M phosphate (pH 7.2) in 0.9% saline was injected i.p.

Mice were contained in an open-ended 25 mm glass NMR tube. The mouse entered the bottom of the tube and was held in a relatively immobile position between two vortex plugs. A large hole in the upper vortex plug provided ventilation for the mouse. The transmitter/receiver coils of the probe covered the abdominal and hindquarter regions of the mouse. Inside the magnet, air was continually vented around the NMR tube to dissipate heat. Probe temperature was 24.0 ± 1.0°C, and was monitored continually.

To determine the half-life of WR-2721 in each mouse, data were fit, using regression analysis, to an exponential of the form $A(t) = 100^* \exp(-Kt)$, where $A(t)$ is the relative area of the WR-2721 signal at time t (in minutes). The half-life (in minutes), $T_{1/2}$, in terms of K is given $T_{1/2} = (\ln 2)/K$. The increase in urinary Pi with time was modeled by the equation $B(t) = C[1 - \exp(-Kt)]$, where $B(t)$ is the area of the

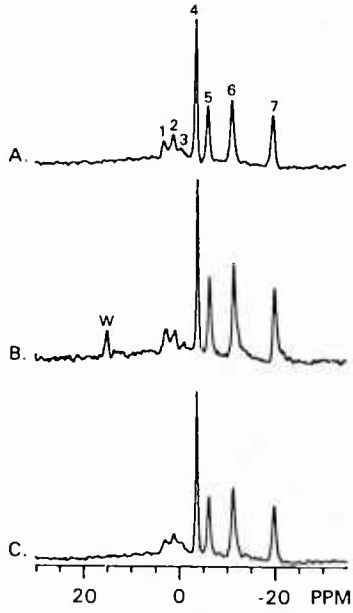

Fig. 1. ^{31}P NMR spectrum of the abdominal and hindquarter regions of a mouse. A, naive mouse before injection; B, after i.p. injection of 600 mg/kg of WR-2721; C, same mouse 24 hr postinjection. Peak assignments are as follows: 1) sugar phosphates (2.8 ppm); 2) Pi (1.05 ppm); 3) unidentified resonances; 4) PCr (−3.75 ppm); 5) γ-ATP phosphate (−6.25 ppm), 6) α-ATP phosphate (−11.30 ppm); 7) β-ATP phosphate (−19.9 ppm); and W, phosphate of WR-2721 (15.10 ppm).

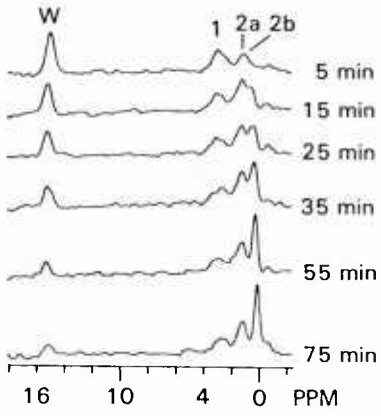

Fig. 2. ^{31}P NMR spectra of representative mouse demonstrating decrease of WR-2721 and increase of Pi with time postinjection. Peak assignments are: W, WR-2721; 2a, cellular Pi; 2b, urinary Pi. Times indicated are midpoint of spectral acquisition time. An increase in urinary Pi, concomitant with an upfield shift, indicating a decrease in pH, is also observable.

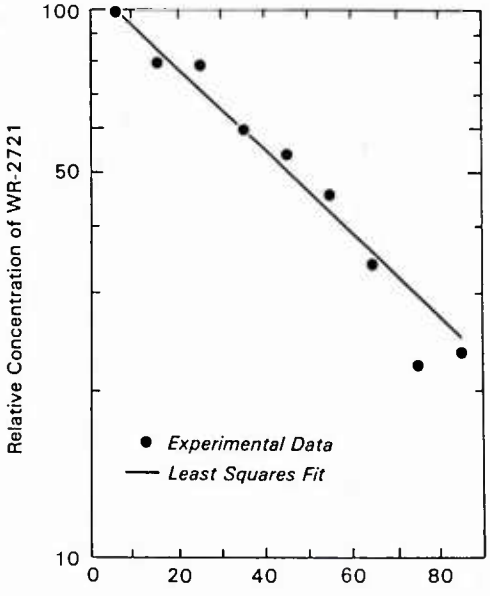

Fig. 3. Decrease in relative concentration of WR-2721 *in vivo* as a function of time after injection; 100% represents integrated area of WR-2721 signal in first spectrum. Using a least-squares analysis, a decreasing exponential was fit to data (see "Methods"), and a half-life of 40.3 ± 2.1 min was obtained for this mouse.

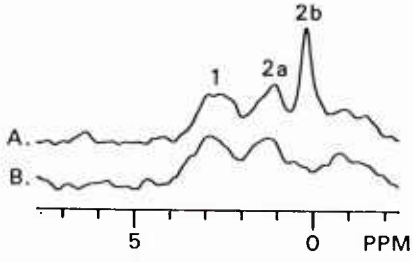

Fig. 4. Pi region of ^{31}P NMR spectrum of mouse. Peak assignments are as in figure 2. Spectrum A was taken 15 min after mouse had been injected with 0.5 ml of 0.5 M phosphate in 0.9% saline. Spectrum B was obtained after mouse was forced to urinate. Cellular pH was calculated to be 7.1 and urinary pH, 6.4 ± 0.1.

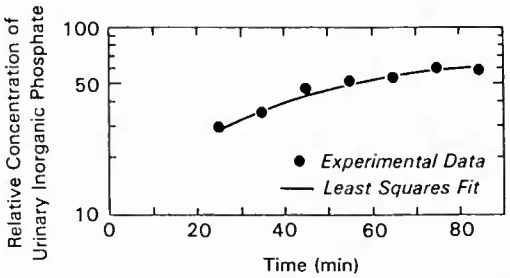

Fig. 5. Increase in relative concentration of urinary Pi *in vivo* as a function of time after injection of WR-2721. Data shown were obtained from same mouse as data in figure 3. Data were fit to an exponential (see "Methods"), using rate constant obtained from decrease of WR-2721 with time.

urinary Pi resonance at time t. The value used for K was that obtained from the decrease of the WR-2721 signal.

Results

The ^{31}P NMR spectrum (fig. 1A) of the abdominal and hindquarter regions of a mouse is similar to that obtained on *in vitro* (Houl *et al.*, 1974; Burt *et al.*, 1976a) and *in vivo* (Burt *et al.*, 1979; Ross *et al.*, 1981) muscle preparations. The peak assignments are given in the caption of figure 1. The chemical shift of the Pi resonance is known to vary with pH (Moon and Richards, 1973) and was therefore used to calculate changes in urinary pH after administration of WR-2721. The minor unidentified resonances appearing in the region between Pi and PCr are typical of phosphodiesters (Burt *et al.*, 1976b). Minor contributions from ADP and NAD to the α-ATP and γ-ATP signals, which are seen in tissue extracts, are usually not detectable in intact tissue.

After i.p. injection of WR-2721 a resonance attributable to its phosphate moiety is immediately evident at 15.1 ppm (fig. 1B). The position of this resonance is typical of phosphorothioates (Smithers and O'Sullivan, 1984), and is well separated from that of endogenous phosphates. Twnety-four hours postinjection another spectrum was acquired, and it can be seen that the WR-2721 signal has disappeared completely (fig. 1C).

Figure 2 demonstrates the disappearance of the WR-2721 phosphate signal with time, and a concurrent increase, and subsequent splitting of the Pi resonance. The rate of decrease in the area of the WR-2721 signal as a function of time, relative to the amount present in the initial spectrum, was monitored for several mice (n = 10). The average half-life of the drug for this group of mice was determined to be 40.9 ± 5.9 (S.D.) min (see fig. 3).

For the mice injected s.c. in the back of their necks, no WR-2721 signal was observable. However, the increase in Pi was noted (figure not shown). The signal attributable to cellular Pi (fig. 2A, peak 2a) is a fairly broad resonance because it represents cytoplasmic Pi and Pi from many subcellular compartments, all of which may have slightly different pH microenvironments. The chemical shift of this resonance signal remains constant during the time course of the dephosphorylation of WR-2721 and corresponds to a pH of 7.0 ± 0.1. The narrowness of the emerging Pi resonance line (labeled 2b) suggests that it was due to Pi located in a homogeneous pH environment. The upfield shift of this resonance with time indicates that this environment is continually becoming more acidic, with the pH decreasing from 6.6 to 6.2 ± 0.1 during the first 75 min postinjection. These observations are highly suggestive that the newly formed resonance may be attributable to Pi in the urine.

To test this hypothesis, a mouse was injected with 0.5 ml of phosphate in 0.9% saline at pH 7.2. Fifteen minutes postinjection the splitting of the Pi signal was clearly observable as is evident in figure 4. The two resonance correspond to pHs of 7.0 (cellular) and 6.4 ± 0.1 (urinary). The mouse was then partially removed from the NMR tube and forced to urinate by application of pressure to the bladder region. Approximately 0.2 ml of clear urine was expelled. Immediately after urination, another spectrum of the same mouse was obtained. It is apparent from figure 4B that after urination the narrow, more acidic phosphate resonance disappeared. The increase in urinary Pi, after injection of WR-2721, with time is shown in figure 5.

Discussion

The nondestructive technique of ^{31}P NMR has been used to monitor *in vivo* dephosphorylation of WR-2721. We interpret our results in terms of two compartmental model,

$$\begin{array}{l} \text{A WR-2721} \xrightarrow{K} \text{WR-1065} + H_3PO_4 \\ \quad K_D \downarrow \\ \text{B WR2721} \end{array}$$

where K is the rate of dephosphorylation and K_D is the rate at which the drug is eliminated out of the region (A) accessed by the receiver coils. Compartment B denotes regions of the mouse outside the volume enclosed by the transmitter/receiver coils of the probe, for example neck and head of mouse. When mice were injected s.c. in back of their necks no WR-2721 phosphate signal was detectable, although an increase in urinary Pi was observed. Thus, the rate of dephosphorylation is faster than is the dispersion rate from site of injection. It is this observation which supports our contention that after i.p. injection of WR-2721 dephosphorylation is being monitored and not diffusion, *i.e.*, $K \gg K_D$. This conclusion assumes the K/K_D is unchanged for the two injection sites. The ^{31}P NMR spectrum of the abdominal and hindquarter regions of a mouse clearly exhibits a resonance attributable to the phosphate moiety of WR-2721 after i.p. administration of this drug. By monitoring the time-dependent decrease of this signal, the half-life of WR-2721 in male $CD2F_1$ mice, after i.p. injection of 600 mg/kg, was determined to be 40.9 ± 5.9 (S.D.) min (n = 10).

Phosphorothioates are among the most effective radioprotectors known, and it is postulated that dephosphorylation of these drugs is a prerequisite to the formation of active radioprotectants. Previous investigations into the metabolism of WR-2721 have predominantly used the ^{35}S radiolabeled form of the drug. When radioactivity due to this label is measured, it must be realized that all metabolic forms of the drug are contributing to the radioactivity and not just WR-2721. This technique is useful for monitoring the biodistribution of WR-2721 and its metabolites, but it cannot be used to determine dephosphorylation kinetics.

Most investigations into the radioprotective effect of WR-2721 on animals have been conducted with administration of the drug 15 or 30 min before irradiation. Few detailed studies have concerned themselves with radioprotective efficiency *vs.* time interval between drug treatment and irradiation. Davidson *et al.* (1980), using ICR mice injected i.p. with 600 mg/kg of WR-2721, found that radioprotection was fairly constant when the time between drug injection and irradiation was varied from

15 min to 3 h. Travis *et al.* (1982) monitored radioprotection of mouse skin as a function of drug pretreatment time and found optimal protection when irradiations were conducted 45 min after drug injection. Stewart and Rojas (1982) also measured protection of mouse skin, and found that most protection occurred at 35 to 45 min postinjection, but maximum protection was obtained at a 60-min time interval. These results are consistent with our determination of an *in vivo* half-life of approximately 41 min.

A drawback of the NMR method that deserves mention is that only mobile compounds present inside the volume enclosed by the transmitter/receiver coils of the probe are observable. In this investigation, this region consists of the abdominal and hindquarters area of the mouse. Previous studies monitoring the biodistribution of ^{35}S-radiolabeled WR-2721 have shown a significant accumulation of the radiolabel in liver, kidney, spleen, small intestines, salivary gland and lung (Utley *et al.*, 1976; Washburn *et al.*, 1974; Yuhas, 1980). Of these tissues, only the lung and salivary gland lie outside the NMR observable region. Another disadvantage is the relative insensitivity of the NMR method. For rapid data collection (5–10 min) concentrations of ^{31}P metabolites must exceed 0.1 M. In this experiment, 10 min were needed to acquire the spectrum; therefore, we cannot exactly measure the total initial amount of WR-2721 present. Instead, all signal areas were related to the area of the WR-2721 signal obtained in the first spectrum. This means that there could be an initial rapid component in the dephosphorylation process which escaped detection by use of nuclear magnetic resonance spectroscopy.

Several reasons for using ^{31}P NMR to observe *in vivo* dephosphorylation of WR-2721 are evident immediately. First, the NMR technique is noninvasive and nondestructive. This makes it possible to perform kinetic metabolic studies on the same subject. Also, each specimen can serve as its own control, that is, it can be examined before and after drug treatment. Compared to other methods used to monitor drug metabolism, the NMR technique is rapid. It does not require the time consuming processes of tissue extractions from several animals before assay. An additional advantage of NMR is its nonselectivity; when performing an *in vivo* ^{31}P NMR experiment, signals from all major mobile phosphorus-containing metabolites are detected. It is this property which permitted the concurrent detection of an increase in urinary Pi, even though our initial attention was focused on the rate of decrease of the WR-2721 phosphate signal. Presently, work is under way examining the *in vivo* dephosphorylation of similar phosphorothioate radioprotectants. The ^{31}P NMR technique can also be used to monitor other *in vivo* and *in vitro* dephosphorylation reactions. Other NMR observable nuclei (*e.g.*, ^{1}H or ^{13}C) could also be used to monitor the metabolism of pharmacologically important compounds, if the sensitivity of the NMR method is adequate.

Acknowledgments

The authors thank Col. D. Davidson, Walter Reed Army Institute of Research, (Washington, DC), for supplying us with S-2-[3-(aminopropylamino)]ethylphosphorothioic acid (WR-2721) and Dr. K. Huhner, University of Tennessee Hospital, for several helpful suggestions. We also thank Pat Noon for regression analysis fit of the experimental data and Mariann Waldbillig for patiently typing this manuscript.

References

Bailey, I. A., Williams, S. R., Radda, G. K. and Gadian, D. G.: Activity of phosphorylase in total global ischemia in the rat heart. Biochem. J. **196:** 171–178, 1981.

Burt, C. T., Glonek, T. and Barany, M.: Analysis of phosphate metabolites, the intracellular pH, and the state of adenosine triphosphate in intact muscle by phosphorous nuclear magnetic resonance. J. Biol. Chem. **251:** 2584–2593, 1976a.

Burt, C. T., Glonek, T. and Barany, M.: Phosphorous-31 nuclear magnetic resonance detection of unexpected phosphodiesters in Muscle. Biochemistry **15:** 4850–4853, 1976b.

Burt, C. T., Cohen, S. M. and Barany, M.: Analysis of intact tissue with ^{31}P-NMR. Annu. Rev. Biophys. Bioeng. **8:** 1–25, 1979.

Campbell, I. D., Dobson, C. M., Williams, R. J. P. and Xavier, A. B.: Resolution enhancement of protein PMR spectra using the difference between a broadened and a normal spectrum. J. Mag. Res. **11:** 172–181, 1973.

Davidson, D. E., Grenan, M. M. and Sweeny, T. R.: Biological characteristics of some improved radioprotectors. *In* Radiation Sensitizers, Their Use in the Clinical Management of Cancer, Chapter 45, pp. 309–320, Masson Publishing Inc., New York, 1980.

Dawson, M. J., Gadian, D. G. and Wilkie, D. R.: Contraction and recovery of living muscles studied by ^{31}P nuclear magnetic resonance. J. Physiol. (Lond.) **267:** 703–735, 1977.

Gadian, D. G. and Radda, G. K.: NMR studies of tissue metabolism. Annu. Rev. Biochem. **50:** 69–83, 1981.

Gadian, D. G., Radda, G. K., Richards, R. E. and Seeley, P. J.: ^{31}P NMR in living tissue: The road from a promising to an important tool in biology. *In* Biological Applications of Magnetic Resonance, ed. by R. G. Shulman, pp. 463–535, Academic Press, New York, 1979.

Harris, J. W. and Phillips, T. L.: Radiohiological and biochemical studies of thiophosphate radioprotective compounds relelated to cysteamine. Rad. Res. **46:** 362–279, 1971.

Hoult, D. I., Busby, S. J. W., Gadian, D. G., Radda, G. K., Richards, R. E. and Seely, P. J.: Observation of tissue metabolites using ^{31}P nuclear magnetic resonance. Nature (Lond.) **252:** 285–287, 1974.

Kligerman, M. M., Shaw, M. T., Slavik, M. and Yuhas, J. M.: Phase I clinical studies with WR-2721. Cancer Clin. Trials **3:** 217–221, 1980.

Kollmann, G., Martin, D. and Shapiro, B.: The distribution and metabolism of the radiation protective agent aminopentylaminoethylphosphorothioate in mice. Rad. Res. **48:** 542–550, 1971.

Moon, R. B. and Richards, J. H.: Determination of intracellular pH by ^{31}P magnetic resonance. J. Biol. Chem. **248:** 7276–7278, 1973.

Ross, B. D., Radda, G. K., Gadian, D. G., Rocker, G., Esiri, M. and Falconer-Smith, J.: Examination of a case of suspected McArdle's syndrome by ^{31}P nuclear magnetic resonnance. N. Engl. J. Med. **304:** 1338–1342, 1981.

Smithers, G. W. and O'Sullivan, W. J.: Phosphorothioate analogues of 5-phosphoribosyl 1-diphosphate: ^{31}P nuclear magnetic resonance study. Biochemistry **23:** 4773–4778, 1984.

Stewart, F. A. and Rojas, A.: Radioprotection of mouse skin by WR-2721 in single and fractionated treatments. Br. J. Radiol. **55:** 42–47, 1982.

Travis, E. L., DeLuca, A. M., Fowler, J. F. and Padikal, T. N.: The time course of radioprotection by WR-2721 in mouse skin. Int. J. Radiat. Oncol. Biol. Phys. **8:** 843–850, 1982.

Utley, J. F., Marlowe, C. and Waddell, W. J.: Distribution of ^{35}S-labeled WR-2721 in normal and malignant tissues of the mouse. Rad. Res. **68:** 289–291, 1976.

Utley, J. F., Seaver, N., Newton, G. L. and Fahey, R. C.: Pharmokinetics of WR-1065 in mouse tissue following treatment with WR-2721. Int. J. Radiat. Oncol. Biol. Phys. **10:** 1525–1528, 1984.

Washburn, L. C., Carlton, J. E., Hayes, R. L. and Yuhas, J. M.: Distribution of WR-2721 in normal and malignant tissues of mice and rats bearing solid tumors: Dependence on tumor type, drug dose and species. Rad. Res. **59:** 475–483, 1974.

Yuhas, J. M.: Biological factors affecting the radioprotective efficiency of S-2-3-aminopropylamino ethylphosphorothioic acid (WR-2721). $LD_{50(30)}$ doses. Rad. Res. **44:** 621–628, 1970.

Yuhas, J. M.: Active versus passive absorption kinetics as the basis for selective protection of normal tissues by S-2-3-(Aminopropylamino) ethylphosphorothioic acid. Cancer Res. **40:** 1519–1514, 1980.

Yuhas, J. M. and Storer, J. B.: Differential chemoprotection of normal and malignant tissues. J. Natl. Cancer Inst. **42:** 331–335, 1969.

Send reprint requests to: Mr. Steve Knizner, Radiation Sciences Department, Division of Biological Spectroscopy, Armed Forces Radiobiology Research Institute, Bethesda, MD 20814.

ARMED FORCES RADIOBIOLOGY
RESEARCH INSTITUTE
SCIENTIFIC REPORT
SR86-5

RADIATION RESEARCH **104**, 293–302 (1985)

Increase in ϕX174 DNA Radiation Sensitivity Due to Electric Fields

PERCIVAL D. MCCORMACK

Division of Cancer Diagnosis and Biology, National Cancer Institute, National Institutes of Health, Bethesda, Maryland 20205

AND

CHARLES E. SWENBERG

Division of Molecular Radiobiology, Armed Forces Radiobiology Research Institute, Bethesda, Maryland 20814-5145

MCCORMACK, P. D., AND SWENBERG, C. E. Increase in ϕX174 DNA Radiation Sensitivity Due to Electric Fields. *Radiat. Res.* **104**, 293–302 (1985).

The application of an external electric field simultaneously with γ irradiation to an aqueous suspension of ϕX174 DNA (in the RFI form) is shown to increase significantly the number of strand breaks. Tritiated DNA allowed the number of single-strand breaks to be estimated from changes in the scintillation of electrophoretic gel band associated with the fastest mobility moiety. At 400 V ($\approx$2400 V cm^{-1}) the corrected increase (corrected for phoresis of DNA on the stainless-steel plates) in the *G*-value yield is 38%. The increase in damage with field strength appears to follow the increase in reduced dichroism. Dichroism results correspond at 400 V to approximately 10% of the maximum orientation. Our results support the conjecture that this significant increase in DNA–radiation interaction with an electric field is due to field-induced conformation changes in the molecule.

INTRODUCTION

The object of the research reported here was to establish whether or not orientation of DNA in electric fields would result in a significant increase in its sensitivity to damage by ionizing radiation. It is well known that linear polyelectrolytes, particularly polynucleotides and polypeptides, are electrically and optically anisotropic and exhibit the phenomena of birefringence and dichroism (*1*). Basic information on the macromolecular dimensions, size, and shape can be inferred from relaxation kinetics of the field-induced changes. It has been shown that the very large dipole moments which are induced in DNA by external electric fields via displacement of the counterion atmospheres are responsible for its orientation along the field direction (*2*, *3*). The induced dipole moments of linear polyelectrolytes may become very large and depend on the length of the molecule and the ionic density of the medium. For rod-like molecules with lengths the order of 1000 Å, at low ionic density (<10 mol d m^{-1}) induced moments of up to 10^5 D have been determined. The induced dipole moment of an individual linear polyelectrolyte dependence on electric field displays a Langevin-

0033-7587/85 $3.00

like behavior (*4*). Saturation of the polarization occurs at moderately high electric fields; when the induced moment becomes independent of the external field and the molecules behave as possessing permanent dipoles. Intramolecular dipole reorientations in polyelectrolytes induced by electric fields can also occur; an excellent example illustrating this is the rapid helix/coil transition of a polypeptide in a viscous solution (*5*).

The overall rotation of a macromolecule in solution is very slow compared to the fast orientation of dipolar helical sequences. In the case of ϕX174 DNA the normal form is a supercoiled circle which has rod-like characteristics and therefore will orient in an external field. In addition to orientation there will be considerable conformational changes as the field strength increases. With significant orientation and conformational effects of electric field on DNA in solution it would not be unexpected to find a corresponding large change in the interaction of ionizing radiation with DNA via the indirect mechanism. A considerable literature exists on the effects of radiation on DNA in aqueous solutions. We have selected ϕX174 DNA because of the well separated and simple band pattern which it produces in gel electrophoresis for the damaged and undamaged forms.

ELECTRIC DICHROISM OF MACROMOLECULES

Orientation of a suspension of macromolecules in solution can be produced by either static or pulsed electric fields. The applied field-induced orientation results from interactions of the field with the permanent molecular electric dipole, the molecular polarizability, and the transition dipoles of the molecules. In general, the polarizability contribution to the orientational interaction energy is a complex function of the ionic atmosphere of the polyion. Model calculations of the effects of the polarization of the surrounding counterions on the macroions have been performed by Rau and Charney (*6*, *7*). Electric linear dichroism refers to the difference in the selective absorption of light polarized perpendicular to the direction of the external field and the absorption of light polarized parallel to the applied field. By analogy with the definition of birefringence the reduced parallel dichroism (*8*) is defined as

$$\Delta A_{11}/A = (A_{11}(E) - A)/A \tag{1}$$

where A is the isotropic absorbance and A_{11} is the optical absorbance of the solution for light polarized parallel to the applied electric field. The isotropic absorbance is taken to be field independent, that is where dichroism arises only from orientational induced anisotropy. The reduced dichroism, $\Delta A_{11}/A$, is concentration independent. For an ensemble of macroions the reduced parallel dichroism can be written as the product of an optical term, $(G(\theta))$, and an orientation function Φ (*9*)

$$\Delta A_{11}/A = G(\theta)\Phi \tag{2}$$

where θ denotes the angle between the field direction and the transition moment of the absorbing moiety. For optical transitions of the nucleic acid bases at $\lambda = 260$ nm, $G(\theta)$ will approach -1 and Φ will approach unity at high fields (saturation orientation). Charney and Yamaoka (*9*) have determined $G(\theta)$ for DNA in aqueous solution at different salt concentrations (0.09 to 1 m*M* NaCl) and found that at $\lambda = 270$ nm, $G(\theta)$ varied between -0.58 to -0.67 depending on the molecular weight of the DNA.

Our measurement of the specific reduced dichroism dependence on field voltage for a dilute aqueous solution of ϕX174 DNA with 0.8 m*M* Tris buffer is shown in Fig. 1.

The optical density of the solution was 0.15 at 260 nm and 0.077 at 280 nm. In the Kerr cell used for the measurement, the electrode spacing was 0.15 cm; thus it is seen that saturation sets in at about 15,000 V cm^{-1} (2400 V). A least-squares fit of the arc tan function is shown in Fig. 1; however, several other expressions can be shown to fit equally well. A theory of optical activity for circular molecules is currently lacking. There is evidence that unfolding of the coiled molecule occurs as part of the orientation effect (*10*). Transient electric dichroism measurements offer a means of studying conformational changes. In general, one expects the decay of the dichroic signal to exhibit at least two decay constants: a fast transient time constant arising from internal molecular reorientation and a much slower time constant due to reorientation of the entire molecule. This has been confirmed by Revzin and Neumann (*11*) in their studies of the effects of electric field impulse of 30 μs on *E. coli* ribosomal RNA in solution. Transient dichroic measurement by Chen and co-workers (*12*) allowed for the determination of the physical extension of the dG-dC polymer on its transition from its B to Z form. Our transient dichroic measurements on ϕX174 DNA will be reported in a separate publication.

EFFECT OF IONIZING RADIATION ON DNA IN SOLUTION

The types of damage induced in DNA by exposure to ionizing radiation include single-strand breaks, double-strand breaks, cross-linking, and base damage. It is known

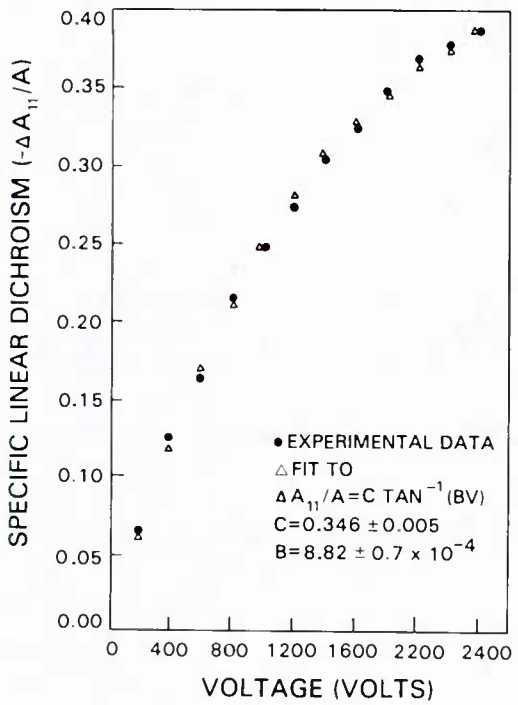

FIG. 1. Specific reduced dichroism versus electric field voltage for ϕX174 DNA in 0.8 m*M* Tris at pH 7.5 with OD = 0.15 at 260 nm.

that DNA damage in aqueous solutions is predominately caused by the indirect action of $OH^{\bullet}$ radicals initially produced by radiolysis of water (*13*). Consider the electrophoretic gel-band pattern for ϕX174 DNA as illustrated in Fig. 2. The normal conformation is that of the supercoiled circle—the RFI form—designated as Band I in Fig. 2. A single-strand break is sufficient to release tension in the RFI form, thereby forming the "nicked" circular form represented in the gel pattern by Band III. This form has the lowest mobility in the gel. A double-strand break causes the circle to unfold and gives rise to the linear form, represented by Band II. In this latter form the DNA would be devoid of any biological activity. If the DNA is tritiated the intensity in each band can be monitored by scintillation counting. Postulating that single hits by γ irradiation produce the "nicked" circular form, then from target theory it can easily be shown that the number of single-strand breaks n_{ssb} (for low total doses) is given by

$$n_{ssb/mol} = \ln \frac{RFI_0}{RFI_D} \tag{3}$$

where RFI_0 denotes the counts/minute in the RFI band for the unirradiated sample and RFI_D is the counts/minute in the RFI band for a total dose of D (rad).

After irradiation of DNA in dilute aqueous solution the number of single-strand breaks per molecule is proportional to the dose,

$$B_{ssb/n\mathrm{T}} = kD \tag{4}$$

where k is the probability of a break per nucleotide (nT) per rad. At a DNA concentration of 0.2 mg/ml the value found for k was 4.15×10^{-7} rad^{-1} (*14*). The molecular weight of ϕX174 DNA is 3.4×10^6 Da, corresponding to 3.5×10^2 Da/nT or approximately 10^4 nT per RFI molecule. Hence the theoretical number of single-strand breaks in ϕX174 DNA per molecule is

$$B_{ssb/mol} = 4 \times 10^{-3} D. \tag{5}$$

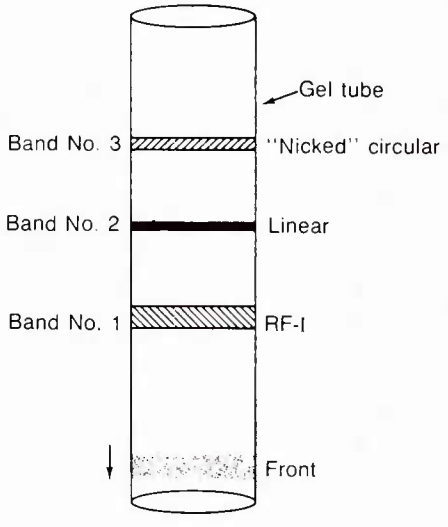

FIG. 2. Gel pattern for ϕX174 DNA.

An alternative expression for the yield of single-strand breaks is the G value, given by

$$G_{\text{ssb/mol}} = 9.65 \times 10^4 C/MD_{37} \tag{6}$$

where C is the concentration of DNA in grams per milliliter, M is the molecular weight in daltons and D_{37} is the 37% survival dose. At a concentration of 0.75 mg/ml the 37% survival dose is the order of 400 rad (*15*).

EXPERIMENTAL DETAILS

Kerr Cell

The same Kerr cell employed in dichroism measurements was used for exposing dilute aqueous solutions of ϕX174 DNA with Tris buffer, EDTA (pH 8.0) to intense ^{60}Co irradiation. A diagram of the cell is shown in Fig. 3. The cell is a high quality Lucite cylinder, out of which a rectangular cavity was cut along the equatorial plane. The cavity was lined by stainless-steel plates spaced 0.15 cm apart. The cavity ends were sealed by Lucite plates screwed down to impinge on Teflon seals. Other fittings included two filling holes, two steel pins which contacted the steel electrodes and connected them via external cables to the power supply. To compute the dose to the solution in the cavity the tissue to air (TAR) ratio was determined both experimentally and theoretically (using the Bragg–Gray principle governing small cavity ionization). With the cell/source configuration used in the experiment, the computed TAR value was 0.94, a value confirmed experimentally. Thus for an air dose rate of 7005 rad/min this gave a solution dose rate of 6505 rad/min. There was an additional dose of 487 rad due to the finite time it takes to raise and lower the cobalt source. The maximum total exposure time was 2 min giving a total dose of 13,627 rad.

Electric Power Supply

The mobility of DNA in solution is quite high, of the order of 5×10^{-4} cm^2 s^{-1} V^{-1} at a sodium ion concentration of 10 mM. With electrode separation of 0.15 cm at 400 V, it is estimated that all DNA would be phoresed on the electrodes in about 125 ms. DNA molecules bind covalently to the metal and field reversal unfortunately does not remove it. The power supply could deliver a maximum of 2000 V at 100 mA. The vacuum relay which accomplished the field reversal had an "ON" time of 140 ms with a "dead" period between reversal of about 50 ms. Figure 4 reports the

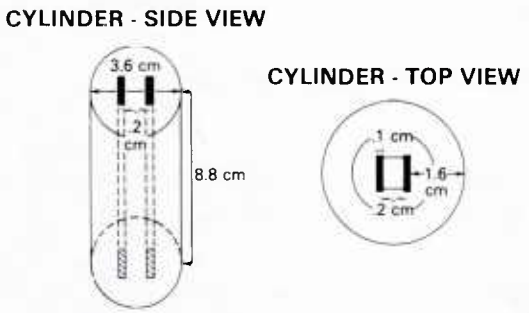

FIG. 3. Schematic of Kerr cell. Cylinder made of high quality Lucite with stainless-steel electrodes.

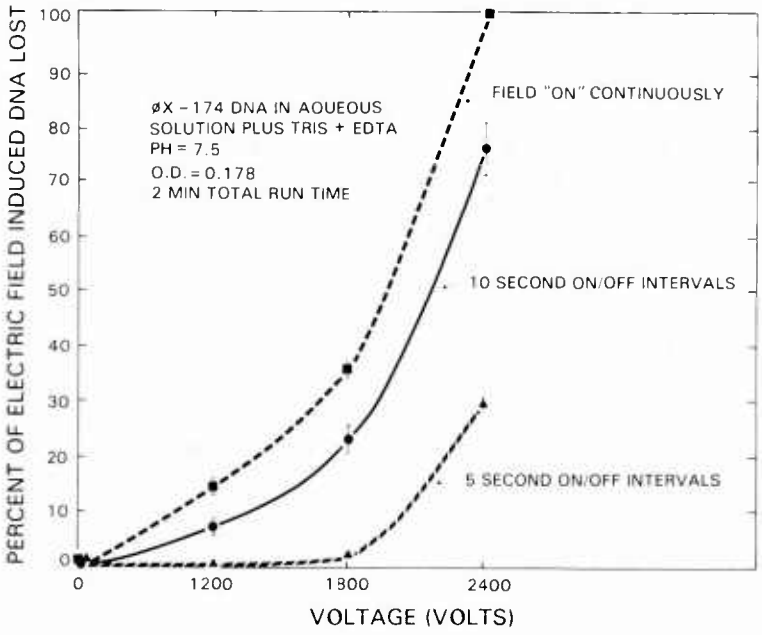

FIG. 4. Electric field-induced loss of DNA by electrophoresis in the Kerr cell.

results of measuring DNA loss by electrophoresis in the cell. The percentage loss of DNA was determined by taking 2 μl of the exposed DNA (to the field dose for periods of 2 min) and adding them to 10 ml of scintillation "cocktail" for counting (the DNA was tritiated). It is evident that there is an unacceptably large loss of DNA even at 400 V. These losses can be reduced by switching the field ON and OFF every 10 s and even more if the interval was reduced to 5 s. In the second radiation experiment, this tactic was resorted to and allowed a field voltage of up to 400 V to be utilized. Under these conditions the total exposed time to the electric field was reduced to 1 min. In our first experiment, the field was applied continuously, but the maximum voltage used was 250 V. In all cases, corrections to computed yield values for electrophoresis losses were made.

ϕX174 DNA

The ϕX174 DNA used was supplied in the Replicative Form I (Genex Corp., Gaithersburg, MD). Some nicked circular form was present. The tritiated DNA allowed for quantitative assessment of damage by scintillation counting as discussed above. The solution concentration was 0.75 mg/ml for the experiment. This was diluted to produce an optical density between 0.18 to 0.20. The solution was buffered with Tris and EDTA to pH 8.

Gel

Gel pattern for the solutions used is shown in Fig. 5 (background—0 V/0 radiation). One percent agarose tube gels were formed and ethidium bromide dye was used after the electrophoresis. The gel tubes were examined under uv light and photographed. The bands (I, II, and III) were dissected out of the gels placed in containers with 20 ml of scintillation "cocktail," and the relative DNA contents were measured in an automatic scintillation counter unit.

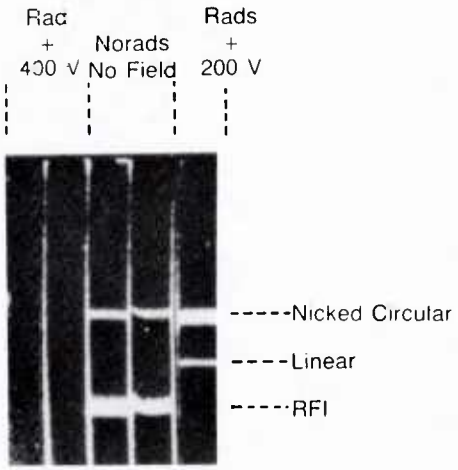

FIG. 5. Gel bands for radiation experiment No. 2.

EXPERIMENTAL RESULTS

First Radiation Experiment

In this experiment three exposures of the ϕX solution in the Kerr cell to the ^{60}Co source were made. The exposures were 2 min long, with a total absorbed dose of 13,622 rad for each exposure. The electric field was ON continuously. The conditions of the three exposures were

Number 1	Radiation + 250-V field
Number 2	Radiation + 200-V field
Number 3	Radiation only.

In addition three control measurements were made:

Number 4	250-V field only
Number 5	200-V field only
Number 6	Background—0 radiation/0 field.

The production of the nicked circular form (Band No. 3) and linear form (Band No. 2) through radiation interaction is clearly seen for the "rad only" case, and these bands are more pronounced in the presence of the electric field (200 and 250 V). A fourth band is evident and corresponds to low mobility material considered to be a contaminant.

Table I summarizes the relative intensities in the various bands in terms of scintillation counts/minute. It is seen that there is a substantial loss of DNA through electrophoresis even at the 250- and 200-V level.

Using Eq. (2) the yield of single-strand breaks (or more) per ϕX molecule, $G_{ssb/mol}$ was computed from Table I for the three radiation runs. These are given in column 1 of Table II and designated as "uncorrected." The corrected values, obtained by subtracting out the electrophoretic losses, are given in column 2. The percentage increase in radiation damage (single-strand breaks and more), attributable to the electric field effect, is also computed and is 40% at 250 V (1800 V/cm) and 27% at 200 V (1200 V/cm).

TABLE I

Scintillation Counts per Minute—Experiment No. 1

Run No./Band No.	*4*	*3*	*2*	*1*
1. rad + 250 V	810	7,100	806	1,612
2. rad + 200 V	680	12,700	218	2,238
3. rad	640	25,400	4,500	5,455
4. 250 V	791	1,100	484	18,621
5. 200 V	740	950	640	20,500
6. Background	868	7,140	545	31,221

Second Radiation Experiment

In this experiment, voltages of 200, 250, 300, 350, and 400 were used. As mentioned earlier, to minimize electrophoretic loss of DNA, the field was switched ON for 5 s and OFF for 5 s sequentially over the 2-min exposure interval. Some reduction in field effect would be expected, and so the results of Experiments 1 and 2 are not exactly comparable. The gel patterns obtained for the 400 V, 300 V, and background cases are shown in Fig. 5. The increase in nicked circular and linear form can be seen at 200 V. Very faint bands were apparent at 400 V and most of the effect here is due to electrophoretic loss.

Table III shows the background, 400 V, and 400 V with γ-radiation results in counts/minute, the uncorrected and corrected single-strand break yields, and the percentage increase in single-strand breaks.

It is seen that at 400 V the corrected increase in the value of the yield, $G_{\text{ssb/mol}}$, is 38%. The predicted number of ssb for ϕX174 DNA molecules at a concentration of 2 mg/ml is

$$G_{\text{ssb/mol}} = 4.15 \times 10^{-3} D$$

where D is the dose in rad. For a total dose of 13,627 rad this relationship predicts a yield of about 56 ssbs per ϕX molecule. The concentration used here was about 0.008 mg/ml and scaling linear, a yield value of about 2 would be expected. Values obtained in the "rad only" cases of experiments 1 and 2 are in the vicinity of 1.7. Within experimental errors (estimated at about ±20%), the correspondence is close enough to confirm the reliability of the results obtained in these experiments.

Figure 6 shows the percentage increase in damage plotted versus field strength. The corrected and uncorrected curves are shown and the specific reduced dichroism curve is superposed. The increase in damage with field strength appears to follow the increase

TABLE II

Single-Strand Break Yields in Experiment No. 1

Run No.	*Uncorr.*	*Corr.*	*% Increase*
1. rad + 250 V	2.96	2.44	40
2. rad + 200 V	2.63	2.21	27
3. rad	1.74	—	—

TABLE III

Radiation Results—Experiment No. 2

	Band No.			*G*		*% Inc. in G*	
Run	*3*	*2*	*1*	*Uncorr.*	*Corr.*	*Uncorr.*	*Corr.*
1. Background	1500	560	8300	—	—	—	—
2. Radiation	6350	1250	1500	1.71	—	—	—
3. 400 V	1250	940	3800	—	—	—	—
4. rad + 400 V	4620	850	358	3.14	2.36	83	38

in reduced dichroism. At a field strength of 2400 V/cm (400 V) the increase is about 38%. Dichroism results correspond at 400 V to only about 10% of the maximum orientation. This observation supports the conjecture that this significant increase in DNA/radiation interaction is due to field-induced conformation changes in the molecule.

CONCLUSIONS

The results demonstrate a significant electric field-induced increase in ^{60}Co γ-ray damage to ϕX174 DNA in dilute aqueous solution, even at field strengths of 2400 V/cm and below. It is likely that the conformational changes in the ϕX molecule are

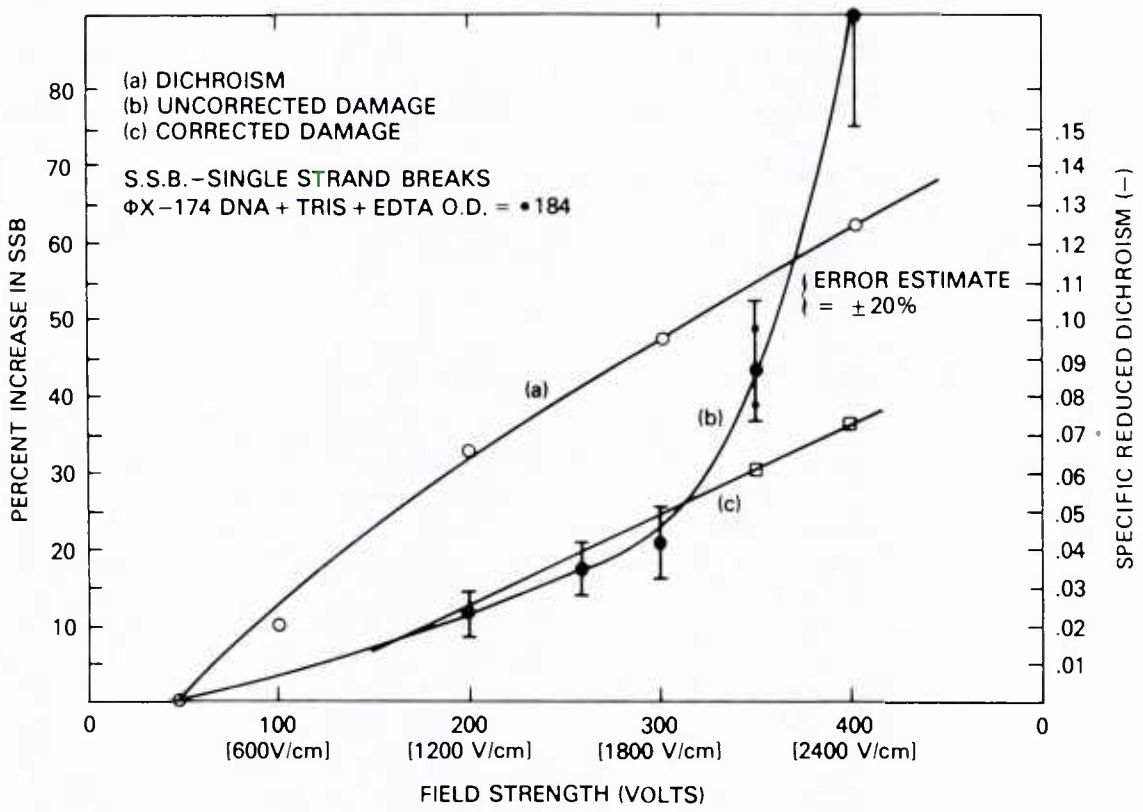

FIG. 6. Increase in radiation damage of ϕX174 versus field strength (V/cm). Open and solid circles and open boxes denote data points. Lines drawn for clarity.

the source of this increased interaction, leading to considerable exposure of reactive sites on the DNA molecule to the action of the $OH^{\cdot}$ radicals. Linear extrapolation of the damage versus field strength curve, to a saturation value of 15,000 V/cm, would predict that the percentage increase in damage would rise to over 250%. This large predicted increase needs to be verified by further experiments. The present results are promising enough to warrant a similar investigation using intracellular DNA. In this connection it must be noted that the phenomena of electric dichroism has already been established for chromatin subunits (*16*, *17*).

ACKNOWLEDGMENTS

The valuable assistance and advice of Major M. Hagan, Armed Forces Radiobiology Research Institute, is gratefully acknowledged and also that of Dr. Charney, Dr. Chen, and Dr. Rau of The Laboratory of Chemical Physics, National Institutes of Health.

RECEIVED: January 14, 1985; REVISED: July 15, 1985

REFERENCES

1. E. FREDERICQ and C. HOUSSIER. *Electric Dichroism and Birefringence.* Oxford Univ. Press (Clarendon), London, 1973.
2. M. EIGEN and G. SCHWARTZ, Ein Orientierungs-Feldeffekt der elektrischen Leitung in Polyelektrolytlösungen. *Z. Phy. Chem. N.F.* **4**, 380 (1955).
3. M. EIGEN and G. SCHWARTZ, In *Electrolytes* (B. Pesce, Ed.), p. 309. Pergamon, New York, 1962.
4. S. KIELICH, Frequency doubling of laser light in an isotropic medium with an electrically destroyed center of inversion. *Opto-electronics*, **2**, 5–20 (1970).
5. K. U. BERGER, Untersuchungen zur Wirkung von monochromatischer Vakuum-UV-Strahlung auf DNA. *Z. Naturforsch.* **24B**, 722–728 (1969).
6. D. RAU and E. CHARNEY, Electric dichrosim of DNA, influence of the ionic environment on the electric polarizability. *Biophys. Chem.* **17**, 35–50 (1983).
7. D. RAU and E. CHARNEY, Polarization of the ion atmosphere of a charged cylinder. *Biophys. Chem.* **14**, 1–9 (1981).
8. E. CHARNEY, The role of the ionic environment in the orientation of nucleic acids in electric fields. *Biophys. Chem.* **11**, 157–166 (1980).
9. E. CHARNEY and K. YAMAOKA, Electric dichroism of deoxyribonucleic acid in aqueous solutions. *Biochemistry* **21**, 834–842 (1982).
10. R. L. JERNIGAN and S. MIYAZAWA, Kerr effects of flexible macromolecules. In *Molecular Electro-Optics* (S. Krause, Ed.), pp. 163–179. Dekker, New York, 1981.
11. A. REVZIN and E. NEUMANN, Conformation changes in rRna induced by electric impulses. *Biophys. Chem.* **2**, 144–150 (1974).
12. H. H. CHEN, E. CHARNEY, and D. RAU, Length changes in solution accompanying the B–Z transition of poly (dG-m.dC) induced by $Co(NH_3)_6^{3+}$. *Nucleic Acids Res.* **10**, 3561–3571 (1982).
13. W. GUNTHER and H. JUNG, Der Einflusse der Temperatur auf die Strahlenempfindlichkeit von Ribonuclease. *Z. Naturforsch.* **22B**, 313–320 (1967).
14. U. HAGEN, Bestimmung von Einzel- and Doppelbruchen in Bestrahlter Desoxyribonucleinsaure durch die Molekulargewichtsverteilung. *Biochim. Biophys. Acta* **134**, 43–58 (1967).
15. J. BLOK and H. LOMAN, The effects of gamma radiation in DNA. *Curr. Top. Radiat. Res. Q.* **9**, 165–245 (1973).
16. J. MCGHEE, E. CHARNEY, and G. FELSENFELD, Orientation of the nucleosome within the higher order structure of chromatin. *Cell* **22**, 87–96 (1980).
17. H. WU, N. DATTAGUPTA, M. HOGAN, and D. CROTHERS, Structural changes of nucleosomes in low salt concentrations. *Biochemistry* **18**, 3960–3965 (1979).

Reprint & Copyright © by
Aerospace Medical Association, Washington, DC

ARMED FORCES RADIOBIOLOGY
RESEARCH INSTITUTE
SCIENTIFIC REPORT
SR86-6

Stimulation of Brain Muscarinic Acetylcholine Receptors Acutely Reverses Radiogenic Hypodipsia

G. ANDREW MICKLEY, M.A., Ph.D., and KAREN E. STEVENS, B.S., M.A.

Behavioral Sciences Department, Armed Forces Radiobiology Research Institute, Bethesda, Maryland, and Department of Behavioral Sciences and Leadership, United States Air Force Academy, Colorado Springs, Colorado

MICKLEY GA, STEVENS KE. *Stimulation of brain muscarinic acetylcholine receptors acutely reverses radiogenic hypodipsia.* Aviat. Space Environ. Med. 1986; 57:250–5.

A sufficiently large dose of ionizing radiation produces changes in water consumption. However, the direction, durations, and physiological substrates of these alterations remain in question. Here we report a 5-d hypodipsia in rats exposed to 600 rads ^{60}Co but a more transient, albeit larger, reduction in drinking after 1000 ^{60}Co. Brain cholinergic neurons have been implicated as mediators of thirst. Therefore, we explored the role of hypothalamic muscarinic receptors in the production of radiation-induced hypodipsia. This was accomplished through the intrahypothalamic injection of carbachol (a muscarinic agonist) or atropine (a muscarinic antagonist) in irradiated rats. Intracranial carbachol produced acute reversal of radiogenic hypodipsia while atropine potentiated the hypodipsia. These post-irradiation drug-induced behaviors were similar to those observed after the same drug treatments before irradiation. Since cholinergic neuronal functions persist and are labile (can be pharmacologically stimulated and blocked) after irradiation, this suggests that other neuronal systems and/or neurochemicals may be more prominently involved in radiogenic hypodipsia.

EXPOSURE TO A sufficiently large dose of ionizing radiation alters consummatory behaviors. A reduction in food intake has been reported almost universally in rats after a variety of doses of radiation (16). Although water consumption usually parallels food intake in rodents, (3) both radiogenic hypodipsia and polydipsia have been described (32). Garcia *et al.* (4) reported that drinking is reduced during multiple low-dose exposures but increases between exposures. Others have found a dose-dependant polydipsia on some days after irradiation and hypodipsia, or no change in drinking, on intervening days (25,31,32). Under many conditions, a reduction in drinking has also been described (2,10,27) as has a radiogenic decrease in thirst-motivated operant responding (2). The brain neuropharmacology which influences these behavioral changes has not been determined.

A large volume of evidence suggests that cholinergic neurons of the hypothalamus are involved in the control of water intake. For example, Grossman (12,14) stimulated a drinking bout in satiated rats by implanting a long-lasting muscarinic acetylcholine receptor agonist (carbachol) into the hypothalamus. Muscarinic receptor blockade of hypothalamic neurons (with atropine or similar compounds) reverses the carbachol-induced hyperdipsic response (13,17,19). Acetylcholine itself is an effective dipsogen (12,30). Inhibition of acetylcholinesterase causes drinking as well (12,20,21). While other neurochemicals are clearly involved in the production of drinking (for review see 7,8) it is generally accepted that regulatory drinking is at least partially mediated by a cholinergic thirst circuit (28).

The neural mechanisms associated with radiation-induced changes in drinking have received relatively little experimental attention (1). The present studies investigated the role of cholinergic brain neurons in radiogenic hypodipsia. We observed a dose-dependent decrease in postirradiation water consumption, which could be acutely reversed by an intrahypothalamic injection of the cholinergic agonist carbachol.

This manuscript was received for review in March 1985. The revised manuscript was accepted for publication in June 1985.

This research was conducted according to the principles enunciated in the "Guide for the Care and Use of Laboratory Animals" prepared by the Institute of Laboratory Animal Resources, National Research Council.

Send correspondence to G. Andrew Mickley, Ph.D., Chief, Experimental Psychology Division, Behavioral Sciences Department, AFRRI, Bethesda, MD 20814–5145.

EXPERIMENT 1

MATERIALS AND METHODS

Subjects: 32 experimentally naive, male, Sprague Dawley rats (200–400 g) were used in these experiments. At least 24 h before the experiment was begun, subjects were individually housed in plastic cages. Rats were in a room illuminated from 6:00 a.m. to 6:00 p.m. daily. Ambient temperature was set at 20°C. Purina rat chow and water were continuously available.

Procedures: We measured water consumption once a day for 2 d prior to irradiation (baseline) and then for 5 d immediately postirradiation.

Rats received a whole-body, midline tissue dose of either 600 rads (N = 10) or 1000 rads (N = 6) ^{60}Cobalt. An equal number of subjects were sham irradiated for times equal to those of the actual radiation exposures.

Irradiated subjects were placed into individual constraining polyethylene tubes immediately before they were exposed. The tops of the tubes were covered by a 0.5-mm lead sheet. Time of exposure was 4.41–4.52 min for 600 rads, and 7.78–8.05 min for 1000 rads. Therefore, within the time of collection of the results reported, the dose rate changed slightly from 136.05 to 132.74 rads · min $^{-1}$ for 600 rads and, during a different time period, from 128.53 to 124.22 rads · min $^{-1}$ for 1000 rads. This was due to the decay of the ^{60}Co source. The source-to-subject distance was 80 cm and the field of exposure varied from 15 × 15 cm (600 rads) to 25 × 25 cm (1000 rads). Radiation originated above the animal from a Theratron 80 irradiator manufactured by Atomic Energy of Canada. The ^{60}Co source was a single sphere of approximately 4580 curies (as of December 1980). It was driven in a horizontal direction by air pressure in the Theratron 80.

Dosimetry was accomplished in air with ionization chambers (Spokas Model 1000) whose calibration is traceable to the National Bureau of Standards. The chambers were equipped with a ^{60}Co build-up cap. The doses and back-scatter factors were computed from depth/dose tables (4).

For purpose of data analysis, changes from-average-baseline statistics were computed for each subject (daily water consumed postirradiation/sham minus average baseline water consumption). We then compared using *t* tests (33) the scores of irradiated and sham-irradiated rats. This was done for the difference scores derived during each of the 5 d after exposure. Baseline drinking was compared in the same way. Since several *t*-tests were computed for each data set, a strict alpha level was set to compensate for the potential of a Type I error (33). An alpha of 0.05 was partitioned over the five comparisons by Bonferroni allocation (22). Thus we assumed statistical significance when individual *t* tests resulted in $p \leq 0.01$.

RESULTS

The lower dose of radiation (600 rads) produced a significant depression in water consumption over the observed time period. The hypodipsia recorded after 1000 rads was initially more pronounced, but transient and variable (Fig. 1,2).

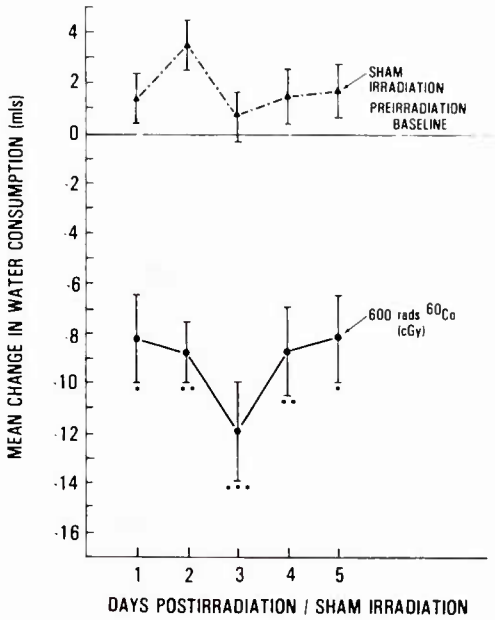

Fig. 1. Changes in average water consumption after either 600 rads ^{60}Co or sham irradiation. Vertical bars represent the S.E.M. (N = 10/point). Asterisks indicate daily statistically significant differences from sham-irradiated group (*t* tests): *p < 0.01; **p < 0.005; ***p < 0.001. Mean 2-d baseline water consumption was: irradiated rats: 37.8 ml (S.D. = 7.4 ml); sham-irradiated rats: 34.2 ml (S.D. = 6.7 ml).

The figures show that baseline water consumption was similar for both experimental and sham-irradiated control subjects within each experiment ($p > 0.05$ for both 600 and 1000 rad-doses).

After 600 rads ^{60}Co, rats consumed less water compared to sham-irradiated controls (Fig. 1) as they significantly reduced their drinking on each of the 5 d after exposure. Similarly, 1000 rads ^{60}Co produced a significant depression in drinking during the first 2 days after irradiation. However, the drinking scores were more variable after a 1000-rad exposure (Fig. 2). Although water consumption was lower than control on post-irradiation days 3–5, it did not achieve statistical significance ($p = 0.07$, 0.06, and 0.06 respectively).

DISCUSSION

The lower dose of ionizing radiation used here (600 rads ^{60}Co) produced a statistically significant hypodipsia for at least the first 5 d after exposure. Similarly, a significant reduction in water intake was noted during the first 2 d after 1000 rads ^{60}Co. Although hypodipsia continued in these subjects for the following 3 d, this decrease in drinking was highly variable and just failed to achieve statistical significance.

This prompt, transient, radiogenic drop in water intake is, in some ways, similar to that reported previously by Afifi *et al.* (1) as well as Smith and Tyree (32). However, this effect may not be characteristic of rats which have received lower and/or fractionated doses of radiation (10,11,25).

Food consumption and body weight often parallel measures of water intake of rats (3,16). We have

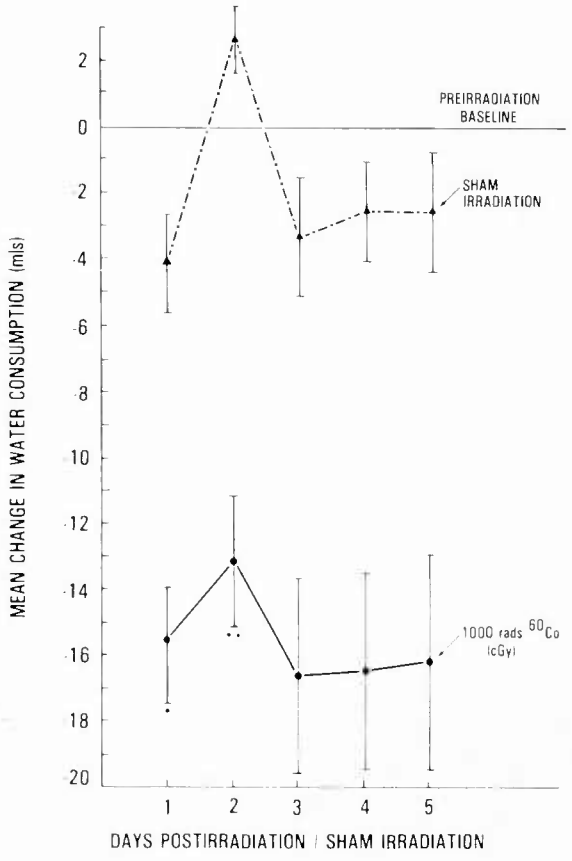

Fig. 2. Changes in average water consumptian after either 1000 rads ^{60}Ca ar sham irradiatian. Vertical bars represent the S.E.M. (N = 6/paint). Asterisks indicate daily statistically significant differences fram sham-irradiated graup (*t* tests): *p<0.01; **p<0.005. Mean 2-d baseline water cansumptian was: irradiated rats: 42.3 ml (S.D. = 8.9 ml); sham-irradiated rats: 46.3 ml (S.D. = 7.8 ml).

previously reported a transient decrease in food consumption and body weight following both 600- and 1000-rad exposures of the animals used in this experiment (23).

EXPERIMENT 2

Experiment 1 demonstrated that whole-body exposure to 600 rads ^{60}Co produces a hypodipsia which lasts for at least 5 d after irradiation. In Experiment 2, we tested the lability of this response through stimulation or blockage of muscarinic cholinergic receptors of the hypothalamus.

MATERIALS AND METHODS

Subjects: 14 experimentally naive male Sprague-Dawley rats (250–350 g) were used in this experiment. Subjects were maintained as described in Experiment 1. Purina rat chow and water were always available.

Procedures: All rats were chronically implanted with bilateral intracranial cannula aimed at the nucleus dorsomedialis hypothalami (DMH). The DMH was selected as an injection site since it is known to contain muscarinic receptors (26,34) and be involved in the regulation of water intake (14,19). Stereotaxic coordinates were 2.0 mm posterior from bregma; ± 0.75 mm lateral from the midline; and −8.0 mm skull depth (18). In preparation for this surgical procedure, rats were anesthetized i.p. with 50 mg · kg^{-1} sodium pentobarbital. Atropine sulfate (0.4 mg · kg^{-1} i.p.) was used as a preanesthetic agent.

Animals were allowed at least a week to recover from surgery. Then, over a several-day period, rats received intrahypothalamic injections of carbachol and/or atropine sulfate. Carbachol (carbamylcholine) is a cholinomimetic drug, not readily metabolized by cholinesterase, that stimulates muscarinic receptors (9,28). Atropine sulfate is a cholinergic antagonist that blocks muscarinic receptors (9,28). Subjects received more than one of the following baseline intracranial injections in a randomized order of presentation: 3.2 μg carbachol (1.6 μg/cannula in 1ul isotonic saline, N=7) or 6.4 μg carbachol (3.2 μg/cannula in 1ul isotonic saline, N=10) and/or 1.6 μg atropine sulfate (0.8 μg/cannula in 1ul sterile water, N=5). One of these injections was given either in the morning (8:00 a.m.) or the afternoon (3:00 p.m.). Vehicle control injections, equal in volume to drug injections, were given at the alternate time of day in a randomized design. Drug injections were given at least 24 h apart. After each injection, rats were replaced in their home cage where water consumption and time spent drinking were monitored for 0.5 h. On the day following the last baseline injection, rats were exposed to 600 rads of ^{60}Co using the procedure described in Experiment 1. The postirradiation drug administration procedures and doses closely paralleled those described before irradiation. Approximately 17 h after radiation exposure, each rat received an intracranial drug injection comparable to one of those given during its baseline. Vehicle control injections again were given at a different time of the same day. Subsequent drug and vehicle injections, comparable to those given before radiation exposure, were administered within the first 5 d after irradiation. The order of drug administrations was randomized. After each of these injections (drug or vehicle), water consumption and time spent drinking were recorded for 0.5 h.

At the time of sacrifice, 1μl of evans blue dye was injected into each cannula to image the flow of drug within the hypothalamus. Animals with extra-hypothalamic dye were not retained in the experiment. All cannula placements were histologically verified (Fig. 3).

RESULTS

Cholinergic stimulation of hypothalamic muscarinic receptors acutely reversed the radiogenic hypodipsia after 600 rads ^{60}Co. Atropine's blockade of these brain receptors further depressed the drinking of irradiated subjects. These effects did not differ significantly from those observed before radiation exposure.

Preliminary computations of group variances suggested that they were not homogeneous and, therefore, nonparametric statistical tests were used in the data analysis (29).

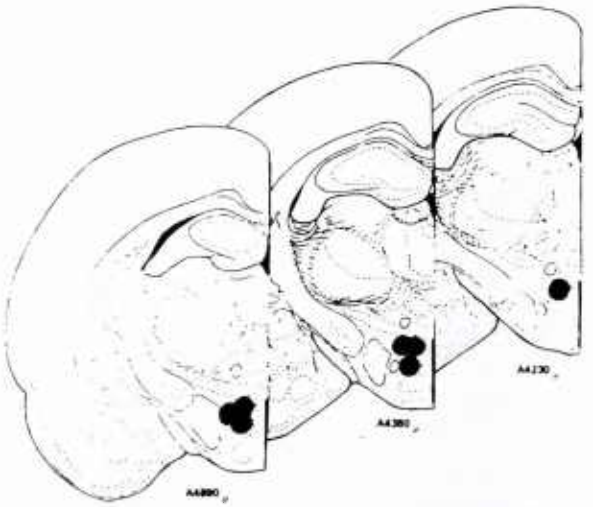

Fig. 3. Locations of injection cannula tips (drawings revised from König and Klippel, 1963. (18).

As in Experiment 1, 600 rads ^{60}Co significantly reduced the water intake of non-drugged rats in this study. We used the Wilcoxon matched pairs sign ranks test (28) (WMPSRT) to compare levels of baseline water consumption, observed after vehicle-control injections, with similarly-derived water consumption postirradiation. This test revealed a significant decrease ($p<0.005$) in total fluid consumed during the observation period following 600 rads ^{60}Co (Fig. 4,5).

Before irradiation, intracranial injections of carbachol significantly enhanced, over vehicle control injections, the amount of water consumed as well as the time spent drinking (3.2 μg carbachol, $p=0.01$, 6.4 μg carbachol, $p<0.005$; both measures, WMPSRT). Intrahypothalamically applied atropine sulfate had the opposite effect or reducing water consumption ($p=0.031$, sign test).

After radiation exposure, these effects persisted. Carbachol enhanced the amount of water drunk and the time spent drinking (3.2 μg carbachol, $p=0.01$; 6.4 μg carbachol, $p<0.005$; both measures, WMPSRT). Atropine injections reduced the already-very-low postir-

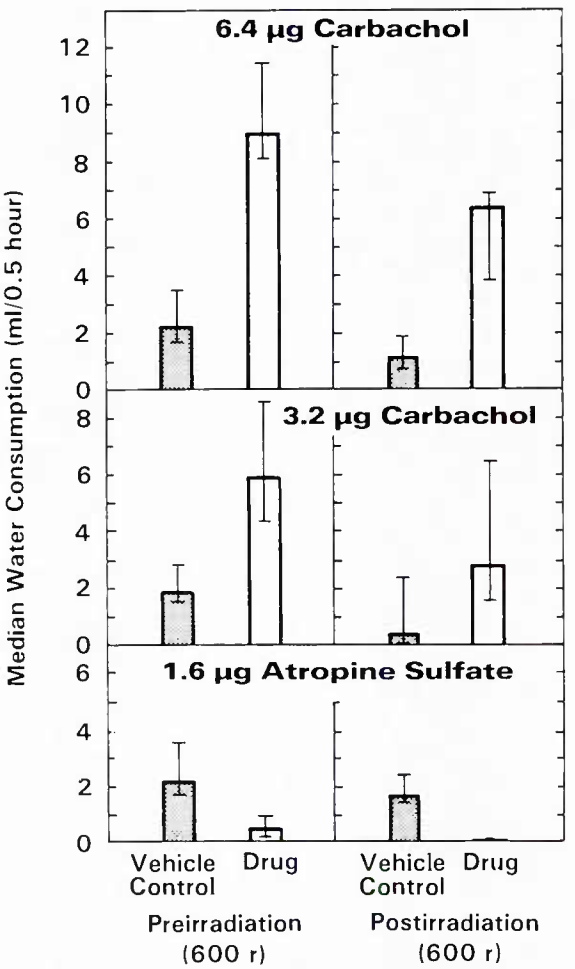

Fig. 4. Median water consumed in a 0.5-h period after an intracranial dose of carbachol (3.2 or 6.4 µg), otropine sulfate (1.6 µg) or vehicle control injections. Carbachal increased water consumption, even after exposure to 600 rads ^{60}Co. Atropine caused a severe hypodipsia. Variance measures are the semi-interquartile range.

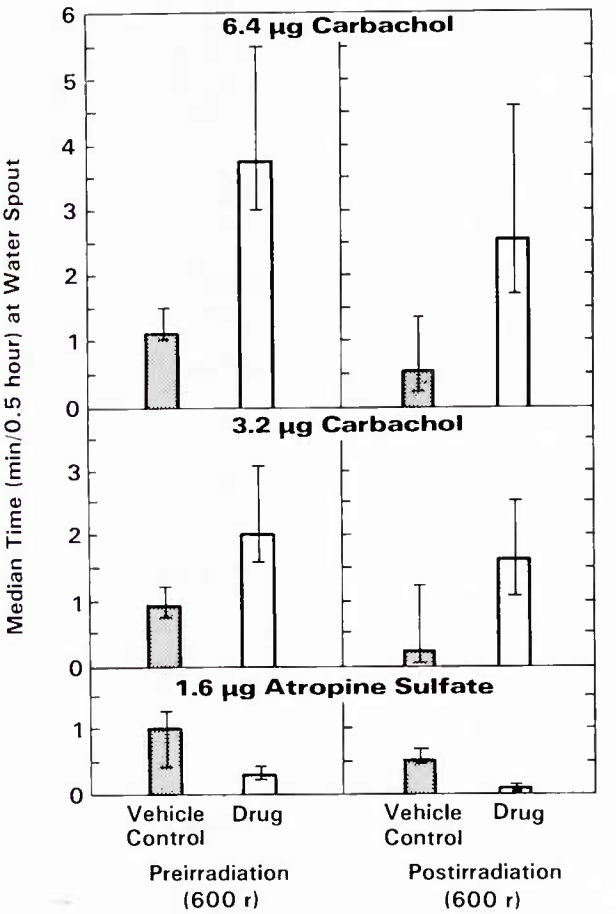

Fig. 5. Median time spent at the water spout in a 0.5-h period after an intracranial dose of carbachol (3.2 or 6.4 µg) atropine sulfate (1.6µg) or vehicle control injections. Carbachal increased the time spent drinking, even after exposure to 600 rads ^{60}Co. Atropine caused a decrease in the time spent at the spout. Variance measures are the semi-interquartile range.

radiation levels of water intake ($p=0.013$, sign test) and time at the water spout ($p=0.013$, sign test). A comparison of these drug effects before and after irradiation suggests that, although both carbachol's and atropine's respective hyperdipsic and hypodipsic effects were slightly diminished postexposure, this decline was not a statistically significant one. Clearly, after irradiation, carbachol (a muscarinic cholinergic agonist) retains its ability to produce drinking in hypodipsic rats and atropine (a muscarinic cholinergic antagonist) can continue to cause a reduction in drinking.

DISCUSSION

Whole-body irradiation at 600 rads ^{60}Co produced a decrease in water consumption during the first 5 d after exposure. Since a reduction in drinking has been, in part, associated with decreased brain muscarinic receptor activity, these behavioral data from Experiment 1 could suggest a radiogenic cholinergic disruption. For example, other studies have revealed a long-term radiation-induced increase in acetylcholinesterase (5) and, after high doses of radiation, a stimulation of high-affinity choline uptake (15). However, the data from Experiment 2 suggest that, after lower doses of radiation, pharmacological manipulation of hypothalamic muscarinic receptors in irradiated animals produces behavioral responses essentially similar to those observed in sham-irradiated subjects. After irradiation, intracranial carbachol continued to produce a voracious drinking response in all subjects. Within a minute of the injection, rats increased their locomotor activity slightly and soon thereafter began drinking. Rats drank almost continuously for 15–20 min. These findings confirm the results of other experiments which have demonstrated the role of muscarinic receptors in the production of drinking (for review see 7,8,28). In addition, these experiments suggest that the muscarinic acetylcholine receptors which mediate drinking remain functional after ^{60}Co irradiation.

Observation of behavioral changes following artificial pharmacological activation and blockage of receptors is only one method of assessing the state of irradiated cholinergic systems. Others have reported that 600 rads ^{60}Co does not significantly alter muscarinic receptor binding for 4-QNB (quinicyclidinic I-124 4-iodobenzilate) in most rat brain areas (6).

Perhaps alterations in the function of other, non-cholinergic, brain neurons might more fully explain radiogenic hypodipsia. For example, others have reported that cholinergic brain neurons interact with angiotensin II-containing neurons to produce thirst (24). It may be that changes in these related, but noncongruent, thirst-stimulating systems may produce acute radiogenic hypodipsia. Future studies should address these issues.

ACKNOWLEDGMENTS

The authors wish to thank Gregory L. Gibbs, Gerald A. White, and Penrose Cancer Hospital, Colorado Springs, CO, for assistance in the ^{60}Co irradiations. We also thank M. Golightly, who typed the manuscript, and William Jackson, who offered statistical advice. A portion of this work was carried out in the Department of Behavioral Sciences and Leadership, United States Air Force Academy, Colorado Springs, CO, and was funded by the USAF School of Aerospace Medicine (SAMTSO 80–3). The work done at the Armed Forces Radiobiology Research Institute was supported by AFRRI work unit number 4332–00125.

REFERENCES

1. Afifi AK, Osborne JW, Mitchell CL. Changes in neurosecretory material, water intake, and urine output in x-irradiated rats. Radiat. Res. 1964; 23:1–12.
2. Arnold WJ. Behavioral effects of cranial irradiation of rats. In: Haley TJ, Snider RS, eds. Response of the nervous system to ionizing radiation. New York: Academic Press, 1962; 669–682.
3. Bolles RC. The interaction of hunger and thirst in the rat. J. Comp. Physiol. Psychol. 1961; 54:580–4.
4. Cohen M, Jones DEA, Green D. Central axis depth dose data for use in radiotherapy. London: British Institute of Radiology, 1972.
5. Davydov, BI. Acetylcholine metabolism in the thalamic region of the brain of dogs after acute radiation sickness. Radiogiologiya 1961; 1:550–4; USAEC Rpt AEC-TR-5424, pp. 132–9.
6. Durakovic A, Eng RR, Conklin JJ. Cholinergic response in the brain after whole-body irradiation. Ann. RCPSC 1984; 17:340.
7. Epstein AN, Kissileff HR, Stellar E. The neuropsychology of thirst: New findings and advances in concepts. Washington, DC: V.H. Winston and Sons, 1973.
8. Epstein AN. The neuropsychology of drinking behavior. In: Satinoff E, Teitelbaum P, eds. Handbook of behavioral neurobiology: Vol 6, Motivation. New York: Plenum Press, 1983; 367–423.
9. Feldman RS, Quenzer LF. Fundamentals of neuropsychopharmacology. Sunderland, MA: Sinauer Associates, Inc., 1984.
10. Garcia J, Kimeldorf DJ, Hunt EL. Conditioned responses to manipulative procedures resulting from exposure to gamma radiation. Radiat. Res. 1956; 5:79–87.
11. Garcia J, Kimeldorf DJ, Hunt EL, Davies BP. Food and water consumption of rats during exposure to gamma radiation. Radiat. Res. 1956; 4:33–41.
12. Grossman SP. Direct adrenergic and cholinergic stimulation of hypothalamic mechanisms. Am. J. Physiol. 1962; 202:872–82.
13. Grossman SP. Effect of adrenergic and cholinergic blocking agents on hypothalamic mechanisms. Am. J. Physiol. 1962; 202:1230–6.
14. Grossman SP. Eating or drinking elicited by direct adrenergic or cholinergic stimulation of hypothalamus. Science 1960; 132:301–2.
15. Hunt WA, Dalton TK, Darden JH. Transient alterations in neurotransmitter activity in the caudate nucleus of rat brain after a high dose of ionizing radiation. Radiat. Res. 1979; 80:556–62.
16. Kimeldorf DJ, Hunt EL. Ionizing radiation: Neural function and behavior. New York: Academic Press, 1965.
17. Kirkstone BJ, Levitt RA. Interactions between water deprivation and chemical brain stimulation. J. Comp. Physiol. Psychol. 1970; 71:334–40.
18. König JFR, Klippel RA. The rat brain: A stereotaxic atlas of the forebrain and lower parts of the brain stem. Baltimore: Williams & Wilkins, 1963.
19. Levitt RA, Fisher AE. Anticholinergic blockage of centrally induced thirst. Science 1966; 154:520–2.
20. Levitt RA, Boley RP. Drinking elicited by injection of eserine or carbachol into rat brain. Physiol. Behav. 1970; 5:693–5.
21. Miller NE, Chien CW. Drinking elicited by injecting eserine into preoptic area of rat brain. Commun. Behav. Biol. 1968; 1:61–3.
22. Miller RG. Simultaneous statistical difference, 2nd Ed. New York: Springer-Verlag, 1981:8.
23. Mickley GA, Stevens KE, Lawrence GH, Gibbs, GL, White GA. Atropine fails to counter radiogenic behavioral deficits. Proceedings, Psychology in the Department of Defense, Eighth Symposium, USAFA-TR-82-10, 498–506, 1982.
24. Moore AF, Drexter AP. A cholinergic link in the centrally mediated actions of angiotensin II. Drug Dev. Res. 1982; 2:241–50.

25. Nims IF, Sutton E. Weight changes and water consumption of rats exposed to whole-body x-irradiation. Am. J. Physiol. 1952; 171:17–21.
26. Nonaka R, Moroji T. Quantitative autoradiography of muscarinic cholinergic receptors in the rat brain. Brain Res. 1984; 296:295–303.
27. Ruch TC, Isaac W, Leary RW. Behavioral and correlated hematologic effects of sublethal whole body irradiation. In: Haley TJ, Snider RS, eds. Response of the nervous system to ionizing radiation, New York: Academic Press, 1962:691–703.
28. Setler PE. The neuroanatomy and neuropharmacology of drinking. In: Iversen LL, Snyder SH, eds. Handbook of psychopharmacology: Vol 8, Drugs, neurotransmitters and behavior. New York: Plenum Press, 1977:131–58.
29. Siegel S. Nonparametric statistics for the behavioral sciences. New York: McGraw-Hill, 1956.
30. Simpson JB, Routtenberg A. Subfornical organ: Acetylcholine application elicits drinking. Brain Res. 1974; 78:49–56.
31. Smith DE, Tyree EB, Patt HM, Bink N. Effect of x-irradiation upon food and water intake and body weight. Fed. Proc. 1952; 11:149.
32. Smith DE, Tyree EB. Effect of x-irradiation upon water consumption by the rat. Am. J. Physiol. 1956; 184:127–33.
33. Winer BJ. Statistical principles in experimental design, 2nd Ed. New York: McGraw-Hill, 1971.
34. Yamamura HI, Kuhar MJ, Snyder SH. *In vivo* identification of muscarinic cholinergic receptor binding in rat brain. Brain Res. 1974; 80:170–6.

ARMED FORCES RADIOBIOLOGY
RESEARCH INSTITUTE
SCIENTIFIC REPORT
SR86-7

RADIATION RESEARCH **105**, 201–210 (1986)

Effect of Radiation on the Regulation of Sodium-Dependent Glucose Transport in LLC-PK$_1$ Epithelial Cell Line: Possible Model for Gene Expression

A. MORAN,[1] L. DAVIS, AND M. HAGAN

Physiology and Experimental Hematology Departments, Armed Forces Radiobiology Research Institute, Bethesda, Maryland 20814-5145

MORAN, A., DAVIS, L., AND HAGAN, M. Effect of Radiation on the Regulation of Sodium-Dependent Glucose Transport in LLC-PK$_1$ Epithelial Cell Line: Possible Model for Gene Expression. *Radiat. Res.* **105**, 201–210 (1986).

Low concentrations of glucose induce cultured kidney epithelial cells (LLC-PK$_1$) to produce hexose transport proteins. We have investigated the effects of ionizing radiation on this induction process in plateau-phase cultures. The induced production of hexose transporters, requiring approximately 6 to 9 days for complete expression, can be inhibited by irradiation during the first 4 days. After the fourth postinduction day, radiation sensitivity decreases with almost no radiation effect on the induction of hexose transport apparent by the sixth day of the induction period. The D_0 value associated with the induction block is approximately 25 Gy, a value which is considerably greater than that necessary to inhibit cell replication. Hexose transport, itself resistant to ionizing radiation at doses in excess of 100 Gy, is sensitive to cycloheximide throughout the induction period. The sensitivity to cycloheximide decreases during the last 2 days of the induction period, approximately 1 day after the reduction in radiosensitivity. Based on these properties hexose transport may be a convenient model for the study of radiation effects upon gene expression in this cell line. © 1986 Academic Press, Inc.

INTRODUCTION

The construction of a successful model to address radiation effects on gene expression has proved to be a difficult effort. Historically, *in vitro* models for the study of development have involved rapidly proliferating cells such as HeLa cells (*1, 2*), murine fibroblasts (*3, 4*), Novikoff hepatoma cells (*5*), chick embryo fibroblasts (*6*), and embryonic myoblasts (*7, 8*). If ionizing radiation were used in these systems, radiation-induced cell killing would quickly dominate the assay (*9*). The recent development, however, of porcine kidney cells (LLC-PK$_1$) which form differentiated epithelia *in vitro* (*10, 11*) and show very little cell replication presents a possible solution (*12*). Epithelial layers formed from these cells show aspects of proximal tubule function such as sodium-coupled transport of phosphate and glucose (*13–17*). With only 2–5% of the cells in the S phase, these cultures are extremely resistant to ionizing radiation (*12*). Moreover, the cultures can be easily maintained in the confluent state for 2 to

[1] Present address: Physiology Department, Faculty of Health Sciences, Ben-Gurion University of the Negev, Beer-Sheva, Israel.

0033-7587/86 $3.00
Copyright © 1986 by Academic Press, Inc.
All rights of reproduction in any form reserved.

6 weeks, compatible with the long periods frequently required for the induction and expression of genetic material in mammalian cells (*10*).

Recently, we have shown that the sodium-coupled transport of glucose in these cultures is regulated by the concentration of glucose in the growth medium (*18, 19*). That is, cells shifted from a high to a low concentration of glucose respond by the development of more glucose transporters (*18*). This phenomenon, defined as up-regulation, is fully reversible with the new steady state in glucose transport expressed in approximately 6–9 days (*18, 19*). Furthermore, up-regulation is independent of cell replication, is completely expressed in cultures in the plateau phase, and is dependent solely upon the concentration of glucose. When 5 m*M* glucose is used to induce glucose transport in these cultures, a maximum increase in glucose transport of some five- to sixfold is observed (*18, 19*). Although plateau-phase cultures can be maintained for several weeks under this condition of low glucose, a modest increase in the rate of cell death occurs (*19*).

Previous studies have shown that down-regulation is unaffected by ionizing radiation. However, doses in the range of 5–50 Gy significantly reduce the capacity of the epithelium to up-regulate (*12*). Since up-regulation requires up to 9 days for complete expression and can be blocked by exposure to ionizing radiation, it is possible that this increased transport requires a change in genetic expression. The inhibition of up-regulation requires significantly higher doses of radiation than does the inhibition of thymidine incorporation, but the clear demonstration of the independence of cell replication and induced glucose transport is still necessary.

As a first step in the evaluation of this model system as a possible candidate for the study of gene expression, we have examined radiation effects on cell replication and sodium-coupled glucose transport during the process of up-regulation. The radiation dose response and the time course of development of induced glucose transport can be clearly separated from requirement for cell replication. Further, the time during the induction periods when the induced glucose transport is sensitive to protein synthesis inhibitor supports the notion that the expression of genetic material is a requirement for the induction process.

MATERIALS AND METHODS

Cell culture. LLC-PK_1 (passages 190 to 220) (American Type Tissue Culture Collection, Bethesda, MD) were grown in Dulbecco's modified Eagle's medium (M. A. Bioproducts, Walkersville, MD) containing 5 or 25 m*M* glucose and supplemented with 2% fetal bovine serum (GIBCO, Grand Island, NY), 10% porcine serum (GIBCO), 0.03% glutamine, 10 units/ml penicillin, and 10 μg/ml streptomycin. Cells were subcultured as previously described (*18*) into wells (4 cm^2) of cluster 12 plates (Costar, Cambridge, MA) and fed (1 ml) three times a week. Cultures were confluent and formed domes on the fourth day after subculture.

Flux measurements. Concentrating capacity (ratio of the intracellular concentration of the sugar to its extracellular concentration) of [^{14}C]-α-methyl glucoside (AMG) was measured as previously described (*18, 19*). In short, cells were washed prior to the experiment with phosphate buffer saline (PBS) containing 0.1 m*M* AMG and raffinose (which serves as an extracellular marker) to remove residual glucose, then incubated on a mechanical shaker at room temperature with the same solution containing labeled AMG and raffinose until a steady state is achieved. At the end of the incubation period, the epithelia were washed using ice cold PBS, solubilized in Triton X 100, and sampled for scintillation counting of the labeled AMG. Cell volume was measured using the nonmetabolizable sugar [^{14}C]-3-*O*-methyl glucose (3OM) that does not accumulate in these cells.

Thymidine incorporation. Thymidine incorporation measurements were done as previously described using the cold chase technique (*12*). In some experiments the radiolabeled thymidine was left on the culture continuously. In these cases the lowest specific activity possible, usually 0.05 μCi/ml, was used.

Autoradiography. Cells were incubated with labeled thymidine 0.05 μCi/ml continuously for the appropriate time. Prior to the autoradiography, nonincorporated labeled thymidine was chased as described earlier (*12*). The epithelia were then trypsinized and spread over a microscope slide using a Cytospin centrifuge (Shandon Elliott). Cells were then immediately fixed using acetic acid 1:3 with methanol. The slides were refrigerated until the emulsion was applied. Nuclear Track Emulsion III (Kodak) was applied and exposed for 5 days at 4°C. After exposure, slides were developed and stained with thiazine/xanthine dye (Diff-Quik). Cells labeled with eight or more grains were scored as positive for thymidine incorporation; results were tallied as number of positives over total number counted.

Radiation. Epithelia were irradiated with γ radiation at the ^{60}Co radiation facility at Armed Forces Radiobiology Research Institute (AFRRI) as previously described (*12*). The dose rate at doses up to 5 Gy was 0.5 Gy/min, and 10 Gy/min for doses higher than that.

Material. [^{14}C]-AMG, 3OM, and [^{3}H]raffinose and thymidine were obtained from New England Nuclear. Unlabeled AMG and 3OM were from CalBiochem (La Jolla, CA). Other chemicals were of the highest purity available from commercial sources. The data points illustrated in figures are means and standard deviations determined from three wells. Results of representative experiments are shown.

RESULTS AND DISCUSSION

The demonstration that the induction of glucose transporters is sensitive to ionizing radiation while glucose transport per se is not (*12*) invoked interest in evaluating whether this system might be useful as a model to study the effects of ionizing radiation on gene expression. An important point in these studies is that the sugar transport measurements are made in cultures in the plateau phase. There is very little cell replication and hence little radiation-induced cell killing (*12*). To illustrate this point, irradiated and nonirradiated epithelia were photographed 7 days after the radiation exposure. The morphologies of the cultures shown in Fig. 1 are virtually indistinguishable. The induction of a new glucose transport state, however, requires more than 6 days to develop. Even a modest rate of cell replication may be significant over this somewhat lengthy period. It is therefore necessary at the outset to show that the abrogation by radiation of the expression of increased glucose transport is not simply a byproduct of reproductive cell death. To address this issue the following set of experiments was performed, comparing properties associated with cell division with those of transport of AMG, a nonmetabolizable sugar.

Since it has been established that 6–9 days are required to effect the new steady state in glucose transport (*12, 19*), cell replication and DNA synthesis were observed during this period in replicate cultures. As can be seen from the data presented in Fig. 2, 80% of the control cells in the culture incorporate tritiated thymidine during 8 days. For cultures irradiated with a dose of 50 Gy, only about 20% of the cells have the capacity to accumulate thymidine. Under these same conditions of irradiation the AMG transport continues to increase to greater than 50% of control value (*12*). These data suggest that the radiation dose response for cell replication may differ significantly from the radiation dose response for induced AMG transport. For a routine assay of proliferation, the incorporation of thymidine per milligram protein was measured and found to be in good agreement with the autoradiographic data for [^{3}H]thymidine uptake. The data presented in Fig. 3 show that the rate of uptake of thymidine into control cultures closely paralleled that which was observed for individual cells through

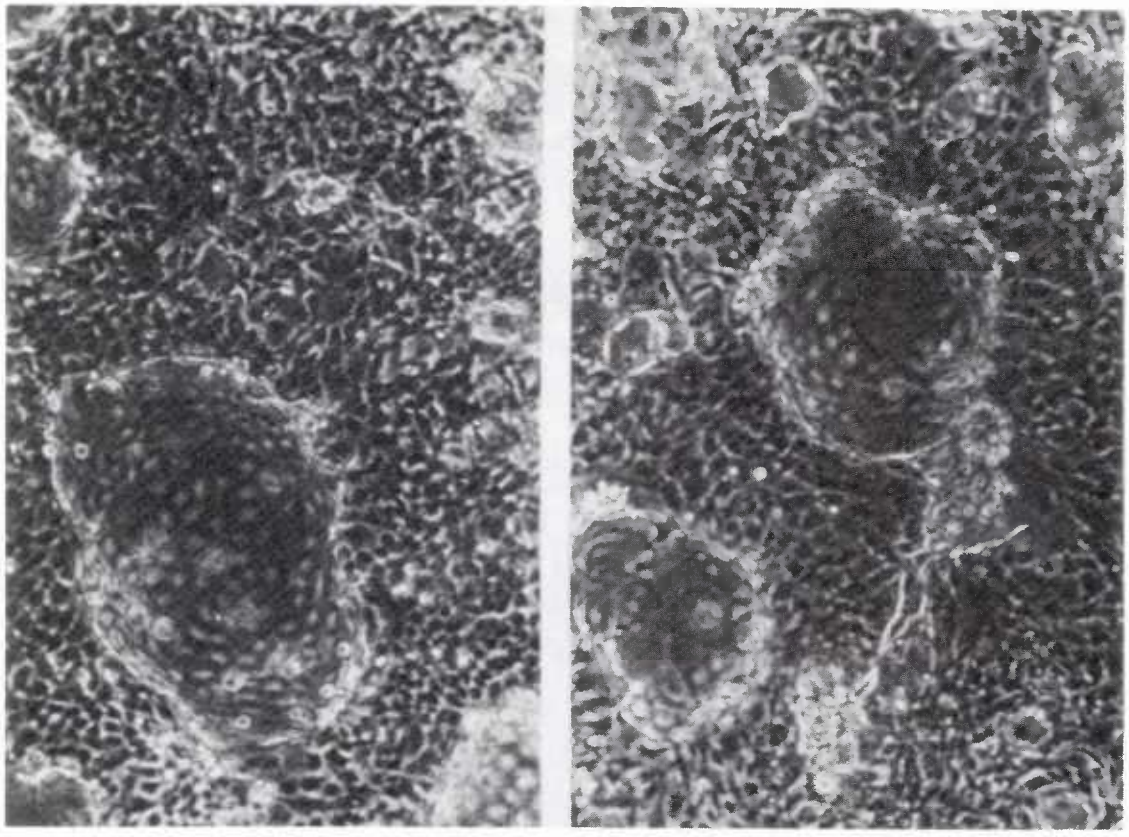

FIG. 1. Phase contrast photomicrograph of epithelial cells before (left) and 7 days after exposure to 50 Gy (right) γ radiation. $\times 140$.

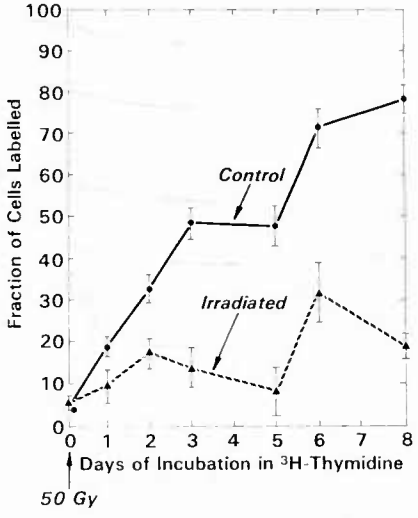

FIG. 2. Percentage of cells labeled as a function of time after irradiation. Fourteen-day-old epithelia were either left unirradiated (●) or irradiated with a dose of 50 Gy administered at a rate of 10 Gy/min (▲). After the irradiation, thymidine remained in the medium (0.05 μCi/ml) for the entire period of the assay. Results shown are the fraction of cells labeled as determined by autoradiography (500 cells/point). Error bars represent 1 SD.

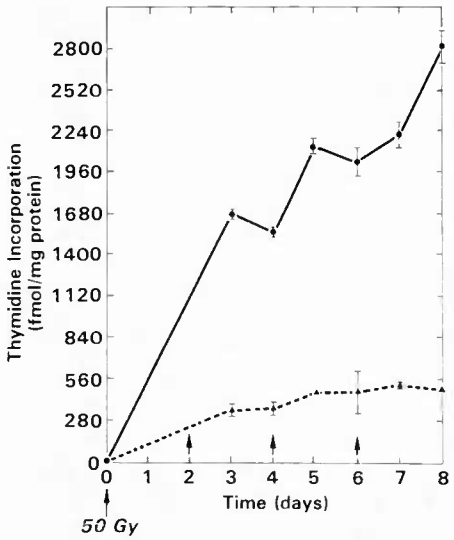

FIG. 3. Accumulative thymidine incorporation into irradiated (▲) and nonirradiated (●) epithelia. Epithelia were irradiated after 2 weeks of culture; conditions of irradiation were the same as for Fig. 2. Thymidine remained in the medium (0.05 μCi/ml) for the entire period of the assay. Arrows indicate times at which the growth media was replenished. Error bars, shown when they are larger than the symbol, represent 1 SD.

the use of autoradiography. The close correlation between autoradiography and thymidine incorporation was also seen for cultures irradiated at a dose of 50 Gy.

Using thymidine uptake as an indicator of cell replication, the radiation dose response for thymidine uptake was compared with the dose response of AMG transport. For these experiments, epithelia were grown to confluency in 25 mM glucose and were either switched to the inducing level of glucose (5 mM) or left at the noninducing level (25 mM). Epithelia were then irradiated and after 7 days scored for their capacity to concentrate AMG. AMG uptake in the noninduced cultures was unperturbed by radiation up to a dose of 100 Gy, demonstrating the resistance to irradiation of the transport process per se. The dose–response curve for induced transport, however, showed a threshold dose of approximately 3 Gy and an approximate D_0 of 25 Gy. In contrast, the data in Fig. 4 show that thymidine uptake decreased below 50% of control values at 2 Gy, a dose of radiation that produced no measurable decrement in the induced transport of AMG.

To test whether the target for this radiation effect is present during the entire induction period, a radiation dose sufficient to reduce inducible AMG uptake by 50% was administered at various times through the induction period. The resulting time course, shown in Fig. 5, identified three phases of the induction period. Categorized by their relative sensitivity to irradiation the three phases are (a) a period of maximum radiosensitivity, days 1–4; (b) a period of decreasing effect occurring between Days 4 and 6 of the induction period; and (c) a refractory period observed 6–7 days into the induction period.

For comparison, Fig. 6 shows the uptake of thymidine following an exposure of 50 Gy administered into cells either switched from 25 to 5 mM or left in 25 mM glucose. Unlike induced AMG transport, the residual incorporation of thymidine showed no

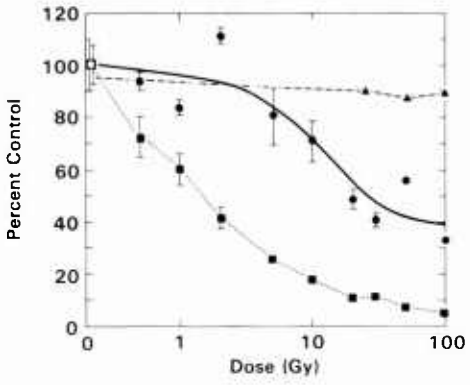

FIG. 4. Dose–response curves for thymidine uptake and either induced or steady-state AMG transport. Epithelia grown for 14 days in 25 m*M* glucose were irradiated and either switched to 5 m*M* glucose (●) or left in 25 m*M* glucose (▲) for an additional 7 days. Epithelia were then scored for AMG uptake (●, ▲) or the ability to incorporate thymidine (■). Error bars, shown when they are larger than the symbol, represent 1 SD.

dependence on the time course of the induction period or on the glucose concentration employed.

Given that (a) the interruption or cessation of DNA synthesis does not correlate well with the block of expression of the new glucose-transport state (Figs. 3, 5, 6) and (b) the direct inhibition of glucose transport per se requires radiation doses in excess of those required to block the induction of the new transport state (Fig. 4), it is reasonable to ask whether protein synthesis, an obvious requirement for gene expression, is required for this induction process. If the synthesis of specific protein(s) is required, a protein synthesis block of short duration administered at a critical time within the

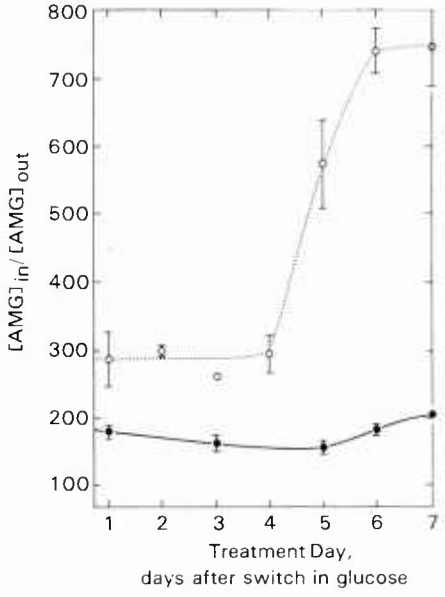

FIG. 5. AMG uptake 7 days after the induction of increased hexose transport. Epithelia 2 weeks of age were switched from medium containing 25 m*M* to medium containing 5 m*M* glucose (○) or left in 25 m*M* glucose (●). Epithelia were irradiated with 50 Gy on the days indicated on thc *x* axis. Error bars represent 1 SD.

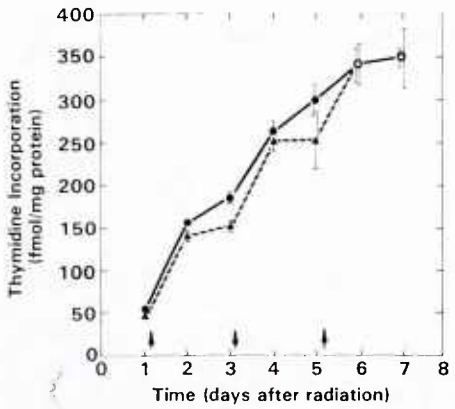

FIG. 6. Cumulative thymidine incorporation into cells irradiated and assayed at 24-h intervals. Epithelia were irradiated and switched from 25 m*M* glucose to 5 m*M* glucose on Day 0 (●) or left in medium containing 25 m*M* glucose (▲). Other conditions are as described for Fig. 3.

period of induction should show significant effect. In addition, the inhibition of protein synthesis may provide another means of distinguishing between thymidine incorporation and induced AMG uptake.

To answer this question, protein synthesis was stopped by an 8-h application of cycloheximide (2 μg/ml in the appropriate growth medium), this treatment given at various times after the "down-shift" in the concentration of glucose. Figure 7 describes the results of the AMG uptake measured 8 days after the "down-shift" in glucose concentration. There appear to be two distinct phases to the kinetics of this phenomenon. When the cycloheximide was administered more than 5 days after the induction, the increase in AMG uptake that was observed was dependent upon the schedule of the treatment. An 8-h inhibition of protein synthesis less than 5 days after the induction produced a maximal inhibition. Similar results were obtained when the length of the block was increased to either 14 or 22 h (data not shown). These results are consistent with an essential requirement for protein synthesis for the full expression of the increased transport of AMG. Demonstration of the efficacy of the protein inhibition, shown in Fig. 8, confirms that protein synthesis was reduced by an order of magnitude

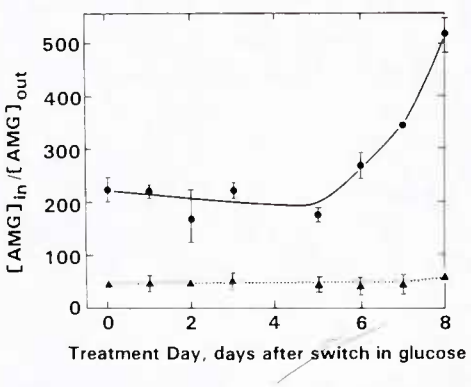

FIG. 7. Effect of an 8-h application of cycloheximide on inducible AMG uptake. Cycloheximide (2 μg/ml) was applied to cultured epithelia for 8 h on the days indicated on the *x* axis; one treatment per epithelium. Epithelia were grown to confluency in 25 m*M* glucose and then switched to 5 m*M* glucose (●) or left in 25 m*M* glucose (▲). Assay for AMG uptake was performed on Day 8.

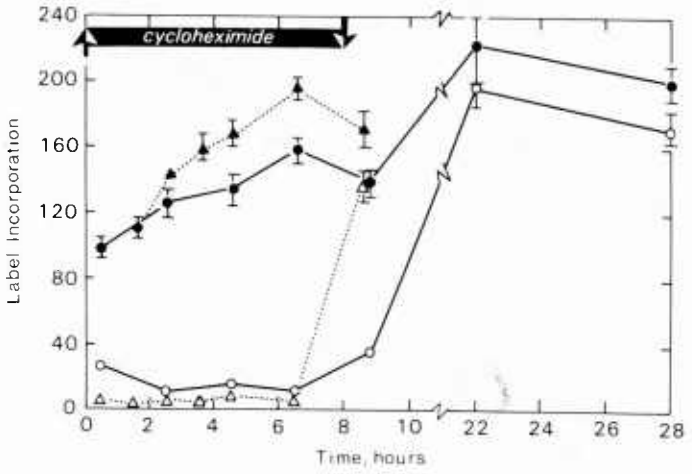

FIG. 8. Effect of an 8-h application of cycloheximide on protein and DNA synthesis. Incorporation of radiolabeled leucine (▲, △) or radiolabeled thymidine (●, ○) was measured as a function of time for cultures incubated either in the presence (○, △) or in absence (●, ▲) of cycloheximide. Incorporation is shown as percentage of incorporation in control cultures.

by the cycloheximide treatment. The data further show that thymidine incorporation recovered quickly after the removal of the cycloheximide, another indication of the independence of thymidine uptake and the induction of AMG uptake.

CONCLUSION

This work differentiates the abrogation by ionizing radiation of the expression of an induced metabolic change from the radiation effect on cell replication. This induced change, a sevenfold increase in the capacity of cultured porcine kidney cells (LLC-PK_1) to transport glucose, was inhibited by ionizing radiation under conditions that excluded radiation effects on cell replication. The following pieces of evidence show a clear separation between the expression of induced glucose transport and the disruption of DNA synthesis: widely disparate radiation dose responses, differences between the percentage of cells impaired in their proliferative function and those impaired in their transport capacity, and differences in kinetics and coupling to protein synthesis. To distinguish the effect of ionizing radiation on the regulation of glucose uptake from the effect on cell replication, we used epithelia formed from plateau-phase cultures of LLC-PK_1 cells. These epithelia exhibited a very low turnover rate: only 80% displayed tritium labeling after 8 days of continuous incubation in [^{3}H]thymidine. This labeling was sensitive to ionizing radiation at doses far less than those which were required to inhibit glucose transport. AMG uptake per se was only moderately impaired at doses of ionizing radiation as high as 200 Gy. However, the induced change in AMG uptake was halved by an exposure to 50 Gy when that exposure was timed to produce its greatest effect. More specifically, an exposure 4 days or less after the induction always maximally impaired the induced change, while exposing epithelia at later postinduction times caused less impairment. Exposures 6 days after induction had little effect on the AMG uptake. Unlike this time-dependent change in AMG uptake, the incorporation of radiolabeled thymidine was maximally impaired within minutes of the exposure

and any residual incorporation increased not in a step-function but monotonically throughout the assay period.

The notion that inhibition of the up-regulatory phenomenon by radiation is due to the effect of radiation on gene expression is strongly supported by the effects of blocking protein synthesis on the same process. As shown in Fig. 7, when the protein synthesis inhibitor cycloheximide is applied to the cells in the same time frame as the radiation challenge with respect to the switch from 25 to 5 m*M* glucose in the growth medium, a similar time course for inhibition is obtained. In fact, these time courses differ only in that the induction process appears to remain sensitive to an inhibition of protein synthesis as radiosensitivity is lost. These findings are consistent with the notion that radiation impairs the expression of the new state of glucose transport and demonstrate that this inhibition stems neither from direct impairment of the glucose transport process nor is a sequela of the disruption of DNA synthesis.

ACKNOWLEDGMENT

This work was supported by the Armed Forces Radiobiology Research Institute, Defense Nuclear Agency, under Research Work Unit MJ 00106. The views presented in this paper are those of the authors; no endorsement by the Defense Nuclear Agency has been given or should be inferred.

RECEIVED: June 21, 1985; REVISED: October 22, 1985

REFERENCES

1. J. E. DARNELL, JR., J. R. NEVINS, and M. ZEEVI, The role of poly (A) in mammalian gene expression. In *Gene Regulation* (B. W. O'Malley, Ed.). Academic Press, New York, 1982.
2. M. ZEEVI, J. R. NEVINS, and J. E. DARNELL, JR., Nuclear RNA is spliced in the absence of poly (A) addition. *Cell* **26,** 39–46 (1981).
3. J. A. MARTIAL, J. D. BAXTER, H. M. GOODMAN, and P. H. SEEBURG, Regulation of growth hormone messenger RNA by thyroid and glucocorticoid hormones. *Proc. Natl. Acad. Sci. USA* **74,** 1816–1820 (1977).
4. L. F. JOHNSON, C. L. FUHRMAN, and L. M. WIEDEMANN, Regulation of dihydrofolate reductase gene expression in mouse fibroblasts during the transition from the resting to growing state. *J. Cell. Physiol.* **97,** 397–406 (1978).
5. A. KROL, H. GALLINARO, E. LAZAR, M. JACOB, and C. BRANLANT, The nuclear 5S RNAs from chicken, rat, and man. U5 RNAs are encoded by multiple genes. *Nucleic Acids Res.* **9,** 769–788 (1981).
6. D. STOPAK and A. K. HARRIS, Connective tissue morphogenesis by fibroflast traction. I. Tissue culture observations. *Dev. Biol.* **90,** 383–398 (1982).
7. C. P. ORDAHL and A. I. CAPLAN, High diversity in the polyadenylated RNA populations of embryonic myoblasts. *J. Biol. Chem.* **253,** 7683–7691 (1978).
8. R. B. DEVLIN and C. P. EMERSON, JR., Coordinate accumulation of contractile protein mRNAs during myoblast differentiation. *Dev. Biol.* **69,** 202–216 (1979).
9. M. M. ELKIND, Repair processes in radiation biology. *Radiat. Res.* **100,** 425–449 (1984).
10. R. N. HULL, W. R. CHERRY, and G. W. WEAVER, The origin and characteristics of a pig kidney cell strain LLC-PK_1. *In Vitro* **12,** 670–677 (1976).
11. J. M. MULLIN, J. WEIBEL, L. DIAMOND, and A. KLEINZELLER, Sugar transport in the LLC-PK_1 renal epithelial cell line: Similarity to mammalian kidney and the influence of cell density. *J. Cell. Physiol.* **104,** 375–389 (1980).
12. A. MORAN, J. S. HANDLER, and M. HAGAN, Cell proliferation and the regulation of sodium-coupled hexose transport in LLC-PK_1 epithelia: Effect of radiation. *Am. J. Physiol.*, in press.
13. K. AMSLER and J. S. COOK, Development of Na^+-dependent hexose transport in a culture line of porcine kidney cells. *Am. J. Physiol.* **242,** C94–C101 (1982).

14. J. BIBER, C. D. A. BROWN, and H. MURER, Sodium-dependent transport of phosphate in LLC-PK_1 cells, *Biochim. Biophys. Acta* **735,** 325–330 (1983).

15. C. D. A. BROWN, M. BODMER, J. BIBER, and H. MURER, Sodium-dependent phosphate transport by apical membrane vesicles from cultured renal epithelial cell line (LLC-PK_1). *Biochim. Biophys. Acta* **769,** 471–478 (1984).

16. D. S. MISFELDT and M. J. SANDERS, Transepithelial transport in cell culture: D-glucose transport by pig kidney cell line (LLC-PK_1). *J. Membrane Biol.* **59,** 13–18 (1981).

17. C. A. RABITO, Localization of the Na^+-sugar transport system in a kidney epithelial cell line. *Biochim. Biophys. Acta* **649,** 286–296 (1981).

18. A. MORAN, R. J. TURNER, and J. S. HANDLER, Regulation of sodium coupled glucose transport by glucose in culture epithelium. *J. Biol. Chem.* **258,** 15087–15090 (1983).

19. A. MORAN, R. J. TURNER, and J. S. HANDLER, Hexose regulation of Sodium-hexose transport in LLC-PK_1 epithelia: The nature of the signal. *J. Membrane Biol.* **82,** 59–65 (1984).

ARMED FORCES RADIOBIOLOGY
RESEARCH INSTITUTE
SCIENTIFIC REPORT
SR86-8

Role of cell replication in regulation of Na-coupled hexose transport in LLC-PK_1 epithelial cells

A. MORAN, J. S. HANDLER, AND M. HAGAN
Physiology and Experimental Hematology Departments, Armed Forces Radiobiology Research Institute, Bethesda 20814-5145; and Laboratory of Kidney and Electrolyte Metabolism, National Heart, Lung, and Blood Institute, National Institutes of Health, Bethesda, Maryland 20205

MORAN, A., J. S. HANDLER, AND M. HAGAN. *Role of cell replication in regulation of Na-coupled hexose transport in LLC-PK_1 epithelial cells.* Am. J. Physiol. 250 (Cell Physiol. 19): C314–C318, 1986.—The glucose concentration in growth medium has been shown to regulate the number of sodium-coupled glucose transporters in LLC-PK_1 epithelial cells. Epithelia grown in high concentrations of glucose express fewer transporters than epithelia grown in low concentrations of glucose. In the present work, the effect of a dose of ionizing radiation sufficient to block the incorporation of thymidine was examined in order to gauge the importance of cell replication in the hexose transport regulatory process. The low rate of thymidine incorporation in the plateau phase was completely eliminated by ionizing radiation. Under conditions of irradiation that completely blocked thymidine incorporation, down-regulation, namely the loss of α-methylglucoside-concentrating capacity, brought about by switching the epithelium from low to high glucose-containing medium, is independent of the irradiation and therefore most likely is also independent of cell replication. In contrast, the up-regulatory phenomenon is strongly impaired by radiation. This impairment may be due to specific radiation impairment of gene expression necessary for the up-regulatory process. It is apparent from the dose-response data that up-regulation is not inhibited by irradiation in a simple manner and is not inhibited at the same radiation dose as cell replication.

radiation; thymidine incorporation

EPITHELIAL CELLS IN CULTURE are, in general, used for the study of both the regulation of cell function and the action of hormones on cells (10, 11). LLC-PK_1, a cell line commonly used for these investigations, grows to confluency by forming a continuous epithelium (12, 20). Furthermore, this cultured epithelium shows properties of normal epithelia in vivo, e.g., polarity of plasma membrane components (14, 15, 26, 27) and the maintenance of proximal tubule functions such as sodium-coupled transport of glucose and phosphate (1, 3, 4, 6, 7, 16–18, 20, 25). LLC-PK_1 cells have also been shown to respond to hormones such as vasopressin, suggesting that this cell line possesses not only the transport system but also the regulatory responses relevant to renal epithelia (2, 23, 24).

Recently, we have shown that the sodium-coupled glucose transport in LLC-PK_1 cells is regulated by the glucose concentration in the growth medium (18). When compared with cells grown in medium containing 25 mM glucose, cells grown in medium containing 5 mM glucose have an increased number of sodium-coupled phlorizin-binding sites (18). The observed difference resulted neither from cell selection from a heterogeneous population nor from a difference in cell density. The trigger for the regulatory process was shown to be the concentration of glucose in the growth medium rather than a factor secreted into or depleted from the medium. Furthermore, although the regulatory process is fully reversible, it is not a direct outcome of the interaction between the carrier and the substrate (19).

Measurements of glucose transport are routinely performed in confluent cultures in the plateau phase of cell growth. Under the assumption that cells are no longer dividing at this stage, the role of cell replication has not been explicitly considered. To evaluate the role of cell replication, we have examined the effect of ionizing radiation on cell replication and the regulation of glucose transport. Since ionizing radiation affects cell replication at doses of a few gray (Gy) and 10–100 Gy (1 Gy = 100 rads) are required to alter membrane permeability (8), a region of radiation doses quite useful for studying hexose transport while eliminating cell replication should exist. We show that the regulatory mechanism can be divided into two distinct components: the down-regulatory process (cells shifted from low- to high-glucose-containing media, thus losing their concentrating capacity) is not affected by irradiation, while the up-regulatory process (cells shifted from high- to low-glucose-containing media, thus increasing their capacity to accumulate glucose) is inhibited by ionizing radiation.

MATERIALS AND METHODS

Cell culture. LLC-PK_1 cells obtained from American Type Culture Collection were grown as previously described (18). Briefly, stock cells were grown in 10-cm-diameter tissue culture dishes (Costar, Kennebunk, ME). Cells in 2- to 3-wk-old cultures were trypsinized (0.25% trypsin in phosphate-buffered saline, PBS) and subcultured (1:10). The cells for the experiment were grown in 12-well clusters (Costar). Most experiments were done at 2 wks when the cell layer was confluent and at steady state with respect to the number of cells in the well and the α-methylglucoside-concentrating capacity [the ratio between the intracellular and the extracellular concen-

tration of α-methylglucoside (AMG) in a steady-state situation] (18).

Uptake measurements. AMG uptake at a steady state was studied as previously described (17). Cell water was determined by measuring the uptake of the nonmetabolizable sugar 3-*O*-methyl-D-glucose, which is not carried on the sodium-coupled glucose transporters in these cells (20). Concentrating capacity was defined as a ratio between the AMG concentration in the cell and in the incubation medium at steady state.

Thymidine incorporation measurements were made as follows: the cells were incubated with complete medium containing 10 μCi/ml [^{3}H]thymidine (78 Ci/mmol) (New England Nuclear, Boston, MA) for 0.5 h in the incubator (37°C and 5% CO_2). Following the incubation, the medium was aspirated, and the cells were rinsed with PBS. The cells were further incubated with medium containing 0.1 mM unlabeled thymidine for another hour in the incubator to chase by competition the remaining unbound [^{3}H]thymidine (22). At the end of the chase period, the cells were washed with PBS, and the cells were solubilized using 0.5% Triton X-100 in water. Samples for radioactivity and protein determinations were then taken. Efflux of AMG was measured as previously described (18).

Irradiation. Cells were irradiated in the ^{60}Co γ-radiation facility at the Armed Forces Radiobiology Research Institute. The cells were exposed to doses of up to 5 Gy with a dose rate of 0.50 Gy/min. Above 5 Gy the dose rate employed was 10 Gy/min. No significant differences were found when 5 Gy were given in either of the two dose rates (data not shown).

Materials. [^{14}C]AMG, 3-*O*-[*methyl*-^{3}H]-methyl-D-glucose, [^{3}H]raffinose (an extracellular marker), and [^{3}H]-thymidine were obtained from New England Nuclear. Unlabeled raffinose and 3-*O*-methyl-D-glucose were from Cal Biochem (La Jolla, CA). Other chemicals were of the highest purity available from commercial sources. The data points illustrated in the figures are the mean and standard deviation determined from three samples. Results of representative experiments are shown.

RESULTS

To observe the effect of ionizing radiation on proliferation, cultures were incubated for 30 min in the presence of [^{3}H]thymidine. Although used extensively, this use of DNA synthesis as an estimate of cell replication was developed largely for fibroblasts (5, 22). For fibroblast cultures in the plateau phase, the incorporation of thymidine is typically reduced to 2% with respect to the same cells grown in log phase (9, 13). In contrast, studies of epithelial cultures in the plateau phase have shown that the incorporation of thymidine is only reduced to 10% with respect to the same cells in log phase (1, 28; A. Moran, unpublished observation). Since nonspecific trapping of radiolabeled thymidine may be a problem during acid precipitation, we used a period of incubation in 1×10^{-4} M thymidine to clear the radiolabel from cellular pools.

Figure 1 shows that exposure to unlabeled thymidine to terminate the labeling period yielded a very sensitive measurement of the incorporation of thymidine. With this technique, the ratio of thymidine incorporation in the log phase to that measured in the plateau phase was between 30 and 200. The low rate of thymidine incorporation could still represent cell replication that plays an important role in the regulatory response, since these epithelia are tested more than 7 days after switching the glucose concentration in the growth media. In plateau-phase cultures, cell replication was affected by the feeding schedule (Fig. 1). No significant difference in replication was observed between cells grown in medium containing 25 mM glucose and cells grown in medium containing 5 mM glucose.

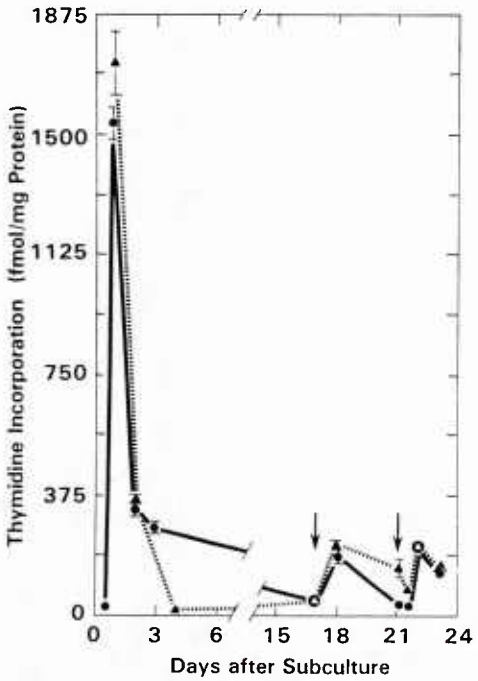

FIG. 1. Thymidine incorporation into epithelial cells grown in media containing 5 (*filled triangles*) or 25 (*filled circles*) mM glucose as a function of time after subculture. *Arrows* indicate feeding times. A difference of 200 times is seen between peak of log phase and lower point at plateau phase. Note no significant difference between thymidine incorporation of epithelial cells grown in medium containing 5 or 25 mM glucose.

When plateau-phase cultures were exposed to ionizing radiation, the residual incorporation of thymidine was significantly reduced. Data presented in Fig. 2 show that DNA synthesis markedly decreased after exposure to a dose of 1–30 Gy. A dose of ~10 Gy reduced thymidine incorporation by nearly one order of magnitude. For the studies that follow, a dose of 50 Gy was used to reduce cell replication to negligible values. As confirmation, Fig. 3 shows thymidine incorporation in cells in the plateau phase with and without 50 Gy of γ-radiation. While there was measurable incorporation of thymidine into nonirradiated cells, the levels shown for irradiated cultures were indistinguishable from background. Once again the results were the same for cells grown in 5 or 25 mM glucose. Thus, although thymidine incorporation may result from processes other than cell replication, the absence of incorporation clearly indicates the absence of cell replication.

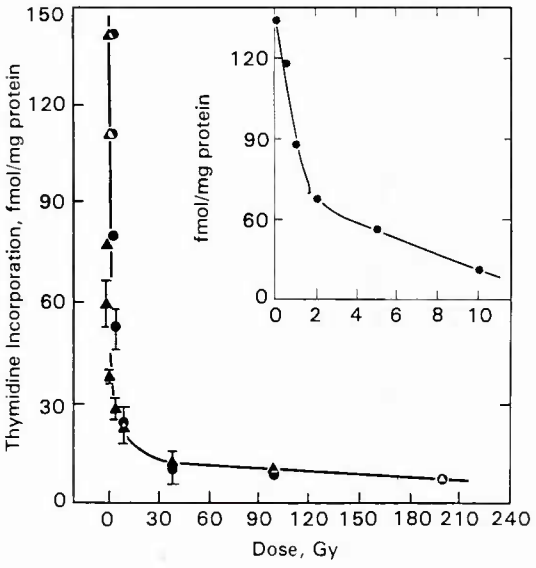

FIG. 2. Radiation dose response of thymidine incorporation into epithelial cells grown in media containing 5 (*filled triangles*) or 25 (*filled circles*) mM glucose 4 days after γ-radiation. Cells were grown for 2 wk in respective media before radiation. Note that effect of radiation on thymidine incorporation is same for epithelia grown in media containing 5 and 25 mM glucose. *Inset* depicts data more accurately for radiation doses up to 10 Gy (only 25 mM glucose is shown).

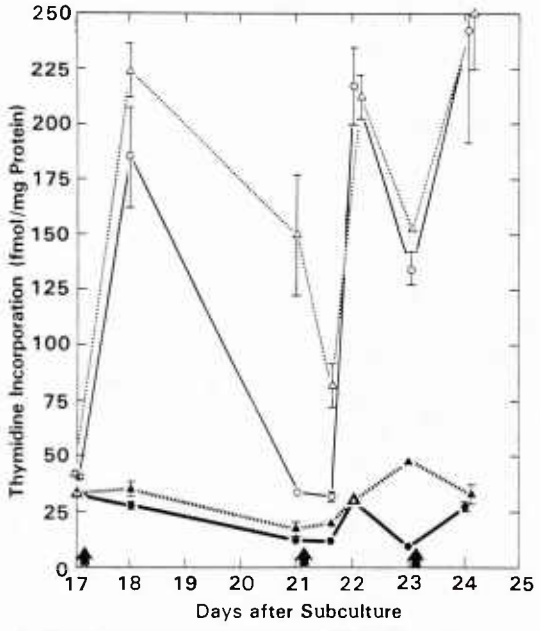

FIG. 3. Thymidine incorporation into LLC-PK$_1$ cells grown in media containing 5 (*open triangles, filled triangles*) or 25 (*open circles, filled circles*) mM glucose prior to measurement, shown as a function of days after subculture. One-half of cultures were irradiated (*filled triangles, filled circles*) on day 17 with 50 Gy. *Arrows* indicate feeding time.

Although the incorporation of thymidine was unaffected by growth in 5 or 25 mM glucose, the striking effect on AMG uptake was evident, as shown in Fig. 4. Uptake of AMG by cells grown in 25 mM glucose was unaffected by radiation doses up to 200 Gy, but doses of radiation above ~5 Gy markedly reduced the AMG-concentrating capacity of cells grown in 5 mM glucose.

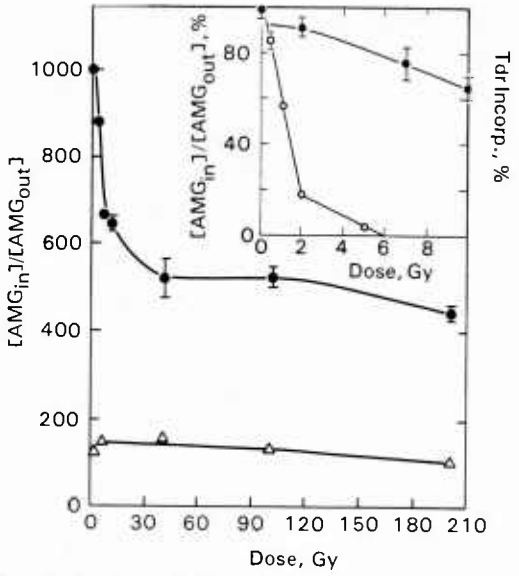

FIG. 4. α-Methylglucoside (AMG) uptake as a function of radiation dose at 7 days after irradiation. (Radiation effect on the AMG uptake was qualitatively same from 1st day of irradiation, with maximum effect observed on 7th day.) LLC-PK$_1$ cells were grown for 14 days in medium containing 5 (*filled circles*) and 25 (*open triangles*) mM glucose. While cells grown in 5 mM glucose were markedly affected, no change was observed when epithelia grown in 25 mM glucose were irradiated. *Inset* depicts percent of control accumulative capacity (*filled circles*) and thymidine incorporation (*open circles*) as a function of radiation dose in cells grown in 5 mM glucose.

The efflux of AMG was affected neither by radiation nor by the concentration of glucose in the growth medium (data not shown).

The effect of irradiation on the down-regulation of the AMG-concentrating capacity by high glucose concentration in the growth medium is depicted in Fig. 5. The cells were grown for 8 days in medium containing 5 mM glucose. On the 8th day of culture, they were divided into two groups. The first group was irradiated with 50 Gy, and the second group was not irradiated. To examine down-regulation, one-half of the cultures were left in medium containing 5 mM glucose, while the rest were switched to medium containing 25 mM glucose. Over a period of ~8 days, epithelial cells switched to 25 mM glucose expressed a reduced capacity to concentrate AMG; 50 Gy of γ-radiation had no effect on this process. The concentrating capacity of the cells left in the original low-glucose medium continued to increase, reaching a plateau value on the 16th day of culture. In contrast, the AMG-concentrating capacity of the irradiated cells left in the original low-glucose medium briefly continued to increase but subsequently decreased to ~50% of the value reached by nonirradiated epithelial cells.

In an inverse experiment to study up-regulation, depicted in Fig. 6, one-half of the cultures grown in 25 mM glucose were switched to medium containing 5 mM glucose. Here, there was a marked difference between the irradiated and nonirradiated cells. The concentrating capacity of the irradiated cells also increased, but the plateau level attained was less than one-half of that achieved by the nonirradiated cells. As in Fig. 4, 50 Gy

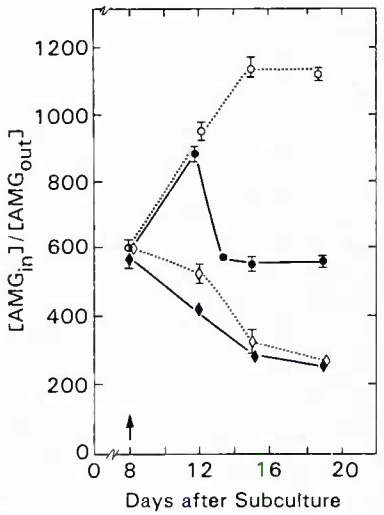

FIG. 5. Effect of radiation on down-regulation of α-methylglucoside-concentrating capacity. LLC-PK$_1$ cells were grown in medium containing 5 mM glucose for 8 days and then switched into medium containing 25 mM glucose (*open diamonds, filled diamonds*). Epithelia not irradiated and left in same medium containing 5 mM glucose (*open circles*) continued to increase their concentrating capacity before leveling off. Irradiated cells (*filled diamonds, filled circles*) left in medium containing 5 mM glucose (*filled circles*) increased their concentrating capacity for a while before it fell. No significant difference was observed in concentrating capacity of cells switched to high glucose-containing medium, regardless of dose of irradiation (*arrow* indicates day of irradiation).

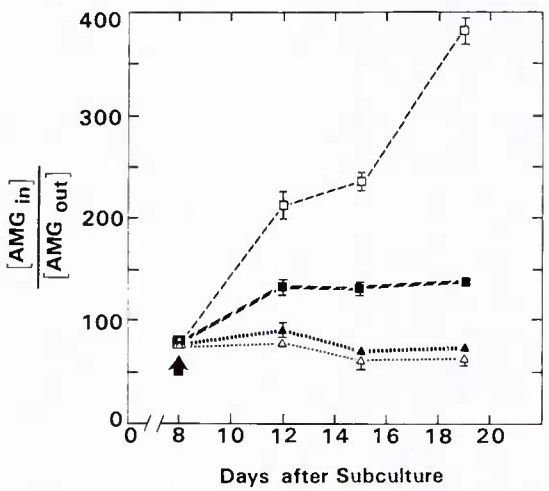

FIG. 6. Effect of radiation on up-regulatory process. LLC-PK$_1$ cells were grown in 25 mM glucose for 8 days before being switched to medium containing 5 mM glucose (*open squares, filled squares*). Nonirradiated cells (*open squares*) continued to increase their capacity after switch. The irradiated cells (*filled squares*) reached only about one half value reached by the nonirradiated cells. As in Fig. 4, no change in α-methylglucoside-concentrating capacity was observed for the cells left in medium containing 25 mM glucose (*open triangles, filled triangles*) (*arrow* indicates day of irradiation).

of γ-radiation did not affect the AMG-concentrating capacity of cells that remained in 25 mM glucose.

DISCUSSION

In the present work, we have examined the effects of ionizing radiation on cell replication and the regulation of sodium-coupled hexose trasport in LLC-PK$_1$ epithelial cells. This was done in an effort to study the dependence of the regulation of glucose transport on cell replication. As these cultures grew from log phase to plateau phase, the amount of thymidine incorporation decreased markedly with some fluctuation related to the schedule of feeding (refer to Fig. 3). Epithelial cells in plateau phase were exposed to ionizing radiation. The dose response for this effect showed a marked decrease in thymidine incorporation with radiation dose; incorporation approached background for doses >10 Gy. After exposure to a test dose of 50 Gy, irradiated epithelial cells showed virtually no capacity for thymidine incorporation. It is important to add that after exposure to radiation doses as high as 200 Gy, these monolayers form domes, metabolize glucose, and remain morphologically indistinguishable (as assessed by phase-contrast microscopy) from nonirradiated controls.

While cell division was practically stopped by radiation, sodium-coupled hexose transport was less profoundly affected. This disparity provided a tool to separate hexose transport regulation that may be coupled to cell replication from that which is not. In this regard, a clear difference was seen between the down-regulatory and up-regulatory processes. The down-regulation was independent of the fact that the cells were irradiated, suggesting that this regulation process and cell division are independent. The fact that in the down-regulated cells no difference was seen between the AMG uptake by irradiated and nonirradiated cells indicates that radiation per se did not impair AMG uptake. The absence of a radiation effect on AMG efflux or the steady-state AMG concentration provided further evidence for the independence of AMG transport per se and cell proliferation. In contrast to the downward regulatory process and AMG transport, the upward regulation was strongly affected by γ-radiation. The irradiated cells achieved only about one-half of the AMG-concentrating capacity achieved by the nonirradiated cells, regardless of whether the epithelia were switched from medium containing 25 to 5 mM glucose or maintained in 5 mM glucose throughout. There are at least two possible reasons for the effect of radiation on the AMG-concentrating capacity of the up-regulating cells: *1*) the process of up-regulation strongly depends on cell replication, and only cells capable of dividing will respond to the low concentration of glucose in the growth medium; *2*) radiation causes additional changes in the cells, independent of cell division, which prevent the expression of the upward regulatory process.

The fact that thymidine incorporation approached zero after a radiation dose of 10 Gy indicates that it is unlikely that residual proliferation could account for the remaining up-regulatory effect. As radiation is known to affect the protein synthesis mechanism directly (7), albeit at much higher doses than those used for this study, it is possible that the impairment of the up-regulatory process resulted from reduction in the concentration of some factor, the absence of which will stop the increase in the AMG-concentrating capacity. Support for such a notion can be obtained from observing the effect of radiation on epithelial cells grown in medium containing

5 mM glucose and left in the same medium after irradiation. Cells grown in medium containing 5 mM glucose normally continue to develop their AMG-concentrating capacity for ~16 days. However, cells irradiated on day 8 and left in medium containing 5 mM glucose continue to develop for only a short while and then decrease their AMG-concentrating capacity. It is more likely that the radiation impairs the synthesis of a new protein but the impairment is expressed only after a few days, meanwhile allowing a short-term increase in the AMG-concentrating capacity. At this time little (if anything) is known about the time scale of the synthesis of the hexose transporter or the number of protein subunits involved.

This work represents the first step in determining whether the induction of sodium-coupled hexose transport can be used as an effective model for the study of radiation effects on gene expression.

This study was supported by Armed Forces Radiobiology Research Institute, Defense Nuclear Agency, under Research Work Unit MJ-00106. A. Moran was supported by a National Research Council Fellowship. The views presented in this paper are those of the authors; no endorsement by the Defense Nuclear Agency has been given or should be inferred.

Received 22 March 1985; accepted in final form 8 July 1985.

REFERENCES

1. AMSLER, K., AND J. S. COOK. Development of Na^+-dependent hexose transport in a culture line of porcine kidney cells. *Am. J. Physiol.* 242 (*Cell Physiol.* 11): C94–C101, 1982.
2. AUSIELLO, D. A., D. H. HALL, AND J. M. DAYER. Modulation of cyclic-AMP dependent protein kinase by vasopressin and calcitonin in cultured porcine renal LLC-PK$_1$ cells. *Biochem. J.* 186: 773–780, 1980.
3. BIBER, J., C. D. A. BROWN, AND H. MURER. Sodium dependent transport of phosphate in LLC-PK$_1$ cells. *Biochim. Biophys. Acto* 735: 325–330, 1983.
4. BROWN, C. D. A., M. BODMER, J. BIBER, AND H. MURER. Sodium-dependent phosphate transport by apical membrane vesicles from cultured renal epithelial cell line (LLC-PK$_1$). *Biochim. Biophys. Acta* 769: 471–478, 1984.
5. CLEAVER, J. E. *Thymidine Metobolism and Cell Kinetics.* Amsterdam: North-Holland, 1967, p. 109–136.
6. COOK, J. S., K. AMSLER, E. R. WEISS, AND C. SHAFFER. Development of Na^+ hexose transport *in vitro*. In: *Membrones in Growth ond Development*, edited by J. F. Hoffman, G. Giebisch, and L. Bolis. New York: Liss, 1982, p. 551–567. (Prog. Clin. Biol. Res. Ser.)
7. CREASEY, W. A. Changes in the sodium and potassium content of cell nuclei after irradiation. *Biochim. Biophys. Acto* 38: 181, 1960.
8. EDWARDS, J. C., D. CHAPMAN, W. A. CRAMP, AND M. B. YATVIN. The effects of ionizing radiation on biomembrane structure and function. *Prog. Biophys. Mol. Biol.* 43: 71–93, 1984.
9. HAHN, G. M., AND B. LITTLE. Plateau-phase culture of mammalian cells: An in vitro model for human cancer. *Curr. Top. Rodiot. Res.* 8: 39–83, 1972.
10. HANDLER, J. S. Use of cultured epithelia to study transport and its regulation. *J. Exp. Biol.* 106: 55–69, 1983.
11. HANDLER, J. S., F. M. PERKINS, AND J. P. JOHNSON. Studies of renal cell function using cell culture techniques. *Am. J. Phyisol.* 238 (*Renol Fluid Electrolyte Physiol.* 7): F1–F9, 1980.
12. HULL, R. N., W. R. CHERRY, AND G. W. WEAVER. The origin and characteristics of a pig kidney cell strain LLC-PK$_1$. *In Vitro* 12: 670–677, 1976.
13. LITTLE, J. B. Repair of sub-lethal and potentially lethal radiation damage in plateau phase cultures of human cells. *Noture Lond.* 224: 804–806, 1969.
14. MILLS, J. W., A. D. C. MACKNIGHT, J.-M. DAYER, AND D. A. AUSIELLO. Localization of [^{3}H]ouabain-sensitive Na^+ pump in sites in cultured pig kidney cells. *Am. J. Physiol.* 236 (*Cell Physiol.* 5): C157–C162, 1979.
15. MILLS, J. W., A. D. C. MACKNIGHT, J. A. JARRELL, J. M. DAYER, AND D. A. AUSIELLO. Interaction of ouabain with the Na^+ pump in intact epithelial cells. *J. Cell Biol.* 88: 637–643, 1981.
16. MISFELDT, D. S., AND M. J. SANDERS. Transepithelial transport in cell culture: D-glucose transport by pig kidney cell line (LLC-PK$_1$). *J. Membr. Biol.* 59: 13–18, 1981.
17. MORAN, A., J. S. HANDLER, AND R. J. TURNER. Na^+-dependent hexose transport in vesicles from cultured renal epithelial cell line. *Am. J. Physiol.* 243 (*Cell Physiol.* 12): C293–C298, 1982.
18. MORAN, A., R. J. TURNER, AND J. S. HANDLER. Regulation of sodium coupled glucose transport by glucose in a cultured epithelium. *J. Biol. Chem.* 258: 15087–15090, 1983.
19. MORAN, A., R. J. TURNER, AND J. S. HANDLER. Hexose regulation of Na-hexose transport in LLC-PK$_1$ epithelia: the nature of the signal. *J. Membr. Biol.* 82: 59–65, 1984.
20. MULLIN, J. M., J. WEIBEL, L. DIAMOND, AND A. KLEINZELLER. Sugar transport in the LLC-PK$_1$ renal epithelial cell line: similarity to mammalian kidney and the influence of cell density. *J. Cell. Physiol.* 104: 375–389, 1980.
21. PAINTER, R. B., AND R. M. DREW. Studies on deoxyribonucleic acid metabolism in human cancer cell cultures (Hela). *Lab. Invest.* 8: 278–285, 1980.
22. PAINTER, R. B., AND B. R. YOUNG. X-rays induced inhibition of DNA synthesis in Chinese hamster ovary, human Hela and mouse L cells. *Rodiot. Res.* 64: 648–656, 1975.
23. ROY, C., AND D. A. AUSIELLO. Characterization of (8-lysine) vasopressin binding sites on a pig kidney cell line (LLC-PK$_1$). *J. Biol. Chem.* 256: 3415–3422, 1981.
24. ROY, C., D. HALL, M. KARISH, AND D. A. AUSIELLO. Relationship of (8-lysine) vasopressin receptor transition to receptor functional properties in a pig kidney cell line (LLC-PK$_1$). *J. Biol. Chem.* 256: 3423–3427, 1981.
25. RABITO, C. A. Phosphate transport by a kidney epithelial cell line. *J. Gen. Physiol.* 76: 20a, 1980.
26. RABITO, C. A. Localization of the Na^+ sugar co-transport system in a kidney epithelial cell line (LLC-PK$_1$). *Biochim. Biophys. Acto* 649: 286–297, 1981.
27. RABITO, C. A., AND M. V. KARISH. Polarized amino acid transport by an epithelial cell line of renal origin (LLC-PK$_1$). The basolateral system. *J. Biol. Chem.* 257: 6802–6808, 1982.
28. RESNIK, V. M., J. VILLELA, AND S. A. MENDOZA. Serum stimulates Na entry and Na-K pump in quiescent cultures of epithelial cells (MDCK). *J. Cell. Physiol.* 17: 211–214, 1983.

ARMED FORCES RADIOBIOLOGY
RESEARCH INSTITUTE
SCIENTIFIC REPORT
SR86-9

0022-3565/85/2322-0413$00.00/0
THE JOURNAL OF PHARMACOLOGY AND EXPERIMENTAL THERAPEUTICS
Copyright © 1985 by The American Society for Pharmacology and Experimental Therapeutics
Vol. 232, No. 2
Printed in U.S.A.

Actions of Ethanol on Voltage-Sensitive Sodium Channels: Effects on Neurotoxin-Stimulated Sodium Uptake in Synaptosomes

MICHAEL J. MULLIN[1] and WALTER A. HUNT

Behavioral Sciences Department, Armed Forces Radiobiology Research Institute, National Naval Medical Center, Bethesda, Maryland

Accepted for publication October 30, 1984

ABSTRACT

Exposure of rat brain synaptosomes to ethanol *in vitro* reduced the neurotoxin-stimulated uptake of $^{22}Na^+$. This effect of ethanol was concentration-dependent, occurred with concentrations of ethanol achieved *in vivo* and was fully reversible. The inhibitory effect of ethanol on neurotoxin-stimulated sodium uptake was due to a decrease in the maximal effect of the neurotoxins. Ethanol reduced the rate of batrachotoxin-stimulated sodium uptake when measured at 3, 5 and 7 but not 10 or 20 sec after the addition of $^{22}Na^+$. In a series of aliphatic alcohols, there was a good correlation between potency for inhibition of batrachotoxin-stimulated $^{22}Na^+$ uptake and the membrane/buffer partition coefficient, suggesting that a hydrophobic site in the membrane was involved in the action of the alcohols. Ethanol did not affect the scorpion venom-induced enhancement of batrachotoxin-stimulated sodium uptake. The inhibitory potency of tetrodotoxin was also unaffected by ethanol. These results demonstrate that ethanol has an inhibitory effect on neurotoxin-stimulated sodium influx occurring in voltage-sensitive sodium channels of brain tissue.

The exact mechanisms by which ethanol causes depression of the CNS and the subsequent behavioral manifestations of intoxification remain undefined. In recent years, a great deal of research has focused on the effects of ethanol on the physical properties of artificial and biological membranes (Seeman, 1972; Goldstein *et al.*, 1980). Through the use of techniques such as electron paramagnetic resonance (Chin and Goldstein, 1977a) and fluorescence spectroscopy (Harris and Schroeder, 1981), it has been demonstrated that pharmacologically relevant concentrations of ethanol *in vitro* cause disordering of membrane lipids as inferred from the measurements of the properties of molecular probes inserted into membranes. By using a variety of molecular probes that insert at different depths in the membrane, it has been shown that the fluidizing effect of ethanol is greater at the hydrophobic inner core than at the superficial membrane surface (Chin and Goldstein, 1981; Harris and Schroeder, 1981). This is somewhat surprising because ethanol is a relatively small, neutral, hydrophilic molecule.

Further evidence that membrane disordering is involved in the intoxicating effects of ethanol has been based on a number of studies that have provided genetic (Goldstein *et al.*, 1982), pharmacological (Lyon *et al.*, 1981) and temporal (Chin and Goldstein, 1977b) correlations between *in vivo* effects and the membrane disordering effect of ethanol *in vitro*. However, because the magnitude of membrane lipid disordering by ethanol is relatively small (Chin and Goldstein, 1977a), it is probable that membrane-mediated biological responses would involve functional entities in membranes. Consequently, ethanol would be expected to interact directly or indirectly with these entities, so that alterations in the functional properties of membrane proteins may also play an important role in the changes in neuronal activity and synaptic function associated with ethanol-induced depression of the CNS. Alterations in lipid fluidity are known to influence the activities of membrane proteins (Lenaz, 1977) and this may represent a mechanism by which the lipid disordering effect of ethanol could be translated into the biochemical and behavioral effects of ethanol.

In the present study, a basic functional unit related to neuronal excitation was investigated with respect to its possible involvement in the actions of ethanol on the brain. An important mechanism in the control of neuroexcitability is the regulation of ion movements at the level of the excitable membrane. Using the squid giant axon, Hodgkin and Huxley (1952) demonstrated that the changes in membrane voltage associated with an action potential were due to a transient increased

Received for publication April 20, 1984.
[1] Supported in part by a Postdoctoral Fellowship from the National Academy of Sciences/National Research Council.

ABBREVIATIONS: CNS, central nervous system; TTX, tetrodotoxin; BTX, batrachotoxin; VER, veratridine; ScV, scorpion venom; HEPES, 4-(2-hydroxyethyl)-1-piperazineethanesulfonic acid.

permeability to sodium followed by an increased permeability to potassium. Apparently, separate channels are utilized by sodium and potassium ions (Hille, 1970; Ulbricht, 1977). The inward movement of sodium ions during excitation occurs through voltage-sensitive sodium channels. The sodium channels that traverse the excitable membrane are composed of complex glycoproteins with multiple polypeptide subunits and contain three distinct receptor sites for various neurotoxins (Catterall, 1980). One receptor site, thought to be located on the extracellular side of the channel (Narahashi, 1966), binds the specific inhibitors saxitoxin and TTX which inhibit the inward movement of sodium (Ritchie and Rogart, 1977). The second neurotoxin receptor site binds the lipid soluble toxins, BTX and VER, which cause persistent activation of sodium channels by blocking the process of channel inactivation and by shifting the voltage-dependence of channel activation to more negative membrane potentials. The third neurotoxin receptor binds small polypeptide toxins present in sea anemone and ScVs. The polypeptide toxins slow channel inactivation and also enhance the effects of BTX and VER. Because the neurotoxins hind to their receptor sites with high affinity and specificity, they have been widely used as chemical tools to study the structure and functional properties of voltage-sensitive sodium channels in a variety of excitable membranes (Narahashi, 1974; Catterall, 1982).

We have studied the effects of ethanol *in vitro* on the functional properties of voltage-sensitive sodium channels in whole rat brain synaptosomes. Ion flux measurements were used as an estimate of sodium ($^{22}Na^+$) ion permeability to assess the function of synaptosomal sodium channels.

Methods

Animals and chemicals. Male Sprague-Dawley rats (200–400 g) were obtained from Charles River Breeding Laboratories, Inc. (Wilmington, MA) and were housed two per cage with free access to water and standard laboratory chow before being used for the experiments. Chemicals and suppliers were as follows: ScV (Leiurus quinquestriatus), TTX and VER from Sigma Chemical Co. (St. Louis, MO); carrier-free $^{22}NaCl$ from New England Nuclear (Boston, MA). BTX was kindly supplied by Dr. John Daly (National Institute of Arthritis, Metabolism and Digestive Diseases, National Institutes of Health, Bethesda, MD). All other chemicals were obtained from commercial sources and were of analytical grade.

Preparation of synaptosomes. A crude synaptosomal (P_2) fraction was prepared by a modification of the method of Gray and Whittaker (1962). Rats were decapitated and the whole brains were removed and homogenized in ice-cold 0.32 M sucrose and 5 mM K_2HPO_4, pH 7.4 (10 ml/g wet wt.), with 10 strokes of a motor-driven Teflon-glass homogenizer. The homogenate was then centrifuged at $1000 \times g$ for 10 min. The resulting supernatant was then centrifuged at $17,000 \times g$ for 60 min. The final pellet was resuspended in ice-cold incubation buffer (8–10 ml/brain) containing (millimolar): KCl, 5.4; $MgSO_4$, 0.8; glucose, 5.5; HEPES-Tris (pH 7.4), 50; and choline chloride, 130. Ten strokes of a loose fitting glass-glass homogenizer were used to resuspend the final pellet. Synaptosomes were kept on ice and were used immediately after preparation.

Measurement of $^{22}Na^+$ uptake. Synaptosomal sodium uptake was determined by a modification of the method of Tamkun and Catterall (1981). Aliquots (50 μl) of the synaptosomal suspension were preincubated at 36°C for 2 min, except in the time course experiments, with incubation buffer or incubation buffer containing the indicated concentration of ethanol. Immediately after the preincubation with ethanol, the indicated concentration of activator toxin (BTX or VER) was added and the samples were incubated for 10 min at 36°C. After 10 min the samples were diluted with a solution containing (final concentration) the indicated concentration of toxin (millimolar): KCl, 5.4; $MgSO_4$, 0.8; glucose, 5.5; HEPES-Tris (pH 7.4), 50; choline chloride, 128; NaCl, 2; ouabain, 5; and 1.3 μCi of carrier-free $^{22}NaCl$ per ml and the indicated concentration of ethanol. After a 5-sec incubation (except where noted), uptake was terminated by the addition of 3 ml of an ice-cold wash solution containing (millimolar): choline chloride, 163; $MgSO_4$, 0.8; $CaCl_2$, 1.8; HEPES-Tris (pH 7.4), 5; and bovine serum albumin, 1 mg/ml. The mixture was filtered rapidly under vacuum through an Amicon 0.45-μm cellulose filter (Amicon, Lexington, MA) and the filters were washed twice with 3 ml of wash solution. The entire halt-filter-wash cycle took less than 10 sec to complete. The filters were placed in scintillation vials, 15 ml of scintillation cocktail were added and filter radioactivity was determined by liquid scintillation spectrometry. The data are presented as corrected specific uptake after subtraction of nonspecific uptake (TTX, 1 μM present in incubation and uptake buffers).

Data analysis. Double reciprocal analysis of the data was performed as described by Catterall (1975) using a modified Michaelis-Menton equation of the form:

$$v = VA/(K_{0.5} + A)$$

where v is the uptake rate at various activator toxin concentrations A, V is maximal uptake rate and $K_{0.5}$ is the apparent dissociation constant of the activator toxin. Statistical analysis was performed using Student's t test for paired samples. Multiple comparisons with a control were done by analysis of variance and Dunnett's test (1964).

Other methods. Drug concentrations in the aqueous and membrane phases were calculated as described by Lyon *et al.* (1981). The membrane/buffer partition coefficients were derived from the data of McCreery and Hunt (1978). Solutions of ScV were prepared according to Catterall (1976). A stock solution of BTX was prepared in absolute ethanol and aliquots were diluted in the appropriate buffer. The final concentration of ethanol in the assay from the addition of BTX was never greater than 0.13 mM. Protein concentrations were determined by the method of Lowry *et al.* (1951). Bovine serum albumin was used as the protein standard.

Results

Preincubation of whole brain synaptosomes with ethanol *in vitro* caused a concentration-dependent inhibition of BTX-stimulated $^{22}Na^+$ uptake (fig. 1). Over the concentration range of ethanol used, the reduction in $^{22}Na^+$ uptake was a linear function of the concentration of ethanol ($r = -0.95$). The inhibitory effect of ethanol occurred at pharmacologically relevant concentrations of ethanol and was fully reversible when ethanol was removed from the sample by washing and centrifugation (fig. 2). Neither the nonspecific (1 μM TTX present) nor the passive, unstimulated (no toxins present) uptake of $^{22}Na^+$ were affected by ethanol *in vitro* (data not shown).

The effects of ethanol on $^{22}Na^+$ uptake were also studied over a range of concentrations of the alkaloid toxins BTX and VER. There was a 6-fold increase in synaptosomal sodium uptake when the concentration of BTX was raised from 0.1 to 5 μM. Ethanol (100 and 400 mM) inhibited $^{22}Na^+$ uptake in synaptosomes exposed to more than 0.1 μM BTX (fig. 3). When VER was used to activate sodium channels and promote $^{22}Na^+$ uptake, a similar effect of ethanol was observed, as shown in figure 4. In order to assess indirectly the interaction of ethanol with the channel receptor site for BTX and VER, we performed a double reciprocal analysis of concentration-effect curves for BTX- and VER-stimulated $^{22}Na^+$ uptake in the absence (control) and presence of two concentrations of ethanol (100 and 400 mM). The data from the double reciprocal analysis are

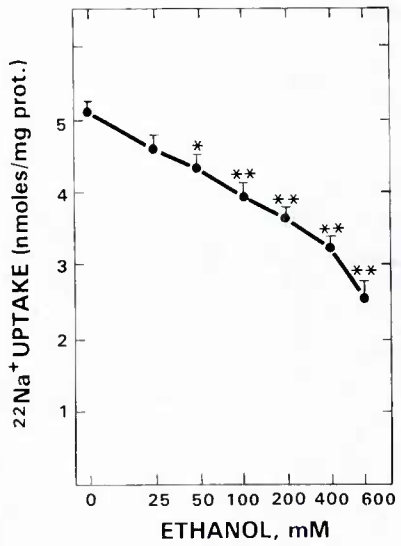

Fig. 1. Concentration-effect curve for inhibition of BTX-stimulated $^{22}Na^+$ uptake. Triplicate samples of whole brain synaptosomes were preincubated for 2 min with the indicated concentration of ethanol followed by a 10-min incubation with 1 μM BTX. Symbols represent the means ± S.E.M., $N = 5$ experiments. The corrected specific uptake of $^{22}Na^+$ during a 5-sec period is shown on the ordinate. The concentration of ethanol is shown on the abscissa, log scale. *P < .01 (Dunnett's test) compared to uptake measured in the absence of ethanol. prot., protein.

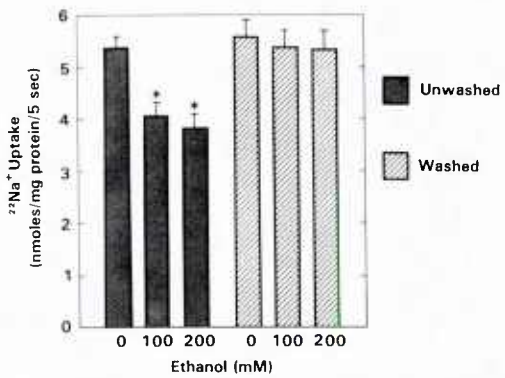

Fig. 2. Reversibility of the inhibitory effect of ethanol on BTX-stimulated $^{22}Na^+$ uptake. After a 2-min preincubation with ethanol, one-half of the samples were centrifuged (1000 × g for 5 min), washed and resuspended in incubation buffer. BTX (1 μM) was added, samples were incubated at 36°C for 10 min and $^{22}Na^+$ uptake was measured as described. The data are expressed as the means ± S.E.M., $N = 4$ experiments. The corrected specific uptake of $^{22}Na^+$ is shown on the ordinate. The concentration of ethanol is shown on the abscissa. *P < .01 (Dunnett's test) compared to uptake in control samples.

summarized in table 1. When sodium channels were activated by BTX, ethanol acted as a noncompetitive inhibitor as the maximum uptake of $^{22}Na^+$ was reduced with no change in the concentration of BTX required for 50% of maximum uptake ($K_{0.5}$). The effects of ethanol on VER-stimulated $^{22}Na^+$ uptake are somewhat more difficult to interpret. Clearly, ethanol significantly reduced the maximum effect of VER. In addition, ethanol reduced the $K_{0.5}$ values for VER but the difference from control was not significant.

The time courses for $^{22}Na^+$ uptake with 1 μM BTX alone and with 1 μM BTX plus 200 mM ethanol are illustrated in figure 5. In the presence of ethanol, the BTX-stimulated uptake of $^{22}Na^+$ was significantly reduced at uptake times of 3, 5 and

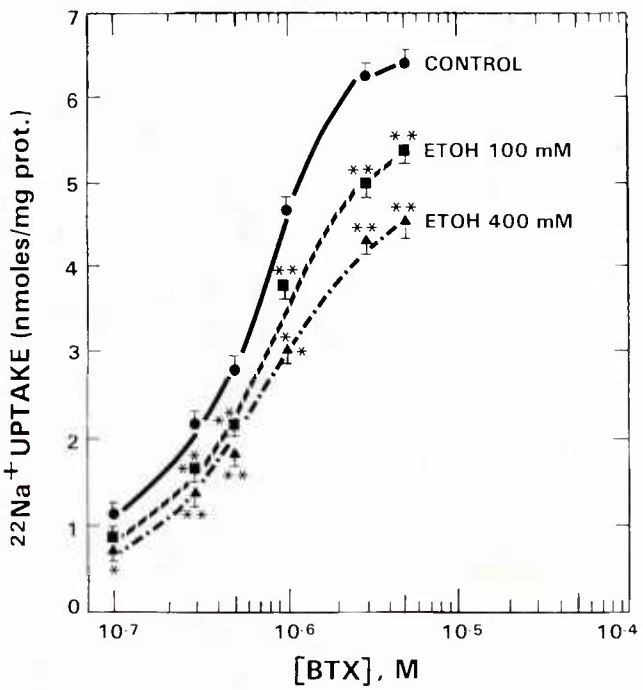

Fig. 3. Effect of ethanol on concentration-effect curve for BTX-stimulated $^{22}Na^+$ uptake. Synaptosomes were preincubated with buffer only or buffer containing ethanol (100 and 400 mM) for 2 min. The indicated concentration of BTX was added and samples were incubated for an additional 10 min and $^{22}Na^+$ uptake was measured for 5 sec as described under "Methods." Symbols represent the means ± S.E.M., $N = 6$ experiments. *P < .05; **P < .01 (Dunnett's test) compared to corresponding control. prot., protein.

7 sec, but not at 10 or 20 sec. Thus, the effect of ethanol on $^{22}Na^+$ uptake is an inhibitory effect on the initial rates of $^{22}Na^+$ uptake. We were unable to measure $^{22}Na^+$ uptake at uptake times shorter than 3 sec with acceptable precision. The results in table 2 demonstrate that the duration of the preincubation period with ethanol was not an important determinant of the inhibitory effect of ethanol. An ethanol concentration of 200 mM reduced the specific uptake to 77.2, 79.3, 74.5 and 77.4% after 0, 0.5, 2 and 10 min, respectively. Thus, the onset of action was immediate and was unchanged over the time periods studied.

The effect of increasing lipid solubility on potency for inhibition of BTX-stimulated $^{22}Na^+$ uptake was studied for a series of aliphatic alcohols. Membrane-buffer partition coefficients were used to calculate the concentration of each alkanol that would result in a similar molar concentration in the nonaqueous (membrane) phase (Lyon *et al.*, 1981). Concentration-effect curves were constructed for each alkanol as percentage of control uptake *vs.* log of the alkanol concentration. Linear regression analysis was used to determine the correlation coefficients, slopes and the concentration of alkanol that inhibited control uptake by 50% (IC_{50}). These values are shown in table 3. For each alkanol tested, the reduction in $^{22}Na^+$ uptake was a linear function of the concentration of alkanol.

The IC_{50} and membrane/buffer partition coefficient values for each alkanol were plotted on a log-log scale (fig. 6). There was a good correlation ($r^2 = 0.997$) between the two parameters, indicating that the ability to partition into a hydrophobic region of the membrane was an important determinant of the potency for inhibition of BTX-stimulated $^{22}Na^+$ uptake.

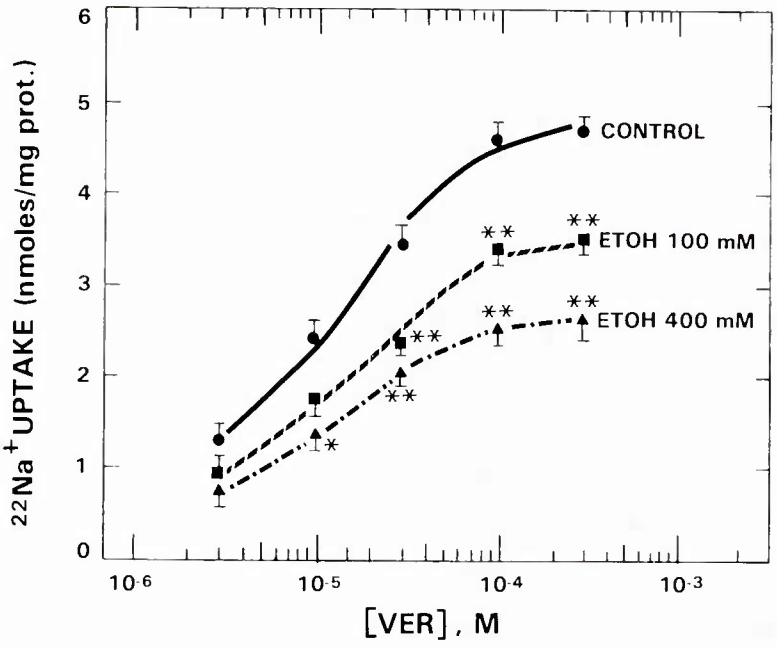

Fig. 4. Effect of ethanol on concentration-curve for VER-stimulated $^{22}Na^+$ uptake. Synaptosomes were preincubated with buffer only or buffer containing ethanol (100 and 400 mM) for 2 min. The indicated concentration of VER was added, samples were incubated for an additional 10 min and $^{22}Na^+$ uptake was measured for 5 sec as described under "Methods." Symbols represent the means ± S.E.M., $N = 4$ experiments. *P < .05; **P < .01 (Dunnett's test) compared to corresponding control. prot., protein.

TABLE 1

Double reciprocal analysis of alkaloid toxin activation of sodium channels

Alkaloid Toxin	Ethanol Conc.	N	V[a]	$K_{0.5}$[a]
	mM		*nmol/mg protein/5 sec*	*μM*
BTX	0	6	6.43 ± 0.27[b]	0.430 ± 0.024
BTX	100	6	4.84 ± 0.15*	0.439 ± 0.042
BTX	400	6	4.09 ± 0.10*	0.431 ± 0.022
VER	0	4	4.62 ± 0.22	9.33 ± 0.70
VER	100	4	3.30 ± 0.29*	7.83 ± 0.94
VER	400	4	2.50 ± 0.12*	6.58 ± 0.63

[a] Values for maximum uptake (V) and $K_{0.5}$ were calculated using a modified Michaelis-Menton equation as described under "Methods."
[b] Values are means ± S.E.M. N = number of experiments.
* Significantly different from control, $P < .01$.

ScV alone does not promote sodium influx. However, ScV enhances alkaloid toxin-stimulated $^{22}Na^+$ uptake, presumably by an allosteric mechanism (Catterall, 1980; Tamkun and Catterall, 1981). The effect of ethanol on the ScV-BTX interaction is shown in figure 7. In control samples, ScV at concentrations of 1 and 10 μg/ml increased BTX-stimulated $^{22}Na^+$ uptake by 26.5 ± 1.6 and 62.5 ± 1.7%, respectively. In the presence of ethanol, a similar enhancement of BTX-stimulated $^{22}Na^+$ uptake was noted (1 μg/ml, 27.3 ± 3.8; 10 μg/ml, 54.2 ± 3.8%). Thus, ethanol does not have a significant effect on the allosteric interaction of ScV and BTX.

The effect of ethanol on the inhibition of BTX-stimulated $^{22}Na^+$ uptake by TTX is shown in figure 8. An ethanol concentration of 200 mM did not affect the potency of the specific inhibitor TTX. The concentration of TTX necessary for a 50% reduction in BTX-stimulated $^{22}Na^+$ uptake in control samples was 12.72 ± 0.61 nM. In the presence of ethanol, a similar value (12.60 ± 0.59 nM) was measured.

Discussion

Incuhation of synaptosomes with ethanol *in vitro* caused a significant inhibition of the initial rates of neurotoxin-stimulated sodium uptake. This effect of ethanol was concentration-

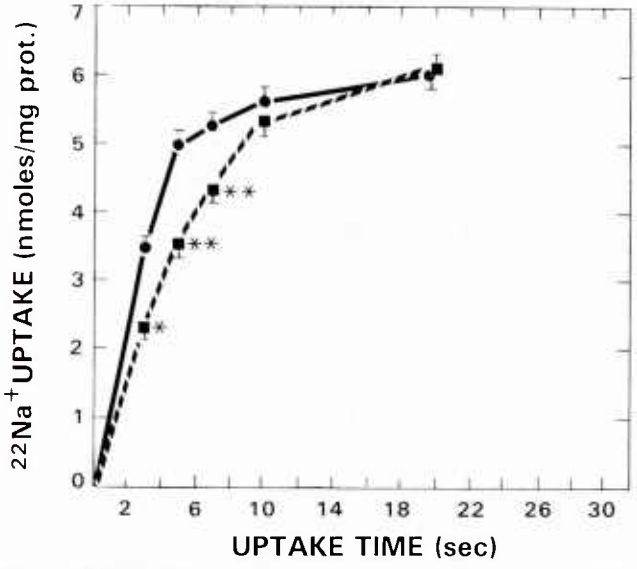

Fig. 5. Effect of ethanol on the time course of BTX-stimulated $^{22}Na^+$ uptake. Synaptosomes were preincubated with buffer only or buffer containing ethanol (200 mM) for 2 min. BTX (1 μM) was added and samples were incubated for an additional 10 min and $^{22}Na^+$ uptake was measured for the indicated time. Symbols represent the means ± S.E.M., $N = 5$ experiments. *P < .05; **P < .01 (paired t test) compared to corresponding control. prot., protein.

TABLE 2

Effect of preincubation time with ethanol on inhibition of BTX-stimulated $^{22}Na^+$ uptake; duration of preincubation[a]

	0 min	0.5 min	2.0 min	10 min
Control	4.72 ± 0.35[b]	4.82 ± 0.39	5.22 ± 0.17	4.65 ± 0.25
Ethanol, 200 mM	3.64 ± 0.39*	3.82 ± 0.38*	3.89 ± 0.20*	3.60 ± 0.21*

[a] Refers to the duration of preincubation of tissue with buffer or buffer containing ethanol (200 mM) before the addition of BTX (1 μM).
[b] Values are means ± S.E.M., $N = 3$ experiments, units are nanomoles of $^{22}Na^+$ per milligram of protein per 5 sec.
* Significantly different from corresponding control, $P < .01$.

TABLE 3

Effects of aliphatic alcohols *in vitro* on BTX-stimulated $^{22}Na^+$ uptake

Alcohol	Pm/b[a]	IC_{50}[b]	Slope[b]	r^2
Ethanol	0.096	582.8 ± 51.8	−71.1 ± 7.2	0.980
Propanol	0.438	104.0 ± 13.6	−72.8 ± 6.9	0.983
Butanol	1.52	35.9 ± 5.4	−65.1 ± 9.2	0.993
Pentanol	5.02	6.6 ± 0.6	−55.9 ± 6.6	0.940
Hexanol	21.4	1.2 ± 0.06	−60.0 ± 9.6	0.936

[a] Membrane/buffer partition coefficient ($P_{m/b}$) values are from McCreery and Hunt (1978).

[b] Values are the means ± S.E.M., N = 4–8 experiments. In each experiment, three or four concentrations of each alkanol were tested. IC_{50}, the concentration of each alcohol necessary to reduce control BTX-stimulated uptake by 50%. Values were derived from linear regression analysis of percentage of control uptake *vs.* log [alkanol].

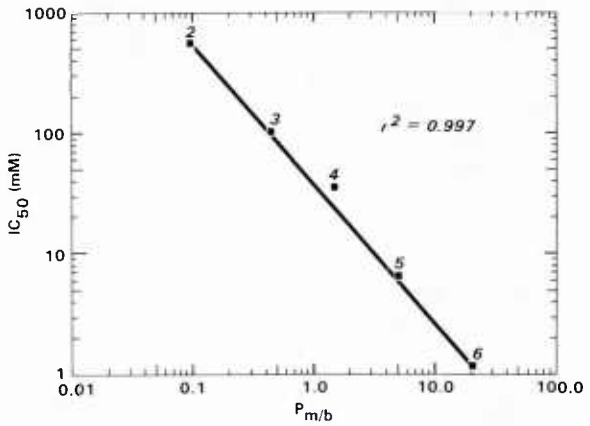

Fig. 6. Correlation of the inhibitory potency of aliphatic alcohols on BTX-stimulated $^{22}Na^+$ uptake with their membrane/buffer partition ($P_{m/b}$) coefficient. The concentration of each alcohol that inhibits BTX-stimulated $^{22}Na^+$ uptake by 50% (IC_{50}, millimolar) is presented on the ordinate. The $P_{m/b}$s are shown on the abscissa. The number above each symbol represents the chain length of the alcohol: 2, ethanol; 3, *n*-propanol; 4, *n*-butanol; 5, *n*-pentanol; and 6, *n*-hexanol. The line was fit by linear regression analysis with a correlation coefficient, r^2 = 0.997. See table 3 for details.

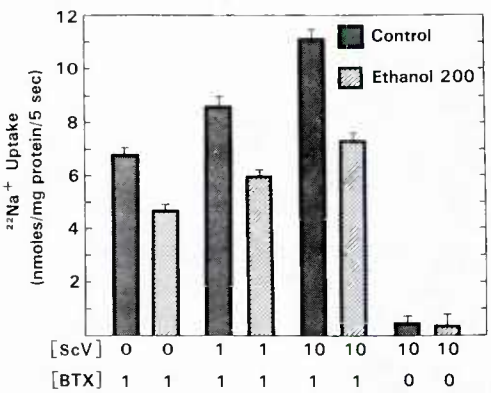

Fig. 7. The effect of ethanol *in vitro* on the BTX-ScV interaction. An aliquot of synaptosomes was preincubated for 2 min with buffer (control) or buffer containing ethanol. The indicated concentrations of BTX and ScV were added and $^{22}Na^+$ uptake was measured as described. The units of concentration for ScV and BTX were micrograms per milliliter and micromolar, respectively. The data are presented as the means ± S.E.M., N = 4 experiments.

dependent, occurred with pharmacologically relevant (50 mM) concentrations of ethanol and was fully reversible when ethanol was removed from the system. In addition, there was a good correlation between potency for inhibition of BTX-stimulated

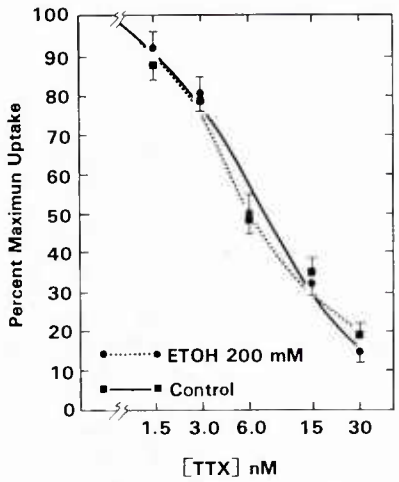

Fig. 8. Effect of ethanol on the inhibition of BTX-stimulated $^{22}Na^+$ uptake by TTX. Triplicate samples of whole brain synaptosomes were preincubated for 2 min with buffer (control) or with buffer containing ethanol. The indicated concentration of TTX was added and 3 min later BTX (1 μM) was added and all samples were incubated for an additional 10 min. Symbols represent the means ± S.E.M., N = 4 experiments. Maximum uptake for control and ethanol samples was 6.50 ± 0.13 and 4.33 ± 0.13 nmol of $^{22}Na^+$ per mg of protein per 5 sec, respectively.

$^{22}Na^+$ uptake and the membrane/buffer partition coefficients for a series of aliphatic alcohols, suggesting that a hydrophobic area of the sodium channel microenvironment was involved in the action of the alkanols. Inasmuch as the neurotoxin-stimulated uptake of sodium was blocked by the specific inhibitor TTX with a $K_{0.5}$ of approximately 13 nM, it appears that the neurotoxin-stimulated sodium uptake that was inhibited by ethanol occurred through voltage-sensitive sodium channels in synaptosomes (Catterall, 1980). Our results with ethanol are consistent with the work of Harris (1984) which showed that a variety of intoxicant anesthetics agents reduced neurotoxin-stimulated sodium uptake.

In the CNS, ionic channels for calcium, potassium and sodium are involved intimately in the control of excitability and each plays an essential role in signal transduction and information processing (Catterall, 1984). At the present time, the structural and functional properties of the voltage-sensitive sodium channels are understood most completely. This is due in part to the existence of a variety of neurotoxins that can be used as tools to study the sodium channel (Narahashi, 1974). In this regard, BTX has been defined as a full agonist (Catterall, 1980; Tamkun and Catterall, 1981) because it activates a larger number of sodium channels and is also more potent ($K_{0.5}$ value is smaller) than the partial agonist VER.

There appeared to be slight differences in the effect of ethanol when different neurotoxins were used to stimulate sodium uptake. When BTX was used to stimulate sodium uptake, the maximum effect of BTX was reduced by ethanol with no change in the $K_{0.5}$ value. Also, the minimum effective concentration of ethanol was 50 mM and the concentration of ethanol required for 50% inhibition (IC_{50}) was approximately 583 mM. VER-stimulated sodium uptake was more sensitive to inhibition by ethanol because the minimum effective concentration of ethanol was 25 mM and the IC_{50} value was approximately 345 mM (Mullin and Hunt, 1984). Ethanol reduced the maximum effect of VER and there was also a clear trend toward reducing the $K_{0.5}$ value of VER. It would be desirable to perform

more experiments with VER to investigate further this point, but during the course of this study VER became unavailable commercially. Even though it is well known that BTX and VER compete for the same binding site in the channel (Catterall, 1975), the mechanism by which each neurotoxin stimulates sodium uptake may be slightly different because of other properties of the toxins (Miller, 1983; Tanaka *et al.*, 1983).

The action of ethanol on the voltage-sensitive sodium channels in synaptosomes appears to be somewhat selective for the site that binds BTX and VER. Ethanol did not interfere with the allosteric interaction that occurred between BTX and ScV. Similarly, the presence of ethanol did not alter the concentration of TTX required to inhibit BTX-stimulated sodium uptake by 50%. However, it must be noted that these findings concerning the effects of ethanol on neurotoxin receptor sites I (TTX) and III (ScV) are based on indirect measurements. Direct measurement using radiolabeled neurotoxins should clarify these points.

Recent studies with fluorescent derivatives of sodium channel neurotoxins (Angelides and Nutter, 1983, 1984) in conjunction with published biochemical evidence (Hartshorne and Catterall, 1981, 1984; Ellisman *et al.*, 1982) have advanced our knowledge of the molecular arrangement of the functional components of the sodium channel. Angelides and Nutter (1984) have proposed a model wherein the TTX binding site resides in a highly polar, hydrophilic area at the extracellular side of the membrane. The binding site for ScV may be located in a more hydrophobic region that is not lipid in nature and may extend 15 A into the cell membrane. The final neurotoxin receptor site (for BTX and VER) is placed in a hydrophobic area directly interacting with the subunit of the channel and the interior of the lipid bilayer. Thus, in this model, the BTX/VER binding site is located in the area of the membrane in which the fluidizing effect of ethanol is greatest (Harris and Schroeder, 1981). An explanation for the observed effects of ethanol on neurotoxin-stimulated sodium uptake may involve changes in the fluidity of the neuronal membrane as a number of other membrane perturbants inhibit sodium uptake with potency for inhibition of sodium uptake being related to lipid solubility (Harris, 1984). Ethanol may alter the arrangement of membrane lipids or hydrophobic proteins in a specific area of the sodium channel microenvironment. In addition, disruption of important lipid-protein interactions by ethanol may result in suboptimal conditions that would adversely affect sodium channel function. Further studies of sodium channel function in systems in which the lipid and protein components are more tightly controlled may answer some of these questions.

It is difficult to determine how important the effect of ethanol on sodium channels is to the intoxicating effect of ethanol. In this study and that of Harris and Bruno (1985), an ethanol concentration of 50 to 100 mM was required to produce a significant inhibitory effect. Previous work from our laboratory demonstrated that an ethanol concentration of 25 mM which is commonly achieved *in vivo* and is associated with moderate intoxication was sufficient to cause a significant inhibition of VER-stimulated $^{22}Na^+$ uptake (Mullin and Hunt, 1984). Additionally, it appears that brain regions differ in sensitivity to this effect of ethanol (Harris and Bruno, 1985).

We have used an ion flux assay to study the effects of ethanol on sodium channel function in synaptosomes in which electrophysiological methods are not practical. Because it is necessary to use toxins to activate the sodium channels, one must consider the possibility that ethanol is interfering with the binding of the toxins to their receptors in the channel. This could explain the results we have presented. This question is currently under study in our laboratory using radiolabeled toxins.

Acknowledgments

The authors thank Dr. John Daly for generously providing BTX, Mr. Tom Dalton for technical assistance, Mrs. Marion Golightly for preparing the manuscript and Drs. R. Adron Harris and E. Majchrowicz for their comments.

References

ANGELIDES, K. J. AND NUTTER, T. J.: Mapping the molecular structure of the voltage-dependent sodium channel: Distances between the tetrodotoxin and Leiurus quinquestriatus scorpion toxin receptors. J. Biol. Chem. **258:** 11958–11967, 1983.

ANGELIDES, K. J. AND NUTTER, T. J.: Molecular and cellular mapping of the voltage-dependent sodium channel. Biophys. J. **45:** 31–34, 1984.

CATTERALL, W. A.: Activation of the action potential Na^+ ionophore of cultured neuroblastoma cells by veratridine and batrachotoxin. J. Biol. Chem. **250:** 4053–4059, 1975.

CATTERALL, W. A.: Purification of a toxic protein from scorpion venom which activates the action potential Na^+ ionophore. J. Biol. Chem. **251:** 5528–5536, 1976.

CATTERALL, W. A.: Neurotoxins that act on voltage-sensitive sodium channels in excitable membranes. Annu. Rev. Pharmacol. Toxicol. **20:** 15–43, 1980.

CATTERALL, W. A.: The emerging molecular view of the sodium channel. Trends Neurosci. **5:** 303–306, 1982.

CATTERALL, W. A.: The molecular basis of neuronal excitability. Science (Wash. DC) **223:** 653–661, 1984.

CHIN, J. H. AND GOLDSTEIN, D. B.: Effects of low concentrations of ethanol on the fluidity of spin-labeled erythrocytes and brain membranes. Mol. Pharmacol. **13:** 435–441, 1977a.

CHIN, J. H. AND GOLDSTEIN, D. B.: Drug tolerance in biomembranes: A spin label study of the effects of ethanol. Science (Wash. DC) **196:** 684–685, 1977b.

CHIN, J. H. AND GOLDSTEIN, D. B.: Membrane-disordering action of ethanol: Variation with membrane cholesterol content and depth of the spin label probe. Mol. Pharmacol. **19:** 425–431, 1981.

DUNNETT, C. W.: New tables for multiple comparisons with a control. Biometrics **20:** 482–491, 1964.

ELLISMAN, M. H., AGNEW, W. S., MILLER, J. A. AND LEVINSON, S. R.: Electron microscopic visualization of the tetrodotoxin-binding protein from Electrophorus electricus. Proc. Natl. Acad. Sci. U.S.A. **79:** 4461–4465, 1982.

GOLDSTEIN, D. B., CHIN, J. H. AND LYON, R. C.: Ethanol disordering of spin-labeled mouse brain membranes: Correlation with genetically determined ethanol sensitivity of mice. Proc. Natl. Acad. Sci. U.S.A. **79:** 4231–4233, 1982.

GOLDSTEIN, D. B., CHIN, J. H., MCCOMB, J. A. AND PARSONS, L. M.: Chronic effects of alcohols on mouse biomembranes. *In* Biological Effects of Alcohol, ed. by H. Begleiter, pp. 1–6, Plenum Press, New York, 1980.

GRAY, E. G. AND WHITTAKER, V. P.: The isolation of nerve endings from brain: An electron-microscopic study of cell fragments derived by homogenization and centrifugation. J. Anat. **96:** 79–87, 1962.

HARRIS, R. A.: Differential effects of membrane perturbants on voltage-activated sodium and calcium channels and calcium-dependent potassium channels. Biophys. J. **45:** 132–134, 1984.

HARRIS, R. A. AND BRUNO, P.: Effects of ethanol and other intoxicant-anesthetics on voltage-dependent sodium channels of brain synaptosomes. J. Pharmacol. Exp. Ther. **232:** 401–406, 1985.

HARRIS, R. A. AND SCHROEDER, F.: Ethanol and the physical properties of brain membranes: Fluorescence studies. Mol. Pharmacol. **20:** 128–137, 1981.

HARTSHORNE, R. P. AND CATTERALL, W. A.: Purification of the saxitoxin receptor of the sodium channel from rat brain. Proc. Natl. Acad. Sci. U.S.A. **78:** 4620–4624, 1981.

HARTSHORNE, R. P. AND CATTERALL, W. A.: The sodium channel from rat brain: Purification and subunit composition. J. Biol. Chem. **259:** 1667–1675, 1984.

HILLE, V.: Ionic channels in nerve membranes. Prog. Biophys. Mol. Biol. **21:** 1–32, 1970.

HODGKIN, A. L. AND HUXLEY, A. F.: A quantitative description of membrane current and its application to conduction and excitation in nerve. J. Physiol. (Lond.) **117:** 500–544, 1952.

LENAZ, G.: Lipid properties and lipid-protein interactions. *In* Membrane Proteins and Their Interactions with Lipids, ed. by R. A. Capaldi, pp. 47–150, Marcel Dekker, New York, 1977.

LOWRY, O. H., ROSEBROUGH, N. J., FARR, A. L. AND RANDALL, R. J.: Protein measurement with the Folin phenol reagent. J. Biol. Chem. **193:** 265–275, 1951.

LYON, R. C., MCCOMB, J. A., SCHREURS, J. AND GOLDSTEIN, D. B.: A relationship between alcohol intoxication and the disordering of brain membranes by a series of short-chain alcohols. J. Pharmacol. Exp. Ther. **21:** 669–675, 1981.

MCCREERY, M. J. AND HUNT, W. A.: Physicochemical correlates of alcohol intoxication. Neuropharmacology **17:** 451–461, 1978.

MILLER, C.: Integral membrane channels: Studies in model membranes. Physiol. Rev. **63:** 1209–1242, 1983.

MULLIN, M. J. AND HUNT, W. A.: Ethanol inhibits veratridine-stimulated sodium uptake in synaptosomes. Life Sci. **34:** 287–292, 1984.

NARAHASHI, T.: Chemicals as tools in the study of excitable membranes. Physiol. Rev. **54:** 813–889, 1974.

NARAHASHI, T., ANDERSON, N. C. AND MOORE, J. W.: Tetrodotoxin does not block excitation from inside the nerve membrane. Science (Wash. DC) **153:** 765–767, 1966.

RITCHIE, J. M. AND ROGART, R. B.: The binding of saxitoxin and tetrodotoxin to excitable tissue. Rev. Physiol. Biochem. Pharmacol. **79:** 1–51, 1977.

SEEMAN, P.: The membrane actions of anesthetics and tranquilizers. Pharmacol. Rev. **24:** 583–655, 1972.

TAMKUN, M. M. AND CATTERALL, W. A.: Ion flux studies of voltage-sensitive sodium channels in synaptic nerve-ending particles. Mol. Pharmacol. **19:** 78–86, 1981.

TANAKA, J. C., ECCLESTON, J. F. AND BARCHI, R. L.: Cation selectivity characteristics of the reconstituted voltage-dependent sodium channel purified from rat skeletal muscle sarcolemma. J. Biol. Chem. **25:** 7519–7526, 1983.

ULBRICHT, W.: Ionic channels and gating currents in excitable membranes. Annu. Rev. Biophys. Bioeng. **6:** 7–31, 1977.

Send reprint requests to: Dr. Michael J. Mullin, Behavioral Sciences Department, Armed Forces Radiobiology Research Institute, Naval Medical Command, National Capital Region, Bethesda, MD 20814-5011.

ARMED FORCES RADIOBIOLOGY
RESEARCH INSTITUTE
SCIENTIFIC REPORT
SR86-10

Journal of Biological Response Modifiers
5:45–60 © 1986 Raven Press, New York

Comparative Effects of Soluble and Particulate Glucans on Survival in Irradiated Mice

M. L. Patchen and T. J. MacVittie

Department of Experimental Hematology, Armed Forces Radiobiology Research Institute, Bethesda, Maryland, U.S.A.

Summary: The survival-enhancing capabilities of particulate (P) and soluble (F) glucan, a B-1,3 polyglycan biological response modifier, were assayed in ^{60}Co irradiated mice. Although glucan-P was slightly more effective than glucan-F, both glucans significantly enhanced survival in otherwise lethally irradiated (9.0–11.0 Gy) C_3H/HeN mice. Following 9.0 Gy, 60% of the glucan-P treated and 53% of the glucan-F treated mice exhibited long-term survival as opposed to 0% of the radiation control mice. The survival-enhancing effects of glucan-P and glucan-F decreased as the radiation dose increased to 11.0 Gy. At higher radiation doses (e.g., 12.0 Gy) neither glucan preparation was capable of enhancing survival. Both glucan-P and glucan-F enchanced the recovery of peripheral blood white cell numbers, platelet numbers, and hematocrit values. In addition, both agents increased endogenous pluripotent hemopoietic stem cell numbers in sublethally irradiated mice. Taken together, these results demonstrate that both glucan-P and glucan-F can significantly enhance survival in lethally irradiated mice. However, these agents appear to function specifically by enhancing hemopoietic recovery and are not effective at radiation doses also known to induce gastrointestinal damage. **Key Words:** Biological response modifiers—Glucan—Hemopoiesis—Polyglycans—Radioprotection

Hemopoietic and immune depression is a well-documented phenomenon following chemotherapy and/or radiotherapy (1,2). In particular, irradiation has been shown to predispose animals to a variety of potentially lethal exogenous and endogenous opportunistic pathogens (2–8). Thus, treatments to combat hemopoietic and immune depression and/or the secondary consequences of hemopoietic and immune depression are of primary clinical concern.

Glucan is a B-1,3 polyglycan biological response modifier (BRM) that is isolated from the yeast *Saccharomyces cerevisiae*. Following the administration of glucan to mice, rats, dogs, and primates, a variety of enhanced reticuloendothelial, immune, and hemopoietic responses have been observed. For example, glucan administration is associated with macrophage activation, increased reticuloendothelial system activity, and stimulated humoral- and cell-mediated immune responses (9–12). Glucan

Received April 30, 1985; accepted August 12, 1985.
Address correspondence and reprint requests to Dr. M. L. Patchen at Department of Experimental Hematology, Armed Forces Radiobiology Research Institute, Bethesda, MD 20814–5145, U.S.A.

treatment also enhances hemopoiesis at the stem cell level in normal mice (13–15) and even enhances hemopoietic recovery in sublethally irradiated mice when administered either before or after the radiation insult (16–19). Probably because of its ability to stimulate reticuloendothelial, immune, and hemopoietic responses, glucan has also proven useful at enhancing host resistance to a variety of experimentally induced bacterial (20–23), fungal (24,25), viral (22,26), and parasitic (27,28) disease states.

Because septicemia is a common lethal secondary consequence of irradiation in doses sufficient to damage the immune and hemopoietic systems, we investigated the possibility that glucan might be able to enhance survival in irradiated mice. In these particular studies the survival-enhancing capabilities of both particulate and soluble glucans were evaluated.

MATERIALS AND METHODS

Mice

In all experiments 10–12-week-old female C_3H/HeN mice, obtained from Charles River Laboratories (Wilmington, MA, U.S.A.), were used. Animals were maintained on a 6:00 a.m.–6:00 p.m. light–dark cycle. Wayne Lab Blox and hyperchlorinated water were available ad libitum. All mice were quarantined and acclimated to laboratory conditions for 2 weeks before experimentation. During this time, the mice were examined and found to be free of lesions of murine pneumonia complex, murine hepatitus virus, and oropharyngeal *Pseudomonas* sp.

Glucans

Particulate glucan (glucan-P) was obtained from Accurate Chemical and Scientific Corporation (Westbury, NY, U.S.A.) and was prepared according to DiLuzio's modification (29) of Hassid's original procedure (30). Stock glucan-P preparations contained 1- to 2-μm glucan particles suspended in sterile saline at a concentration of 5 mg/ml. Glucan-P was further diluted in sterile saline, and 1.5 mg in a volume of 0.5 ml was intravenously injected into experimental mice via the lateral tail veins. Soluble glucan (glucan-F) was obtained from Dr. N. R. DiLuzio (Tulane University Medical Center, New Orleans, LA, U.S.A.) and was prepared as described by DiLuzio et al. (29). Stock glucan-F preparations contained 10 mg of soluble glucan per ml of sterile saline. All mice were intravenously injected with 0.5 ml of the stock glucan-F (i.e., 5.0 mg). In some experiments 5.0 mg (in a 0.5 ml volume) of three other soluble B-1,3 polyglycan BRMs were also intravenously injected into mice. These agents consisted of Krestin (PSK), Schizophyllan (SPG), and mannan-R, which were generously provided by Dr. P. Jacques (Catholic University of Louvain, Brussels, Belgium). Table 1 provides additional information on each of these polyglycan BRMs. Control mice were injected with 0.5 ml of sterile saline. The *Limulus* lysate assay was used to ensure that all polyglycan preparations were free from endotoxin contamination.

Irradiation

Bilateral total body irradiation from the AFRRI ^{60}Co source at a dose rate of 0.4 Gy/min was used in all experiments.

TABLE 1. *Biological and physical characteristics of one particulate and four soluble B-1,3 polyglycans*

Compound	Solubility	Biological source	Structure	Molecular weight	Commercial source
Glucan-P	No	*Saccharomyces cerevisiae*	B-1,3 glucan B-1,6 glucan	(1–2 μm particle)	Accurate Chemical & Scientific Co., Westbury, NY, U.S.A.
Glucan-F	Yes	*S. cerevisiae*	B-1,3 glucan	10×10^5	—
Krestin	Yes	Coriolus versicolor	B-1,4 glucan B-1,3 glucan B-1,6 glucan (25–38% protein)	1×10^5	Kureha Chemical Co., Tokyo, Japan
Mannan-R	Yes	*Rhodotorulum rubrum*	B-1,3 mannan B-1,4 mannan	—	—
Schizophyllan	Yes	Schizophyllum commune media	B-1,3 glucan B-1,6 glucan	5×10^5	Kaken Co., Tokyo, Japan

Survival Measurements

Mice used in survival studies were exposed to various doses of total-body irradiation, and their survival was checked daily for a period of 30 days.

Endogenous Spleen Colony-Forming Unit Assay

Endogenous spleen colony-forming units (E-CFU) were evaluated by the method of Till and McCulloch (31). Mice were exposed to doses of 6.5, 7.0, 7.5, 8.0, or 8.5 Gy of total-body irradiation to partially oblate endogenous hemopoietic stem cells. Ten days after irradiation, the mice were killed; their spleens were removed and fixed in Bouins's fixative; and the number of grossly visible spleen colonies were counted.

Peripheral Blood White Cell Counts, Platelet Counts, and Hematocrit Determinations

Mice were ether anesthetized and bled from the retroorbital sinus. White blood cell counts and platelet counts were performed by collecting 20 μl of blood into a calibrated capillary tube, dispensing it into 1.98 ml of ammonium oxalate diluent (Unopettes, Becton-Dickinson, Rutherford, NJ, U.S.A.), and counting white blood cells and platelets on a hemocytometer. Hematocrits were used as an indicator of red blood cellularity.

Statistical Analyses

The Kruskal Wallis test was used to compare 30 day survival levels in polyglycan-treated versus control irradiated mice. The Student's *t* test was used to analyze E-CFU and spleen weight data.

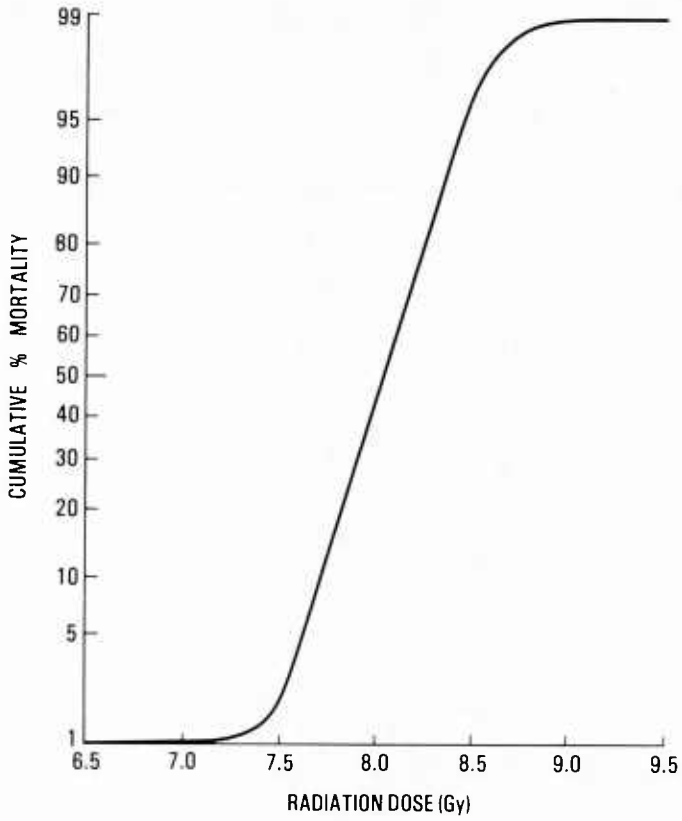

FIG. 1. Effect of irradiation on survival of C_3H/HeN mice exposed to graduated doses of ^{60}Co irradiation. Cumulative mortality data were calculated from 31–35 mice at each radiation dose.

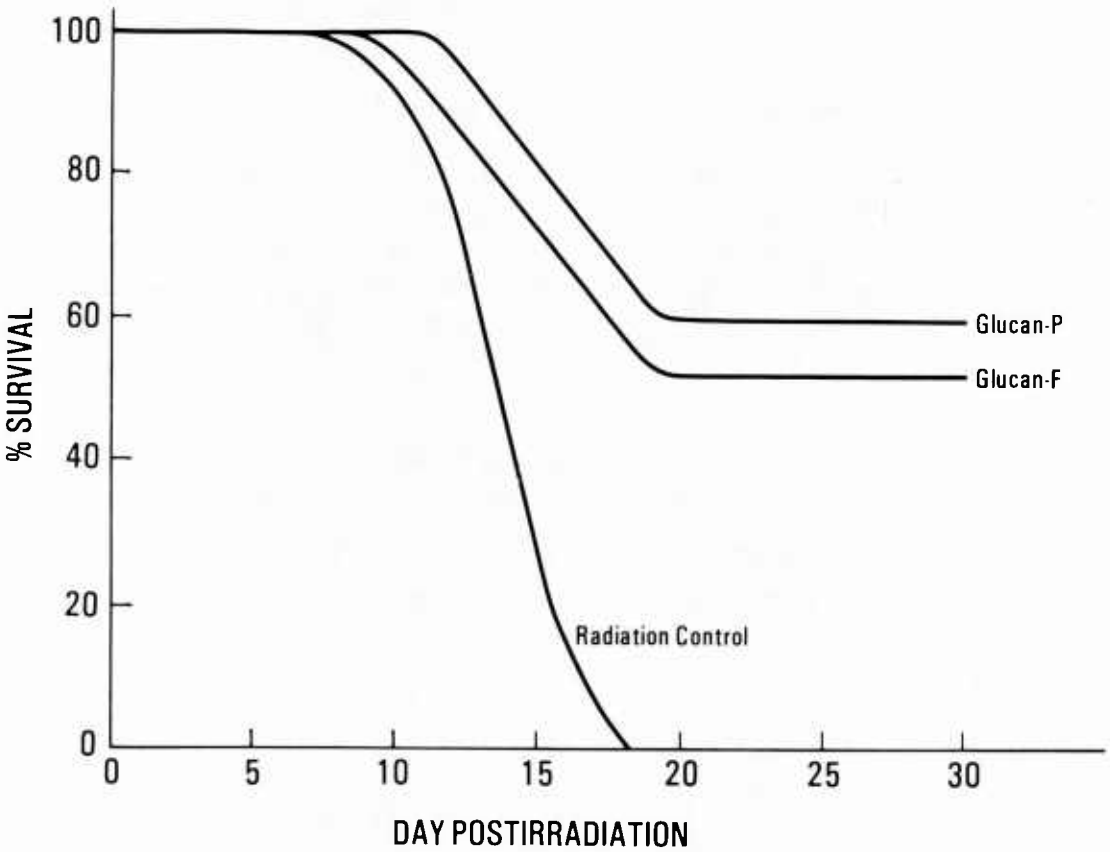

FIG. 2. Effects of glucan-P and glucan-F on survival in C_3H/HeN mice exposed to 9.0 Gy ^{60}Co irradiation 1 day after glucan injections. Cumulative survival data were calculated from 49 radiation control mice, 50 glucan-P-treated mice ($p \leq 0.01$), and 48 glucan-F-treated mice ($p \leq 0.01$).

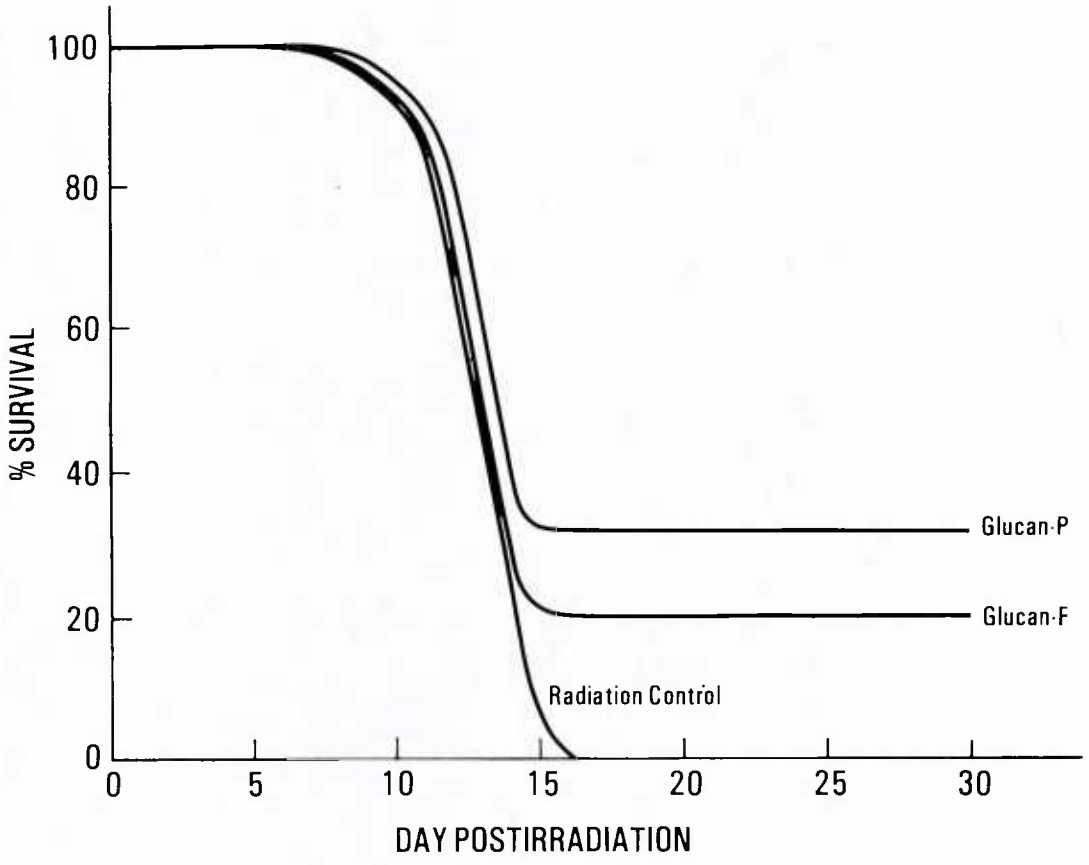

FIG. 3. Effects of glucan-P and glucan-F on survival in C_3H/HeN mice exposed to 10.0 Gy ^{60}Co irradiation 1 day after glucan injections. Cumulative survival data were calculated from 47 radiation control mice, 48 glucan-P-treated mice ($p \leq 0.01$), and 49 glucan-F-treated mice ($p \leq 0.01$).

RESULTS

Dose Response of Radiation-Induced Mortality

Prior to undertaking studies to compare the radioprotective abilities of soluble and particulate glucans, it was necessary to establish a radiation dose response mortality curve for the mouse strain used in these experiments. Figure 1 illustrates a probit plot of 30 day cumulative mortality in normal C_3H/HeN mice exposed to increasing doses of ^{60}Co radiation. As can be seen, mice that had been exposed to radiation doses less than 7.0 Gy rarely died (<1% mortality), whereas, >99% of mice that had been exposed to radiation doses greater than or equal to 9.0 Gy died. Because we were interested in evaluating the ability of glucan to alter radiation-induced mortality in a "worse case" scenario, radiation doses $\geq$9.0 Gy were used in all subsequent survival studies.

Effects of Glucan-P and Glucan-F on Radiation-Induced Mortality

To determine whether glucan-P and glucan-F could enhance the survival of otherwise lethally irradiated mice, mice were injected with glucan-P, glucan-F, or sterile saline 24 h before exposure to 9.0, 10.0, 11.0, or 12.0 Gy of ^{60}Co radiation. The cumulative 30-day survival data from these experiments are presented in Figs. 2–5,

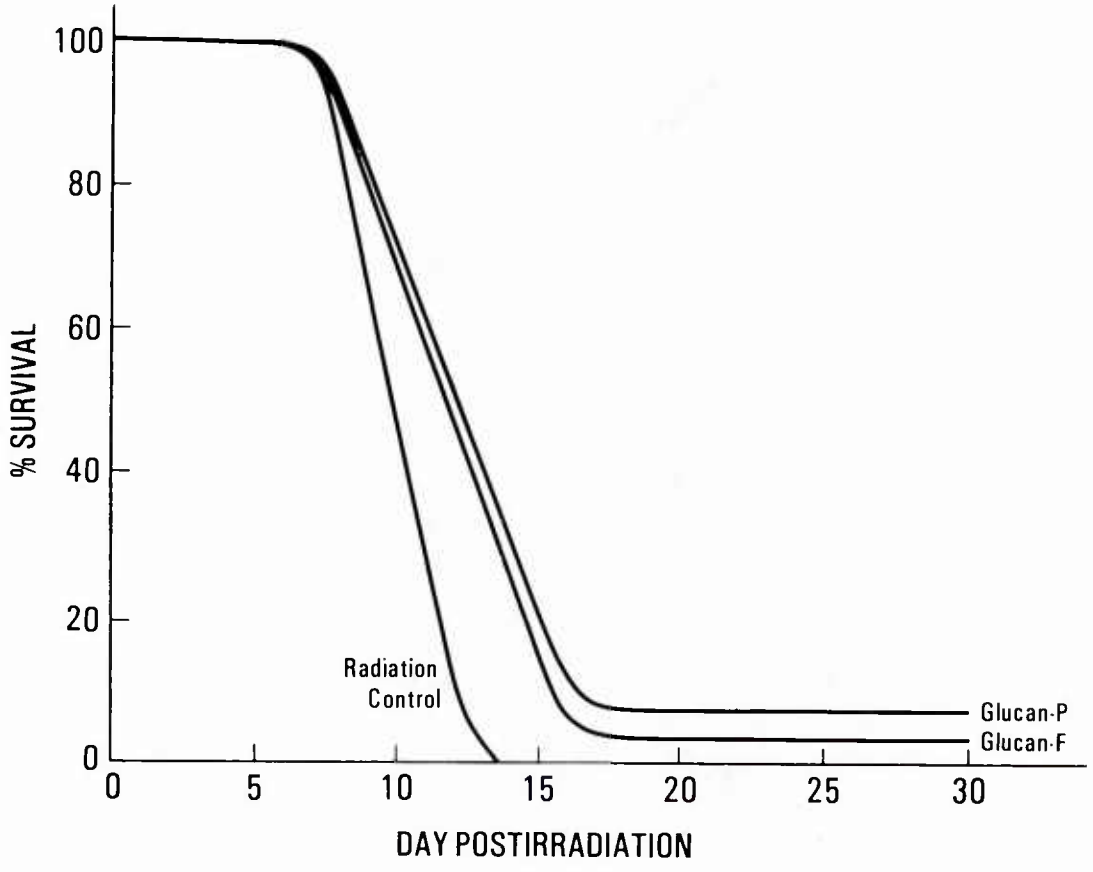

FIG. 4. Effects of glucan-P and glucan-F on survival in C_3H/HeN mice exposed to 11.0 Gy ^{60}Co irradiation 1 day after glucan injections. Cumulative survival data were calculated from 51 radiation control mice, 49 glucan-P-treated mice ($p \leq 0.05$), and 50 glucan-F-treated mice.

respectively. When either glucan-P or glucan-F was injected prior to a 9.0, 10.0, or 11.0 Gy irradiation, survival was significantly increased above that of radiation controls. This effect was radiation dose-dependent, in that a greater enhancement was observed after a 9.0 Gy exposure than after a 10.0 Gy exposure; and a greater enhancement was seen after a 10.0 Gy exposure than after an 11.0 Gy exposure. In addition, at each radiation dose examined, glucan-P consistently provided slightly better protection than did glucan-F. When the radiation dose was increased to 12.0 Gy, neither glucan-P nor glucan-F enhanced survival.

Effects of Various Glucan Injection Schedules on Radiation-Induced Mortality

To investigate whether glucan-mediated radioprotection might be further enhanced by manipulating the time of glucan administration, mice were injected with glucan-P at either 5 days, 2 days, or 1 day prior to a 9.0 Gy exposure of ^{60}Co. The results of these studies are presented in Fig. 6. As can be seen, day -2 glucan-P administration was less effective than day -1 glucan-P administration, and day -5 glucan-P administration offered no radioprotection. Experiments testing the ability of multiple glucan-P treatments to further enhance the radioprotection of glucan-P were also performed (Fig. 7). Multiple glucan-P treatments were ineffective at further enhancing survival; and, in fact, they appeared to provide even less protection than did a single glucan-P injection administered 1 day prior to radiation exposure.

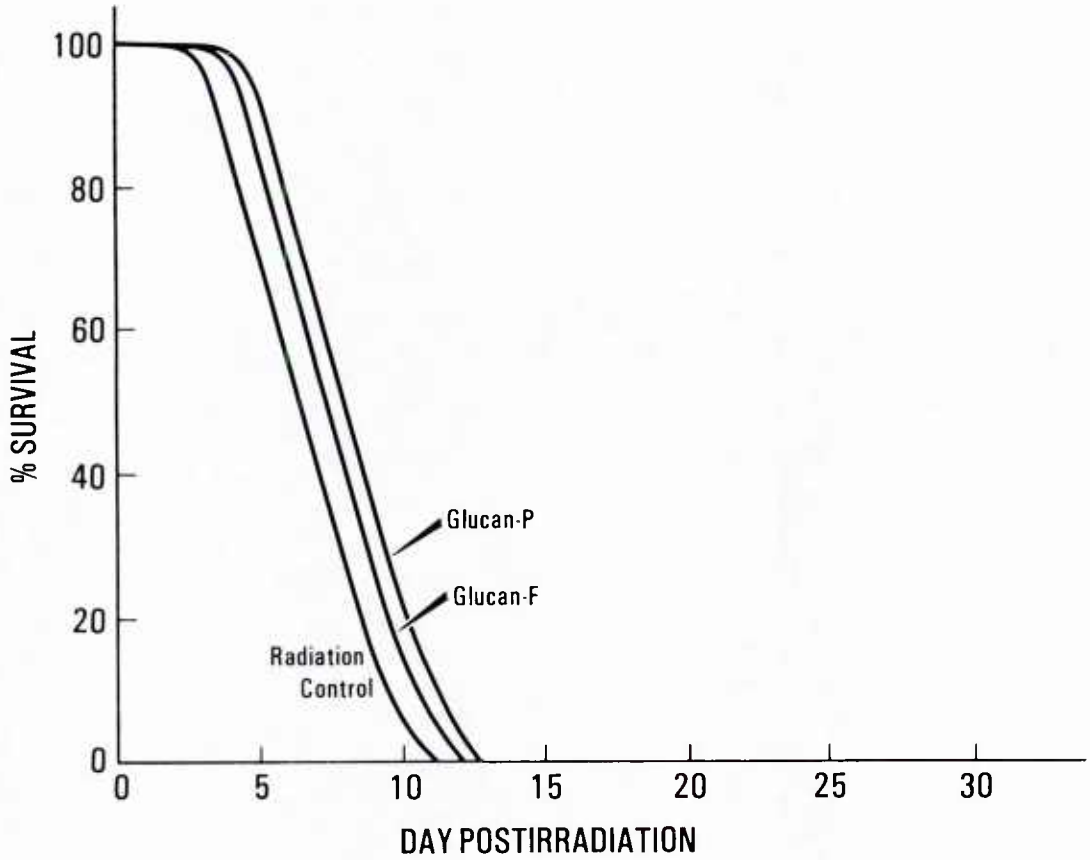

FIG. 5. Effects of glucan-P and glucan-F on survival in C_3H/HeN mice exposed to 12.0 Gy ^{60}Co irradiation 1 day after glucan injections. Cummulative survival data were calculated from 46 radiation control mice, 49 glucan-P-treated mice (NS), and 49 glucan-F-treated mice (NS). NS, not significant.

Effects of Other Polyglycans on Radiation-Induced Mortality

To distinguish whether the survival-enhancing effects provided by day − 1 glucan treatments were unique to glucan or were a general property of B-1,3 polyglycan BRMs, two soluble B-1,3 glucan-containing BRMs (PSK and SPG) and one soluble B-1,3 mannan-containing BRM (mannan-R) were injected 1 day prior to irradiation and the survival-enhancing capability of these polyglycans compared with that produced by soluble glucan-F. Although none of these agents was as effective as glucan-F at enhancing survival, the two agents containing B-1,3 glucan were somewhat protective and the agent containing B-1,3 mannan was not at all effective at enhancing survival (Fig. 8).

Hemopoietic Effects of Glucan-P and Glucan-F

Because glucan-P and glucan-F appeared to be radioprotective in the hemopoietic syndrome dose range (e.g., 9.0–11.0 Gy) but not at higher radiation doses, which also affect the gastrointestinal tract (e.g., 12.0 Gy), experiments were performed to assay the ability of glucan-P and glucan-F to enhance hemopoietic recovery. Specifically, the endogenous spleen colony-forming assay was used to assay the ability of these two BRMs to protect and/or enhance the recovery of pluripotent hemopoietic stem cells in irradiated mice. Glucan-P and glucan-F were administered 1 day prior

TABLE 2. *Effect of glucan-P and glucan-F on peripheral blood parameters in 9.0 Gy irradiated mice*

	Day post 9.0 Gy irradiation											
	1	2	3	6	8	10	13	15	17	20	24	30
Number of white blood cells ($\times 10^3$)/mm^3 peripheral blood												
Radiation control	1,595.0 ± 260	2,273.0 ± 352	73.0 ± 37	0.0	0.0	0.0	0.0	0.0	0.0	—	—	—
Glucan-P	550.0 ± 168	403.0 ± 132	0.0	0.0	0.0	37.0 ± 18	73.0 ± 36	183.0 ± 97	366.0 ± 160	623.0 ± 200	935.0 ± 386	1,595.0 ± 386
Glucan-F	1,833.0 ± 223	503.0 ± 130	37.0 ± 30	0.0	0.0	0.0	0.0	37.0 ± 18	73.0 ± 36	165.0 ± 45	1,110.0 ± 309	1,335.0 ± 368
Hematocrit (%)												
Radiation control	40.7 ± 0.3	40.2 ± 0.5	38.2 ± 0.6	33.2 ± 0.5	30.7 ± 0.8	21.0 ± 0.9	6.2 ± 1.6	4.8 ± 0.4	5.0 ± 1.0	—	—	—
Glucan-P	42.7 ± 0.9	38.0 ± 1.5	36.3 ± 0.7	27.3 ± 2.2	26.7 ± 0.9	18.7 ± 0.9	14.0 ± 3.0	10.3 ± 3.8	13.7 ± 5.2	19.3 ± 3.5	36.0 ± 2.0	38.5 ± 1.5
Glucan-F	41.0 ± 1.5	40.0 ± 1.0	35.7 ± 2.7	34.7 ± 2.7	26.0 ± 1.0	16.0 ± 1.0	5.6 ± 0.3	7.2 ± 0.3	8.6 ± 0.9	11.2 ± 1.3	26.0 ± 1.0	31.3 ± 2.3
Number of platelets ($\times 10^3$)/mm^3 peripheral blood												
Radiation control	1,099.0 ± 94	795.0 ± 40	679.0 ± 127	295.0 ± 57	29.0 ± 3	2.0 ± 1	1.0 ± 1	5.0 ± 3	7.0 ± 2	—	—	—
Glucan-P	476.0 ± 22	308.0 ± 6	173.0 ± 18	10.0 ± 3	5.0 ± 1	4.0 ± 1	15.0 ± 9	36.0 ± 5	46.0 ± 19	74.0 ± 20	209.0 ± 30	247.0 ± 38
Glucan-F	950.0 ± 47	872.0 ± 50	824.0 ± 13	275.0 ± 97	15.0 ± 9	3.0 ± 1	2.0 ± 1	15.0 ± 7	27.0 ± 9	31.0 ± 10	120.0 ± 30	187.0 ± 41

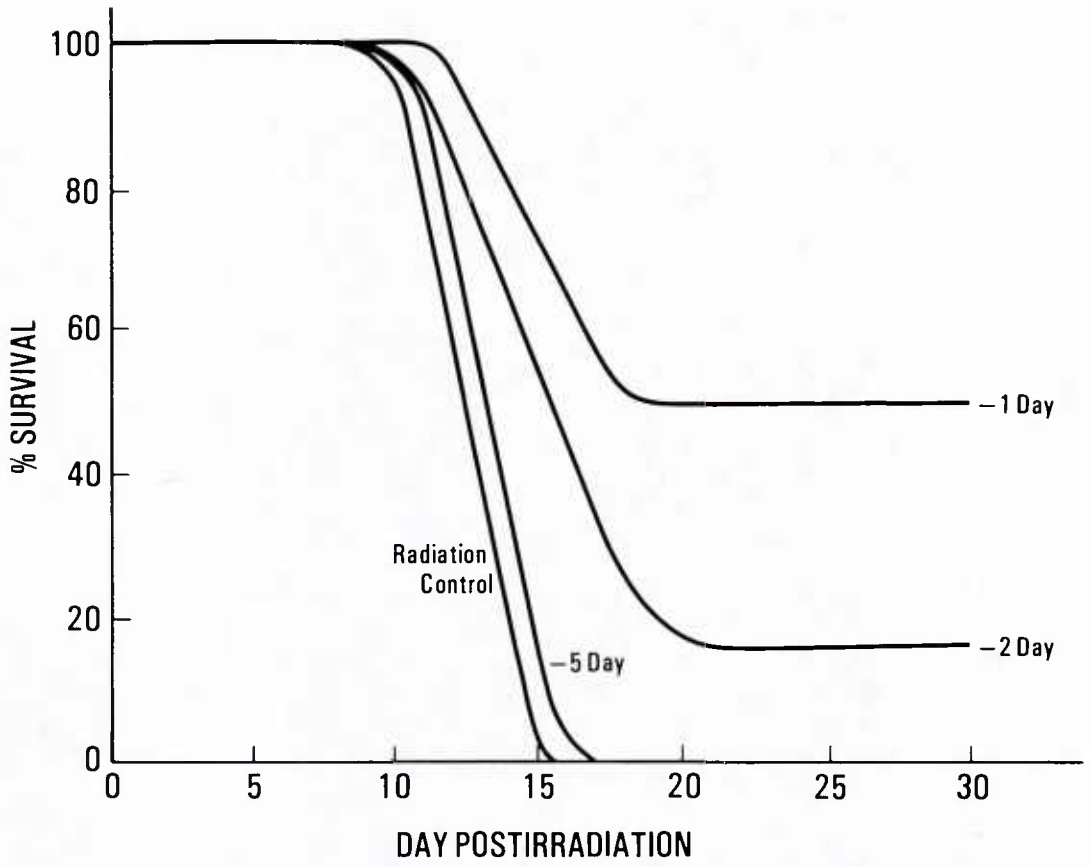

FIG. 6. Effects of time of glucan-P administration on survival in C_3H/HeN mice irradiated with 9.0 Gy ^{60}Co. Cummulative survival data were calculated from 59 radiation controls, 43 mice treated at day −1 ($p \leq 0.01$), 39 mice treated at day −2 ($p \leq 0.05$), and 43 mice treated at day −5 (NS). NS, not significant.

to various sublethal radiation exposures (6.5–8.5 Gy) and the number of E-CFU was determined (Fig. 9). At each radiation dose examined, both glucan-P and glucan-F significantly increased E-CFU numbers above radiation control values; glucan-P, however, was more stimulatory than was glucan-F. A similar phenomenon was observed when the spleen weights of these animals were examined (Fig. 10). When recovery of peripheral blood white cell counts, platelet counts, and hematocrit values were examined, mice treated with glucan-P and glucan-F prior to a 9.0 Gy radiation exposure also exhibited accelerated recovery of these hemopoietic parameters (Table 2).

Effects of Glucan-P and Glucan-F on Radiation-Induced Mortality When Administered Postirradiation

Glucan-P and glucan-F were administered to mice 1 h after a 9.0 Gy radiation exposure, and survival was monitored (Fig. 11). Glucan-F was still capable of slightly enhancing survival when administered postirradiation. On the other hand, glucan-P not only was not protective, but it actually induced death more rapidly than in radiation control mice.

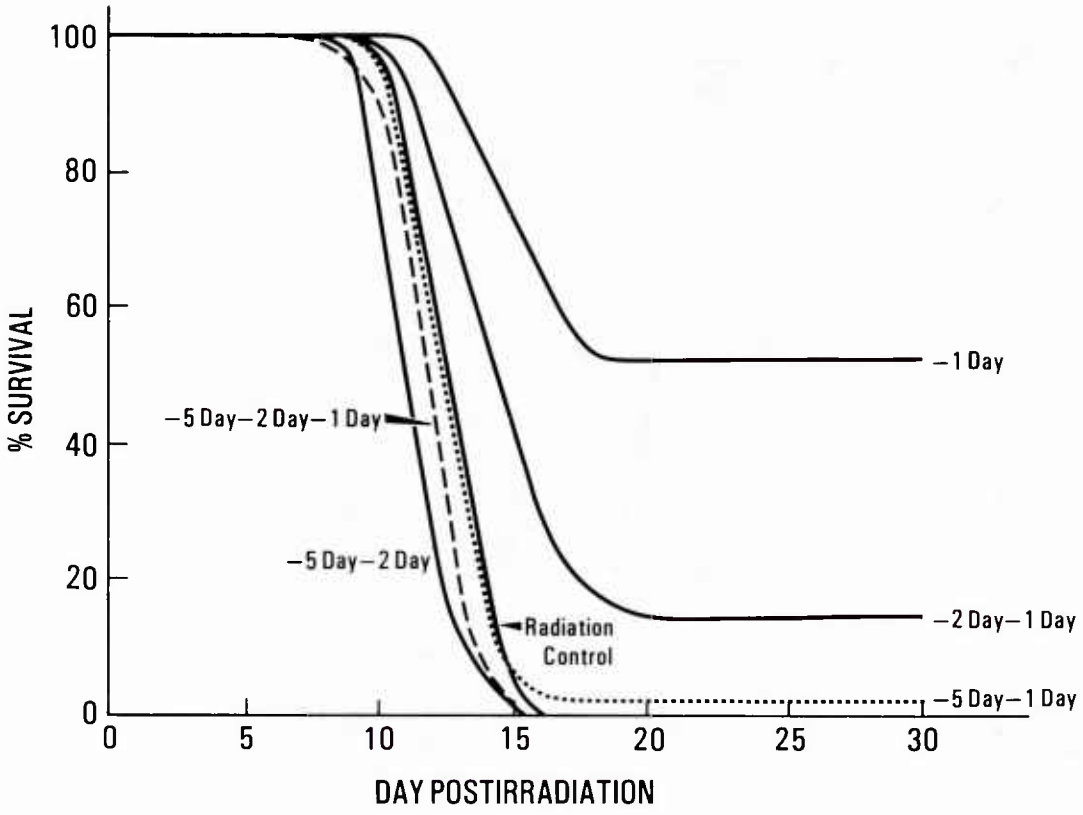

FIG. 7. Effects of multiple glucan-P injections on survival in C_3H/HeN mice irradiated with 9.0 Gy ^{60}Co. Cummulative survival data were calculated from 51 radiation control mice, 38 mice treated at day −1 ($p \leq 0.01$), 40 mice treated at day −2 and −1 ($p \leq 0.05$), 43 mice treated at day −5 and −1 (NS), 41 mice treated at day −5 and −2 (NS), and 40 mice treated at day −5, −2, and −1 (NS). NS, not significant.

DISCUSSION

We have previously demonstrated that glucan-P can enhance the survival of mice if administered prior to a 9.0 Gy dose of ^{60}Co radiation (18). The studies presented here have demonstrated the survival-enhancing capabilities of not only glucan-P but also glucan-F in ^{60}Co-irradiated mice. The ability of these agents to enhance survival was inversely related to the radiation dose. Survival enhancement was best in 9.0 Gy irradiated mice, and decreased as the exposure dose increased to 11.0 Gy. In addition, glucan treatment was effective only in the hemopoietic-syndrome radiation dose range since no radioprotection was observed following a 12.0 Gy radiation exposure (which induces both significant hemopoietic and gastrointestinal injury) (8). Both particulate and soluble glucan produced these survival-enhancing effects, with glucan-P being somewhat more effective than glucan-F. Approximately three times more glucan-F was required to produce effects similar to those produced by 1.5 mg of glucan-P. Over the time course of these experiments, eight batches of glucan-P and four batches of glucan-F were used. All required the respective 1.5 mg glucan-P or 5.0 mg glucan-F doses and yielded consistent glucan-P and glucan-F responses. The exact reasons for this difference in dosage are not known. However, soluble glucan-F has a smaller molecular weight than particulate glucan-P, and thus the effective dose of glucan-F in vivo may be reduced due to its ability to escape phagocytosis and/or be more rapidly cleared and excreted from the body.

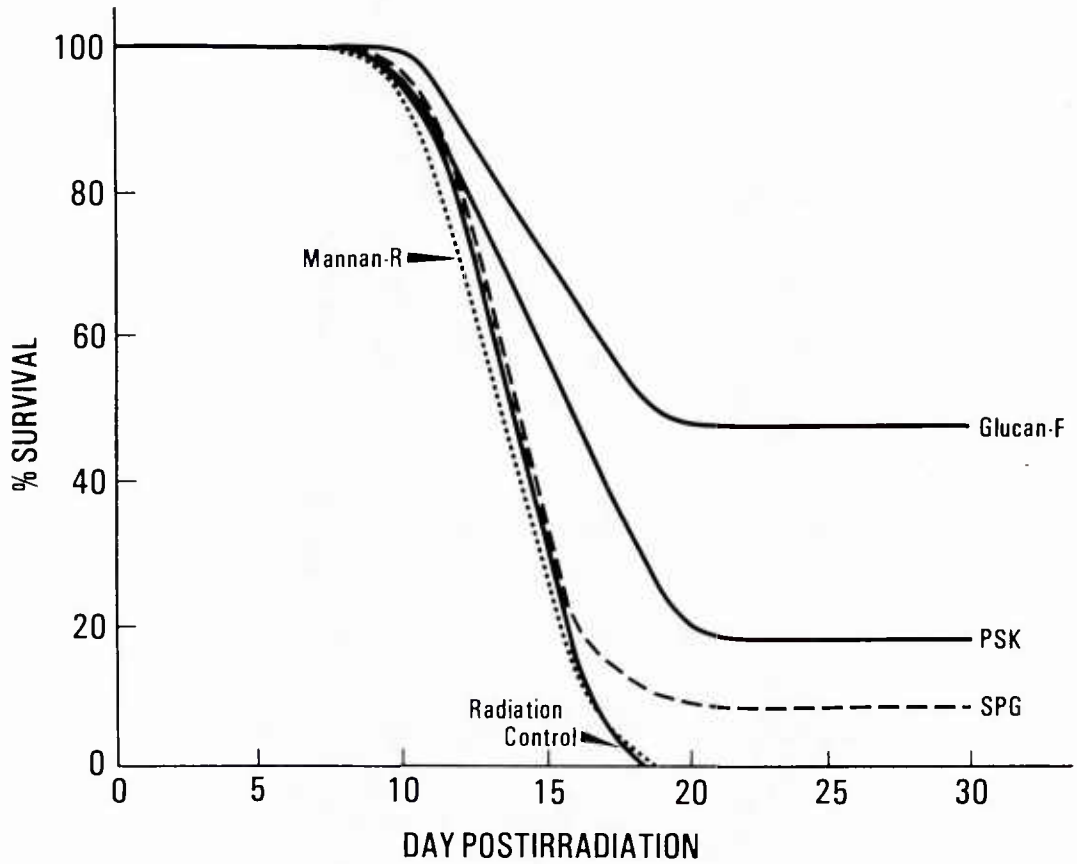

FIG. 8. Effects of four soluble B-1,3 polyglycans on survival in C_3H/HeN mice exposed to 9.0 Gy ^{60}Co irradiation 1 day after polyglycan injections. Cumulative survival data were calculated from 73 radiation control mice, 45 glucan-F-treated mice ($p \leq 0.01$), 36 PSK-treated-mice ($p \leq 0.05$), 45 SPG-treated mice ($p \leq 0.05$), and 45 mannan-R-treated mice (NS). NS, not significant.

Interestingly, at doses of glucan-P and glucan-F up to 1.5 and 5.0 mg per mouse, respectively, the survival-enhancing effects of glucan-P and glucan-F were dose-related (M. L. Patchen, unpublished observations). However, at greater doses, effectiveness of glucan-F could not be further increased, and effectiveness of glucan-P could not be determined due to lethal side effects. In particular, intravenous doses of glucan-P greater than 1.5 mg per mouse resulted in microemboli-induced lethality (32). Additional attempts to increase the glucan-P dose by administering multiple 1.5 mg glucan-P injections did not further increase, and in fact appeared to decrease, its survival-enhancing effects. Whether this phenomenon may be related to immunological suppression, which has sometimes been observed after multiple high dose injections of other BRMs, is not known at this time. However, a similar negative effect of glucan-P on survival was also observed when even a single glucan-P injection was administered 1 h postirradiation. In fact, in postirradiation glucan-P-treated mice we have previously noted that as glucan-P doses increase to 1.5 mg per mouse, these mice die progressively more rapidly than do radiation control mice (33). A similar effect was not observed with glucan-F, which was even somewhat protective when administered postirradiation. The mechanisms behind these differential effects of glucan-P and glucan-F are currently being investigated in our laboratory.

The exact mechanisms by which preirradiation glucan-P and glucan-F administration enhance survival in otherwise lethally irradiated mice are still largely unknown.

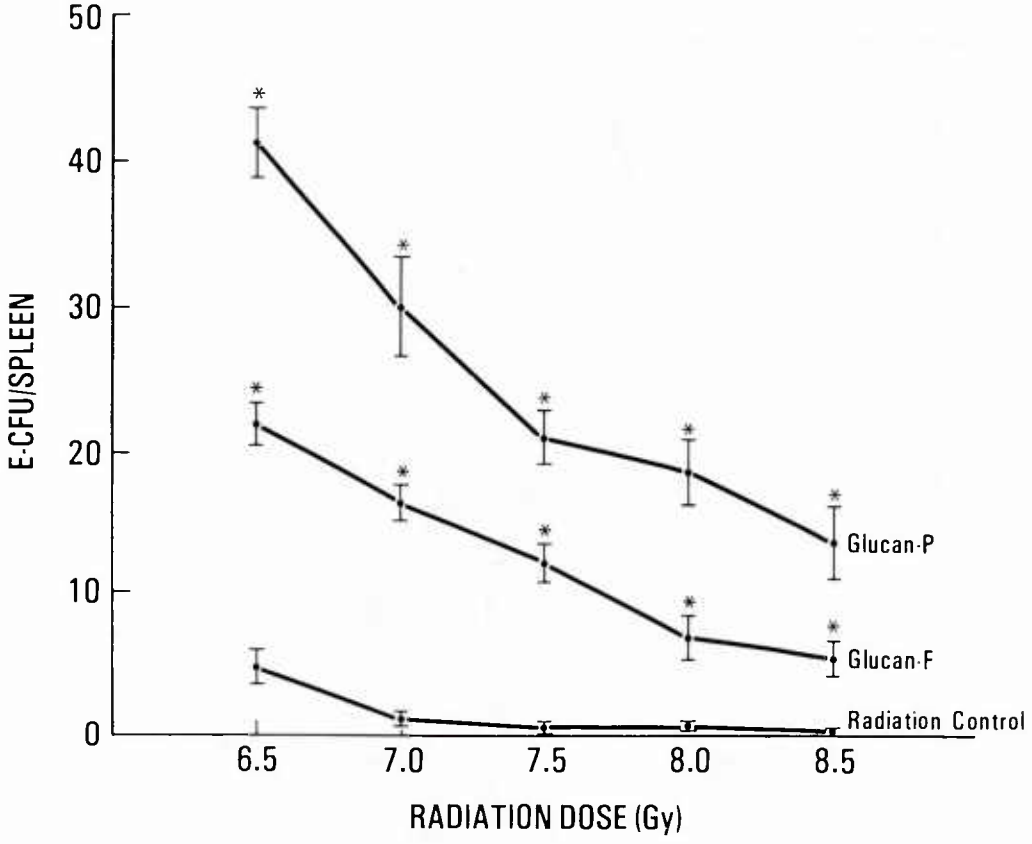

FIG. 9. Effects of glucan-P and glucan-F on endogenous spleen colony-forming unit (E-CFU) formation in C_3H/HeN mice exposed to various doses of ^{60}Co irradiation 1 day after glucan injections. Each datum point represents the mean ± 1 SE of data obtained from 13 to 15 individual mice. With respect to radiation control values, *$p \leq 0.01$.

Both glucan-P and glucan-F have been shown to be potent hemopoietic stimulants in normal mice (13–15,34). This, coupled with the fact that these agents are most effective in the hemopoietic syndrome radiation dose range, suggests that glucan-mediated hemopoietic repopulation may play a major part in glucan-mediated survival enhancement. The E-CFU data presented here clearly illustrate that both glucan-P and glucan-F can enhance endogenous hemopoietic stem cell proliferation and/or recovery in irradiated mice. In fact, we have previously reported a similar phenomenon for both glucan-P and glucan-F when administered 1 h before or 1 h after a 6.5 Gy radiation exposure (32). In addition, these current studies indicate that hemopoietic stem cells not only increase in number but also apparently proliferate, differentiate, mature, and migrate to the peripheral circulation since peripheral blood white cells, platelets, and hematocrit values all recovered more quickly in glucan-P- and glucan-F-treated mice than in radiation control mice. The recovery of peripheral blood white cell numbers is of particular interest because of the critical first-line defense they play in combating infections. White blood cell numbers in glucan-P- and glucan-F-treated mice began to recover ~10–15 days postirradiation, whereas no peripheral blood white cell recovery was observed in radiation controls. Since 10 days postirradiation has been shown to be the time when septicemia first becomes apparent in untreated irradiated mice (15,35), it may be possible that in glucan-P- and glucan-F-treated mice, the increased white cell numbers play a role in preventing them from

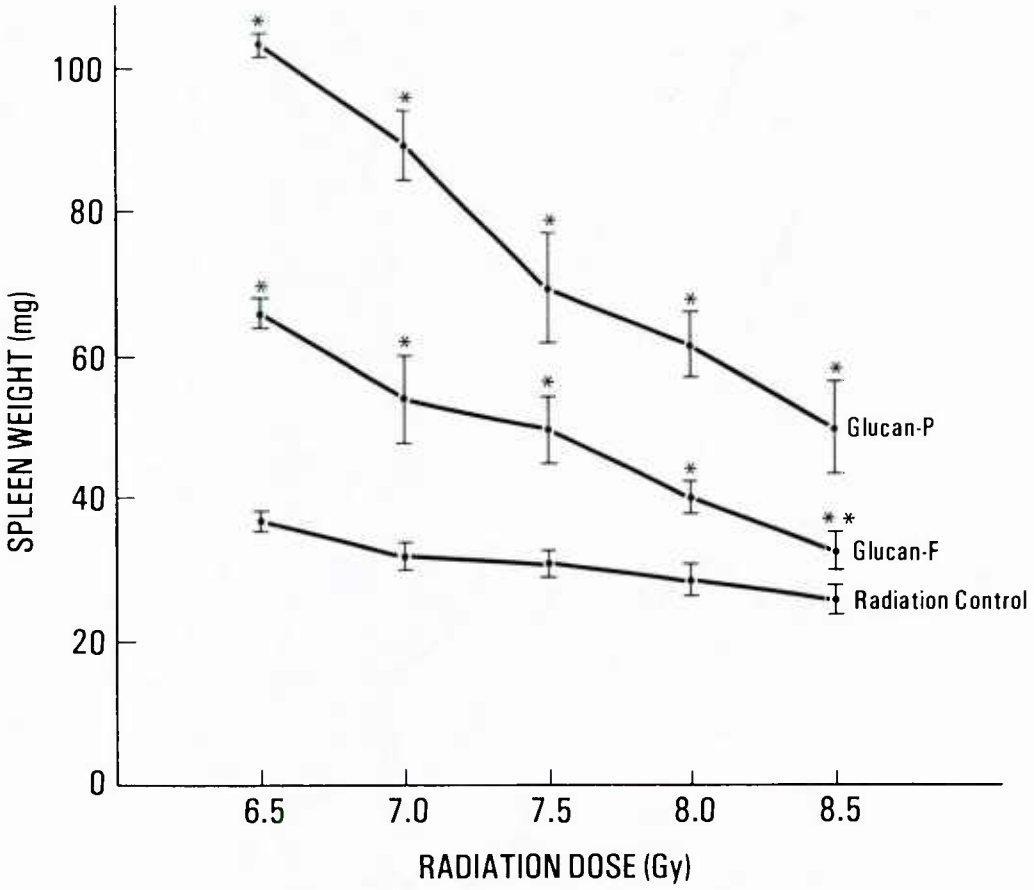

FIG. 10. Effects of glucan-P and glucan-F on spleen weights in C_3H/HeN mice exposed to various doses of ^{60}Co irradiation 1 day after glucan injections. Each datum point represents the mean ± 1 SE of data obtained from 13 to 15 individual spleens. With respect to radiation control values, *$p \leq 0.01$ and **$p \leq 0.05$.

succumbing to such secondary infections associated with irradiation. In fact, recent experiments in our laboratory have demonstrated that glucan-treated irradiated mice develop far fewer infections than do the radiation control mice.

In addition to this information on the possible biological mechanisms of glucan-mediated survival enhancement our studies using various other B-1,3 polyglycans have shed some light on the possible biochemical mechanisms of glucan-mediated survival enhancement. In studies comparing the survival-enhancing capabilities of three other soluble B-1,3 polyglycan BRMs, two of these, PSK and SPG, also appeared to be slightly radioprotective. These two protective agents also contained B-1,3 glucan components, whereas the ineffective polyglycan (mannan-R) contained a B-1,3 mannan rather than a B-1,3 glucan component. Although PSK and SPG were considerably less effective than glucan-F at enhancing survival, this might be expected if B-1,3 glucan is the active survival enhancing component, since both PSK and SPG only partially consist of B-1,3 glucan and glucan-F consists only of B-1,3 glucan (Table 1). Thus, perhaps the manner in which the B-1,3 glucan linkages are recognized and/or processed is associated with the ability of these agents to modify radiation-induced lethality. Whatever the mechanism, however, it does not appear to be strain-specific or species-specific, since we have also observed enhanced hemopoietic re-

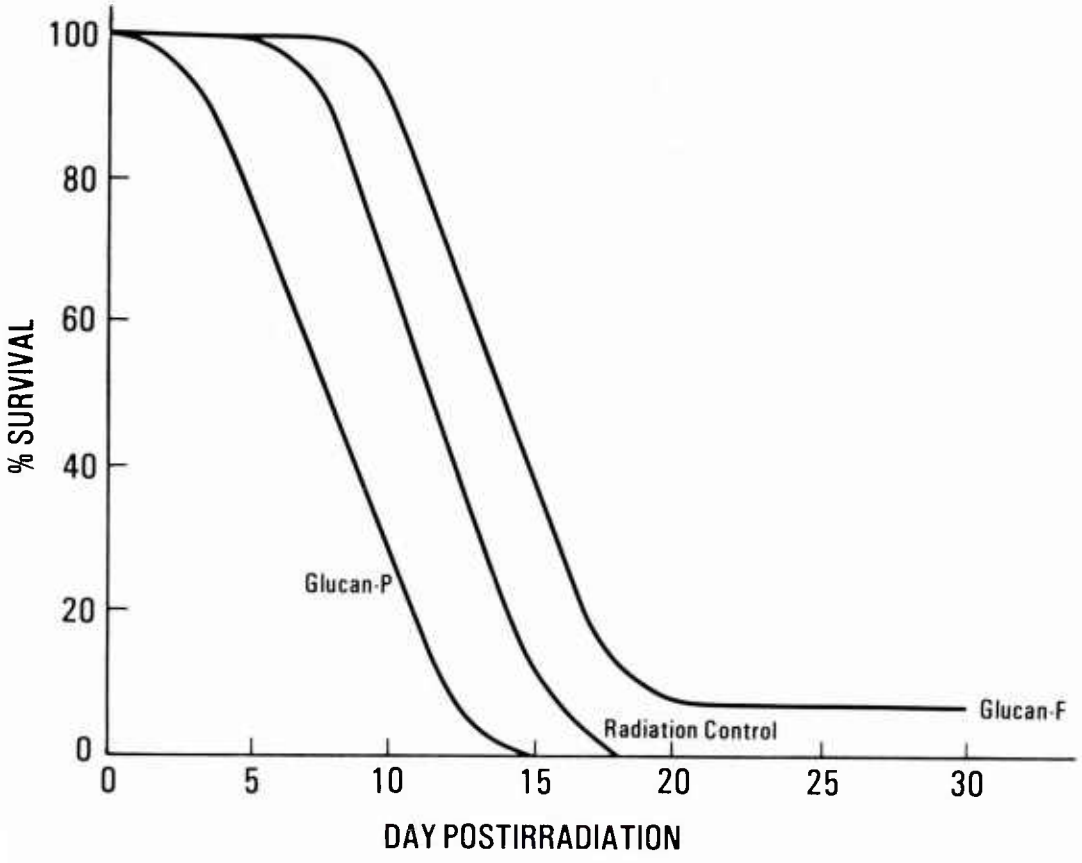

FIG. 11. Effects of glucan-P and glucan-F on survival when administered 1 h after exposure to a 9.0 Gy dose of ^{60}Co irradiation. Cumulative survival data were calculated from 37 radiation control mice, 36 glucan-P-treated mice (NS), and 36 glucan-F-treated mice ($p \leq 0.05$). NS, not significant.

covery and prolonged survival in irradiated B6D2F_1 and C57B1/6 mice, as well as in canines and primates (M. L. Patchen, unpublished observations).

The fact that glucan-F appears to be nearly as potent as glucan-P at enhancing postirradiation survival is of particular clinical interest since the undesirable severe hepatosplenomegally and granuloma formation known to be associated with intravenous glucan-P administration do not occur with glucan-F administration (36–38). Even at extremely high intravenous doses, glucan-F has failed to produce detrimental side effects in mice, dogs, or primates, and it is currently undergoing Phase I drug evaluation in humans. Thus, even in humans, glucan-F may prove to be useful for combating radiation and/or chemical hemopoietic and immune depression and the sometimes lethal consequences of such depression.

Acknowledgment: The authors acknowledge the excellent technical assistance of Brenda Bell, James Atkinson, and Brian Solberg. The excellent editorial and typing skills of Junith Van Deusen and Gloria Contreras also greatly contributed to the completion of this manuscript. Research was supported by Armed Forces Radiobiology Research Institute, Defense Nuclear Agency, under Research Work Unit 00132. The views presented in this paper are those of the authors; no endorsement by the Defense Nuclear Agency has been given or should be inferred.

REFERENCES

1. Blackett NM, Marsh JC, Gordon MY, Okell SF, Aguado M. Simultaneous assay by six methods of the effect on hemopoietic precursor cells of adriamycin, methyl-CCNU, ^{60}Co rays, vinblastine, and cytosine arabinoside. *Exp Hematol* 1978;6:2–12.

2. Lohrmann HP, Schreml W. *Cytotoxic drugs and the granulopoietic system*. Berlin: Springer Verlag, 1982.
3. Benacerrof B. Influence of irradiation and resistance to infection. *Bact Rev* 1960;24:35–40.
4. Broerse JJ, MacVittie TJ. *Response of different species to total body irradiation*. Amsterdam, The Netherlands: Martin Nijhoff Publishers, 1984.
5. Hammond C, Tomkins M, Miller P. Studies on susceptibility to infection following ionizing radiation (I). *J Exp Med* 1954;99:405–10.
6. Hammond C, Colling M, Cooper D, Miller P. Studies on susceptibility to infection following ionizing radiation (II). *J Exp Med* 1954;99:411–8.
7. Hammond C, Ruml D, Cooper D, Miller P. Studies on susceptibility to infection following ionizing radiation (III). *J Exp Med* 1955;102:403–11.
8. Gordon L, Ruml D, Hahne H, Miller P. Studies on susceptibility to infection following ionizing radiation (IV). *J Exp Med* 1955;102:413–25.
9. Wooles WR, DiLuzio NR. The phagocytic and proliferative response of the RES following glucan administration. *J Reticuloendothel Soc* 1964;1:160–9.
10. DiLuzio NR, Pisano JC, Saba TM. Evaluation of the mechanism of glucan-induced stimulation of the reticuloendothelial system. *R Reticuloendothel Soc* 1970;7:731–42.
11. Wooles WR, DiLuzio NR. Influence of RE hyperfunction on bone marrow transplantation. *Am J Physiol* 1962;203:404–8.
12. Wooles WR, DiLuzio NR. Reticuloendothelial function and the immune response. *Science* 1963;142:1078–80.
13. Burgaleta C, Golde DW. Effect of glucan on granulopoiesis and macrophage genesis in mice. *Cancer Res* 1977;37:1739–42.
14. Patchen ML, Lotzova E. Modulation of murine hemopoiesis by glucan. *Exp Hematol* 1980;8:409–22.
15. Patchen ML, MacVittie TJ. Dose-dependent responses of murine pluripotent stem cells and myeloid and erythroid progenitor cells following administration of the immunomodulating agent glucan. *Immunopharmacology* 1983;5:303–13.
16. Patchen ML, MacVittie TJ. Use of glucan to enhance hemopoietic recovery after exposure to cobalt-60 irradiation. *Adv Exp Med Biol* 1982;155:267–72.
17. Popisil M, Jary J, Netikova J, Marek M. Glucan-induced enhancement of hemopoietic recovery in gamma-irradiated mice. *Experientia* 1982;38:1232–4.
18. Patchen ML. Immunomodulators and hemopoiesis. *Surv Immunol Res* 1983;2:237–42.
19. Patchen ML, MacVittie TJ, Wathen LM. Effect of pre and post irradiation glucan treatment on pluripotent stem cells, granulocyte, macrophage and erythroid progenitor cells and hemopoietic stromal cells. *Experientia* 1984;4:1240–4.
20. DiLuzio NR, Williams DL. Protective effect of glucan against systemic *Staphylococcus aureus* septicemia in normal and leukemic mice. *Infect Immun* 1978;20:804–10.
21. DiLuzio NR, Williams DL. Glucan induced modification of the increased susceptibility of cyclophorphamide-treated mice to *Staphylococcus aureus* infection. *Cancer Immunol Immunother* 1979;6:73–9.
22. Reynolds JA, Kastello MD, Harrington DG, et al. Glucan-induced enhancement of host resistance to selected infectious diseases. *Infect Immun* 1980;30:51–7.
23. Williams DL, Browder IW, DiLuzio NR Immunotherapeutic modification of *E. coli* induced experimental peritonitis and bacteremia by glucan. *Surgery* 1983;93:448–54.
24. Williams DL, Cook JA, Hoffman EO, DiLuzio NR. Protective effect of glucan in experimentally induced Candidiasis. *J Reticuloendothel Soc* 1978;23:479–90.
25. Browder WD, Williams DL, Kitahama A, DiLuzio NR. Modification of post-operative C-albicans sepsis by glucan immunostimulation. *Int J Immunopharmacol* 1984;6:19–26.
26. Williams DL, DiLuzio NR. Glucan-induced modification of murine viral hepatitis. *Science* 1980;200:67–9.
27. Cook JA, Holbrook TW, Parker BW. Visceral leishmaniasis in mice: protective effects of glucan. *J Reticuloendothel Soc* 1980;27:567–73.
28. Cook JA, Runey GL, Holbrook TW. Immunomodulation of protozoa diseases. *Surv Immunol Res* 1983;2:243–5.
29. DiLuzio NR, Williams DL, McNamee RB, Edwards BF, Kilahama A. Comparative tumor-inhibitory and antibacterial activity of soluble and particulate glucan. *Int J Cancer* 1979;24:773–9.
30. Hassid WZ, Joslyn MA, McCready M. The molecular constitution of an insoluble polysaccharide from yeast, *Saccharomyces cerevisiae*. *J Am Chem Soc* 1941;63:295–8.
31. Till JE, McCulloch EA. Early repair processes in marrow cells irradiated and proliferating in vivo. *Radiat Res* 1963;18:96–105.

32. Patchen ML, DiLuzio NR, Jacques P, MacVittie TJ. Soluble polyglycans enhance recovery from cobalt-60 induced hemopoietic injury. *J Biol Response Mod* 1984;3:627–33.
33. Patchen ML, MacVittie TJ. Stimulated hemopoiesis and enhanced survival following glucan treatment in sublethally and lethally irradiated mice. *Int J Immunopharmacol* (in press).
34. Patchen ML, MacVittie TJ. Hemopoietic effects of intravenous soluble glucan administration. *Exp Hematol* (submitted).
35. Patchen ML, Walker RI, Brook I, MacVittie TJ. Glucan, an immunologic and hemopoietic agent, inhibits sepsis and enhances survival of lethally irradiated mice. In: Broerse J, Barendsen G, Kal H, Van der Kogel A, eds. *Proceedings of the 7th International Congress of Radiation Research*. Amsterdam, The Netherlands: Martinus Nijhoff, 1983:D5–30.
35a. Riggi S, DiLuzio NR. Identification of a reticulocndothelial stimulating agent in zymosan. *Am J Physiol* 1961;200:297–300.
36. Deimann W, Fahimi H. Induction of focal hemopoiesis in adult rat liver by glucan, a macrophage activator. *Lab Invest* 1980;42:217–24.
37. DiLuzio, NR. Immunopharmacology of glucan: a broad spectrum enhancer of host defense mechanisms. *Trends Pharm Sci* 1983;4:344–7.

ARMED FORCES RADIOBIOLOGY RESEARCH INSTITUTE
SCIENTIFIC REPORT
SR86-11

Meth and Find Exptl Clin Pharmacol 1986;8(3):151-155

Glucan-Induced Hemopoietic and Immune Stimulation: Therapeutic Effects in Sublethally and Lethally Irradiated Mice

M.L. Patchen, T.J. MacVittie and I. Brook

Department of Experimental Hematology, Armed Forces Radiobiology Research Institute, Bethesda, MD, USA

SUMMARY

The hemopoietic effects of glucan, a beta 1,3 polyglycan biological response modifier, were assayed in normal and irradiated mice. In normal mice, glucan administration increased the content of bone marrow and splenic transplantable pluripotent hemopoietic stem cells (CFU-s), committed granulocyte-macrophage progenitor cells (GM-CFC), and pure macrophage progenitor cells (M-CFC). In mice partially hemopoietic depleted by exposure to 6.5 Gy of ^{60}Co irradiation glucan increased the number of endogenous pluripotent hemopoietic stem cells (E-CFU). The most pronounced effects were observed when glucan was administered 1 day before irradiation. In addition, the administration of glucan 1 day before lethal (9.0 Gy) irradiation-enhanced survival. The enhanced survival in glucan-treated mice in part appeared to be mediated by an enhanced resistance to the surgence of enteric opportunistic pathogens that occurs following radiation-induced hemopoietic and immune depression.

Key words: Hemopoiesis - Radioprotection - Glucan - Polyglycans - Stem cells

INTRODUCTION

Although most biological response modifiers (BRMs) have traditionally been evaluated for their immunomodulating capabilities, it has been demonstrated that a variety of such agents can also exert effects on the hemopoietic system (1-7). Since bone marrow suppression is a common detrimental side effect in patients undergoing radiotherapy and/or chemotherapy, agents capable of modulating hemopoiesis might be therapeutically useful for enhancing hemopoietic reconstitution and thus contributing to the prevention of potentially lethal opportunistic infections in such patients (8-9).

In the past several years studies have concentrated on investigating the hemopoietic effects of glucan, a B, 1-3 polyglucose isolated from the yeast *Saccharomyces cerevisiae* (7,10-12). As opposed to numerous other naturally obtained BRMs, glucan is not potentially infectious, is not antigenic, and has a known molecular structure (13). The data presented in this paper demonstrates that this nontoxic BRM is a potent hemopoietic stimulant in both normal and irradiated mice, and that glucan administration in otherwise lethally irradiated mice can significantly increase survival in the hemopoietic syndrome radiation dose range.

MATERIALS AND METHODS

Mice

In all experiments 20- to 25-gram C_3H/HeN female mice were used. All mice were quarantined and acclimated to laboratory conditions for at least 2 weeks prior to experimentation. During this time mice were examined and found to be free of lesions of murine pneumonia complex and oropharyngeal *Pseudomonas* sp.

Glucan

Particulate endotoxin-free glucan, prepared as described by DiLuzio *et al.* (14), was obtained from Accurate Chemical and Scientific Corporation (Westbury, NY). Glucan was intravenously administered in a 0.5 ml volume via the lateral tail veins in the dose of 1.5 mg per mouse. Control mice were injected with an equivalent volume of sterile saline.

0379-0355/86/$5.00 + $2.00
Copyright © 1986 J.R. Prous, S.A.

Hemopoietic cell supensions

Each cell suspension represented the pool of tissues from three mice. Single cell suspensions of femoral bone marrow cells or spleen cells were prepared in Hank's balanced salt solution as previously described (12). The total number of nucleated cells in each suspension was determined by counting the cells on a hemocytometer.

Hemopoietic stem and progenitor cell assays

Pluripotent hemopoietic stem cells were assayed *in vivo* by the exogenous (CFU-s) or endogenous (E-CFU) spleen colony-forming unit assays originally described by Till and McCulloch (15-16). Spleens were harvested 10 days post irradiation and fixed in Bouin's Solution; the number of grossly visible colonies were then counted. Hemopoietic progenitor cells committed to granulocyte-macrophage (GM-CFC) or pure macrophage (M-CFC) differentiation were assayed *in vitro* by the double-layer agar culture techniques originally described by Bradley and Metcalf (17) and MacVittie (3), respectively. Specific modifications of these assays have been described previously in detail (12).

Irradiation

Bilateral total-body irradiation administered from the AFRRI ^{60}Co source at a dose rate of 0.4 Gy per minute was used in all radiation experiments.

Survival studies

Mice used in survival studies were exposed to 9.0 Gy of total-body irradiation, and their survival was checked daily for a period of 30 days.

Bacteriological studies

The liver and spleen of individual mice were aseptically removed, homogenated, and streaked onto two enriched BHI agar plates. One plate was incubated for 48 h at 37°C and 5% CO_2 for isolation of aerobic bacteria. The other plate was incubated for 48 h in an anaerobic environment for the isolation of anaerobic bacteria. The number of colonies was semiquantitatively estimated, and the microorganisms were identified utilizing standard criteria (18-19).

RESULTS

Effect of glucan on hemopoietic stem and progenitor cells in normal mice

Glucan was administered to normal mice, and the bone marrow and splenic content of pluripotent hemopoietic stem cells (CFU-s), granulocyte-macrophage progenitor cells (GM-CFC), and pure macrophage progenitor cells (M-CFC) were assayed 1, 5, 11, and 17 days later (Table 1). Glucan stimulated CFU-s, GM-CFC, and M-CFC production in both the bone marrow and the spleen. Although glucan's hemopoietic stimulatory effect in the femoral bone marrow occurred later, was of a shorter duration, and appeared to be of a smaller magnitude than in the spleen, glucan's total bone marrow effect was no doubt at least as great as its splenic effect since the femoral marrow represents only approximately 7 percent of the total murine bone marrow content.

Effect of glucan on hemopoietic stem cells in irradiated mice

The endogenous spleen colony-forming unit assay (E-CFU) was used to evaluate the ability of glucan to enhance hemopoietic stem cell recovery in radiation-

TABLE 1. Effect of glucan on hemopoietic stem and progenitor cells in normal mice[a]

Day Post Glucan	CFU-s/Organ[b] ($\times 10^3$)		GM-CFC/Organ[b] ($\times 10^4$)		M-CFC/Organ[b] ($\times 10^5$)	
Treatment	Bone Marrow	Spleen	Bone Marrow	Spleen	Bone Marrow	Spleen
0 (Controls)	2.66 ± 0.19	6.23 ± 0.55	1.95 ± 0.12	1.11 ± 0.16	0.89 ± 0.11	1.54 ± 0.35
1	2.11 ± 0.19	9.57 ± 1.82[c]	1.92 ± 0.16	2.89 ± 0.58[c]	0.89 ± 0.07	2.97 ± 0.22[c]
5	3.55 ± 0.43[c]	18.82 ± 8.06[c]	2.30 ± 0.20	5.63 ± 0.44[c]	0.92 ± 0.10	4.20 ± 0.44[c]
11	3.01 ± 0.41	9.86 ± 1.83[c]	2.41 ± 0.24[c]	3.34 ± 0.82[c]	1.10 ± 0.12[c]	3.97 ± 0.59[c]
17	2.54 ± 0.14	7.40 ± 1.28	2.22 ± 0.16	1.78 ± 0.21[c]	0.98 ± 0.05	2.98 ± 0.22[c]

[a] Mean ± standard deviation of data obtained from 3-4 individual experiments.
[b] Bone marrow values represent CFUs, GM-CFC-, and M-CFC values per femur.
[c] $p \leq .05$.

TABLE 2. Effect of glucan on endogenous spleen colony formation in 6.5-Gy irradiated mice

Time of Treatment Prior to Irradiation	E-CFU/Spleen[a]	
	Saline + Irradiation	Glucan + Irradiation
1 day	2.6 ± 0.3	44.2 ± 4.0[b]
5 days	3.1 ± 0.4	31.4 ± 3.6[b]
11 days	2.9 ± 0.3	15.3 ± 2.1[b]

[a]Mean ± standard error of values obtained from 17-25 individual spleens.
[b]$p \leq .05$.

injured mice (Table 2). E-CFU numbers were significantly increased whether injected with glucan at 1, 5 or 11 days prior to the radiation injury. However, the largest increase in E-CFU numbers was observed when glucan was injected 1 day before irradiation.

Effect of glucan on survival in lethally irradiated mice

Since mice exposed to irradiation in the dose of 8.0-10.0 Gy (the hemopoietic syndrome dose range) ultimately die 2-3 weeks later due to hemopoietic and immune suppression, attempts were made to alter the survival in such mice with glucan therapy (Table 3). Although glucan administration was not effective at altering 30-day survival when administered 5 or 11 days prior to irradiation, it did significantly enhance survival when administered 1 day prior to an otherwise lethal radiation exposure.

Bacteriological effects of glucan in lethally irradiated mice

The effect of glucan on the surgence of opportunistic pathogens that occurs following radiation exposure in the hemopoietic syndrome dose range was evaluated by measuring bacterial translocation in the livers and spleens of mice 7, 9, 11, and 13 days after radiation exposure (Table 4). At 7 and 9 days postirradiation, more microorganisms were recovered in glucan-treated mice than in saline-treated mice. However, at days 11 and 13 postirradiation the livers and spleens from glucan-treated mice were essentially free of bacteria while 60-70 percent of those from saline-treated mice exhibited the presence of bacteria.

DISCUSSION AND CONCLUSIONS

These studies demonstrate that glucan is a potent hemopoietic stimulant in normal mice and in radiation-injured mice. In addition, these studies clearly demonstrate that glucan is capable of significantly enhancing survival in mice that would otherwise die from the infectious consequences of radiation-induced hemopoietic and immune suppression.

Whether glucan's ability to enhance survival in lethally irradiated mice is mediated solely via enhanced repopulation of the granulocyte and macrophage cell populations (which are so critically important as a first-line defense against bacterial invasion) is not absolutely certain. It has been observed that CFU-s, GM-CFC, M-CFC and peripheral white blood cell numbers in glucan-treated 9.0-Gy irradiated mice begin to recover approximately 10-15 days postirradiation (Patchen *et al.*, data not included here). Such recovery was not observed in saline-treated 9.0-Gy irradiated mice, which

TABLE 3. Effect of glucan on survival in 9.0-Gy irradiated mice

Time of Treatment Prior to Irradiation	Percent Survival at 30 Days Postirradiation	
	Saline + Irradiation	Glucan + Irradiation
1 day	0[a]	59[a]
5 days	0[b]	0[b]
11 days	0[c]	0[c]

[a] Based on cumulative survival data in experiments involving 163-178 mice.
[b] Based on cumulative survival data in experiments involving 42-50 mice.
[c] Based on cumulative survival data in experiments involved 43-51 mice.

TABLE 4. Effect of glucan on bacterial translocation in 9.0-Gy irradiated mice[a]

Day Post-Irradiation	Percent Positive Bacterial Cultures[b]			
	Liver		Spleen	
	Saline + Irradiation	Glucan + Irradiation	Saline + Irradiation	Glucan + Irradiation
7	0	20	0	10
9	0	10	0	20
11	30	20	20	0
13	60[c]	0	70[c]	0

[a]Saline or glucan was administered 1 day prior to irradiation.
[b]Organisms detected were *Proteus mirabilis, Staphylococcus aureus,* and *Escherichia coli.*
[c]Many mice exhibited multiple types of infection within the same animal.

interestingly begin to die approximately 10-15 days postirradiation. Although the time course of hemopoietic recovery and survival appear to closely correlate, this does not exclude the possibility that other mechanisms may also be contributing to glucan's ability to enhance survival in lethally irradiated mice. For instance, macrophages have been demonstrated to be radioresistant (20). Since glucan is an extremely potent macrophage activator it could no doubt also function to control the surgence of postirradiation opportunistic enteric pathogens by providing the presence of large radioresistant activated macrophage cell populations. In addition, macrophages have been shown to produce and release hemopoietic and immune factors (21) that might further facilitate hemopoietic and immune reconstitution in irradiated mice.

The results presented in this paper have dealt solely with the effects of particulate glucan (glucan-P). Although glucan-P has few side effects compared to most other BRMs, intravenous administration of glucan-P has been shown to produce severe hepatosplenomegaly and granuloma formation (13, 22). Recently the experiments presented here were repeated using a newly-produced soluble glucan preparation (glucan-F) that does not induce severe hepatosplenomegaly and granuloma formation, and thus is more clinically applicable. In those experiments, glucan-F produce results very similar to those produced by glucan-P with the exception that a 5.0 mg glucan-F dose was required to produce the same effects as a 1.5 mg dose of glucan-P (Patchen *et al.*, manuscript submitted). Clearly, glucan appears to be a BRM that possesses clinically promising hemopoietic and radioprotective capabilities.

REFERENCES

1. Fisher, B. et al. *Effect of Mycobacterium bovis (Strain Bacillus Calmette Guerin) on macrophage production by the bone marrow of tumor bearing mice.* Cancer Res 1974; 34: 1668-1670.
2. Dimitrov, N. et al. *Effect of Corynebacterium parvum on bone marrow cell cultures.* Proc Soc Exp Biol Med 1975; 148: 440-442.
3. MacVittie, T.J. *Alterations induced in macrophage and granulocyte-macrophage colony-forming cells by a single injection of mice with Corynebacterium parvum.* Reticuloendothel Soc 1979; 26: 479-490.
4. Mahmood, T. et al. *Effect of levamisole on human granulopoiesis in vitro.* Proc Soc Exp Biol Med 1977; 156: 359-364.
5. Wuest, B. et al. *Stimulatory effect of N-Acetyl muramyl dipeptide in vivo: proliferation of bone marrow progenitor cells in mice.* Infection and Immunity 1982; 37: 452-462.
6. Niskanen, E.O. et al. *Effect of glucan, macrophage activator, on murine hemopoietic cell proliferation in diffusion chambers in mice.* Cancer Res 1978; 38: 1406-1409.
7. Patchen, M.L. et al. *Modulation of murine hemopoiesis by glucan.* Exp Hematol 1980; 8: 409-422.
8. Blackett, N.M. et al. *Simultaneous assay by six methods of the effect on hemopoietic precursor cells of adriamycin, methyl-CCNU, ^{60}Co x-rays, vinblastine, and cytosine arabinoside.* Exp Hematol 1978; 6: 2-13.
9. Talmage, D.W. *Effect of ionizing radiation on resistance to infection.* Ann Rev Microbiol 1955; 9: 335-346.
10. Patchen, M.L. et al. *The role of macrophages and T-lymphocytes in glucan-mediated alteration of murine hemopoiesis.* Biomed 1981; 34: 71-77.
11. Patchen, M.L. et al. *Temporal response of murine pluripotent stem cells and myeloid and erythroid progenitor cells to low-dose glucan treatment.* Acta Hematol 1983; 70: 281-288.
12. Patchen, M.L. et al. *Dose-dependent responses of murine pluripotent stem cells and myeloid and erythroid progenitor cells following administration of the immunomodulating agent glucan.* Immunopharmacol 1983; 5: 303-313.
13. DiLuzio, N.R. *Immunopharmacology of glucan: A broad spectrum enhancer of host defense mechanisms.* Trends in Pharmaceutical Sci 1983; 4: 344-347.
14. DiLuzio, N.R. et al. *Comparative tumor-inhibitory and an-*

tibacterial activity of a soluble and particulate glucan. Int J Cancer 1979; 24: 773-779.
15. Till, J.E. et al. *A direct measurements of radiation sensitivity of normal bone marrow cells.* Rad Res 1961; 14: 213-222.
16. Till, J.E. et al. *Early repair processes in marrow cells irradiated and proliferating in vivo.* Rad Res 1973; 18: 96-105.
17. Bradley, T.R. et al. *The growth of mouse bone marrow cells in vitro.* Aust J Exp Med Sci 1966; 448: 287-300.
18. Manual of Clinical Microbiology. E.H. Lennette et al. (Eds.).American Society for Microbiology: Washington 1980.
19. Wadsworth Anaerobic Bacteriology Manual. V.L. Sutter et al. (Eds.). The C.V. Mosby Co: St. Louis 1980.
20. Brecher, G.K. et al. *Effects of x-ray on lymphoid and hemopoietic tissues of mice.* Blood 1948; 3: 1259-1264..
21. Cellular Functions in Immunity and Inflammation. *J.J. Oppenheim, et al.* (Eds.). Elsevier North Holland: Amsterdam 1981.
22. Deimann, W. et al. *Induction of focal hemopoiesis in adult rat liver by glucan, a macrophage activator.* Lab Invest 1980; 42: 217-224.

Send reprint requests to: Dr. Myra L. Patchen, Department of Experimental Hematology, Armed Forces Radiobiology Research Institute, Bethesda, MD 20814-5145, USA.

Brain Research, 364 (1986) 377–381
Elsevier

BRE 21316

ARMED FORCES RADIOBIOLOGY RESEARCH INSTITUTE
SCIENTIFIC REPORT
SR86-12

Electrophysiological correlates of peroxide damage in guinea pig hippocampus in vitro

TERRY PELLMAR

Physiology Department, Armed Forces Radiobiology Research Institute, Bethesda, MD 20814-5145 (U.S.A.)

(Accepted September 18th, 1985)

Key words: hydrogen peroxide — hippocampus — Fenton reaction — active oxygen — hydroxyl free radical

To study the effects of active oxygen on neuronal electrophysiology, hippocampal brain slices were exposed to hydrogen peroxide plus ferrous sulfate which react to produce hydroxyl free radicals. Analysis of extracellularly recorded somatic and dendritic responses to orthodromic stimulation indicated a decrease in both synaptic efficacy and impairment of action potential generation.

Active oxygen (superoxide, peroxide and hydroxyl radicals) and other free radicals occur naturally as intermediates in oxidative metabolism. There are many enzymes and free radical scavengers present in normal tissue to maintain these compounds within non-toxic levels[4]. In some pathological states of the nervous system, however, free radicals in brain tissue can increase to abnormally high levels[1]. One such state is ischemia and subsequent reperfusion[1,2,17–19]. The free radicals produced by this insult are likely to react with unsaturated fatty acids and initiate lipid peroxidation[3,15,17,22], disrupting the integrity of cell membranes.

CA1 neurons of the hippocampus are particularly sensitive to ischemic damage[5,6,8,9,16,20]. The spontaneous electrical activity of the neurons, studied in vivo, disappears during ischemia, returns 10–20 min after reperfusion and then increases above normal levels during the next 24 h[20]. In vitro studies on the hippocampal brain slice preparation demonstrated that ischemia was accompanied by a reduction in synaptically elicited electrical activity in the dentate and CA3 regions of the hippocampus[11,14].

The present study was initiated to determine the electrophysiological correlates of active oxygen damage in CA1 pyramidal cells of the hippocampus in vitro. Hydrogen peroxide was combined with ferrous sulfate to generate hydroxyl free radicals. Through analysis of the dendritic and somatic field potentials, it was found that synaptic efficacy and spike generation mechanisms were impaired.

Male guinea pigs were killed by cervical dislocation under halothane anesthesia. The brain was removed and immediately placed in oxygenated, iced solution (composition below). Within 5 min both hippocampi were dissected and thin slices (350–400 μm) were cut. The slices were incubated at room temperature for at least 1 h before use. In the recording chamber, the submerged slice was constantly perfused with oxygenated solution at 30 ± 1 °C. Normal bathing solution contained (in mM): NaCl 124, KCl 3, $CaCl_2$ 2.4, $MgSO_4$ 1.3, KH_2PO_4 1.24, glucose 10 and $NaHCO_3$ 26. The solution was oxygenated by constant bubbling with 95% O_2/5% CO_2. Potentials were recorded with a high gain DC amplifier and were digitized, stored and analyzed on a LSI 11-03 minicomputer. In most experiments a bipolar stainless steel stimulating electrode was positioned in the stratum radiatum to activate the Schaffer collateral pathway as well as other afferents to the CA1 pyramidal cells. Constant current stimuli (0.1–1 mA, 100 μs) were provided at 0.33 Hz. (Threshold for evoking a population spike was always less than 0.3 mA.) Recording electrodes (less than 10 MΩ) filled with 2 M

Correspondence: T. Pellmar, Physiology Department, Armed Forces Radiobiology Research Institute, Bethesda, MD 20814-5145, U.S.A.

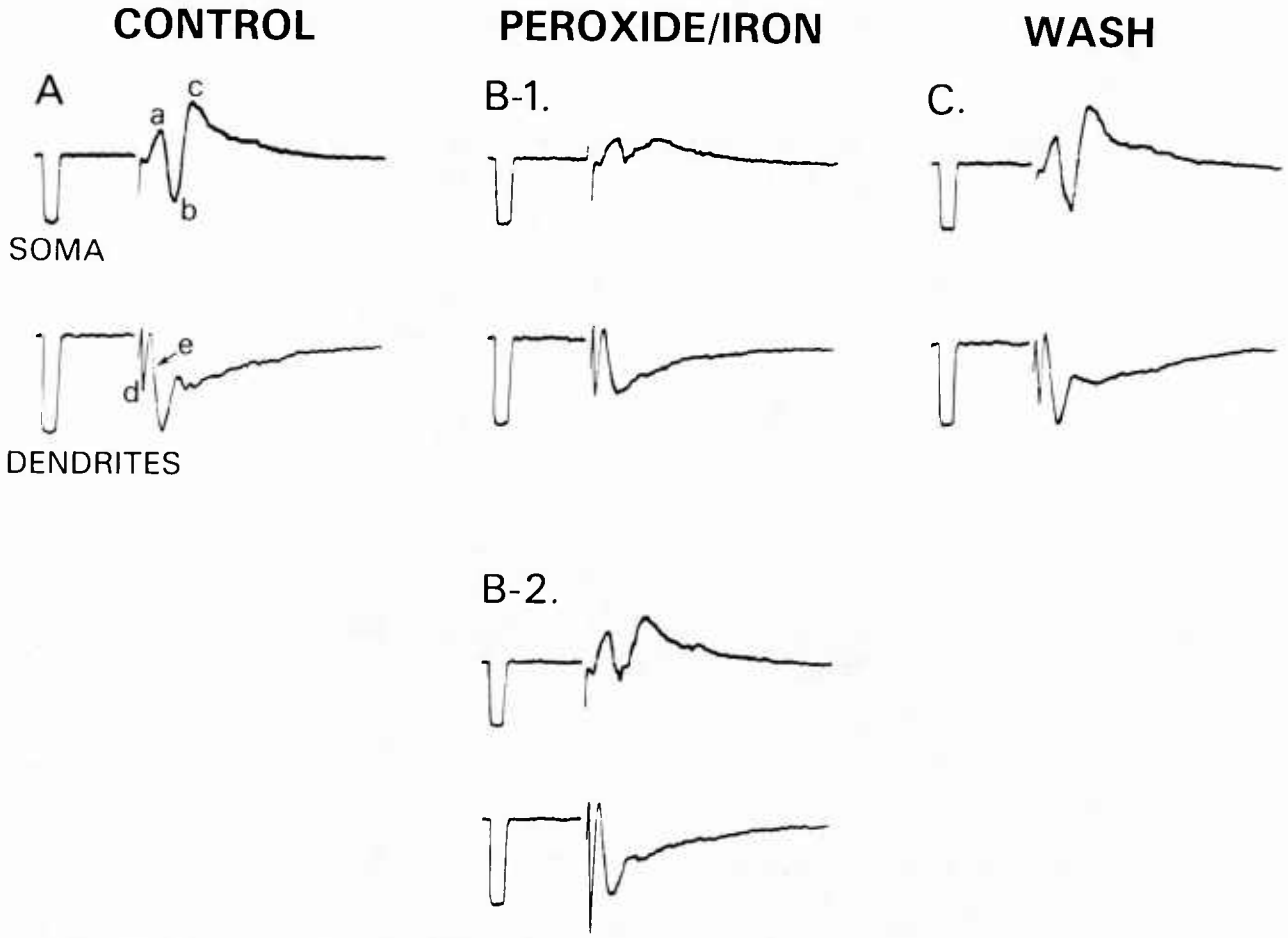

Fig. 1. Effects of 0.01% peroxide with 100 μM ferrous sulfate on somatic and dendritic responses of CA1 neurons of the hippocampus. A: top trace shows the population response recorded in the cell body layer to stimulation of the stratum radiatum. Bottom trace shows the response recorded simultaneously in the dendritic layer. The traces are preceded by a calibration pulse of 1 mV, 2 ms. All records are the average of 3 traces. The amplitude of the population spike in the cell body layer is defined as the average amplitude from point a to point b and from point c to point b. The presynaptic volley is indicated at point d. The size of the synaptic response is defined as the slope of the population PSP at point e. B: the somatic and dendritic responses of the same tissue after 15 min exposure to peroxide/iron. Both the population spike and the population PSP are reduced. In B-1 stimulus parameters were identical to those in A. In B-2 stimulus strength was increased until dendritic response was similar to that of control. The population response is still smaller than in control. C: somatic and dendritic responses following 30 min wash. Stimulus intensity is same as that in A. Both responses are partially recovered.

NaCl were placed in the cell body layer of CA1 to record the somatic response. A second recording electrode was positioned in stratum radiatum to record the dendritic response to afferent stimulation. All records are the average of 3–4 traces.

A typical orthodromic response is shown in Fig. 1A. The population spike, the synchronous firing of CA1 pyramidal cells, is measured as the average of the amplitude from point a to point b and the amplitude from point b to point c. The response recorded in the dendritic layer shows the afferent volley (point d) and the synaptic response of the population of neurons (postsynaptic potential, PSP). The PSP is quantified by measuring the slope early in the response (point e). The slope was used as a measure since the amplitude was frequently obscured by generation of a population spike.

As illustrated in Fig. 1, the application of 0.01% H_2O_2 plus 100 μM ferrous sulfate (peroxide/iron) resulted in a decrease in the orthodromically elicited population spike (n = 14). Recovery of the population spike occurred in 5 out of 6 slices when normal oxygenated saline was washed through for 20–30 min (Fig. 1C). At these concentrations of peroxide and iron, the population spike elicited by antidromic stimulation through a bipolar electrode in the alveus

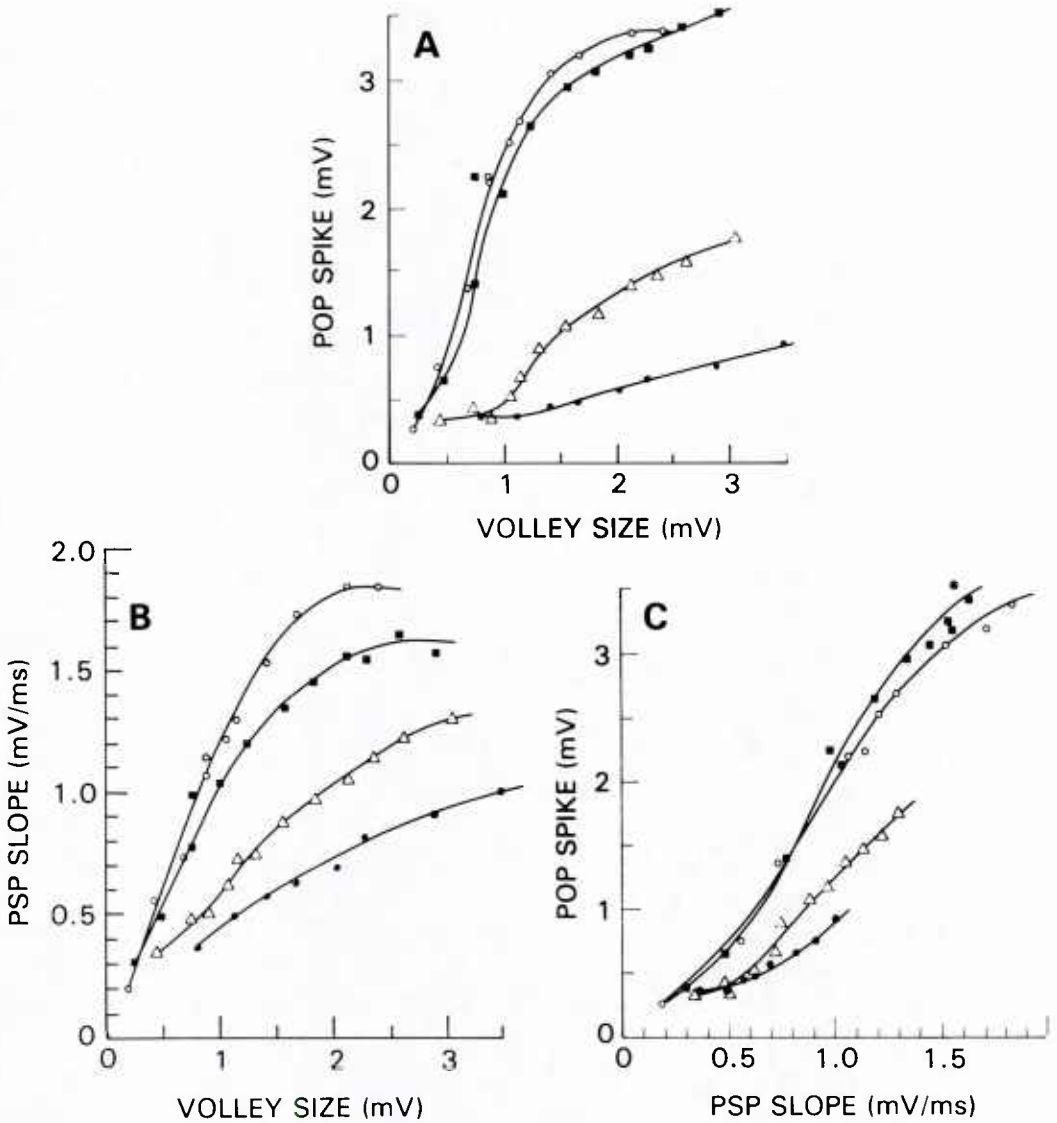

Fig. 2. Input–output curves illustrating the effects of 0.01% peroxide with 100 μM ferrous sulfate in same experiment as Fig. 1. A: amplitude of the presynaptic volley is plotted against the resulting population spike amplitude. ○, control; △, 15 min exposure to peroxide/iron; ●, 25 min exposure to peroxide/iron; ■, 30 min of wash. The population spike is reduced by peroxide/iron but partially recovers with wash. B: graph of volley size vs slope of the dendritic response. Symbols are the same as in A. PSP is reduced by peroxide/iron and only partially recovers in wash. C: the dendritic response is plotted against the amplitude of the population spike. Symbols are the same as in A. The same size PSP is less effective in eliciting a population response in peroxide/iron as compared to control. This effect is completely reversed by wash in this experiment.

was unaffected. Only at much higher concentrations (0.1% H_2O_2) was the antidromic spike significantly attenuated. The action of peroxide/iron was not pathway specific. In two experiments the afferents to the basal dendrites of the CA1 pyramidal cells were activated with a stimulating electrode in stratum oriens. The population response to this afferent stimulus was similarly reduced.

The neuronal damage caused by peroxide/iron is likely to result from the generation of free radicals and initiation of lipid peroxidation. Two observations support this. (1) While peroxide (0.01%) alone was found to reduce the orthodromic population spike, addition of ferrous ions seemed to potentiate the effect by speeding its onset. Addition of Fe^{2+} to H_2O_2 promotes the formation of hydroxyl free radicals through the Fenton reaction. Ferrous sulfate alone (100 μM), however, did not cause any change in the elicited field potentials (n = 5). (2) The longer the tissue was incubated before the experiment, the more

sensitive to peroxidative damage it appeared. It is probable that lipid peroxidation occurs spontaneously during incubation as observed by Kovachich and Mishra[10].

To analyze the site of action of the peroxide and iron, input/output curves were generated. Stimulus strength was varied to elicit a range of sizes of population spikes. The afferent volley was used as an index of activated presynaptic fibers. Peroxide/iron did not change the afferent volley size elicited by a given stimulus strength. As the size of the volley increased the somatic population spike increased (Fig. 2A). Addition of peroxide/iron resulted in a progressive decrease of the amplitude of the population spike. The population spike recovered substantially with a 30-min wash. An increase in afferent volley was also reflected in an increase in the slope of the dendritic potential (PSP slope) (Fig. 2B). In the presence of peroxide and iron, the same size volley produced a smaller PSP indicating a decrease in synaptic efficacy. This effect was only partially reversible. These two actions of peroxide and iron, reflected in Fig. 2A and B, can also be observed in Fig. 1A, B-1, and C. In Fig. 1, the stimulus strength used to evoke the response remained constant and the afferent volley size (d) was unchanged. Both the amplitude of the population spike and the slope of the PSP were reduced.

Fig. 2C illustrates the change in the relationship between the slope of the PSP and the population spike with peroxide/iron. For a PSP of the same size, a smaller population spike was evoked in peroxide/iron than in the control, suggesting that the mechanism for spike generation was impaired. This is also reflected in Fig. 1B-2 where the stimulus strength was increased sufficiently to evoke a dendritic response similar to that seen in the control (Fig. 1A), but the population spike was still substantially smaller than in the control.

The actions of peroxide/iron on generation of the PSP and on generation of the population spike appear to be independent effects. The two mechanisms were usually, but not always, simultaneously affected. In 3 out of 14 slices the PSP was not reduced. In 3 other experiments, the ability of the PSP to evoke a population spike was not reduced. Within a single experiment, the two effects were independent in their reversibility with wash. For example in Fig. 2, the impaired spike generation was completely reversed with wash while the decrease in synaptic efficacy was not. In other experiments, only synaptic efficacy was reversed or both mechanisms were only partially reversed.

In some laboratories, peroxide is added to the perfusion solution to supplement oxygenation of neural tissue in vitro. Lower concentrations of peroxide may be capable of increasing available oxygen, through the enzyme catalase, without inducing free radical damage. Llinas and Sugimori[12] found that addition of 0.001% H_2O_2 improved the viability of cerebellar slices, while Llinas et al.[13] found that they required 0.003% H_2O_2 in the intact perfused cerebellum preparation to keep it alive. Walton and Fulton[21] found that 0.004% H_2O_2 optimally increased fields in the isolated spinal cord preparation and that this effect was reversed by inhibition of catalase. The results of the present study suggest that this approach should only be taken with caution.

Although the molecular mechanism of peroxide/iron damage is not definite, it is likely to result from lipid peroxidation. The reversibility of the electrophysiological effects are difficult to explain since one would not expect lipid peroxidation to reverse. It is possible that there is functional recovery despite continued presence of lipid damage. Noda et al.[15] found only transient increases in lipid peroxidation products following hyperbaric oxygen. They suggested that either the lipid peroxides or malondialdehyde were metabolized fairly rapidly in vivo.

The data presented here suggest that increased free radicals, that can result from ischemia and reperfusion, are able to produce profound changes in neuronal activity. Two mechanisms are affected by the peroxide/iron: synaptic efficacy and spike generating mechanisms. Antidromically elicited population spikes were only affected by very high concentrations of peroxide. The results of Lipton and Whittingham[11] similarly show that hypoxia has a greater effect on orthodromic activity than the antidromic spike in granule cells of the dentate. Because potassium and ouabain accelerated the effects of hypoxia, these authors suggested that hypoxia caused a depolarization due to inhibition of the sodium/potassium pump. Misgeld and Frotscher[14] on the other hand, saw a hyperpolarization with anoxia in CA3 neurons of the hippocampus. The ionic mechanism of the reduced synaptic efficacy seen here with peroxidative damage will be ex-

amined in future studies with intracellular techniques.

An increase in free radical concentrations and lipid peroxidation can also be induced with oxygen under pressure[3,15]. King and Parmentier[7] studied the changes in electrical activity in the hippocampal brain slice produced by oxygen at high pressure. In agreement with the present study, they reported that the presynaptic volley was less efficient in evoking a synaptic response. While in the present study no change in the presynaptic volley was observed with peroxide and iron, King and Parmentier[7] found that oxygen at high pressure increased the volley size.

In conclusion peroxide/iron decreases synaptic efficacy and impairs action potential generation. This functional damage probably results from generation of hydroxyl free radicals and subsequent lipid peroxidation.

I thank Drs. W. Hunt and P. Gunter-Smith for helpful discussions. This work was supported by the Armed Forces Radiobiology Research Institute, Defense Nuclear Agency under Research Work Unit 00105. The views presented in this paper are those of the author; no endorsement by the Defense Nuclear Agency has been given or should be inferred.

1 Demopoulos, H.B., Flamm, E., Seligman, M. and Pietronigro, D.D., Oxygen free radicals in central nervous system ischemia and trauma, *Pathology of Oxygen*, Academic Press, New York, 1982, pp. 127–155.
2 Demopoulos, H.B., Flamm, E., Pietronigro, D.D. and Seligman, M., The free radical pathology and the microcirculation in the major central nervous system disorders, *Acta Physiol. Scand. Suppl.*, 492 (1980) 91–119.
3 Dirks, R.C. and Faiman, M.D., Free radical formation and lipid peroxidation in rat and mouse cerebral cortex slices exposed to high oxygen pressure, *Brain Research*, 248 (1982) 355–360.
4 Fridovich, I., The Biology of oxygen radicals, *Science*, 201 (1978) 875–880.
5 Johansen, F.F., Jorgensen, M.B., Ekstrom von Lubitz, D.K.J. and Diemer, N.H., Selective dendritic damage in hippocampal CA1 stratum radiatum with unchanged axon ultrastructure and glutamate uptake after transient cerebral ischaemia in the rat, *Brain Research*, 291 (1984) 373–377.
6 Karnushina, I., Suzuki, R., Padgett, W. and Daly, W., Degeneration of CA1 neurons in hippocampus after ischemia in mongolian gerbils: cyclic AMP systems, *Brain Research*, 268 (1983) 87–94.
7 King, G.L. and Parmentier, J.L., Oxygen toxicity of hippocampal tissue in vitro, *Brain Research*, 260 (1983) 139–142.
8 Kirino, T., Delayed neuronal death in the gerbil hippocampus following ischemia, *Brain Research*, 239 (1982) 57–69.
9 Kirino, T. and Sano, K., Selective vulnerability in the gerbil hippocampus following transient ischemia, *Acta Neuropathol.*, 62 (1984) 201–208.
10 Kovachich, G.B. and Mishra, O.P., The effect of ascorbic acid on malonaldehyde formation, K^+, Na^+ and water content of brain slices, *Exp. Brain Res.*, 50 (1983) 62–68.
11 Lipton, P. and Whittingham, T.S., The effect of hypoxia on evoked potentials in the in vitro hippocampus, *J. Physiol. (London)*, 287 (1979) 427–438.
12 Llinas, R. and Sugimori, M., Electrophysiological properties of in vitro Purkinje cell somata in mammalian cerebellar slices, *J. Physiol. (London)*, 305 (1980) 171–195.
13 Llinas, R., Yarom, Y. and Sugimori, M., The isolated mammalian brain in vitro: A new technique for the analysis of electrical activity of neuronal circuit function, *Fed. Proc. Fed. Am. Soc. Exp. Biol.*, 40 (1981) 2240–2245.
14 Misgeld, U. and Frotscher, M., Dependence of the viability of neurons in hippocampal slices on oxygen supply, *Brain Res. Bull.*, 8 (1982) 95–100.
15 Noda, Y., McGeer, P.L. and McGeer, E.G., Lipid peroxide distribution in brain and the effect of hyperbaric oxygen, *J. Neurochem.*, 40 (1983) 1329–1332.
16 Petito, C.K. and Pulsinelli, W.A., Delayed neuronal recovery and neuronal death in rat hippocampus following severe cerebral ischemia: possible relationship to abnormalities in neuronal processes, *J. Cerebral Blood Flow and Metabolism*, 4 (1984) 194–205.
17 Rehncrona, S., Siesjo, B.K. and Smith, D.S., Reversible ischemia of the brain: biochemical factors influencing restitution, *Acta Physiol. Scand. Suppl.*, 492 (1980) 135–140.
18 Shaller, C.A., Jaques, S. and Shelden, C.H., The pathophysiology of stroke: a review with molecular considerations, *Surg. Neurol.*, 14 (1980) 433–443.
19 Smith, D.S., Rehncrona, S. and Siesjo, B.K., Barbiturates as protective agents in brain ischemia and as free radical scavengers in vitro, *Acta Physiol. Scand. Suppl.*, 492 (1980) 129–134.
20 Suzuki, R., Yamaguchi, T., Li, C. and Klatzo, I., The effects of 5-minute ischemia in mongolian gerbils: II. Changes of spontaneous neuronal activity in cerebral cortex and CA1 sector of hippocampus, *Acta Neuropathol.*, 60 (1983) 217–222.
21 Walton, K. and Fulton, B., Hydrogen peroxide as a source of molecular oxygen for in vitro mammalian CNS preparations, *Brain Research*, 278 (1983) 387–393.
22 Watson, B.D., Busto, R., Goldberg, W.J., Santiso, M., Yoshida, S. and Ginsberg, M.D., Lipid peroxidation in vivo induced by reversible global ischemia in rat brain, *J. Neurochem.*, 42 (1984) 268–274.

ARMED FORCES RADIOBIOLOGY
RESEARCH INSTITUTE
SCIENTIFIC REPORT
SR86-13

Neuroscience & Biobehavioral Reviews, Vol. 10, pp. 55–65, 1986. © Ankho International Inc. Printed in the U.S.A. 0149-7634/86 $3.00 + .00

Mechanisms of Radiation-Induced Conditioned Taste Aversion Learning

BERNARD M. RABIN*† AND WALTER A. HUNT*[1]

**Behavioral Sciences Department, Armed Forces Radiobiology Research Institute*
Bethesda, MD 20814-5145
and †Department of Psychology, University of Maryland Baltimore County, Catonsville, MD 21228

Received 25 March 1985

RABIN, B. M. AND W. A HUNT. *Mechanisms of radiation-induced conditioned taste aversion learning.* NEUROSCI BIOBEHAV REV 10(1) 55–65, 1986.—The literature on taste aversion learning is reviewed and discussed, with particular emphasis on those studies that have used exposure to ionizing radiation as an unconditioned stimulus to produce a conditioned taste aversion. The primary aim of the review is to attempt to define the mechanisms that lead to the initiation of the taste aversion response following exposure to ionizing radiation. Studies using drug treatments to produce a taste aversion have been included to the extent that they are relevant to understanding the mechanisms by which exposure to ionizing radiation can affect the behavior of the organism.

Ionizing radiation Conditioned taste aversion Lithium chloride Area postrema Behavior

THE toxicity of ionizing radiation generally is expressed as the loss of rapidly turning over cells. This results from an impairment of the synthesis of these cells, especially those in bone marrow. However, since neurons in the mature central nervous system do not undergo cellular turnover, the brain generally has been believed to be insensitive to exposure to ionizing radiation [71], thereby allowing for the routine use of radiation in treating brain tumors. However, little attention has been given to evidence appearing over the years that raises doubts about this conclusion. For example, exposure to ionizing radiation at doses of 15–500 rad significantly reduces the electroshock seizure threshold, an effect lasting up to 8 months [97]. Also, in this dose range emesis is induced. Transient increases in the spontaneous locomotor activity of C57BL mice and arousal in rats have been observed after exposure to 1000–1500 rad [60,83]. And, on the molecular level, the functioning of sodium channels is impaired after radiation exposure to as little as 10 rad [140]. These observations suggest that exposure to ionizing radiation may have behavioral consequences not previously appreciated.

High lethal doses of ionizing radiation can severely disrupt behavior. Depending upon the species, the quality of radiation, and the nature of the behavioral measurements, 1000–10000 rad degrades performance on a number of tasks. Under some conditions the effects are transient, generally lasting up to one hr after irradiation [7, 14, 15, 36, 64], but after sufficiently high doses of radiation a permanent incapacitation is induced, culminating in the death of the organism. Possible effects of lower doses (<1000 rad) of radiation have not been adequately explored. Therefore, given the available evidence, such as that cited above, exposure to ionizing radiation may have subtle actions on the brain that may have clinical significance.

In addition to emesis, exposure to lower doses of ionizing radiation induces a conditioned taste aversion (CTA) in experimental animals and humans. A CTA can result when a novel tasting solution is paired with a toxin, so that when the solution is presented subsequently, further ingestion is avoided. This avoidance behavior is typically acquired after a single pairing of the solution with the toxin. Taste aversions can be produced, using saccharin or sucrose solutions, after injection of a wide variety of drugs, such as lithium chloride (LiCl), amphetamine, copper sulfate, and apomorphine [44,113], as well as after exposure to ionizing radiation [124]. Since radiation-induced taste aversions are obtained typically after exposure to 37–150 rad doses, examining the underlying mechanisms associated with development of this type of CTA might provide information on other possible behavioral consequences of low-dose irradiation. Such a model has the additional benefit of having an extensive behavioral and physiological database relating to taste aversions in general (see [1, 47, 117] for recent reviews of drug-induced CTA learning).

The goal of this paper is to review the variety of studies that have used radiation to produce a CTA in order to define the general mechanisms by which exposure to nonlethal levels of radiation might alter behavior. Our purpose is not to review CTA learning in general. However, studies with toxins in addition to radiation will be presented when they are relevant to the discussion.

A number of methods are used to produce a CTA. Since interpretation of information derived from some procedures

[1]Requests for reprints should be addressed to Walter A. Hunt.

can be misleading, we will begin with a brief discussion of the various methods employed for producing a CTA and their advantages and disadvantages.

METHODOLOGICAL CONSIDERATIONS

The general procedure for producing a conditioned taste aversion involves placing the subjects on a water deprivation schedule. Once the animal has adapted to the schedule, a novel tasting solution is substituted for the regular water bottle as the conditioned stimulus (CS). Ingestion of the novel solution is followed by treatment with the toxin, the unconditioned stimulus (UCS). The dependent measure, the conditioned response (CR), is the amount of the solution ingested at a subsequent presentation of the CS.

Within this general paradigm, a number of variations are used in quantifying the dependent measure, although the suggestion has been made that these different procedures may be measuring different aspects of CTA learning [131]. One such variation involves the use of either a one-bottle or two-bottle test to study taste aversion learning. In a single-bottle test, the animal is presented with only a single bottle containing the CS during the period in which fluid is available. In a two-bottle test, the animal can choose between the CS or a neutral fluid such as tap water. In a single-bottle test the subject is forced to choose between ingesting the solution that has been paired with the UCS or "going thirsty"; whereas with a two-bottle test, an alternative is available to drinking the CS.

A second variation in the dependent measure involves determining either the absolute or the relative intake. In a single-bottle test, the most typical dependent measure is the actual amount of the CS ingested by the subject, although postconditioning intake may also be expressed as a percentage of CS intake on the conditioning day prior to treatment. When a two-bottle design is used, the data are typically presented in terms of the relative intake of both the neutral and conditioned stimuli. While the data from a two-bottle test may be presented in terms of the actual intakes of each solution, the data can also be presented as a sucrose preference score, calculated by dividing the CS intake by total fluid intake. Because this preference measure is relatively insensitive to variations in total fluid intake, the preference score has been considered to be a more sensitive indicator of CTA learning [31,53], particularly under conditions in which the taste aversion produced by the UCS is relatively weak.

Using a single-bottle design may also introduce a potential conflict that can result from forcing the animal to ingest the solution which has been paired with the UCS. The only other alternative for the animal is not to drink at all. Conflict is not involved with a two-bottle design because the subject can choose which solution to drink. The introduction of conflict into the CTA learning paradigm can complicate the interpretation of data relating to possible mechanisms underlying CTA acquisition. This is a significant problem is studies that have attempted to assess a possible role of pituitary/adrenal hormones in CTA learning. In a series of studies using single-bottle designs, Smotherman *et al.* [128,129] have reported that acquisition of an LiCl-induced CTA is associated with the activation of the pituitary/adrenal system. Manipulation of corticosteroid levels by injection of ACTH or dexamethasone produces corresponding changes in the acquisition or extinction of the CTA response [56, 57, 127]. However, more recent work has shown that it is possible to dissociate the corticosteroid and behavioral responses to LiCl injection by varying the number of LiCl preexposures to which the animals are subjected [130]. This observation suggests that CTA acquisition is not dependent upon the LiCl-induced changes in pituitary/adrenal function. Consistent with this finding is the report by Rabin *et al.* [104] that hypophysectomy has no effect on the acquisition of an LiCl-induced CTA in rats tested using a two-bottle procedure.

Similar findings have been reported with radiation-induced taste aversion learning. Garcia and Kimeldorf [40] working with non-deprived rats in a single-bottle design reported that hypophysectomy had no effect on the acquisition of a radiation-induced CTA in rats. Similarly, Rabin *et al.* [104] found that hypophysectomy had no effect on radiation-induced CTA learning in rats tested with a two-bottle procedure. In contrast, Cairnie and Leach [16], using a single-bottle test with deprived animals, reported that injections of dexamethasone produced a significant attenuation of a radiation-induced CTA in rats. However, using a two-bottle test Rabin *et al.* (unpublished manuscript) found no effect of the drug. Since hormones of the pituitary/adrenal system have been shown to play a role in mediating conflict-induced arousal [55,138], these results suggest that activation of the pituitary/adrenal system or manipulation of corticosteroid levels in a CTA paradigm is related more to conflict produced using a single-bottle experimental design than to the CTA learning itself.

A second potential confounding artifact in studies attempting to evaluate the mechanisms involved in mediating CTA learning may result from a failure to control for the effects of state-dependent learning [94]. State-dependent learning results from a failure to maintain identical conditions (states) on both the conditioning and test days. Consequently, a CTA that is learned on the conditioning day is not recalled on the subsequent test day because the test conditions are different than the conditions under which the response was originally learned. In experiments designed to evaluate the effects of a variety of potentially disruptive treatments on CTA acquisition the usual procedure is to interpolate some treatment during the interval between the presentation of the CS and UCS on the conditioning day. Under these conditions, the subjects are exposed to the CS in the same treatment-free environment on both conditioning and test days. Some experimental manipulations, however, may require that the disruptive treatment be administered prior to, or coincident with, the presentation of the CS on the conditioning day. If the identical treatment is not subsequently administered together with the presentation of the CS on the test day, then the different conditions on the two days can interfere with the recall of the previously acquired CTA response. Under these conditions, identical treatments must be administered on both conditioning and test days to maintain identical states on both days.

That state-dependent learning can present a serious problem for studies designed to analyze the mechanisms of CTA learning has been shown by a number of studies using a variety of unconditioned stimuli and disruptive treatments. Working with ionizing radiation, Levy *et al.* [75] reported that treatment of rats with an antihistamine (chlorpheniramine maleate) on the conditioning day attenuated the acquisition of a CTA to saccharin. However, they administered the antihistamine prior to the initial exposure of the CS and failed to give a corresponding treatment on the test day. When the antihistamine is administered together with the CS on both conditioning and test days, treatment with the antihistamine has no effect on the acquisition of a radiation-

induced CTA [102]. Alternatively, when the antihistamine is given after the presentation of the CS, so that the animals are in a drug-free state on both conditioning and test days, neither intraperitoneal [16, 102, 119] nor intraventricular [101] injections of antihistamine have an effect on the acquisition of a radiation-induced CTA.

In addition to the use of a radiation UCS, state-dependent effects have also been observed in studies of drug-induced CTA learning. Phillips and LePiane [96] have reported that the disruption of LiCl-induced CTA learning produced by stimulation of the basolateral amygdala is not observed when that stimulation is given on both the conditioning and test day. Similarly, in a pilot experiment, Rabin and Hunt (unpublished manuscript) found that the reported disruption of an amphetamine-induced CTA by pretreatment with alpha-methyltyrosine [50] is greatly attenuated if the treatment sequence is administered prior to the presentation of the CS on both the conditioning and the test day. It would therefore seem that the problems posed by state-dependent learning are general, affecting a variety of unconditioned stimuli and disruptive treatments. As a result, appropriate controls for state-dependent effects must be employed where a disruptive treatment is administered prior to or during the presentation of the CS.

THE RADIATION-INDUCED CTA

Some Parametric Considerations

Ionizing radiation is only one of many potential unconditioned stimuli which can be used to produce a CTA [44, 113, 124]. Therefore, it would be important to review some of the parametric factors associated with the acquisition of taste aversions produced by exposure to ionizing radiation or by injection of chemical compounds. A consideration of some of the similarities and differences in taste aversion learning produced by these various unconditioned stimuli will facilitate a comparison of the mechanisms involved in the acquisition of a CTA.

As indicated above, the dose of radiation used to produce CTA learning is well below the lethal dose [45,124]. Threshold doses for whole body exposures in rats have been variously reported to range from 7.5 rad [45] to between 20–25 rad [108]. These variations probably reflect differences in the radiation quality and in the conditions associated with the behavioral testing [124]. Further increases in the dose produce a non-linear increase in the strength of the aversion [108], such that whole body exposures of 50–100 rad produce a nearly total avoidance of the CS (e.g., [45, 124, 126]).

Similar results are obtained with LiCl. The threshold dose for an LiCl-induced aversion is between 0.15 and 0.30 mEq/kg [91,108]. Further increases in the dose of LiCl also produce a non-linear increase in the strength of the aversion, with the maximum aversion being reached with doses of 3 mEq/kg [91].

Amphetamine, in contrast to both radiation and LiCl, does not show this dose/response relationship. The threshold dose for amphetamine-induced CTA is between 0.5 and 1.0 mg/kg, but further increases in dose up to 2.0 mg/kg do not produce a corresponding increase in the strength of the aversion [108].

Despite the similar dose/response relationships between radiation and LiCl, there are significant differences in time-courses of the conditioning effects. This is primarily reflected in the capacity of the radiation UCS to produce a CTA when presented in a backwards conditioning paradigm [2]. A radiation-induced CTA can be acquired when the radiation UCS is presented up to 6 hr preceding the presentation of the CS. The strength of the aversion seems to be the greatest when the UCS precedes the CS y 90 min [19]. LiCl, in contrast, is not capable of inducing a CTA under these conditions. These observations indicate that exposing the organism to ionizing radiation, unlike treatment with LiCl, causes a long-lasting change that produces the temporal overlap necessary for the acquisition of a CR.

A related issue concerns the dose equivalence of different unconditioned stimuli when comparing their mechanisms of action. When a given treatment or manipulation shows an equivalent effectiveness in modulating a CTA produced by different unconditioned stimuli, the empirical observation is, by itself, sufficient evidence for a similarity of mechanism as it relates to those specific experimental conditions. In contrast, the observation that an experimental manipulation is effective in modulating a CTA produced by one UCS but not by another UCS may mean either that the mechanisms of action of these stimuli are different, or that there are differences in the initial effectiveness of those stimuli in producing a CTA. In part, the validity of the two hypotheses can be determined by comparing the experimental dose of the CTA-inducing agents with the threshold doses of those agents. In general, a given manipulation is less likely to be effective in modulating a CTA the greater the experimental dose is above the threshold dose (e.g., [35,110]). In addition, the two alternatives can be evaluated by comparing the effects of the manipulations on a variety of response measures. Thus, for example, LiCl- and amphetamine-induced aversions are different not only in terms of the effects of area postrema lesions on the acquisition of the response, but also in terms of the non-consummatory responses elicited by the two stimuli [95,114].

Role of Illness

One of the major unknowns in the acquisition of a radiation-induced CTA concerns the nature of the UCS. What are the specific characteristics of the UCS that lead to the subsequent avoidance of a "food" with which the UCS has been associated? With injections of toxic unconditioned stimuli that produce obvious signs of illness in the organism such as LiCl or copper sulfate, for example, a direct relationship is assumed between the gastrointestinal effects of the UCS and the resultant CTA learning [22, 23, 118]. Consistent with this hypothesis is the observation that lesions of the area postrema, the chemoreceptive trigger zone for emesis [9], disrupt the acquisition of a CTA produced by injections of methylscopolamine [4,114] and by injections of LiCl [103,114]. That the acquisition of a CTA requires a relatively specific UCS is shown by the observation that pairing a novel CS with a painful exteroceptive UCS, such as shock, does not readily result in CTA learning [41,73]. This observation which shows that pain *per se* is not an effective UCS for CTA learning suggests that the UCS may in some way involve the gastrointestinal system. However, even assuming, for the moment, that the toxic character of some stimuli constitutes the direct antecedent condition for CTA learning, a CTA can also be produced by pairing a novel CS with a variety of unconditioned stimuli (such as amphetamine, cannabinols, sesame oil and morphine) that are not only non-toxic, but will also be self-administered [3, 28, 38, 49]. This would suggest that the toxicity of a UCS is not a necessary condition for CTA learning to occur.

Whether the toxicity of radiation is important for the development of a CTA is not clear. As indicated in the preceding section, high doses of radiation (>500 rad) are clearly toxic stimuli which can produce a variety of changes in neural [67, 112, 136, 141] and behavioral [30, 82, 89, 90] functioning. In addition, like both LiCl and copper sulfate, irradiation can lead to emesis [8,12] and, in humans, to nausea [120]. In contrast, the dose of radiation (37–150 rad) typically used to produce a CTA, has no apparent effect on the unrestrained behavior of the organism [124]. However, lesions of the area postrema attenuate a radiation-induced CTA just as they attenuate a CTA following an injection of LiCl [93,103]. This might suggest that a radiation-induced change, possibly related to emesis, is a factor in the acquisition of a radiation-induced CTA, and that, therefore, there is some relationship between the toxic nature of radiation and the capacity of exposure to ionizing radiation to lead to CTA learning.

If an effect on the gastrointestinal system related to emesis does play a role in the acquisition of a CTA when a toxic UCS is used, then it should be possible to disrupt the CTA by treating the organisms with an antiemetic to prevent the development of the malaise. Initial experiments did not support the hypothesis of a link between the antiemetic-sensitive gastrointestinal distress and CTA learning. Levy *et al.* [75] reported that pretreating rats with the antiemetic trimethobenzamide did not disrupt the acquisition of a radiation-induced CTA, and Gadusek and Kalat [37] reported that treatment with scopolamine did not attenuate the recall of a previously acquired LiCl-induced CTA. However, reasoning that these previous investigations used doses of antiemetics that were much higher than the clinically effective doses, Coil *et al.* [23] tested the effects of several doses of a variety of antiemetics on the recall of a LiCl-induced CTA. They found that treatment with the clinically effective doses of scopolamine, trimethobenzamide, prochlorperazine and cyclizine produced a significant attenuation of the previously acquired CTA. Doses of antiemetics either greater or less than the clinically effective dose had no effect on CTA recall. These results would be consistent with the hypothesis that a UCS-induced illness plays a role in CTA learning when LiCl is used as the UCS.

More recent research, however, has failed to confirm these findings. Goudie *et al.* [51], working with taste aversions produced by a variety of drugs including LiCl, reported that treatment with the clinically effective doses of scopolamine or prochlorperazine had no effect on the recall of a previously acquired CTA. In a more detailed study, Rabin and Hunt [99] looked at the effect of antiemetic treatment on both the acquisition and recall of taste aversions produced by injection of LiCl or by exposure to ionizing radiation. Treatment with the previously reported effective doses of trimethobenzamide, prochlorperazine or cyclizine [23] did not attenuate the acquisition of either a radiation- or LiCl-induced CTA. Because radiation exposure can produce a CTA when administered up to 6 hr prior to ingestion of the CS [2] and because the maximal effects of irradiation on CTA learning are observed 90 min after exposure [19], additional groups of rats were included in this study that were given one injection of prochlorperazine 15 min prior to irradiation or to injection of LiCl and a second antiemetic treatment 3 hr later. This extended antiemetic treatment, which would be expected to overlap the period of radiation effects, also had no effect on the acquisition of a CTA. As would be expected, given the lack of effect of antiemetic treatment on CTA acquisition, there were also no effects on the recall of a previously acquired radiation- or LiCl-induced CTA. In this part of the experiment the procedures used were similar to those of Coil *et al.* [23], which would suggest that any possible effect of antiemetic treatment on CTA learning is marginal at best. Consistent with this interpretation is the observation that, in humans, nausea is not a necessary symptom in subjects that acquire a CTA [5]. Therefore, the data do not provide compelling evidence that a UCS-induced illness is a direct antecedent condition to CTA learning.

The failure to find a consistent effect of antiemetic treatment on CTA learning produced by a toxic UCS raises some questions about the role of a UCS-produced illness as an antecedent condition to the acquisition of a radiation-induced CTA. Possibly the toxicity of the UCS is a side-effect of the treatment that is not required for the acquisition of the CTA. Some additional evidence is concordant with this possibility. Several studies have provided evidence which indicates that pairing a novel CS with the illness produced by various poisons is not, by itself, sufficient to produce a CTA [66,92]. Similarly, both radiation- and LiCl-induced taste aversions can be acquired by rats that are exposed to the UCS while under deep surgical anesthesia and maintained under the anesthesia for an additional 4–8 hr [100,116]. Under these conditions, it is difficult to understand how the experience of a possible UCS-induced illness could contribute to the acquisition of the CTA.

Role of the Gastrointestinal System

Even though the data on radiation presented above suggest the possibility of a subtle effect on nervous system function following exposure to low doses of ionizing radiation, these radiation-induced changes in nervous system activity do not seem to be critical for the occurrence of CTA learning [61]. Garcia and Kimeldorf [40] reported that radiation exposure restricted to the abdomen of rats could serve as the UCS for CTA learning. Although a higher dose of abdomen-only radiation is needed to produce an aversion equivalent to that produced by whole-body exposure, irradiation restricted to the abdomen is much more effective in producing a CTA than is irradiation restricted to the head, pelvis, or thorax alone. These basic results have been replicated in a number of investigations that, despite utilizing a variety of procedures, all show that body-only radiation exposure will produce a stronger aversion and at a lower dose than will head-only irradiations [106,126]. Since exposure of pelvis or thorax would be expected to affect the spinal cord and peripheral nerves to a similar extent as irradiation of the abdomen, the greater effectiveness of exposure of the abdomen in producing a CTA would be consistent with the hypothesis that some effect of the radiation related to the gastrointestinal system may be involved in mediating the acquisition of the radiation-induced CTA.

There are two possible mechanisms by which exposure of the abdomen can lead to taste CTA learning. First, the radiation may have a direct effect on the activity of the gastrointestinal system. Second, it may act as a nonspecific toxin causing the release of some humoral factor related to a generalized irritation of the gastrointestinal system. In support of the first possibility, Hulse and Mizon [58] have reported that exposing the abdomen of rats to ionizing radiation at doses of 20–100 rad produces a delay in gastric emptying which is correlated with the strength of an aversion to a

barium meal. Exposing the head and shoulders of rats to radiation doses of up to 200 rad does not have an effect on gastric emptying and produces only a weak aversion, at best, to the barium meal. However, while treating rats with insulin reverses the radiation-induced delay in gastric emptying [59], it does not disrupt the acquisition of a radiation-induced CTA [16].

A second approach to evaluating a possible role for direct gastrointestinal effects in CTA learning has involved sectioning the vagus nerve. The vagus constitutes the most extensive afferent source from the gut to the central nervous system [88] and has been implicated in the regulation of a wide range of visceral homeostatic functions [79, 80, 137]. If disruption of gastric function is the UCS for the acquisition of a radiation-induced CTA and this information is relayed to the brain by neural pathways from the stomach, then sectioning the vagus might he expected to produce some changes in the acquisition of the CTA [22,80]. However, Rabin, Hunt and Lee [105] found that subdiaphragmatic vagotomy in rats did not disrupt the acquisition of a CTA following exposure to either 200 rad whole-body or body-only irradiation. The results obtained with taste aversions produced by exposure to ionizing radiation generally parallel those obtained with drugs. In general, vagotomy has no effect on the acquisition of taste aversions induced by systemic toxins such as apomorphine, LiCl or ethanol [68, 69, 80, 105]. While these studies do not eliminate the possibility that the relevant information for CTA learning may be carried from the gut to the central nervous system by alternate pathways (e.g., splanchnic), it does not seem likely that a radiation-induced change in gastric function mediated by the vagus nerve, which provides the most extensive afferent source, serves as the proximate UCS for CTA learning following exposure to radiation.

In contrast, the emetic response to gastric irritation produced by intragastrically administered copper sulfate is greatly attenuated by vagotomy [137]. Concordant with this finding is the report that subdiaphragmatic vagotomy in rats disrupts CTA acquisition following intragastric and intraperitoneal copper sulfate, but not following intravenous administration [24]. While this finding would suggest that vagally-mediated changes in gastrointestinal function can play a role in CTA learning, Rabin *et al.* [105,109] have been unable to replicate this finding. Although more work is needed to resolve this discrepancy, the evidence suggesting a direct gastrointestinal involvement in CTA learning is not compelling.

Role of Humoral and Neural Mechanisms

In contrast to the above, there is good support for the hypothesis that exposure to ionizing radiation causes the release of a humoral factor, which in turn serves to mediate the acquisition of a CTA. Using a standard CTA paradigm, Hunt *et al.* [62] exposed one member of a parabiotic pair of rats to 360 rad of ionizing radiation while the other member of the pair was shielded. When tested for a saccharin preference, the shielded member of the pair showed a significant aversion to the saccharin solution. Since the parabiotic pair share a common blood supply, the inference is that some blood transferable humoral factor is produced in the irradiated member that can act as a UCS for the shielded member. There appears to be a dose/response relationship between the dose of radiation and the release of the humoral factor because the strength of the aversion produced in the shielded member of the parabiotic pair varies as a function of the dose to which the unshielded member is exposed [63].

Additional support for the hypothesis that a radiation-released humoral factor which serves to mediate CTA learning following exposure to ionizing radiation comes from the observation that a CTA can be produced in rats by injecting them with serum from rats that have been previously exposed to radiation [43]. However, caution must be used in interpreting the results of this experiment because the donor rats were subjected to extreme doses of radiation (30000 rad) and because the recipient rats were given injections of 12 ml of serum in 3 injections separated by 15 min each on 4 separate experimental days. This procedure is so different from the standard procedures for producing a CTA that the degree to which we can generalize from these results to the more typical experiment is not certain.

Another line of evidence that is consistent with the hypothesis of humoral mediation of the radiation-induced CTA comes from studies of the effect of area postrema lesions on CTA learning. The area postrema is the chemoreceptive trigger zone for emesis which functions to monitor the blood and cerebrospinal fluid for toxins [9]. Lesions of the area postrema disrupt the emetic response to a variety of blood-borne toxins [9] as well as to intraventricular histamine [6]. Similarly, lesions of the area postrema disrupt the emetic response to ionizing radiation in monkeys [12] and in dogs [20], suggesting that a humoral factor mediates the emetic response to irradiation. This conclusion is limited by the observation that area postrema lesions have been reported to have no effect on emesis produced by whole body irradiation in the cat [8]. However, more recent work indicates that area postrema lesions are effective in disrupting emesis in cats exposed to body-only radiation (Rabin, Hunt, Chedester and Lee, in preparation).

As with blood-borne emetic stimuli, lesions of the area postrema disrupt CTA acquisition to systemically-administered drugs. Area postrema lesions have been shown to attenuate CTA learning following intraperitoneal injections of methylscopolamine [4], LiCl [103,114] and histamine [103], as well as following an intravenous injection of copper sulfate [22]. The area postrema thus seems to mediate CTA learning for a particular class of unconditioned stimuli that are apparently related in some manner to emesis because the area postrema lesions do not disrupt the CTA produced by injections of amphetamine [4,114]. A similar distinction between LiCl and amphetamine as representing different classes of unconditioned stimuli for CTA learning has been made by Parker [95] based upon the observation of different nonconsummatory behavioral responses produced by treatment with these stimuli.

It therefore seems that there are two classes of UCS for CTA learning: one mediated by the area postrema and the other which does not depend upon the integrity of the area postrema. The CTA produced by exposure to ionizing radiation, for the most part, falls within the class of UCS that is mediated by the area postrema. Lesions of the area postrema produce an equivalent attenuation of taste aversions produced by exposure to gamma radiation and by injection of LiCl and histamine [93,101]. Also consistent with this hypothesis is the observation that lesions of the area postrema after the initial pairing of a novel sucrose solution with either radiation or LiCl on the conditioning day has no effect on the subsequent recall of the CTA [107]. This observation further confirms the function of the area postrema as a transfer point by which information about potential toxins in the blood and

cerebrospinal fluid is transmitted into the central nervous system.

As indicated above, a comparison of aversions produced by partial-body exposures indicates that irradiation of the body-only is more effective in producing a CTA than is irradiation of the head-only [40, 126]. This finding raises the possibility that taste aversions produced by head- and body-only exposures may involve different mechanisms. This possibility was evaluated in an experiment comparing the effects of area postrema lesions on the acquisition of a CTA produced by head- or body-only exposure [106]. Lesions of the area postrema of rats exposed to body-only radiation produced a complete disruption of CTA learning. In contrast, area postrema lesions in rats exposed to head-only radiation, while producing a significant attenuation of the CTA, did not prevent the occurrence of a significant reduction in test day sucrose preference compared to conditioning day preference. These results indicate that the acquisition of a CTA following partial-body exposures is mediated by the area postrema and also involves additional mechanisms not dependent upon the integrity of the area postrema. A direct effect of radiation on the brain mediating the acquisition of a CTA would be consistent with studies indicating changes in electrocortical activity [24, 86, 87], in seizure thresholds [88,97], and in sodium channel function [140] at radiation doses of less than 300 rad.

Role of Central Neurotransmitters

So far, there is little indication what brain mechanisms may mediate radiation-induced CTA learning in the absence of the area postrema. One possible approach to determining potential mechanisms would be to examine the effects of irradiation on central neurotransmitters. For example, neurochemical studies have, in fact, indicated that exposing an organism to ionizing radiation can affect biogenic amines in the brain [65].

A number of neurobehavioral studies have been undertaken in an attempt to determine the mechanisms of CTA learning produced by a variety of unconditioned stimuli. Most of these studies use lesions of various areas of the brain and drugs that modify the actions of neurotransmitters. The relationship of these studies to the mechanisms of radiation-induced taste aversions is not clear, since they generally have involved unconditioned stimuli other than radiation. However, based on the discussions in previous sections of this review, it may be possible to infer potential mechanisms of radiation-induced taste aversions through the actions of unconditioned stimuli that seem to act in a manner similar to radiation. One way to group these stimuli is by the ability of lesions of the area postrema to block specific aversions. Since both radiation- and LiCl-induced aversions are prevented by area postrema lesions, actions of lithium relative to the development of a CTA might have some bearing on how radiation induces a CTA.

The manipulation of the actions of neurotransmitters has been a major means by which possible mechanisms underlying CTA learning have been examined. These manipulations have been accomplished either by administering drugs that either facilitate or suppress the activity of a given transmitter or by applying selective lesions to areas of the brain that send afferents containing that transmitter or contain the synaptic endings. Most of the research, though limited, has focused on the biogenic amines that include the catecholamines, dopamine and norepinephrine, and the indoleamine, serotonin. A few studies have appeared examining cholinergic mechanisms.

One difficulty inherent in this approach, however, is the possible confounding of the processes that lead to the initiation of the behavior with those that lead to the association of the CS with the UCS or to the expression of the behavior. Since the acquisition of a response can only be demonstrated through its subsequent performance, the failure of an organism to show a CTA following neurochemical manipulation of the brain may reflect a deficit in either process. Since the present concern is with the mechanisms responsible for the initiation of the CTA response, care must be taken to separate out these various processes that lead to the performance of a learned response. Ideally, the experiment should be designed to show that a given manipulation disrupts CTA learning to a class of unconditioned stimuli presumed to have a similar mechanism of action while having no effect on the acquisition of a CTA induced by stimuli presumed to have a different mechanism of action.

This approach has been utilized in the comparison of LiCl and amphetamine as unconditioned stimuli for taste aversion learning. Lesions of the area postrema disrupt the acquisition of a CTA produced by injection of LiCl and methylscopolamine, but have no effect on an aversion produced by amphetamine [4,114]. Conversely, manipulation of catecholaminergic systems, either by injection of 6-hydroxydopamine [115,135] or by lesions of the dorsolateral tegmentum [139] attenuate a CTA produced by injection of amphetamine, but have no effect on the acquisition of a CTA following injection of LiCl. Because these experiments show that the effects of manipulation of catecholaminergic systems on CTA learning are restricted to a single class of unconditioned stimuli, it would suggest that the effects of manipulation of these systems are on the mechanisms responsible for the initiation of the response and not on the processes responsible for the association or performance of the response.

One transmitter whose activity correlates with the development of an LiCl-induced CTA is serotonin. Various manipulations that alter serotonergic activity can modify the magnitude of the CTA. Lesions of the median raphe nucleus, but not the dorsal raphe nucleus prior to conditioning enhance the LiCl-induced CTA [76]. On the other hand, pretreatment of either raphe-lesioned or unlesioned animals are pretreated before conditioning with 5-hydroxytryptophan, the precursor of serotonin, or with inhibitors of serotonin uptake results in the acquisition of an attenuated CTA [77,78]. Since medial raphe lesions deplete serotonin in limbic structures such as the hippocampus and septum, the results of these studies are interpreted as indicating that the role of serotonin may be to modulate the perceived intensity of the toxic stimulus.

In general, there is little evidence for a role of catecholamines in radiation- or LiCl-induced CTA learning. Blockade of catecholamine synthesis or dopaminergic receptors does not alter the subsequent development of a CTA [99,122]. Also, as indicated above, depletion of forebrain norepinephrine with the neurotoxin 6-hydroxydopamine or electrolytic lesions of the dorsolateral tegmentum are ineffective [81, 139]. On the other hand, infusions of beta-adrenergic agonists and antagonists into the ventricular system of the brain have been reported to modify the development of LiCl-induced taste aversions. The agonist enhances the CTA and the antagonist reduces it [72]. Because similar infusions into the lateral hypothalamus can alter the aversiveness of

certain tastes, these treatments may be related to the magnitude of an animal's response to taste. Also, because lesions of the amygdala produce a nonselective disruption of CTA learning produced by X-irradiation [32] as well as to both LiCl and amphetamine injection [54], and because the depletion of norepinephrine produced by injection of 6-hydroxydopamine into the basolateral amygdala also disrupts CTA learning [11], it may be that catecholamines are more related to the association of the CTA response to a CS than to the nature of the UCS.

Results from experiments studying the effect of drugs that block acetylcholine receptors have depended upon the doses used. With low doses of atropine (0.6 mg/kg, SC) or scopolamine (0.05–1.0 mg/kg, SC), the development of a radiation- or LiCl-induced CTA is not altered [37,125]. After higher doses of atropine (15 mg/kg, SC or 100 mg/kg, IP), radiation- and LiCl-induced taste aversions are attenuated [29,52]. However, interpretation of these results is further complicated by the observation that treatment with atropine sulfate (25 mg/kg, IP) itself produces a CTA [98].

Although its relevance to radiation-induced CTA learning has yet to be directly established, endogenous opioids have been implicated as mediating some of the behavioral changes observed following exposure to ionizing radiation [83,84]. Mickley [83] has reported that treatment with naloxone prevents the occurrence of a radiation-induced stereotypic hyperactivity in C57BL/6J mice that is similar to the behavioral response of these mice to treatment with morphine. Also, morphine-tolerant rats show a smaller radiation-induced performance decrement than do non-tolerant rats [84]. Similar results have been reported by Tesky and Kavaliers [132] who observed a radiation-induced analgesia in CF-1 mice which could be reversed by treatment with naloxone. Because treatment with morphine produces a CTA that can be attenuated by treatment with naloxone [74,134], it may be that endogenous opioids play a role in the acquisition of a radiation-induced CTA. However, Rabin and Hunt (unpublished manuscript) found that pretreating rats with a single injection of naloxone did not attenuate the acquisition of a radiation-induced CTA.

From this discussion, there is no clear role for the major transmitters in initiating a CTA induced by radiation- or drug-released toxins acting through the area postrema. The effects observed after transmitter manipulation appear to be related more to the expression of the CTA.

CONCLUSIONS

Overall, the research reviewed in this report would be consistent with the hypothesis that there are at least two classes of unconditioned stimuli that can lead to the acquisition of a CTA. The first class consists of those unconditioned stimuli, such as amphetamine, that do not require the mediation of the area postrema for CTA learning. In the second class, there are those stimuli, such as LiCl, which require the mediation of the area postrema for the acquisition of a CTA. For the most part, radiation, as a UCS for CTA learning, seems to belong to the second class of stimuli.

The area postrema is one of a group of circumventricular organs that is characterized by a relatively weak blood/brain barrier [28]. As such, it may be assumed that the role of the area postrema in CTA learning is to transfer to the central nervous system information about the presence of toxins in blood and cerebrospinal fluid when those toxins cannot cross the blood/brain barrier [107]. This hypothesis would be consistent with the observation that lesions of the area postrema disrupt CTA learning following injection of methylscopolamine, which cannot cross the blood/brain barrier, but have no effect on CTA learning when the UCS is a drug such as amphetamine, which can cross the barrier [4,114]. However, this hypothesis does not account for the disruption of an LiCl-induced CTA by area postrema lesions because LiCl does cross the blood/brain barrier [25]. Therefore, other factors, in addition to the ability of a substance to cross the blood/brain barrier, might determine whether or not the area postrema plays a necessary role in the acquisition of a CTA. It may be that the central effects of LiCl, unlike those of amphetamine, are not relevant for the acquisition of a CTA.

While the data indicate that activation of the area postrema is not a necessary condition for CTA learning, there are some very limited data which suggests that it might be a sufficient condition. In the cat, but not in the rat, the cardiovascular effects of angiotensin II are mediated by the area postrema [121]. In agreement with these findings is the observation that injection of angiotensin II produces changes in the activity of single units in the area postrema of the cat [10], but has no such effects in the rat [13]. Concordant with the electrophysiological data on the area postrema is the observation by Rabin *et al.* [111] that injection of angiotensin II will produce a CTA in cats, but not in rats. To more fully evaluate this possibility that activation of the area postrema may constitute a sufficient condition for CTA learning, however, would require additional electrophysiological studies monitoring the response of area postrema neurons to toxins that do not cause a CTA.

One other question concerns the specific nature of the UCS. The data reviewed in previous sections do not provide clear evidence as to whether the potential toxicity of a certain class of unconditioned stimuli, such as ionizing radiation and LiCl, is the proximal antecedent condition for CTA learning. Because a CTA can be produced by nontoxic stimuli that organisms will self-administer, a UCS-produced illness cannot be considered a necessary condition for CTA learning. Even where a toxic UCS is utilized, the data do not provide unequivocal support for the common assumption that a stimulus-induced illness is a sufficient condition for CTA learning. This is true not only for a UCS such as LiCl, which produces overt signs of distress, but even more so for exposure to ionizing radiation, which produces no overt changes in unrestrained behavior. It may be that radiation is able to produce a CTA because it activates the neural circuits associated with illness even in the absence of the experience of the illness by the awake organism [100]. Alternatively, it may be, as suggested by Gamzu [38], that the basis for taste aversion learning lies in the novelty of the treatment-induced state: that any treatment will produce a CTA as long as it produces a novel, discriminable state within the organism. In this view, ionizing radiation is able to lead to CTA learning because irradiation produces a discriminable change in nervous system activity. The potentially toxic character of the radiation UCS, or any other UCS such as LiCl, is not directly relevant to the CTA learning as long as that UCS is capable of producing a discriminably different state. As such, the UCS-produced illness may not be the direct antecedent cause of the CTA, but may rather simply be an unavoidable side-effect of the treatment that produces such a novel state.

The final question concerns the nature of the interaction between the UCS and the area postrema. When a CTA is

acquired following treatment with a systemic toxin, such as LiCl, which involves the mediation of the area postrema, an implicit assumption is that the toxin exerts direct effects on neuronal activity of the area postrema leading to CTA learning. This assumption, however, might not be correct. Smith [123] reported that injection of LiCl directly into the fourth ventricle, unlike systemically administered LiCl, did not produce a CTA. The implication of this finding is that CTA learning following systemic (intraperitoneal or intragastric) treatment with LiCl does not result from a direct action of lithium on area postrema neurons, but rather that systemic treatment with LiCl causes the release of an endogenous mediator to which the area postrema is sensitive. Thus, the LiCl-induced CTA, like the radiation-induced CTA, may depend upon a treatment-released humoral factor which serves as the proximate UCS for CTA learning. It is interesting to speculate that, because manipulations which affect LiCl-induced CTA learning also affect the radiation-induced CTA, the same endogenous humoral factor mediates CTA learning following treatment with either UCS; or, indeed, any UCS that requires the mediation of the area postrema.

Electrophysiological studies have shown that the area postrema is sensitive to a variety of endogenous peptides. Working with dogs, Carpenter and his coworkers [17,18] have reported that iontophoretic application of a variety of peptides causes changes in the activity of area postrema neurons and that systemic treatment with these same peptides causes emesis. In rats, treatment with the gastrointestinal hormone cholecystokinin may produce a CTA ([27,33], but see [48] for contrary data) that is mediated by the area postrema [133]. A CTA has also been reported to result from repeated systemic injection of arginine vasopressin [34]. Whether any of these peptides can, in fact, serve as the factor which is the proximal UCS for CTA learning following exposure to ionizing radiation or following systemic treatment with LiCl remains to be established.

It is, however, clear that the CTA, as a CR to a CS associated with toxic consequences to the organism, has definite implications for the survival of the organism. Given the wide range of unconditioned stimuli which can elicit a CTA, it is unlikely that the area postrema would have evolved specific receptors for each potential toxin. Rather, it is more likely that a class of toxic stimuli produce a series of similar effects resulting in the release of an endogenous factor. This factor may alter the activity of neurons within the area postrema with the consequent development of a CTA. Radiation is capable of functioning as a UCS for CTA learning because it too is capable of causing the release of this humoral factor. Ionizing radiation is, therefore, just one member of a class of environmental toxins that induce a CTA through the release of some endogenous factor affecting the activity of the area postrema. The validity of this hypothesis and the definition of a potential endogenous factor remain to be established by further research.

REFERENCES

1. Ashe, J. H. and M. Nachman. Neural mechanisms in taste aversion learning. In: *Progress in Psychobiology and Physiological Psychology*, vol 9, edited by J. M. Sprague and A. N. Epstein. New York: Academic Press, 1980, pp. 233–262.
2. Barker, L. M. and J. C. Smith. A comparison of taste aversions induced by radiation and lithium chloride in CS-US and US-CS paradigms. *J Comp Physiol Psychol* **87**: 644–654, 1974.
3. Berger, B. D. Conditioning of food aversions by injections of psychoactive drugs. *J Comp Physiol Psychol* **81**: 21–26, 1972.
4. Berger, B. D., C. D. Wise and L. Stein. Area postrema damage and bait shyness. *J Comp Physiol Psychol* **82**: 475–479, 1973.
5. Bernstein, I. L. and M. M. Webster. Learned taste aversions in humans. *Physiol Behav* **25**: 363–366, 1980.
6. Bhargava, K. P. and K. S. Dixit. Role of the chemoreceptive trigger zone in histamine-induced emesis. *Br J Pharmacol* **34**: 508–513, 1968.
7. Bogo, V. Effects of bremsstrahlung and electron radiation on rat motor performance. *Radiat Res* **100**: 313–320, 1984.
8. Borison, H. L. Site of emetic action of X-radiation in the cat. *J Comp Neurol* **107**: 439–453, 1957.
9. Borison, H. L. Area postrema: Chemoreceptive trigger zone for vomiting—is that all? *Life Sci* **14**: 1807–1817, 1974.
10. Borison, H. L., M. J. Hawken, J. I. Hubbard and N. E. Sirett. Unit activity from cat postrema influenced by drugs. *Brain Res* **92**: 153–156, 1975.
11. Borsini, F. and E. T. Rolls. Role of noradrenaline and serotonin in the basolateral region of the amygdala in food preferences and learned taste aversions in the rat. *Physiol Behav* **33**: 37–43, 1984.
12. Brizzee, K. R. Effects of localized brain stem lesions and supradiaphragmatic vagotomy on X-irradiation emesis in the monkey. *Am J Physiol* **187**: 567–570, 1956.
13. Brooks, M. J., J. I. Hubbard and N. E. Sirett. Extracellular recording in rat area postrema in vitro and the effects of cholinergic drugs, serotonin and angiotensin II. *Brain Res* **261**: 85–90, 1983.
14. Bruner, A., V. Bogo and R. K. Jones. Delayed match-to-sample early performance decrement in monkeys after ^{60}Co irradiation. *Radiat Res* **63**: 83–96, 1975.
15. Burghardt, W. B. and W. A. Hunt. Characterization of radiation-induced performance decrement using a two-lever shock-avoidance task. *Radiat Res* **103**: 149–157, 1985.
16. Cairnie, A. B. and K. E. Leach. Dexamethasone: A potent blocker for radiation-induced taste aversion in rats. *Pharmacol Biochem Behav* **17**: 305–311, 1982.
17. Carpenter, D. O., D. B. Briggs and N. Strominger. Responses of canine area postrema to neurotransmitters and peptides. *Cell Mol Neurobiol* **3**: 113–126, 1983.
18. Carpenter, D. O., D. B. Briggs and N. Strominger. Peptide-induced emesis in dogs. *Behav Brain Res* **11**: 277–281, 1984.
19. Carroll, M. E. and J. C. Smith. Time course of radiation-induced taste aversion conditioning. *Physiol Behav* **13**: 809–812, 1974.
20. Chinn, H. I. and S. C. Wang. Locus of emetic action following irradiation. *Proc Soc Exp Biol Med* **85**: 472–474, 1954.
21. Coil, J. D. and R. Norgren. Taste aversions conditioned with intravenous copper sulfate: Attenuation by ablation of the area postrema. *Brain Res* **212**: 425–433, 1981.
22. Coil, J. D., R. C. Rogers, J. Garcia and D. Novin. Conditioned taste aversions: Vagal and circulatory mediation of the toxic unconditioned stimulus. *Behav Biol* **24**: 509–519, 1978.
23. Coil, J. D., W. G. Hankins, D. J. Jenden and J. Garcia. The attenuation of a specific cue-to-consequence association by antiemetic agents. *Psychopharmacology (Berlin)* **56**: 21–25, 1978.
24. Daugherty, J. H. and C. D. Barnes. Effect of X-irradiation on the interaction of flash-evoked cortical potentials. *Radiat Res* **49**: 359–366, 1972.
25. Davenport, V. D. Distribution of parenterally administered lithium chloride in plasma, brain and muscle of rats. *Am J Physiol* **163**: 633–641, 1950.

26. Dempsey, E. W. Neural and vascular ultrastructure of the area postrema in the rat. *J Comp Neurol* **150**: 177–200, 1973.
27. Deutsch, J. A. and W. T. Hardy. Cholecystokinin produces bait shyness in rats. *Nature* **266**: 196, 1977.
28. Deutsch, J. A., F. Molina and A. Puerto. Conditioned taste aversion caused by palatable nontoxic nutrients. *Behav Biol* **16**: 161–174, 1976.
29. Deutsch, R. Effects of atropine on conditioned taste aversion. *Pharmacol Biochem Behav* **8**: 685–694, 1978.
30. Doyle, T. F., C. R. Curran and J. E. Turns. The prevention of radiation-induced, early, transient incapacitation of monkeys by an antihistamine. *Proc Soc Exp Biol Med* **145**: 1018–1024, 1974.
31. Dragoin, W., G. E. McCleary and P. McCleary. A comparison of two methods of measuring conditioned taste aversions. *Behav Res Meth Instr* **3**: 309–310, 1971.
32. Elkins, R. L. Attenuation of X-ray-induced taste aversions by olfactory bulb or amygdaloid lesions. *Physiol Behav* **24**: 515–521, 1980.
33. Ettenberg, A. and G. F. Koob. Different effects of cholecystokinin and satiety on lateral hypothalmic self-stimulation. *Physiol Behav* **32**: 127–130, 1984.
34. Ettenberg, A., D. van der Kooy, M. Le Moal, G. F. Koob and F. E. Bloom. Can aversive properties of (peripherally-injected) vasopressin account for its putative role in memory? *Behav Brain Res* **7**: 331–350, 1983.
35. Fenner, D. P. and I. L. Bernstein. Interference in food aversion conditioning by reducing drug dose or conditioning trials. *Behav Neural Biol* **40**: 114–118, 1984.
36. Franz, C. G. Effects of mixed neutron-gamma total-body irradiation on physical activity performance of rhesus monkeys. *Radiat Res* **101**: 434–441, 1985.
37. Gadusek, F. J. and J. W. Kalat. Effects of scopolamine on retention of taste-aversion learning in rats. *Physiol Psychol* **3**: 130–132, 1975.
38. Gamzu, E. The multifaceted nature of taste-aversion-inducing agents: Is there a single common factor? In: *Learning Mechanisms in Food Selection*, edited by L. M. Barker, M. R. Best and M. Domjam. Waco, TX: Baylor Univ. Press, 1977, pp. 477–509.
39. Garcia, J. and D. J. Kimeldorf. Temporal relationship within the conditioning of a saccharin aversion through radiation exposure. *J Comp Physiol Psychol* **50**: 180–183, 1957.
40. Garcia, J. and D. J. Kimeldorf. Some factors which influence radiation-conditioned behavior of rats. *Radiat Res* **12**: 719–727, 1960.
41. Garcia, J. and R. A. Koelling. Relation of cue to consequence in avoidance learning. *Psychon Sci* **4**: 123–124, 1966.
42. Garcia, J. and R. A. Koelling. A comparison of aversions induced by X-rays, toxins, and drugs in the rat. *Radiat Res* Suppl 7: 439–450, 1967.
43. Garcia, J., E. R. Ervin and R. A. Koelling. Toxicity of serum from irradiated donors. *Nature* **213**: 682–683, 1967.
44. Garcia, J., W. G. Hankins and K. W. Rusiniak. Behavioral regulation of the milieu interne in man and rat. *Science* **185**: 824–831, 1974.
45. Garcia, J., D. J. Kimeldorf and E. L. Hunt. The use of ionizing radiation as a motivating stimulus. *Psychol Rev* **68**: 383–395, 1961.
46. Garcia, J., D. J. Kimeldorf and R. A. Koelling. Conditioned aversion to saccharin resulting from exposure to gamma radiation. *Science* **122**: 157–158, 1955.
47. Gaston, K. E. Brain mechanisms of conditioned taste aversion learning: A review of the literature. *Physiol Psychol* **6**: 340–345, 1978.
48. Gibbs, J., R. C. Young and G. P. Smith. Cholecystokinin decreases food intake in rats. *J Comp Physiol Psychol* **84**: 488–495, 1973.
49. Goudie, A. J. Aversive stimulus properties of drugs. *Neuropharmacology* **18**: 971–979, 1979.
50. Goudie, A. J., E. W. Thornton and J. Wheatley. Attenuation by alpha-methyltyrosine of amphetamine-induced conditioned taste aversion. *Psychopharmacologia* **45**: 119–123, 1975.
51. Goudie, A. J., I. P. Stolerman, C. Demellweek and G. D'Mello. Does conditioned nausea mediate drug-induced taste aversion. *Psychopharmacology (Berlin)* **78**: 277–281, 1982.
52. Gould, M. N. and N. B. Yatvin. Atropine-caused central nervous system interference with radiation-induced learned and unlearned behaviours. *Int J Radiat Biol* **24**: 463–468, 1973.
53. Grote, F. W. and R. T. Brown. Conditioned taste aversions: Two-stimulus tests are more sensitive than one-stimulus tests. *Behav Res Meth Instr* **3**: 311–312, 1971.
54. Grupp, L. A., M. A. Linseman and H. Cappell. Effects of amygdala lesions on taste aversions produced by amphetamine and LiCl. *Pharmacol Biochem Behav* **4**: 541–544, 1976.
55. Hennessy, J. W. and S. Levine. Stress arousal and the pituitary adrenal system. A psychoendocrine hypothesis. In: *Progress in Psychobiology and Physiological Psychology*, vol 8, edited by J. M. Sprague and A. N. Epstein. New York: Academic Press, 1979, pp. 133–178.
56. Hennessy, J. W., W. P. Smotherman and S. Levine. Conditioned taste aversion and the pituitary-adrenal system. *Behav Biol* **16**: 413–424, 1976.
57. Hennessy, J. W., W. P. Smotherman and S. Levine. Investigations into the nature of dexamethasone and ACTH effects upon learned taste aversion. *Physiol Behav* **24**: 645–649, 1980.
58. Hulse, E. V. and L. G. Mizon. Radiation-conditioned aversion in rats after part-body X-irradiation and its relationship to gastric emptying. *Int J Radiat Biol* **12**: 515–522, 1967.
59. Hulse, E. V. and G. Patrick. A model for treating post-irradiation nausea and vomiting in man: The action of insulin in abolishing radiation-induced delay in gastric emptying in the rat. *Br J Radiol* **50**: 645–651, 1977.
60. Hunt, E. L. and D. J. Kimeldorf. Behavioral arousal and neural activation as radiosensitive reactions. *Radiat Res* **21**: 91–110, 1964.
61. Hunt, E. L. and D. J. Kimeldorf. The humoral factor in radiation-induced motivation. *Radiat Res* **30**: 404–419, 1967.
62. Hunt, E. L., H. W. Carroll and D. J. Kimeldorf. Humoral mediation of radiation-induced motivation in parabiont rats. *Science* **150**: 1747–1748, 1965.
63. Hunt, E. L., H. W. Carroll and D. J. Kimeldorf. Effects of dose and of partial-body exposure on conditioning through a radiation-induced humoral factor. *Physiol Behav* **3**: 809–813, 1968.
64. Hunt, W. A. Comparative effects of exposure to high energy electrons and gamma radiation on active avoidance behavior. *Int J Radiat Biol* **44**: 257–260, 1983.
65. Hunt, W. A., T. K. Dalton and J. H. Darden. Transient alterations in neurotransmitter activity in the caudate nucleus of rat brain after a high dose of ionizing radiation. *Radiat Res* **80**: 556–562, 1979.
66. Ionescu, E. and O. Buresova. Failure to elicit conditioned taste aversion by severe poisoning. *Pharmacol Biochem Behav* **6**: 251–254, 1977.
67. Kemper, T. L., R. O'Neill and W. F. Caveness. Effects of single dose supervoltage whole brain radiation in macaca mulatta. *J Neuropathol Exp Neurol* **36**: 916–940, 1977.
68. Kiefer, S. W., K. W. Rusiniak and J. Garcia. Vagotomy facilitates extinction of conditioned taste aversions in rats. *J Comp Physiol Psychol* **95**: 114–122, 1981.
69. Kiefer, S. W., R. J. Cabral, K. W. Rusiniak and J. Garcia. Ethanol-induced flavor aversions in rats with subdiaphragmatic vagotomies. *Behav Neural Biol* **29**: 246–254, 1980.
70. Kimeldorf, D. J. and E. L. Hunt. *Ionizing Radiation: Neural Function and Behavior*. New York: Academic Press, 1965.
71. Kimeldorf, D. J., J. Garcia and D. O. Rubadeau. Radiation-induced conditioned avoidance behavior in rats, mice, and cats. *Radiat Res* **12**: 710–718, 1966.
72. Kral, P. A. and V. V. St. Omer. Beta adrenergic receptor involvement in the mediation of learned taste aversions. *Psychopharmacologia* **26**: 79–83, 1972.

73. Lasiter, P. S. and J. J. Braun. Shock facilitation of taste aversion learning. *Behav Neural Biol* **32**: 277–281, 1981.
74. LeBlanc, A. and H. Cappell. Antagonism of morphine-induced aversive conditioning by naloxone. *Pharmacol Biochem Behav* **3**: 185–188, 1975.
75. Levy, C. J., M. E. Carroll, J. C. Smith and K. G. Hofer. Antihistamines block radiation-induced taste aversions. *Science* **186**: 1044–1046, 1974.
76. Lorden, J. F. and D. L. Margules. Enhancement of conditioned taste aversions by lesions of the midbrain raphe nuclei that deplete serotonin. *Physiol Psychol* **5**: 273–279, 1977.
77. Lorden, J. F. and W. B. Nunn. Effects of central and peripheral pretreatment with fluoxetine in gustatory conditioning. *Pharmacol Biochem Behav* **17**: 435–443, 1982.
78. Lorden, J. F. and G. A. Oltmans. Alteration of the characteristics of learned taste aversion by manipulation of serotonin levels in the brain. *Pharmacol Biochem Behav* **8**: 13–18, 1978.
79. Louis-Sylvestre, J. Validation of tests of completeness of vagotomy in rats. *J Auton Nerv Syst* **9**: 301–314, 1983.
80. Martin, J. R., F. Y. Cheng and D. Novin. Acquisition of learned taste aversion following bilateral subdiaphragmatic vagotomy in rats. *Physiol Behav* **21**: 13–17, 1978.
81. Mason, S. T. and H. C. Fibiger. Noradrenaline and extinction of conditioned taste aversions in the rat. *Behav Neural Biol* **25**: 206–216, 1979.
82. Mickley, G. A. Behavioral and physiological changes produced by a supralethal dose of ionizing radiation: Evidence for hormone-influenced sex differences in the rat. *Radiat Res* **81**: 48–75, 1980.
83. Mickley, G. A., K. E. Stevens, G. A. White and G. L. Gibbs. Endogenous opiates mediate radiogenic behavioral change. *Science* **220**: 1185–1187, 1983.
84. Mickley, G. A., K. E. Stevens, J. M. Burrows, G. A. White and G. L. Gibbs. Morphine tolerance offers protection from radiogenic performance deficits. *Radiat Res* **93**: 381–387, 1983.
85. Miller, D. S. Effects of low level radiation on audiogenic convulsive seizures in mice. In: *Response of the Nervous System to Ionizing Radiation*, edited by T. J. Haley and R. S. Snider. New York: Academic Press, 1962, pp. 513–531.
86. Minamisawa, T. and T. Tsuchiya. Long-term changes in the averaged evoked potentials of the rabbit after irradiation with moderate X-ray doses. *Electroencephalogr Clin Neurophysiol* **42**: 416–424, 1977.
87. Minamisawa, T., K. Yamamoto and T. Tsuchiya. Long-term effects of moderate X-ray doses on the averaged evoked potentials in the rabbit. *Electroencephalogr Clin Neurophysiol* **50**: 59–70, 1980.
88. Minkler, J. *Introduction to Neuroscience*. Saint-Louis, MO: C. V. Mosby Co., 1972.
89. Mossman, K. L., A. J. Martini and R. I. Heinkin. Radiation-induced changes in sodium preference and fluid intake in the rat. *Int J Radiat Biol* **36**: 191–196, 1979.
90. Mossman, K. L., J. D. Chencharick, A. C. Scheer, W. P. Walker, R. D. Ornitz, C. C. Rogers and R. I. Henkin. Radiation-induced changes in gustatory function, comparison of effects of neutron and photon irradiation. *Int J Radiat Oncol Biol Phys* **5**: 521–528, 1979.
91. Nachman, M. and J. H. Ashe. Learned taste aversions in rats as a function of dosage, concentration, and route of administration of LiCl. *Physiol Behav* **10**: 73–78, 1973.
92. Nachman, M. and P. L. Hartley. Role of illness in producing learned taste aversion in rats: A comparison of several rodenticides. *J Comp Physiol Psychol* **89**: 1010–1018, 1975.
93. Ossenkopp, K.-P. Taste aversion conditioned with gamma radiation: Attenuation by area postrema lesions in rats. *Behav Brain Res* **7**: 295–305, 1983.
94. Overton, D. A. Experimental methods for the study of state-dependent learning. *Fed Proc* **33**: 1800–1813, 1974.
95. Parker, L. A. Nonconsummatory and consummatory behavioral CRs elicited by lithium- and amphetamine-paired flavors. *Learn Mot* **13**: 281–303, 1982.
96. Phillips, A. G. and F. G. LePiane. Disruption of conditioned taste aversion in the rat by stimulation of amygdala: A conditioning effect, not amnesia. *J Comp Physiol Psychol* **94**: 664–674, 1980.
97. Pollack, M. and P. S. Timiras. X-ray dose and electroconvulsive responses in adult rats. *Radiat Res* **21**: 111–119, 1964.
98. Preston, K. L. and C. R. Schuster. Conditioned gustatory avoidance by three cholinergic agents. *Pharmacol Biochem Behav* **15**: 827–828, 1981.
99. Rabin, B. M. and W. A. Hunt. Effects of antiemetics on the acquisition and recall of radiation- and lithium chloride-induced conditioned taste aversions. *Pharmacol Biochem Behav* **18**: 629–635, 1983.
100. Rabin, B. M. and J. S. Rabin. Acquisition of radiation- and lithium chloride-induced conditioned taste aversions in anesthetized rats. *Anim Learn Behav* **12**: 439–441, 1984.
101. Rabin, B. M., W. A. Hunt and J. Lee. Studies on the role of central histamine in the acquisition of a radiation-induced conditioned taste aversion. *Radiat Res* **90**: 609–620, 1982.
102. Rabin, B. M., W. A. Hunt and J. Lee. State-dependent interactions in the antihistamine-induced disruption of a radiation-induced taste aversion. *Radiat Res* **90**: 621–627, 1982.
103. Rabin, B. M., W. A. Hunt and J. Lee. Attenuation of radiation- and drug-induced conditioned taste aversions following area postrema lesions in the rat. *Radiat Res* **93**: 388–394, 1983.
104. Rabin, B. M., W. A. Hunt and J. Lee. Acquisition of lithium chloride- and radiation-induced taste aversions in hypophysectomized rats. *Pharmacol Biochem Behav* **18**: 463–465, 1983.
105. Rabin, B. M., W. A. Hunt and J. Lee. Taste aversion learning in vagotomized rats. Paper presented at the 1983 Meeting of the American Psychological Association, Anaheim, CA.
106. Rabin, B. M., W. A. Hunt and J. Lee. Effects of dose and of partial body ionizing radiation on taste aversion learning in rats with lesions of the area postrema. *Physiol Behav* **32**: 119–122, 1984.
107. Rabin, B. M., W. A. Hunt and J. Lee. Recall of a previously acquired conditioned taste aversion in rats following lesions of the area postrema. *Physiol Behav* **32**: 503–506, 1984.
108. Rabin, B. M., W. A. Hunt and J. Lee. Interactions between unconditioned stimuli that produce taste aversion learning. *Soc Neurosci Abstr* **11**: 535, 1985.
109. Rabin, B. M., W. A. Hunt and J. Lee. Intragastric copper sulfate produces a more reliable conditioned taste aversion in vagotomized rats than in intact rats. *Behav Neural Biol*, in press, 1985.
110. Rabin, B. M., W. A. Hunt and J. Lee. Effect of area postrema lesions on taste aversions produced by treatment with WR-2721 in the rat. *Neurobehav Toxicol Teratol* **8**: in press, 1986.
111. Rabin, B. M., W. A. Hunt, A. C. Bakarich, A. L. Chedester and J. Lee. Angiotensin II produces a taste aversion in cats but not in rats. *Soc Neurosci Abstr* **10**: 1011, 1984.
112. Remler, M. P. and W. H. Marcussen. Time course of early delayed blood-brain barrier changes in individual cats after ionizing radiation. *Exp Neurol* **73**: 310–314, 1981.
113. Riley, A. L. and L. L. Baril. Conditioned taste aversions: A bibliography. *Anim Learn Behav* **4**: 1S-13S, 1976.
114. Ritter, S., J. L. McGlone and K. W. Kelly. Absence of lithium-induced taste aversion after area postrema lesion. *Brain Res* **201**: 501–506, 1980.
115. Roberts, D. C. and H. C. Fibiger. Attenuation of amphetamine-induced conditioned taste aversion following intraventricular 6-hydroxy-dopamine. *Neurosci Lett* **1**: 343–347, 1975.
116. Roll, D. L. and J. C. Smith. Conditioned taste aversion in anesthetized rats. In: *Biological Foundations of Learning*, edited by M. E. P. Seligman and J. L. Hager. New York: Appleton-Century-Crofts, 1972, pp. 98–102.
117. Rondeau, D. B., F. B. Jolicoeur, A. D. Merkel and M. J. Wayner. Drugs and taste aversion. *Neurosci Biobehav Rev* **5**: 279–294, 1981.

118. Rusiniak, K. W., C. C. Palmerino, A. G. Rice, D. L. Forthman and J. Garcia. Flavor-illness aversions: Potentiation of odor by taste with toxin but not shock in rats. *J Comp Physiol Psychol* **96**: 527–539, 1982.
119. Sessions, G. R. Histamine and radiation-induced taste aversion conditioning. *Science* **190**: 402–403, 1975.
120. Sheline, G. E., W. M. Wara and V. Smith. Therapeutic irradiation and brain injury. *Int J Radiat Oncol Biol Phys* **6**: 1215–1228, 1980.
121. Simpson, J. B. The circumventricular organs and the central actions of angiotensin. *Neuroendocrinology* **32**: 248–256, 1981.
122. Sklar, L. S. and Z. Amit. Manipulations of catecholamine systems block the conditioned taste aversion induced by self-administered drugs. *Neuropharmacology* **16**: 649–655, 1977.
123. Smith, D. F. Central and peripheral effects of lithium on conditioned taste aversions in rats. *Psychopharmacology* **68**: 315–317, 1980.
124. Smith, J. C. Radiation: Its detection and its effects on taste preferences. In: *Progress in Physiological Psychology*, vol 4, edited by E. Stellar and J. M. Sprague. New York: Academic Press, 1971, pp. 53–117.
125. Smith, J. C. and D. D. Morris. Effects of atropine sulfate on the conditioned aversion to saccharin fluid with X-rays as the unconditioned stimulus. *Radiat Res* **28**: 186–190, 1963.
126. Smith, J. C., G. R. Hollander and A. C. Spector. Taste aversions conditioned with partial body radiation exposures. *Physiol Behav* **27**: 903–913, 1981.
127. Smotherman, W. P. and S. Levine. ACTH and $ACTH_{1-10}$ modification of neophobia and taste aversion responses in the rat. *J Comp Physiol Psychol* **92**: 22–33, 1978.
128. Smotherman, W. P., J. W. Hennessy and S. Levine. Plasma corticosterone levels during recovery from LiCl produced taste aversions. *Behav Biol* **16**: 401–412, 1976.
129. Smotherman, W. P., J. W. Hennessy and S. Levine. Plasma corticosterone levels as an index of the strength of illness induced taste aversions. *Physiol Behav* **17**: 903–908, 1976.
130. Smotherman, W. P., A. Margolis and S. Levine. Flavor preexposures in a conditioned taste aversion situation: A dissociation of behavioral and endocrine effects in rats. *J Comp Physiol Psychol* **94**: 25–35, 1980.
131. Spector, A. C., J. C. Smith and G. R. Hollander. A comparison of measures used to quantify radiation-induced taste aversion. *Physiol Behav* **27**: 887–901, 1981.
132. Teskey, G. C. and M. Kavaliers. Ionizing radiation induces opioid-mediated analgesia in male mice. *Life Sci* **35**: 1547–1552, 1984.
133. Van der Kooy, D. Area postrema: site where cholecystokinin acts to decrease food intake. *Brain Res* **295**: 345–347, 1984.
134. Van der Kooy, D. and A. Phillips. Temporal analysis of naloxone attenuation of morphine-induced taste aversion. *Pharmacol Biochem Behav* **6**: 637–641, 1977.
135. Wagner, G. C., R. W. Foltin, L. S. Seiden and C. R. Schuster. Dopamine depletion by 6-hydroxydopamine prevents conditioned taste aversion induced by methylamphetamine but not lithium chloride. *Pharmacol Biochem Behav* **14**: 85–88, 1981.
136. Wakisaka, S., R. R. O'Neil, T. L. Kemper, D. M. Verrelli and W. F. Caveness. Delayed brain damage in adult monkeys from radiation in the therapeutic range. *Radiat Res* **80**: 277–291, 1979.
137. Wang, S. C. and H. L. Borison. Copper sulfate emesis: A study of afferent pathways from the gastrointestinal tract. *Am J Physiol* **164**: 520–526, 1951.
138. Weinberg, J., M. R. Gunnar, L. P. Brett, C. A. Gonzalez and S. Levine. Sex differences in biobehavioral responses to conflict in a taste aversion paradigm. *Physiol Behav* **29**: 201–210, 1982.
139. Wellman, P. J., P. McIntosh and E. Guidi. Effects of dorsolateral tegmental lesions on amphetamine- and lithium-induced taste aversions. *Physiol Behav* **26**: 341–344, 1981.
140. Wixon, H. N. and W. A. Hunt. Ionizing radiation decreases veratridine-stimulated uptake of sodium in rat brain synaptosomes. *Science* **220**: 1073–1074, 1983.
141. Zook, B. C., E. W. Bradley, G. W. Casarett and C. C. Rogers. Pathologic findings in canine brains irradiated with fractionated fast neutrons or photons. *Radiat Res* **84**: 562–568, 1980.